UNCLASSIFIED
SECURITY CLASSIFICATION OF THIS PAGE (When Data Entered)

REPORT DOCUMENTATION PAGE

READ INSTRUCTIONS BEFORE COMPLETING FORM

1. REPORT NUMBER: IIHR Report No. 304
2. GOVT ACCESSION NO.:
3. RECIPIENT'S CATALOG NUMBER:

4. TITLE (and Subtitle): Viscous-Inviscid Interaction With Higher-Order Viscous-Flow Equations

5. TYPE OF REPORT & PERIOD COVERED: Technical Report, Sept. 1983 - August 1986

6. PERFORMING ORG. REPORT NUMBER: IIHR Report No. 304

7. AUTHOR(s): Frederick Stern, Sungyul Yoo, and Virendra C. Patel

8. CONTRACT OR GRANT NUMBER(s): N000-14-83-K-0136

9. PERFORMING ORGANIZATION NAME AND ADDRESS: Iowa Institute of Hydraulic Research, The University of Iowa, Iowa City, Iowa 52242

10. PROGRAM ELEMENT, PROJECT, TASK AREA & WORK UNIT NUMBERS: NR 655-002

11. CONTROLLING OFFICE NAME AND ADDRESS: Office of Naval Research, 800 North Quincy Street, Arlington, Virginia 22217

12. REPORT DATE: August 1986

13. NUMBER OF PAGES:

14. MONITORING AGENCY NAME & ADDRESS(if different from Controlling Office): Office of Naval Research, 536 South Clark Street, Chicago, Illinois 60605

15. SECURITY CLASS. (of this report): Unclassified

15a. DECLASSIFICATION/DOWNGRADING SCHEDULE:

16. DISTRIBUTION STATEMENT (of this Report): Approval for Public Release; Distribution unlimited

17. DISTRIBUTION STATEMENT (of the abstract entered in Block 20, if different from Report):

18. SUPPLEMENTARY NOTES:

19. KEY WORDS (Continue on reverse side if necessary and identify by block number): Thick 3 D Boundary Layer, Viscous-Inviscid Interaction, Partially-Parabolic Equations, Computational Fluid Dynamics

20. ABSTRACT (Continue on reverse side if necessary and identify by block number)

The partially-parabolic, or parabolised, Navier-Stokes equations for laminar flow, and the corresponding Reynolds equations for turbulent flow, are coupled with an inviscid-flow solution procedure to develop a viscous-inviscid interaction method which can be used in three-dimensional flows which cannot be treated by means of the classical boundary-layer equations. Potential applications of such a higher-order matching procedure are, for example: thick boundary layers on ship sterns and bodies at incidence, interacting shear layers (wakes, wall jets), solid-solid and solid-fluid corners.

DD FORM 1 JAN 73 1473 EDITION OF 1 NOV 65 IS OBSOLETE S/N 0102-014-6601

Unclassified
SECURITY CLASSIFICATION OF THIS PAGE (When Data Entered)

This report provides a detailed overview of the approach for general three-dimensional flows, and presents the results of applications to some simple test cases. The Reynolds equations are derived in nonorthogonal curvilinear coordinates, with velocity components along the coordinate directions, using vector techniques. This approach differs from the commonly-used tensor methods but serves to establish a connection with the more familiar boundary-layer methods. The k-ε model is used for turbulent flows. The partially-parabolic viscous-flow equations are solved using an implicit finite-difference scheme and the SIMPLER algorithm for pressure-velocity coupling. The inviscid-flow solutions are obtained with a conforming panel, source-panel method. Interaction between the viscous and inviscid regions is accounted for using the displacement-body concept. The relative merits of interactive and global solution procedures are evaluated by comparing the viscous-inviscid interaction solutions with large-domain solutions of only the viscous-flow equations. Comparisons are also made with experimental data and other computational methods. Although the test cases are restricted to two-dimensional and axisymmetric flows, the results clearly demonstrate the feasibility of higher-order viscous-inviscid interaction procedures.

VISCOUS-INVISCID INTERACTION WITH HIGHER-ORDER VISCOUS-FLOW EQUATIONS

by

F. Stern, S. Y. Yoo, and V. C. Patel

Sponsored by

Office of Naval Research
Accelerated Research Initiative (Special Focus)
Program in Ship Hydrodynamics

Contract No. N00014-83-K-0136

IIHR Report No. 304

Iowa Institute of Hydraulic Research
The University of Iowa
Iowa City, Iowa 52242

August 1986

Approved for Public Release: Distribution Unlimited

VISCOUS-INVISCID INTERACTION WITH HIGHER-ORDER VISCOUS-FLOW EQUATIONS

by

F. Stern, S.Y. Yoo, and V.C. Patel

Sponsored by

Office of Naval Research
Accelerated Research Initiative (Special Focus) Program in Ship Hydrodynamics
Contract No. N00014-83-K-0136

IIHR Report No. 304

Iowa Institute of Hydraulic Research
The University of Iowa
Iowa City, Iowa, 52242

August 1986

ABSTRACT

The partially-parabolic, or parabolised, Navier-Stokes equations for laminar flow, and the corresponding Reynolds equations for turbulent flow, are coupled with an inviscid-flow solution procedure to develop a viscous-inviscid interaction method which can be used in three-dimensional flows which cannot be treated by means of the classical boundary-layer equations. Potential applications of such a higher-order matching procedure are, for example: thick boundary layers on ship sterns and bodies at incidence, interacting shear layers (wakes, wall jets), solid-solid and solid-fluid corners.

This report provides a detailed overview of the approach for general three-dimensional flows, and presents the results of applications to some simple test cases. The Reynolds equations are derived in nonorthogonal curvilinear coordinates, with velocity components along the coordinate directions, using vector techniques. This approach differs from the commonly-used tensor methods but serves to establish a connection with the more familiar boundary-layer methods. The k-ϵ model is used for turbulent flows. The partially-parabolic viscous-flow equations are solved using an implicit finite-difference scheme and the SIMPLER algorithm for pressure-velocity coupling. The inviscid-flow solutions are obtained with a conforming panel, source-panel method. Interaction between the viscous and inviscid regions is accounted for using the displacement-body concept. The relative merits of interactive and global solution procedures are evaluated by comparing the viscous-inviscid interaction solutions with large-domain solutions of only the viscous-flow equations. Comparisons are also made with experimental data and other computational methods. Although the test cases are restricted to two-dimensional and axisymmetric flows, the results clearly demonstrate the feasibility of higher-order viscous-inviscid interaction procedures.

ACKNOWLEDGEMENTS

This research was sponsored by the Office of Naval Research, Accelerated Research Initiative (Special Focus) Program in Ship Hydrodynamics, under Contract N000-14-83-K-0136. The Graduate College of the University of Iowa provided a large part of the computer funds.

LIST OF SYMBOLS

Alphabetical Symbols

A,B,C,F,G,H	components of the inverse metric tensor
$A_\delta{}^*$, A_δ	cross-sectional area beteween the actual-body surface and the δ^* surface, and the δ surface respectively
a_i,b_i,c_i,d_i,e_i	coefficients in the discretized form of the momentum and turbulence-model equations
B	constant in the log-law
b	half-width of the wake
C_μ, $C_{\varepsilon 1}$, $C_{\varepsilon 2}$	constants in the k-ϵ equations
C_p	pressure coefficient = $2(p - p_o)/ \rho U_o^2$
D	diameter of body
$\hat{e}_i$	unit vectors in the (x,y,z) coordinate directions
f_i	coefficients in the pressure and pressure-correction equations
$\tilde{G}$	turbulence generation term in the k-ϵ equations
g_{ij}	inverse metric tensor
H	shape parameter
h_i	metric coefficients
IT	global iteration number
k	turbulent kinetic energy
L	body length
L_s	closing length of the body
n_1	x-component of the unit normal to the body
$O()$	order of magnitude
p	mean pressure
$\hat{p}$	pressure correction
p_o	ambient pressure

q	magnitude of $\underline{V}$
$\underline{R}$	body cartesian-coordinate position vector
Rn	Reynolds number based on body length
s	triple product
S	Jacobian defined by $S = s/h_1h_2h_3$
S_B	body surface boundary
S_E	exit boundary
S_I	inlet boundary
S_o	outer boundary
Sp	source term in the pressure and pressure-correction equations
$S\phi$	source term in the momentum and turbulence equations
U_o	uniform stream velocity
U_τ	wall-shear velocity
$(\tilde{U},\tilde{V},\tilde{W})$	pseudovelocity components
$\underline{V}$	mean velocity $\underline{V} = (U,V,W)$
$\underline{v}$	turbulent velocity $\underline{v} = (u,v,w)$
$\overline{v_iv_j}$	Reynolds stresses
$\underline{V}_p$	potential-flow velocity
x_u	transition location from thin to thick boundary
y_o	outer boundary where uniform-stream conditions exist
(X,Y,Z)	body cartesian coordinates
(x,y,z)	nonorthogonal curvilinear coordinates
y^+	y nondimensionalized as an inner variable

Greek Symbols

$\alpha(x)$	arc length of the body cross-section
α	under-relaxation factor for the momentum equations
α_p	under-relaxation factor for the pressure equation
$\alpha_p^{\wedge}$	under-relaxation factor for the pressure-correction equation
$\gamma_{y,z}$	expansion ratio and grid distribution in y-z directions
δ	boundary layer thickness
δ^*	displacement thickness
Δ	difference
Δ_p	dimensionless pressure gradient
Δ_τ	dimensionless shear stress gradient
ε	rate of turbulent energy dissipation
ε_{ij}	rate-of-strain tensor
θ	momentum thickness
κ	von Karman constant
(λ,μ,ν)	angles between respective coordinates (x,y,z)
ν	kinematic viscosity
ν_t	eddy viscosity
ρ	density
σ	source strength
σ_B	source strength due to original body
σ_{BL}	source strength due to viscous effect
σ_k, σ_ε	constants for turbulence modelling
τ_w	wall-shear stress
Φ	perturbation velocity potential
∇	gradient

$\nabla\cdot$	divergence
∇^2	Laplacian
$\nabla\times$	curl
$\underline{\omega}$	the mean vorticity

Subscripts

B	body
BL	boundary layer
CL	wake centerline
d	downstream
E	exit
e	value at edge of viscous-flow domain
I	inlet
m	node-point index in y-direction
MM	maximum number of node-points in y-direction
n	node-point index in z-direction
NN	maximum number of node-points in z-direction
o	outer boundary
p	potential-flow value
u	upstream

Superscripts

l	node-point index in x-direction
LL	maximum number of node-points in the x-direction
T	transpose of matrix

TABLE OF CONTENTS

I. INTRODUCTION

The classical boundary-layer equations, which are based on the assumption that the viscous layer is thin relative to the local radii of curvature of the surface, are parabolic and neglect all influences of the downstream flow other than those contained in the inviscid-flow pressure field. Also, in the classical theory, the inviscid flow is calculated without accounting for the boundary-layer displacement effects. In spite of these approximations, there would seem to be no question as to the tremendous success of boundary-layer theory. The requirements of the theory are met in many practical flow situations, at least for a portion of the flow domain, and for cases where they are not met it provides a formal framework upon which refinements and modifications can be applied and understood. The conditions of boundary-layer theory are not met in a variety of practical circumstances, for example: in regions or in the vicinity of flow separation; near leading and trailing edges; in corners; at the juncture of the boundary layer and the free surface for surface-piercing bodies; in regions of strong mass injection; and in regions of strong shock-wave boundary-layer interaction. In these cases, some or all of the terms neglected in the Navier-Stokes equations to obtain the boundary-layer equations become important and, as a result, the classical approach fails to predict such flows. There is, therefore, a need for approaches which solve viscous-flow equations which are more general than the boundary-layer equations.

There are two possible approaches to the solution of higher-order viscous-flow equations: a global approach in which one set of governing equations that are appropriate for both the inviscid-and viscous-flow regions are solved using a large solution domain so as to capture the entire zone of viscous-

inviscid interaction; and an interactive approach in which different sets of governing equations are used for the viscous- and inviscid-flow field regions and the complete solution is obtained iteratively and interactively through the use of an interaction law, i.e., patching or matching conditions. The latter approach is often referred to as a zonal approach. It should be recognized that the former approach is somewhat more rigorous since it does not rely on the patching conditions which are not exact. Nonetheless, for a variety of reasons, some of which will be discussed subsequently, both types of approaches are of interest. A complete review of the literature is beyond the scope of this report. However, an overview is given using selected references as examples for the purpose of putting the present work in perspective.

Traditionally, interaction studies have coupled the thin-boundary-layer equations with inviscid-flow solutions which include viscous-flow effects using displacement-body or equivalent-source methods. Usually, only one iteration is performed either because sufficient accuracy has been obtained or due to slow convergence. Such methods have been successful in predicting flows where the boundary-layer equations are, in fact, a good approximation in the viscous-flow region, e.g., thin airfoils and wings at sufficiently small angles of attack such that there is no flow separation. Extensions for thicker airfoils and wings and/or larger angles of attack, such that only a limited separation occurs that is confined to a thin layer adjacent to the surface, have also been made. In this case, the singularity of the boundary-layer equations at separation is removed by using the inverse mode and single-pass solutions can be obtained using the FLARE approximation. Here again, the results are very good and under most circumstances the interactive boundary layer procedures can predict the flow as well as the global Navier-Stokes or

partially-parabolic Navier-Stokes solutions (McDonald and Briley, 1983; Mehta et al., 1985). The interactive procedures have the advantage of computational efficiency over the global methods.

Applications of either the traditional (direct-mode) or inverse-mode interactive procedures to flows in which the boundary-layer equations do not represent a good approximation (e.g., axisymmetric bodies and ship hulls) have generally had only a limited success. In the case of the traditional procedures this has been well demonstrated by the extensive experimental and theoretical studies of Huang and associates at the David Taylor Naval Ship Research and Development Center (DTNSRDC) (Huang et al., 1978, 1980, 1983). For axisymmetric bodies with relatively sharp trailing edges, the viscous-inviscid interaction is relatively weak, and the traditional procedures allow the boundary-layer calculations to go beyond the premature separation predicted by the classical theory and show good agreement with the experimental data except at the extreme tail region. This improvement over the without interaction solutions is no doubt due to the removal of the rear stagnation point in the inviscid-flow solution. However, for axisymmetric bodies with blunt trailing edges and more complex three-dimensional bodies the viscous-inviscid interaction is strong and the agreement with the experimental data has not been satisfactory. There have, in fact, been only a very limited number of inverse-mode interaction studies for axisymmetric and three-dimensional bodies. Here again, difficulties have been encountered for strong interaction applications (Piquet and Visonneau, 1985).

Patel (1982) has reviewed the experimental data for the viscous-flow over the stern of axisymmetric bodies and ship hulls, which he refers to as thick-boundary-layer flows, and points out the following features: (a) for practical

body geometries there is an absence of flow separation; (b) a rapid thickening of the boundary layer; (c) variation of pressure across the boundary layer implying strong viscous-inviscid interaction; (d) the development of a large longitudinal vorticity component which may or may not lead to a free-vortex type separation; (e) a general reduction in the level of turbulence. Patel concludes that the appropriate governing equations for the viscous-flow region are the partially-parabolic Navier-Stokes or Reynolds equations. Thus, higher-order equations must be used in the viscous-flow region for such applications.

Investigations using higher-order equations for axisymmetric and three-dimensional bodies have been quite varied in the approximations embodied and the turbulence model and numerical procedures utilized. Generally speaking, the results from most of these investigations have shown an improvement over the traditional interaction procedures; however, they do not show overall good agreement with the experimental data. This can be attributed to a variety of causes: lack of, incomplete, or incorrect viscous-inviscid interaction procedures; inconsistent approximations in the equations; velocity-pressure coupling procedures; turbulence modeling; and coordinates and grid dependence. For axisymmetric bodies, see for example, Brune et al. (1975), Lee (1978), Dietz (1980), Muraoka (1980), Markatos (1984), and Marlin et al. (1985). For three-dimensional bodies, see for example, Abdelmeguid et al. (1979), Markatos et al. (1980), Muraoka (1980, 1982), Tzabiras and Loukakis (1983), Tzabiras (1983), and Hoekstra and Raven (1985). In most of the above references the outer boundary was placed at about two boundary-layer thicknesses from the body surface where conditions are prescribed based on the potential-flow solution without including the viscous-flow displacement effects which are

presumed to be small at this distance; however, as pointed out by Chen and Patel (1985) and also by the present work, viscous-inviscid interaction is important even at such distances from the body. Thus, these previous solutions are not complete. Also, in one case (Tzabiras 1983), the use of the experimental displacement-body to compute the potential flow actually led to a less accurate prediction of the surface pressure distribution, indicating other numerical difficulties.

Only Chen and Patel (1985) and Zhou (1982) have taken a sufficiently large solution domain in the solution of the partially-parabolic Reynolds equations to capture the entire zone of viscous-inviscid interaction. The two methods are very different. Zhou uses a streamline iteration method which may not be easily extended to three-dimensional flows. Chen and Patel use the novel finite-analytic method to discretize the equations and have presented results for both two- and three-dimensional flows. Also, see the recent review article by Patel and Chen (1985) of the state-of-the-art for axisymmetric bodies (not including the present work). Thus far, these large domain solutions have proven to be the most successful.

In the present investigation, a viscous-inviscid interaction method has been developed in which the partially-parabolic, or parabolised, Navier-Stokes equations for laminar flow, and the corresponding Reynolds equations for turbulent flow, are coupled with a displacement-body inviscid-flow solution procedure in an interactive and iterative manner. There are numerous potential applications of such a higher-order matching procedure, for example: thick-boundary-layers on ship sterns and bodies at incidence, interacting shear layers, solid-solid and solid-fluid corners. Herein, of particular interest are thick-boundary-layer trailing-edge flows, e.g., ship boundary

layers. For such applications the interaction approach has the advantage over the global approach in that it is most easily extendable to the calculation of ship boundary layers at nonzero Froude numbers.

This report provides a detailed overview of the approach for general three-dimensional flows, and presents the results of applications to some simple test cases. The Reynolds equations are derived in nonorthogonal curvilinear coordinates, with velocity components along the coordinate directions, using vector techniques. This approach differs from the commonly-used tensor methods but serves to establish a connection with the more familiar boundary-layer methods. The k-ε model is used for turbulent flows. The partially-parabolic viscous-flow equations are solved using an implicit finite-difference scheme and the SIMPLER algorithm for pressure-velocity coupling. The inviscid-flow solutions are obtained with a conforming panel, source-panel method. Interaction between the viscous and inviscid regions is accounted for using the displacement-body concept. The relative merits of interactive and global solution procedures are evaluated by comparing the viscous-inviscid interaction solutions with large-domain solutions of only the viscous-flow equations. Comparisons are also made with experimental data and other computational methods. Although the test cases are restricted to two-dimensional and axisymmetric flows, the results clearly demonstrate the feasibility of higher-order viscous-inviscid interaction procedures.

II. METHOD OF APPROACH

Consider the flow field in the vicinity of a body fixed in a uniform stream with velocity U_o of an incompressible viscous fluid. The body shape is

assumed to be sufficiently streamlined and the Reynolds number sufficiently large such that no flow separation occurs and viscous effects are confined to a relatively narrow region adjacent to the body surface and in the wake. As depicted in figure 1, the flow field can be divided into three regions. Region 1 is the inviscid-flow region. Region 2 is the thin-boundary-layer which ends at a station x_u beyond which boundary-layer approximations are no longer valid. Region 3 ($X > x_u$) is the thick-boundary-layer and wake region in which it is assumed that only streamwise gradients of viscous and turbulent stresses can be neglected. The inviscid-flow region extends to a distance y_o beyond which uniform stream conditions may be assumed. Appropriate computational methods can be used for each of the three regions. They are related through their boundary conditions and are not necessarily independent. In particular, the flow fields in regions 3 and 1 are interdependent such that a complete solution for each region has to be determined iteratively through the use of a viscous-inviscid interaction procedure. Alternatively, the flow fields in regions 3 and 1 can be solved simultaneously by simply extending region 3 to also include the portion of region 1 influenced by the interaction. Such a large-domain solution captures the entire zone of viscous-inviscid interaction and can be used to assess the accuracy of a small-domain interaction solution. Herein, both types of solutions will be obtained in order to explicate the nature of an interactive solution.

III. VISCOUS-INVISCID INTERACTION

In an interactive approach to the present problem, the viscous- and inviscid-flow regions 3 and 1 are demarcated by the common boundary δ , as

shown in figure 1. This boundary must be placed at a sufficient distance from the body surface and wake centerplane such that, exterior to δ (region 1), viscous effects can be neglected. Traditionally, this boundary is placed at or just beyond the edge of the boundary layer. Note that this should be considered as the minimum value for δ , and it is also possible to place δ at distances greater than the boundary-layer thickness, as has been done by other investigators. Herein, the traditional definition is used. The flow-field solutions in regions 3 and 1 are obtained separately and by quite different means, but they are interdependent through the common boundary condition that the two solutions merge smoothly at δ. That is, the viscous-flow solution (region 3) is obtained with edge conditions at δ specified based on the inviscid-flow solution (region 1) which is obtained with recognition of the displacement effect of the viscous flow. The complete solution is obtained iteratively until convergence is achieved.

It has long been recognized that the viscous-flow region displaces the inviscid-flow streamlines such that the inviscid flow is not the same as that about the actual body, but rather that about a surface displaced into the fluid a distance δ^* referred to as the displacement surface. The displacement surface can be defined unambiguously by the following two requirements: (a) that it be a stream surface of the inviscid flow continued from outside the boundary layer; (b) that the inviscid-flow discharge between this surface and any stream surface exterior to the boundary layer be equal to the actual discharge between the body and the latter stream surface. The second condition implies that the flow reduction inside the viscous flow is compensated by an outward displacement of such a stream surface through a distance δ^* , i.e.

$$\int_{A_{\delta^*}} \underline{V}_p \cdot \underline{dA} = \int_{A_\delta} (\underline{V}_p - \underline{V}) \cdot \underline{dA} \qquad \text{(III-1)}$$

where $\underline{V}_p$ is the velocity vector of the outer inviscid flow analytically continued into the viscous-flow region, $\underline{V}$ is the viscous-flow velocity vector, and A_{δ^*} and A_δ are the cross-sectional areas between the actual-body surface and the displacement-body surface and the boundary-layer surface respectively. Thus, the inviscid-flow solution is obtained for the displacement body. This solution then provides the boundary conditions for the viscous flow

$$\begin{aligned} U(\delta) &= U_p(\delta) = U_e \\ W(\delta) &= W_p(\delta) = W_e \qquad \text{(III-2)} \\ p(\delta) &= p_p(\delta) = p_e \end{aligned}$$

Since δ^* and $\underline{V}_p(\delta)$ are not known a priori, an initial guess must be provided and the complete solution obtained by iteratively updating the viscous- and inviscid-flow solutions until the "patching" conditions (III-1) and (III-2) are satisfied. Note that, in the present viscous-inviscid interaction procedure, no assumptions have been made with regard to the thickness of the boundary layer. The primary assumption is that the inviscid- and viscous-flow solutions can be patched together through conditions (III-1) and (III-2).

Within the context of thin-boundary-layer theory, and for two-dimensional flow, equation (III-1) becomes

$$\delta^* = \frac{1}{U_e} \int_o^\delta (1 - U/U_e)\, dy \qquad \text{(III-3)}$$

where

$$U_e = U_p(o) = U_p(\delta).$$

Lighthill (1958) refers to this definition of δ^* (III-3) as the flow-reduction method which he shows, for both two- and (with the appropriate definition) three-dimensional flow, is completely equivalent, within the context of thin-boundary-layer theory, to three other definitions: equivalent source, velocity comparison, and mean vorticity. The velocity-comparison method was first introduced by Moore (1953) and is closely related to the equivalent-source method, in which it is shown that the displacement effect of the boundary layer on the inviscid flow can be represented by an additional distribution of sources on the actual body surface of strength

$$\sigma_{BL} = \frac{1}{2\pi} \frac{d}{dx} (U_e \delta^*) \qquad \text{(III-4)}$$

where x is the distance along the body surface in the streamwise direction. Landweber (1978) has pointed out that (III-4) is just the first approximation to the solution of the general integral equation for σ_{BL} due to the boundary-layer outflow velocity distribution $\frac{d}{dx} (U_e \delta^*)$. To the same order of approximation, the source distribution for the actual body is given by

$$\sigma_B = \frac{1}{2\pi} (U_o n_1) \qquad \text{(III-5)}$$

where n_1 is the x-component of the unit normal to the body surface. Based on either thin- or thick-boundary-layer order-of-magnitude estimates (see Table

1) $\sigma_{BL} / U_o \sim O(\varepsilon)$ where ε is the nondimensional boundary-layer thickness and $\sigma_B / U_o \sim O(n_1)$. The equivalent-source method has been used extensively and with success in viscous-inviscid interaction procedures for airfoils and wings where n_1 is small in the region of interaction. However, for the problems of present interest (e.g. axisymmetric bodies and ship hulls), n_1 is not necessarily small near the trailing edge and the equivalent-source method is not useful for representing the viscous-flow displacement effect on the inviscid flow.

IV. VISCOUS FLOW

In the thick boundary layer and wake (region 3 in figure 1) it is assumed that only streamwise gradients of viscous and turbulent stresses can be neglected. Under this assumption, the Reynolds equations are reduced to a simplified form referred to as the partially-parabolic (Reynolds) equations. In these equations, the velocity field is elliptic in transverse planes and parabolic in the streamwise direction while the pressure field is fully elliptic. Solutions to the partially-parabolic equations can be obtained iteratively by solving the parabolic equations that result when the pressure field is specified and subsequently updating the pressure field using the results from the latest parabolic solution. Of crucial importance is the manner in which the velocity and pressure fields are coupled. Many procedures have been tried for this purpose (e.g., Anderson et al. 1984). In the present work, a modified form of the SIMPLER algorithm (Patanker, 1980) that enhances global convergence has been used (Chen and Patel, 1985). Selection of the appropriate coordinate system and grid generation technique used to obtain the coor-

dinates is also important. A streamline coordinate system is the most consistent with the assumptions of the partially-parabolic equations; however, such a coordinate system is difficult to generate. Alternatively, body-fitted coordinates can be used in which the axial coordinate should be roughly aligned with the streamlines since they are coincident on the body surface itself. The partially-parabolic assumptions are made in this preselected axial coordinate direction. In the present work, both simplified analytic and numerically generated body-fitted coordinate systems have been used. The Reynolds stresses are modeled using the k-ϵ turbulence model. A complete transformation of the governing equations is used such that the directions of the velocity components are along the grid lines. It should be recognized that very few investigators have used a complete transformation of the governing equations, no doubt due to the complexity of their derivation as will become apparent subsequently. The more common approach is a partial transformation in which only the coordinates are transformed and the velocity components are maintained in either cartesian or polar coordinates. The governing equations are reduced to algebraic form using finite differences and solved implicitly by the method of lines. In the subsections to follow, the details of these computational procedures are discussed.

A. Equations and Coordinate System. The partially-parabolic equations are solved using a nonorthogonal curvilinear coordinate system in which the x-coordinate is roughly aligned with the flow direction and the y-coordinate is in a plane transverse to the body axis X (see figure 1a). For three-dimensional flow, the z-coordinate is also in the transverse plane and in the girthwise direction (see figure 1b). The Reynolds equations in nonorthogonal curvilinear coordinates can be derived either through the use of vector or

tensor analysis. Here, a vector approach has been used since it lends itself to more physical insight. Recently, Richmond et al. (1986) have provided a derivation using tensor analysis.

The Reynolds, continuity, turbulent-kinetic-energy k, and its dissipation-rate ε equations for steady incompressible flow can be written in the following vector form:

$$\frac{1}{2}\nabla(\underline{V}\cdot\underline{V}) - \underline{V}\times\underline{\omega} = -\nabla\, p/\rho + \nu\{\nabla(\nabla\cdot\underline{V}) - \nabla\times\underline{\omega}\} - \nabla\cdot\overline{v_i v_j} + \overline{(v_i)\,\nabla\cdot\underline{v}} \qquad \text{(IV-1)}$$

$$\nabla\cdot\underline{V} = 0 \qquad \text{(IV-2)}$$

$$\underline{V}\cdot\nabla k = \nabla\cdot\left(\frac{\nu_t}{\sigma_k}\nabla k\right) + \tilde{G} - \varepsilon \qquad \text{(IV-3)}$$

$$\underline{V}\cdot\nabla\varepsilon = \nabla\cdot\left(\frac{\nu_t}{\sigma_\varepsilon}\nabla\varepsilon\right) + C_{\varepsilon 1}\,\tilde{G}\,\frac{\varepsilon}{k} - C_{\varepsilon 2}\,\frac{\varepsilon^2}{k} \qquad \text{(IV-4)}$$

where $\underline{V} = (U,V,W)$ are the mean velocity components, $\underline{v} = (u,v,w)$ are the turbulent velocity components, p is the mean pressure, $\underline{\omega} = \nabla \times \underline{V}$ is the mean vorticity, $\overline{v_i v_j}$ are the Reynolds stresses (the overbar denotes time averaging), $k = \frac{1}{2}\overline{\underline{v}\cdot\underline{v}}$ is the turbulent kinetic energy, $\nu_t = C_\mu\, k^2/\varepsilon$ is the eddy viscosity, and $\tilde{G}$ is the turbulence generation. Since the fluid is assumed to be incompressible, the terms involving $\nabla \cdot \underline{V}$ and $\nabla \cdot \underline{v}$ in equation (IV-1) are identically zero, but have been included since they aid in putting the transformed equations into a more compact form. The usual values are used for the constants in the k-ε equations, namely, $(C_\mu, \sigma_k, \sigma_\varepsilon, C_{\varepsilon 1}, C_{\varepsilon 2}) = (.09,\ 1.,\ 1.3,\ 1.44,\ 1.92)$. The turbulence generation term is defined by

$$\tilde{G} = \nu_t [2(\varepsilon_{11}^2 + \varepsilon_{22}^2 + \varepsilon_{33}^2) + 4\,(\varepsilon_{12}^2 + \varepsilon_{23}^2 + \varepsilon_{31}^2)] \qquad \text{(IV-5)}$$

where ε_{ij} is the rate-of-strain tensor

$$\varepsilon_{ij} = \frac{1}{2}\,[\nabla \underline{V} + \nabla \underline{V}^T] \qquad \text{(IV-6)}$$

In (IV-6) $\nabla \underline{V}$ is the deformation-rate tensor e_{ij} and $\nabla \underline{V}^T$ its transpose, i.e. $\nabla \underline{V}^T = e_{ji}$. The Reynolds stresses required in (IV-1) are related to k and ε through the isotropic eddy viscosity concept:

$$\overline{v_i v_j} = -\,2\nu_t \varepsilon_{ij} + \frac{2}{3}\,k(h_i h_j g_{ij}) \qquad \text{(IV-7)}$$

where the h_i are the metric coefficients and g_{ij} is the inverse metric tensor both of which are defined below.

Equations (IV-1) - (IV-7) can be transformed into any coordinate system through the use of appropriate definitions of the gradient (∇), divergence ($\nabla\cdot$), and curl ($\nabla\times$) vector operators. The details of this procedure for orthogonal curvilinear coordinates are provided by Rouse (1959). For nonorthogonal curvilinear coordinates the appropriate vector operator definitions are not readily available. They were probably first derived by Weatherburn (1926). Following Weatherburn, and referring to figures 1 and 2 for the present notation, the unit vectors $\hat{e}_i = (\hat{e}_1, \hat{e}_2, \hat{e}_3)$ in the directions of the nonorthogonal curvilinear coordinates (x,y,z) are defined in terms of the body cartesian-coordinate position vector

$$\underline{R} = X(x,y,z)\,\hat{i} + Y(x,y,z)\,\hat{j} + Z(x,y,z)\,\hat{k} \qquad \text{(IV-8)}$$

by

$$\hat{e}_1 = \underline{R_x}/h_1,\ \hat{e}_2 = \underline{R_y}/h_2,\ \hat{e}_3 = \underline{R_z}/h_3 \qquad \text{(IV-9)}$$

where

$$h_1 = |\underline{R_x}|,\ h_2 = |\underline{R_y}|,\ h_3 = |\underline{R_z}| \qquad \text{(IV-10)}$$

and a lettered subscript denotes a partial derivative. The angles (λ, μ, ν) between the (x,y,z) coordinate axes are given by

$$\begin{aligned} \cos\lambda &= \hat{e}_2 \cdot \hat{e}_3 \\ \cos\mu &= \hat{e}_1 \cdot \hat{e}_3 \\ \cos\nu &= \hat{e}_1 \cdot \hat{e}_2 \end{aligned} \qquad \text{(IV-11)}$$

and the unit normals to constant x- y- and z-surfaces are given respectively by

$$\begin{aligned} \hat{e}_2 \times \hat{e}_3 &= \frac{1}{h_2 h_3 s}\left[Ah_1\hat{e}_1 + Hh_2\hat{e}_2 + Gh_3\hat{e}_3\right] \\ \hat{e}_3 \times \hat{e}_1 &= \frac{1}{h_1 h_3 s}\left[Hh_1\hat{e}_1 + Bh_2\hat{e}_2 + Fh_3\hat{e}_3\right] \\ \hat{e}_1 \times \hat{e}_2 &= \frac{1}{h_1 h_2 s}\left[Gh_1\hat{e}_1 + Fh_2\hat{e}_2\ \ Ch_3\hat{e}_3\right] \end{aligned} \qquad \text{(IV-12)}$$

where s is the triple product

$$s = (h_1 h_2 h_3)\ (\hat{e}_1 \cdot \hat{e}_2 \times \hat{e}_3)$$

$$= [A h_1^2 + H h_1 h_2 \cos\nu + G h_1 h_3 \cos\mu]^{1/2} \qquad \text{(IV-13)}$$

and

$$\begin{aligned} A &= h_2^2 h_3^2 \sin^2\lambda \\ B &= h_1^2 h_3^2 \sin^2\mu \\ C &= h_1^2 h_2^2 \sin^2\nu \\ F &= (h_1 h_3 \cos\mu)\ (h_1 h_2 \cos\nu) - h_1^2\ (h_2 h_3 \cos\lambda) \\ G &= (h_1 h_2 \cos\nu)\ (h_2 h_3 \cos\lambda) - h_2^2\ (h_1 h_3 \cos\mu) \\ H &= (h_2 h_3 \cos\lambda)\ (h_1 h_3 \cos\mu) - h_3^2 (h_1 h_2 \cos\nu) \end{aligned} \qquad \text{(IV-14)}$$

The inverse metric tensor is defined by

$$g_{ij} = (h_i \hat{e}_i \cdot h_j \hat{e}_j)^{-1}$$

$$= \frac{1}{s} \begin{bmatrix} A & H & G \\ H & B & F \\ G & F & C \end{bmatrix} \qquad \text{(IV-14.1)}$$

In terms of the above quantities, the gradient of any scalar $Q(x,y,z)$ and divergence and curl for any vector $\underline{V}(x,y,z) = V_1\hat{e}_1 + V_2\hat{e}_2 + V_3\hat{e}_3$ are given by:

$$\nabla Q = \frac{1}{s^2} \{ (AQ_x + HQ_y + GQ_z)\ h_1\hat{e}_1 + (HQ_x + BQ_y + FQ_z)\ h_2\hat{e}_2$$

$$+ (GQ_x + FQ_y + CQ_z)\, h_3\hat{e}_3\} \qquad \text{(IV-15)}$$

$$\nabla\cdot\underline{V} = \frac{1}{s}\left[\frac{\partial}{\partial x}\left(\frac{sV_1}{h_1}\right) + \frac{\partial}{\partial y}\left(\frac{sV_2}{h_2}\right) + \frac{\partial}{\partial z}\left(\frac{sV_3}{h_3}\right)\right] \qquad \text{(IV-16)}$$

$$\nabla\times\underline{V} = \frac{1}{s}\left\{\frac{\partial}{\partial y}\left[V_1h_3\cos\mu + V_2h_3\cos\lambda + V_3h_3\right]\right.$$

$$\left. - \frac{\partial}{\partial z}\left[V_1h_2\cos\nu + V_2h_2 + V_3h_2\cos\lambda\right]\right\} h_1\hat{e}_1$$

$$+ \frac{1}{s}\left\{\frac{\partial}{\partial z}\left[V_1h_1 + V_2h_1\cos\nu + V_3h_1\cos\mu\right]\right.$$

$$\left. - \frac{\partial}{\partial x}\left[V_1h_3\cos\mu + V_2h_3\cos\lambda + V_3h_3\right]\right\} h_2\hat{e}_2$$

$$+ \frac{1}{s}\left\{\frac{\partial}{\partial x}\left[V_1h_2\cos\nu + V_2h_2 + V_3h_2\cos\lambda\right]\right.$$

$$\left. - \frac{\partial}{\partial y}\left[V_1h_1 + V_2h_1\cos\nu + V_3h_1\cos\mu\right]\right\} h_3\hat{e}_3 \qquad \text{(IV-17)}$$

The transformed equations are very lengthy and are provided in Appendix I. The equations have been put in a form that is similar to that used by Nash and Patel (1972) for orthogonal curvilinear coordinates. By comparison, it is seen that, for the present circumstances, the coefficients in the governing equations depend on terms related to not only the curvatures of the coordinates but also their angular orientation. Due to the complexity of the derivation of the transformed equations it was desired to check their accuracy; however, this was made difficult by the fact that no other presentations of the governing equations in nonorthogonal curvilinear coordinates in a format

and notation similar to the present one are known to exist. The following checks were made: for $(\lambda,\mu,\nu) \to 90°$, the orthogonal form of the equations was recovered; for $(\lambda,\nu) \to 90°$, and subject to the boundary-layer assumptions the boundary-layer equations of Cebeci et al. (1978) were recovered; and some of the coefficients were compared with their corresponding counterparts in the tensor form of the equations presented by Richmond et al. (1986).

The partially-parabolic equations are obtained from the complete set of equations in Appendix I through the use of the order-of-magnitude estimates given in Table 1.

Table 1: Order-of-Magnitude Estimates for a Thick Boundary Layer

Quantity	Order-of-Magnitude
U	1
V	ε
W	ε
$\partial/\partial x$	1
$\partial/\partial y$	ε^{-1}
$\partial/\partial z$	ε^{-1}
ν	ε^{2}
$\overline{v_i v_j}$	ε

Patel (1982) has shown that these order-of-magnitude estimates are consistent with the partially-parabolic assumptions. Also, in obtaining the partially-

parabolic equations no assumptions are made with regard to geometrical quantities; that is, all geometrical quantities are considered O(1). The x-momentum equation is obtained by retaining terms of O(1) only. All other equations are obtained by retaining terms of $O(1) + O(\varepsilon)$. The partially-parabolic equations are provided in Appendix II. Lastly, it should be mentioned that, strictly speaking, the complete equations can also be rendered partially-parabolic by simply only neglecting the viscous- and turbulent-diffusion terms (second-order derivatives) in the x direction.

B. Discretization. The governing equations are reduced to algebraic form by approximating all the spatial derivatives by finite differences. A staggered-grid system has been used in order to avoid difficulties in the velocity-pressure coupling procedure to be discussed subsequently. The grid arrangement and notation are as shown in figure 3. An implicit finite-difference scheme is used which is basically only first-order accurate; however, certain derivatives have been evaluated using second-order central differences and all terms have been evaluated at the proper grid location by using averages of the surrounding values. The detailed finite-difference formulas are provided in Appendix III. The overall procedure is described below.

The x-momentum equation is discretized with reference to control volume I of figure 3. Referring to the partially-parabolic form of the x-momentum equation (B-1), figure 3, and Appendix III.A: only the x- and y-derivatives in the convective acceleration and the y-diffusion terms are maintained on the left hand side to form the tridiagonal matrix; the remaining terms are grouped into a single source term and are put on the right hand side; and all terms are evaluated at the location of $U^{\ell}_{m,n}$.

The y-momentum equation is discretized with reference to control volume II of figure 3. Referring to the partially-parabolic form of the y-momentum equation (B-2), figure 3, and Appendix III.A: only the x- and y-derivatives in the convective acceleration and y-diffusion terms are maintained on the left hand side to form the tridiagonal matrix; the remaining terms are grouped into a single source term and are put on the right hand side; and all terms are evaluated at the location of $V^{\ell}_{m,n}$.

The z-momentum equation is discretized with reference to control volume III of figure 3. Referring to the partially-parabolic form of the z-momentum equation (B-3), figure 3, and Appendix III.A: only the x- and z-derivatives in the convective acceleration and z-diffusion terms are maintained on the left hand side to form the tridiagonal matrix; the remaining terms are grouped into a single source term and are put on the right hand side; and all terms are evaluated at the location of $W^{\ell}_{m,n}$.

The k-ϵ equations are discretized with reference to control volume IV of figure 3. Referring to the partially-parabolic form of the k-ϵ equations (B-4) and (B-5) respectively, figure 3, and Appendix III.B: only the x- and y-derivatives in the convective acceleration and y-diffusion terms are maintained on the left hand side to form the tridiagonal matrix; the remaining terms are grouped into a single source term and are put on the right hand side; and all terms are evaluated at the location of $k^{\ell}_{m,n}$ and $\varepsilon^{\ell}_{m,n}$.

By means of the above finite difference scheme, the three momentum and the k-ϵ turbulence-model equations can be put in the form:

$$a_1 U^{\ell}_{m-1,n} + a_2 U^{\ell}_{m,n} + a_3 U^{\ell}_{m+1,n} = Su^{\ell}_{m,n} + Pu^{\ell}_{m,n} \qquad \text{(IV-18)}$$

$$b_1 V^{\ell}_{m-1,n} + b_2 V^{\ell}_{m,n} + b_3 V^{\ell}_{m+1,n} = Sv^{\ell}_{m,n} + Pv^{\ell}_{m,n} \qquad \text{(IV-19)}$$

$$c_1 W^{\ell}_{m,n-1} + c_2 W^{\ell}_{m,n} + c_3 W^{\ell}_{m,n+1} = Sw^{\ell}_{m,n} + Pw^{\ell}_{m,n} \qquad \text{(IV-20)}$$

$$d_1 k^{\ell}_{m-1,n} + d_2 k^{\ell}_{m,n} + d_3 k^{\ell}_{m+1,n} = Sk^{\ell}_{m,n} \qquad \text{(IV-21)}$$

$$e_1 \varepsilon^{\ell}_{m-1,n} + e_2 \varepsilon^{\ell}_{m,n} + e_3 \varepsilon^{\ell}_{m+1,n} = S\varepsilon^{\ell}_{m,n} \qquad \text{(IV-22)}$$

where the $S\phi$ terms are the source terms and $P\phi$ are the pressure-gradient terms (ϕ = (U,V,W,k,ε)). Note that equations (IV-18) - (IV-22) are nonlinear since both the coefficients a_i through e_i and the source terms are functions of the unknowns (U,V,W,k,ε) (see Appendix III). If the pressure field is known then equations (IV-18) - (IV-22) can be solved directly for the velocity field (U,V,W) and turbulence parameters (k,ε); however, since the pressure field is unknown, it must be determined such that the continuity equation is also satisfied. The velocity-pressure coupling procedure is the subject of the next section.

C. Velocity-Pressure Coupling. The coupling of the velocity and pressure fields is accomplished through the use of a two-step iterative procedure involving the continuity equation. In the first step, the solution to the momentum equations for a guessed pressure field is corrected at each cross section such that continuity is satisfied. However, in general, the corrected velocities are no longer a consistent solution to the momentum equations for the guessed p. Thus, the pressure field must also be corrected. In the second step, the pressure field is updated again through the use of the continuity equation. This is done after a complete solution to the velocity field

has been obtained for all cross-sections in a manner that properly accounts for the elliptic nature of the pressure field and also accelerates convergence. Repeated global iterations are thus required in order to obtain the converged solution. The details of the derivation of the pressure-correction and pressure equations are provided in Appendix III. C. The overall procedure is described below.

Both the pressure-correction and pressure equations have the same form and are derived in the same manner from the discretized form of the continuity equation, i.e.

$$\frac{1}{(\Delta x)^{\ell}_{m,n}}\left(\overline{U}^{\ell}_{m,n} - \overline{U}^{\ell-1}_{m,n}\right) + \frac{1}{(\Delta y)^{\ell-1/2}_{m+1/2,n}}\left(\overline{V}^{\ell}_{m+1,n} - \overline{V}^{\ell}_{m,n}\right)$$

$$+ \frac{1}{(\Delta z)^{\ell-1/2}_{m,n+1/2}}\left(\overline{W}^{\ell}_{m,n+1} - \overline{W}^{\ell}_{m,n}\right) = 0 \qquad \text{(IV-26)}$$

where

$$\overline{U}^{\ell}_{m,n} = \left(\frac{s}{h_1}\right)^{\ell}_{m,n} U^{\ell}_{m,n}$$

$$\overline{V}^{\ell}_{m,n} = \left(\frac{s}{h_2}\right)^{\ell}_{m,n} V^{\ell}_{m,n} \qquad \text{(IV-27)}$$

$$\overline{W}^{\ell}_{m,n} = \left(\frac{s}{h_3}\right)^{\ell}_{m,n} W^{\ell}_{m,n}$$

The velocity components ($U^{\ell}_{m,n}$, $V^{\ell}_{m,n}$, $W^{\ell}_{m,n}$) required in (IV-27) are obtained from the discretized form of the momentum equations (IV-18)-(IV-20) by putting equations (IV-18)-(IV-20) in the form

$$U^{\ell}_{m,n} = \tilde{U}^{\ell}_{m,n} + a_7 p_x + a_8 p_y + a_9 p_z$$

$$V^{\ell}_{m,n} = \tilde{V}^{\ell}_{m,n} + b_7 p_x + b_8 p_y + b_9 p_z \qquad \text{(IV-28)}$$

$$W^{\ell}_{m,n} = \tilde{W}^{\ell}_{m,n} + c_7 p_x + c_8 p_y + c_9 p_z$$

where $\tilde{U}^{\ell}_{m,n}, \tilde{V}^{\ell}_{m,n}, \tilde{W}^{\ell}_{m,n}$ are referred to as pseudovelocities.

Substituting (IV-28) and (IV-27) into (IV-26) and representing the pressure gradient terms in (IV-28) by finite differences results in the desired equation for pressure. In the $U^{\ell}_{m,n}$ equation, a forward difference is used for p_x and central differences for p_y and p_z. In the $V^{\ell}_{m,n}$ equation, a backward difference is used for p_y and central differences for p_x and p_z. In the $W^{\ell}_{m,n}$ equation, a backward difference is used for p_z and central differences for p_x and p_y. All terms are evaluated at the respective velocity component location by using averages of the surrounding values. The resulting equation for pressure involves 20 of the 27 nodes corresponding to x indices (ℓ-1, ℓ, ℓ+1) and y and z indices, (m-1, m, m+1) and (n-1, n, n+1), respectively; however, only certain terms are maintained on the left hand side to subsequently form the tridiagonal matrix, and all remaining terms are grouped into a single source term and put on the right hand side:

$$f_1 p^{\ell+1}_{m,n} + f_2 p^{\ell}_{m,n} + f_3 p^{\ell-1}_{m,n} + f_4 p^{\ell}_{m+1,n} + f_5 p^{\ell}_{m-1,n}$$

$$+ f_6 p^{\ell}_{m,n+1} + f_7 p^{\ell}_{m,n-1} = Sp \qquad \text{(IV-29)}$$

It should be recognized that no approximations have been made in deriving (IV-29) and as such it is an exact representation of the equation of continuity in terms of pressure.

Equation (IV-29) is first used to correct the velocity field obtained from the solution of the momentum equations for a guessed pressure field. In this case, p is designated as $\hat{p}$ and both upstream and downstream values of $\hat{p}$ are neglected. The resulting pressure-correction equation is

$$f_2\hat{p}^{\ell}_{m,n} + f_4\hat{p}^{\ell}_{m+1,n} + f_5\hat{p}^{\ell}_{m-1,n} + f_6\hat{p}^{\ell}_{m,n+1}$$

$$+ f_7\hat{p}^{\ell}_{m,n-1} = \hat{Sp} \qquad \text{(IV-30)}$$

where $\hat{Sp}$ is obtained by evaluating Sp (C-61) with the current solution to the momentum equations $U^{\ell}_{m,n}$, $V^{\ell}_{m,n}$, $W^{\ell}_{m,n}$ substituted for $\tilde{U}^{\ell}_{m,n}$, $\tilde{V}^{\ell}_{m,n}$, $\tilde{W}^{\ell}_{m,n}$. The pressure-correction equation (IV-30) is approximate since both upstream and downstream values of $\hat{p}$ have been neglected as well as the influence of pressure corrections on the neighboring velocities. The latter approximation neglects the indirect or implicit influence of the pressure correction on velocity and is the reason for the words semi-implicit in the name SIMPLER. Note that both approximations are justified since the corrected velocity field is only an intermediate solution, and when the solution converges, $\hat{p}$ is zero. Equation (IV-30) is solved at each cross-section ℓ using the method of lines for two-dimensional and axisymmetric flow applications and an alternating direction implicit method (ADI) for three-dimensional flow applications. Subsequently, the velocity field is corrected using equations (IV-28) with $\hat{p}$ substituted for p and with the current solution to the momentum equations $U^{\ell}_{m,n}$, $V^{\ell}_{m,n}$, $W^{\ell}_{m,n}$ substituted for $\tilde{U}^{\ell}_{m,n}$, $\tilde{V}^{\ell}_{m,n}$, $\tilde{W}^{\ell}_{m,n}$.

When the exit cross-section ℓ=LL is reached, equation (IV-29) is again used to update the pressure field. In this case, no approximations are made. The pressure equation is solved by marching from downstream to upstream using the method of lines for two-dimensional and axisymmetric flow applications and an ADI method for three-dimensional flow applications at each cross-section ℓ with the $\ell+1$ and $\ell-1$ values considered as known from the previous iteration. With a new pressure field thus obtained, the entire process is repeated until the results converge; that is, a compatible velocity- and pressure-field solution is found.

D. Boundary Conditions. The partially-parabolic equations require boundary conditions for the pressure, either explicit or implicit, on all boundaries. Boundary conditions are required only from upstream and in the cross-section for the velocity components and turbulence parameters. Note that only three of the unknowns (U,V,W,p) can be specified on each boundary or the problem is over specified. The fourth unknown is determined through the solution of the governing equations.

Referring to figure 4, the boundary conditions used in solving the momentum and k-ε equations (IV-18)-(IV-22), and the pressure (IV-29) and pressure-correction (IV-30) equations are as follows:

Inlet Boundary S_I

Initial conditions for (U,V,W,k,ε) are specified based on simple flat-plate solutions. Initial conditions for p and $\hat{p}$ are not required.

Exit Boundary S_E

A zero-gradient condition is used for p and $\hat{p}$ and no conditions are required for the velocity components and k-ϵ .

Outer Boundary S_O

$$U = U_e, \quad W = W_e, \quad p = p_e$$

$$\frac{\partial k}{\partial y} = \frac{\partial \epsilon}{\partial y} = \hat{p} = 0 \qquad \text{(IV-31)}$$

where (U_e, W_e, p_e) are specified from the inviscid-flow solution. Large-domain solutions are obtained by placing the outer boundary at a sufficient distance from the body surface and simply specifying (U_e, W_e, p_e) = (1, 0., 0.).

Body Surface Boundary S_B

For laminar flow, the solution is carried out up to the body surface where the no-slip condition is applied: U = V = W = 0. For turbulent flow, the wall-function approach of Chen and Patel (1985) is used. In this procedure, the first two grid points are placed in the log-law region. With a guessed value of the wall-shear velocity U_τ the required boundary conditions at the first grid point for the velocity components (U,V,W) and k and ϵ are obtained from the log-law and the assumption of local equilibrium:

$$\frac{q}{U_\tau} = \frac{1}{\kappa}\left\{\ln\left[\frac{4}{\Delta_\tau}\frac{(1+\Delta_\tau y^+)^{1/2}-1}{(1+\Delta_\tau y^+)^{1/2}+1}\right] + 2\left[(1+\Delta_\tau y^+)^{1/2}-1\right]\right\}$$

$$+ B + 3.7\,\Delta_p \qquad \text{(IV-32)}$$

$$k = U_\tau^2/\sqrt{c_\mu}$$

$$\varepsilon = U_\tau^3/\kappa y \qquad \text{(IV-33)}$$

where U_τ is the wall-shear velocity defined by $U_\tau = \sqrt{\tau_w/\rho}$, $y^+ = yU_\tau/\nu$ is the dimensionless distance measured in the direction normal to the surface, $\Delta_p = \frac{\nu \nabla p}{\rho U_\tau^3}$ is the dimensionless pressure gradient, Δ_τ is the dimensionless shear-stress gradient and is assumed to be $1/2\ \Delta_p$, q is the magnitude of the velocity, $\kappa = 0.42$ is the von Karman constant, and $B = 5.45$. Since the log-law (IV-32) only provides the velocity magnitude, in order to obtain the velocity components, it is assumed that the velocity vector in the (x,y) plane is parallel to the wall and in the (x,z) plane has the same direction as at the second grid point. Since the second grid point is also in the log-law region, after a field solution has been obtained, the solution at the second grid point can be used to update the guessed value of U_τ and the procedure repeated until convergence. Lastly, conditions on p and $\hat{p}$ are not required on S_B.

Symmetry Plane S_W

$$\frac{\partial}{\partial y}(U,W,p,\hat{p},k,\varepsilon) = 0 \qquad \text{(IV-34)}$$

$$V = 0$$

Symmetry Planes S_{WL} and S_K

$$\frac{\partial}{\partial z}(U,V,p,\hat{p},k,\varepsilon) = 0 \qquad \text{(IV-35)}$$

$$W = 0$$

E. Grid Generation. Grid generation is an important aspect of the overall numerical procedures. This is primarily due to the fact that the partially-parabolic assumptions are made with reference to a preselected grid coordinate curve which is presumed to be sufficiently close to the streamwise direction. Also, grids that are not sufficiently smooth can cause erroneous instabilities in the solution. Two body-fitted grid-generation techniques have been used.

For the small-domain interactive calculations a simple analytic grid-generation technique has been used in which local expanding grids for each cross-section are pieced together in the streamwise direction. That is, the nonorthogonal curvilinear coordinates (x,y,z) are defined by

$$x = X$$

$$y = \Delta y \frac{(\gamma_y^m - 1)}{\gamma_y - 1} \delta(x,z) \qquad \text{(IV-36)}$$

$$z = \Delta z \frac{(\gamma_z^n - 1)}{\gamma_z - 1} \alpha(x)$$

where $\Delta y = y^+\nu/U_\tau$ is the initial y-direction spacing, γ_y is the expansion ratio in the y-direction, $\delta(x,z)$ is the boundary-layer thickness, Δz is the initial z-direction spacing, γ_z is the expansion ratio in the z-direction, and $\alpha(x)$ is the arclength of the body cross-section.

For the large-domain solutions it was not possible to use such a simple analytic technique as (IV-36). This is due to the fact that, as the outer boundary is placed at further distances from the body surface, the piecewise local-expansions technique produces a grid in which the coordinates display humps and hollows near the body trailing edge and midway across the flow domain. Such irregularities cause instability in the solution. Consequently, for the large-domain solutions, a more sophisticated body-fitted grid-generation technique, developed by Chen and Patel (1985), was used in which the coordinates are obtained numerically from the solution of a set of Poisson equations for specified boundaries and control functions.

F. Global Solution Procedure. In the previous subsections (IV.A)-(IV.E) the various aspects of the viscous-flow-solution method have been described. The inviscid-flow-solution method is described in section V. In this section, the global and interactive solution procedures are outlined. The main steps are as follows:

1) Specify all boundary and initial conditions, including an initial guess for the entire pressure field and, for the interaction solutions, the boundary-layer thickness.

2) Construct the grid and calculate all the required geometric data.

3) Evaluate all the coefficients in the momentum, pressure-correction, and pressure equations.

4) Solve the momentum equations. An under-relaxation factor α is used.

5) Solve the pressure-correction equation and correct the velocities. An under-relaxation factor $\alpha_p^{\wedge}$ is used.

6) Calculate the pseudovelocities and store for use in solving the pressure equation.

7) Evaluate all the coefficients in the k-ϵ equations and solve the k-ϵ equations.

8) Repeat steps 3) - 7) for each cross-section until the exit plane is reached.

9) Calculate the displacement body and for the interaction solution the new inviscid-flow solution.

10) Solve the pressure equation elliptically. For the interaction solution the edge conditions are updated based on the new inviscid-flow solution. An under-relaxation factor α_p is used.

11) Repeat steps 3) - 10) until convergence is reached within a specified tolerance. Actually, the convergence criterion used for the results

to be presented was simply that there was no noticeable change in the body surface and wake centerline pressure distribution when viewed on the plotting device. Below, the notation IT is used to refer to the global iteration number.

V. INVISCID FLOW

A. Source-Panel Method. In the inviscid-flow region (region 1 in figure 1), the flow is assumed to be irrotational. A velocity potential Φ is defined such that $\nabla\Phi$ is the perturbation velocity field, i.e.

$$\underline{V}_p = U_o \hat{i} + \nabla\Phi \tag{V-1}$$

The perturbation potential must satisfy the Laplace equation

$$\nabla^2\Phi = 0 \tag{V-2}$$

subject to the boundary condition

$$\Phi_n = - U_o n_1 \qquad \text{on } S_B \tag{V-3}$$

on the body, and the condition

$$\nabla\Phi \to o \tag{V-4}$$

at infinity. The boundary-value problem (V-2) - (V-4) for the perturbation-potential can be solved by the source-distribution method. The conforming

panel, source-panel method of von Kerczek et al. (1983) has been used here. The perturbation potential is expressed by

$$\Phi = \int_{S_B} \sigma \, G \, dS \tag{V-5}$$

where σ is the source strength and G is the Green function

$$G = 1/R$$

$$R = |\underline{X} - \underline{\xi}| \tag{V-6}$$

with $\underline{X} = (x,y,z)$ the field point and $\underline{\xi} = (\xi,\mu,\zeta)$ the source point. Note that equation (V-5) automatically satisfies condition (V-4). Substitution of (V-5) into (V-3) results in the integral equation for the source strength σ, i.e.

$$- 2\pi\sigma + \int_{S_B} \sigma \frac{\partial G}{\partial n} \, dS = - U_o n_1 \tag{V-7}$$

Equation (V-7) is solved by discretizing the body surface into a number of conforming surface panels, on each of which the source strength is assumed constant, and evaluating the integral in (V-7) over each panel approximately by using Gauss quadrature.

This procedure is facilitated through the use of a parametric surface equation representation for the body surface:

$$\underline{R_B} = X \, \hat{i} + Y \, (X,\alpha) \, \hat{j} + Z \, (X,\alpha) \, \hat{k} \tag{V-8}$$

where $\underline{R}_B$ is a position vector which describes the body surface. Here X is the usual lengthwise coordinate and α is a parameter which varies along the girth of each section. The following procedures are implemented. First, the body offsets for one side are mapped into the X-α plane. That is, corresponding (X,α) pairs are assigned for each given offset $\underline{R}_B$. Second, the derivatives, $\underline{R}_X$, $\underline{R}_\alpha$, and $\underline{R}_{X\alpha}$, are obtained by three-point finite-difference approximations. Third, the offsets and derivatives are interpolated using cubic-Hermite splines onto a uniform $\{X_i, \alpha_j\}$ grid chosen so as to provide a good surface coverage with regard to surface features. With the surface vector, $\underline{R}_B$, and its derivatives, $\underline{R}_X$, $\underline{R}_\alpha$ and $\underline{R}_{X\alpha}$, known at each gridpoint, their values at any arbitrary point (X,α) on the grid can easily be obtained by reinterpolation, again using cubic-Hermite splines. Lastly, (X,α) are specified to form the input needed for the evaluation of the integral in (V-7). That is,

$$\int_{S_{B_j}} \frac{\partial G}{\partial n}\, dS_j = \Delta X_j\, \Delta \alpha_j \sum_{k=1}^{N} w_k \frac{\partial G}{\partial n}(X_k, \alpha_k) \qquad \text{(V-9)}$$

where w_k is the weighting factor and (X_k, α_k) are the nodes of the Gauss quadrature formula. The resulting system of linear equations is solved for σ by Gauss-Seidel iteration. With σ known, the surface and field point velocities are readily calculated, again using Gauss quadrature, from

$$\underline{V}_p = U_o \hat{i} + \int_{S_B} \sigma \nabla G\, dS$$

and the pressure is obtained from the Bernoulli equation

$$C_p = 1 - (\underline{V}_p \cdot \underline{V}_p)/U_o^2$$

where $C_p = p-p_o/\frac{1}{2}\rho U_o^2$ is the pressure coefficient.

B. Displacement Body. As explained previously, in the interaction calculation, the body boundary condition (V-3) is applied not on the actual-body surface but on the displacement-body surface. In terms of the present nonorthogonal curvilinear coordinate system the displacement body is defined by

$$\int_{A_{\delta *}} \underline{V_p} \cdot \underline{dA} = \int_{A_\delta} (\underline{V_p} - \underline{V}) \cdot \underline{dA} \qquad \text{(V-10)}$$

where $\underline{V_p}$ is the velocity vector of the outer potential flow analytically continued into the viscous-flow region, $\underline{V}$ is the viscous-flow velocity vector, $A_{\delta *}$ and A_δ are the cross-sectional areas between the actual-body surface and the displacement-body surface and the boundary-layer surface respectively, and $\underline{dA} = \hat{e}_2 \times \hat{e}_3 \, h_2 h_3 dydz$. In evaluating (V-10), for axisymmetric flow applications, the approximation was used that $\underline{V_p}$ is constant across $A_\delta *$, i.e.

$$\int_o^{\delta^*} h_2 h_3 \, dy = \frac{1}{\underline{V_p}(\delta^*)\cdot\hat{i}} \int_o^{\delta} (\underline{V_p} - \underline{V}) \cdot \hat{i} \, h_2 h_3 \, dy \qquad \text{(V-11)}$$

This approximation can be removed by analytically continuing the displacement-body potential-flow solution inside the displacement body; however, this requires an inviscid-flow solution method based on the symmetric form of Green's theorem (i.e. source and dipole distributions) which is continuous across the body surface whereas the present source-panel method is not. Lastly, some comments should be made with regard to the evaluation of (V-10) for three-dimensional flow applications. A straightforward but approximate

procedure is to again assume $\underline{V}_p$ is constant across $A_{\delta *}$ and make the additional approximation that $\delta^*(x,z)$ can be defined in terms of a local flux balance, i.e.

$$\int_0^{\delta^*} h_2 h_3 dy = \frac{1}{\int_{z_1}^{z_2} \underline{V}_p(\delta^*)\cdot\hat{i}dz} \int_{z_1}^{z_2} \int_0^{\delta} (\underline{V}_p - \underline{V})\cdot\hat{i} h_2 h_3 dy dz$$

Landweber (1986) has pointed out that such an approximation does not guarantee that δ^* is a stream surface of the continued potential flow and suggests an alternative method for evaluating (V-10) subject to an explicit condition that δ^* is a stream surface.

C. Equivalent-Source Method. For the flat-plate boundary-layer and wake test case (see Section VI.A.) the displacement effect of the boundary layer was included through the use of the equivalent-source method. In this case, such a method is acceptable since the body surface is flat. A two-dimensional potential function is defined by

$$\Phi = U_o X + \int_{X_1}^{X_2} \sigma G dX \qquad \text{(V-12)}$$

where

$$G = \ell n R$$

$$\sigma = \frac{d}{dx}(U_e \delta^*)$$

VI. APPLICATIONS FOR TWO-DIMENSIONAL AND AXISYMMETRIC FLOWS

Results are now presented from the application of the computational procedures described in Sections II - V for two-dimensional and axisymmetric flows. The two-dimensional-flow application is a simple flat-plate boundary layer and wake. Results are presented for both laminar and turbulent flow. For the axisymmetric-flow applications, results are presented for turbulent flow only, and for two of the family of afterbodies for which experimental data have been obtained by Huang and associates at DTNSRDC. The two afterbodies investigated represent examples of medium and strong viscous-inviscid interaction. In the discussions to follow, all coordinates are nondimensionalized using the body length L, with X = 0 at the body leading edge (nose), and velocities and pressure are normalized using the free-stream velocity U_o and the fluid density.

A. Flat Plate Boundary Layer and Wake. The simple case of a flat-plate boundary layer and wake has been the subject of many previous investigations. For laminar flow, solutions have been obtained using a variety of approaches: thin-boundary-layer; thin-boundary-layer including viscous-inviscid interaction; triple-deck theory; partially-parabolic Navier-Stokes; and Navier-Stokes. Recently, Chen and Patel (1986) have performed a comprehensive investigation in order to establish the capabilities of their partially-parabolic method, extended for complete Navier-Stokes solutions, by comparing their results with the solutions obtained using alternative approaches and systematically studying the influence of the boundary conditions, the size of the solution domain, and the grid resolution. A direct comparison will be made between results using the present approach and that of Chen and Patel. For turbulent flow, results have also been obtained using a variety of approaches;

however, in this case, a direct comparison is made more difficult by the fact that the results additionally depend upon the turbulence model utilized and the numerical details of its implementation. Patel and Chen (1986) have also performed turbulent flow calculations using the complete Reynolds equations and the k-ϵ turbulence model with two different treatments of the flow close to the wall: wall-function approach; and an eddy-viscosity distribution. The present turbulent-flow results are compared with both the results of Patel and Chen and the near-wake experimental data of Pot (1979).

1. Laminar Flow. The laminar-flow calculations were performed for a plate Reynolds number $Rn = \frac{U_\infty L}{\nu} = 10^5$ (where L is the plate length) which is the value used by Chen and Patel and others. Typical large- and small-domain grids used for the calculations are shown in figures 5 and 6, respectively. Referring to figures 5 and 1 for notation: the number of axial grid points is 40; the number of transverse grid points is 15; the inlet boundary S_I is at x_u=.4; the exit boundary S_E is at x_d=2.5; and the outer boundary S_o is at y_o=12. Referring to figures 6 and 1 for notation: the number of axial grid points is 40; the number of transverse grid points is 11; the inlet and exit boundaries have the same values as the large-domain grid; and the outer boundary is at y_o=1.26 δ where $\delta(x)$ is the boundary-layer thickness which was specified based on the Blasius solution. The y-direction grid expansion for the grids shown was specified based on the turbulent flow conditions since these grids were actually used for the turbulent-flow calculations to be discussed subsequently. The y-direction expansion for the laminar-flow calculations was more gradual. The Blasius solution was used to specify the initial streamwise profile and a zero-gradient condition was used for the normal velocity component on the inlet boundary in both the large-domain and small-

domain calculations. All other boundary conditions are prescribed as discussed in Section IV.D.

Figure 7 shows the pressure distribution on the surface of the plate and along the wake centerline. Results are shown from the present methods both for a large solution domain and a small solution domain, including viscous-inviscid interaction (interaction solution). Also shown for comparison are results from the Navier-Stokes calculations of Chen and Patel (1986), triple-deck theory (Melnik and Chow, 1975), and interactive thin-boundary-layer theory (Veldman, 1979). It is seen that the agreement between both the present solutions and the solution of Chen and Patel for $x_u = .5421$ is excellent. The reason that the partially parabolic and Navier-Stokes solutions are in such a close agreement is that, at this high Rn, the influence of streamwise diffusion is important only in a region very close to the plate trailing edge and not resolvable with the present grid. In fact, the interactive thin-boundary-layer results are also in good agreement, indicating that, for this very simple trailing-edge flow, the influence of the pressure variation within the boundary layer is also small. As explained by Chen and Patel, the solution is very dependent on the location of the upstream boundary. Thus, their solution for $x_u = .1349$, which has also been included on figure 7 for comparison, shows large differences. Note that the triple-deck solution for which $x_u = .1$ is consistent with the solution of Chen and Patel for $x_u = .1349$ on the plate but not in the wake. In the wake, the triple-deck solution is more consistent with the other solutions obtained using larger values of $x_u \sim .5$. Apparently, this is due to the treatment of the downstream boundary in the triple-deck solution which is matched to the 1/3 power law solution at too great a distance.

The skin-friction coefficient and the wake-centerline velocity are shown in figures 8 and 9, respectively. As seen from figure 8, all the solutions for the skin-friction coefficient are in close agreement and show about the same deviation from the Blasius solution. This indicates that the prediction of the skin-friction coefficient is not very sensitive to the details of the numerical procedures employed. As seen from figure 9, the differences between the solutions for the wake-centerline velocity are also not large except for the triple-deck solution which shows larger values than the the other solutions for $X > 1.3$ for the reason discussed previously. The close agreement among all but the triple-deck solutions for the wake-centerline velocity indicates that the prediction of the wake properties is not sensitive to upstream conditions beyond $x_u \sim .5$.

Figures 10 and 11 show the converged values for the displacement thickness and edge velocity, respectively, used in the interaction solution. Referring to figures 10 and 11, it is seen that the magnitude of the viscous-inviscid interaction for the flat-plate boundary layer and wake is weak; however, its features are characteristic of more complex trailing-edge flows. Note that for the flat plate test case the equivalent-source method is used (see Section V.C.) to represent the displacement effect of the boundary layer in the interaction solution.

The interaction calculations were started with free-stream edge conditions ($U_e = 1.$, and $p_e = 0.$) which were subsequently updated after each global iteration. The large-domain solution converged in 60 global iterations and the interaction solution in 40. In both solutions, the relaxation factors used were $(\alpha, \alpha_p, \alpha\hat{}_p) = (.5, .7, 1.)$. Also, both solutions required about 5 minutes cpu on a Prime 9950 minicomputer.

2. Turbulent Flow. The turbulent flow calculations were performed for a plate Reynolds number $Rn = 1.2 \times 10^6$ which results in a momentum-thickness Reynolds number at the plate trailing edge of $Rn_\theta = 3000$. This corresponds fairly closely to the experimental condition of the wake measurements of Pot (1979) for which $Rn_\theta = 2940$. The large- and small-domain grids used in the calculations are shown in figures 5 and 6 respectively. Referring to figures 5 and 1 for notation: the number of axial grid points is 56; the number of transverse grid points is 15; the inlet boundary S_I is at $x_u = .4$; the exit boundary S_E is at $x_d = 16.25$; the outer boundary S_o is at $y_o = 1$; and the first grid point off the body surface was located at $y^+ \sim 40$. Referring to figures 6 and 1 for notation: the number of axial grid points is 56; the number of transverse grid points is 15; the inlet and exit boundaries as well as the first grid point off the body surface have the same values as the large-domain grid; and the outer boundary is at $y_o = 1.26\,\delta$ for $X \leq 1.$ and varied linearly to $y_o = .25$ at the exit.

Figures 12 and 13 show the pressure distribution on the surface of the plate and along the wake centerline and the skin-friction coefficient respectively. It is seen that the large-domain and interaction solutions are in excellent agreement. By comparing figures 7 and 12 it is seen that, for turbulent flow, the extent of the region of pressure variation is reduced for the boundary-layer region upstream of the trailing edge and increased for the wake region downstream of the trailing edge. Also, the pressure recovery in the wake occurs with a favorable pressure gradient for laminar flow and an adverse pressure gradient for turbulent flow. Also shown for comparison on figures 12 and 13 are the results from Patel and Chen (1986) using the k-ϵ turbulence model with wall functions. Note that their results are for a

slightly different Reynolds number (Rn = 2.48 x 10^6) and that their grid resolution was similar to the present one except the first grid point off the body surface was located at y+~100 . The comparison between the pressure distributions is excellent for X >.9. For X <.9 the solution of Patel and Chen shows lower pressures. This is due to the initial conditions used in their calculations. In order to compare skin-friction coefficients the results of Patel and Chen were Rn scaled. Referring to figure 13, it is seen that although the trends are identical their result is slightly lower than the present one. This is due to the larger value of y+ for the first grid point off the body surface used by Patel and Chen.

Figure 14 shows the usual overall parameters for describing the near wake, the half-width b, the centerline velocity defect $w_o = 1-U_{CL}$, and also the shape parameter $H = \delta^*/\theta$. Also shown for comparison is Pot's experimental data and the results of Patel and Chen for w_o. It is seen that the agreement between the large-domain and interaction solutions for w_o and H is very good; however, both solutions deviate from the experimental data for $100 \leq X/\theta \leq 600$. A similar deviation from the experimental data is seen for the large-domain solution for b. The interaction solution for b agrees with the large-domain solution only in the very near wake and elsewhere shows larger values. In general, the calculations show larger values for b, w_o and H indicating a thicker wake region. The agreement between the present results for w_o and Patel and Chen is quite good with the differences being attributable to the different values of y+ used for the first grid point off the body surface. Patel and Scheuerer (1982) have compared results from wake calculations using thin-boundary-layer equations and the k-ϵ turbulence model with these same experimental data. Their results show better agreement in the near

wake ($X/\theta < 350$) but poorer agreement in the far wake. The differences between the partially-parabolic calculations and the results from thin-boundary-layer theory are consistent; that is, the influence of the adverse pressure gradient in the near wake results in a thicker wake region in the partially-parabolic solutions. The reason for the poorer agreement of the partially-parabolic solution than the thin-boundary-layer solution with the experimental data in the near wake is not known. The reason for the discrepancy between the large-domain and interaction solutions for b is due to the width of the interaction solution domain in the wake (see figure 6). Further calculations using a larger growth rate for δ in the wake region indicate a closer agreement of b with the large-domain solution.

Figures 15 and 16 show the wake momentum thickness and centerline eddy viscosity respectively. Referring to figure 15, it is seen that the present results from both the large-domain and interaction solutions indicate larger values of θ than the experimental data. This is probably due to the difference in the trailing edge values of Rn_θ . Referring to figure 16, it is seen that the present results indicate a larger value for ν_t than the calculations of Patel and Chen. From the results for ν_t and θ it was determined that the asymptotic value of $\nu_t/U_o\theta$ for the large-domain solution is .0333 and for the interaction solution is .0406. The value from the experimental data for the range $400 \leq X/\theta \leq 1000$ is .035. Patel and Scheuerer and Patel and Chen obtained values of .024 and .022 respectively. Figures 17 and 18 show the asymptotic (velocity-defect $w = 1-U$ and stress $\tau = -\overline{uv}$) profiles for the large-domain and interaction solutions. Also shown for comparison is Pot's experimental data. Both solutions for the velocity-defect profile show excellent agreement with the experimental data. Both solutions for the stress

profile are in agreement and show a peak value of about .029. The experimental stress profile indicates larger values with a peak value of about .051. Patel and Scheuerer and Patel and Chen also obtained lower values for the stress profile than the experimental data. Their peak values are about .033 and .03 respectively. One of the conclusions of Patel and Scheuerer is that the k-ε model does not adequately predict the observed asymptotic behavior. This was confirmed in the present investigation.

Figures 19 and 20 show the converged values for the displacement thickness and edge velocity, respectively, predicted in the interaction solution. By comparing these figures with figures 10 and 11 it is seen that the influence of turbulence is to reduce the extent of the viscous-inviscid interaction.

The interaction calculations were started with edge conditions (U_e = 1, p_e = 0.) which were subsequently updated after each global iteration. The large-domain solution converged in 40 global iterations and the interaction solution in 25. In both solutions, the relaxation factors used were $(\alpha, \alpha_p, \alpha_p^\wedge)$ = (.5, .45, 1.). Also, both solutions required about 5 minutes of cpu on a Prime 9950 minicomputer.

B. Axisymmetric Bodies. For axisymmetric flow, calculations have been performed for DTNSRDC afterbodies 1 (Huang et al., 1978) and 5 (Huang et al., 1980). Afterbody 1 is the parent form of a family of three-dimensional bodies with elliptical cross-sections (Huang et al., 1983). Referring to figure 21, which shows a comparison of afterbodies 1 and 5, it is seen that both bodies have similar length/diameter ratios but very different tail forms. In particular, afterbody 5 (L_s/D = 2.04) is blunter than afterbody 1 (L_s/D = 4.3) and has greater curvature with an inflection point. Note that afterbody 5 is

almost as blunt as afterbody 3 ($L_s/D = 1.5$) which exhibited a small region of flow separation near the tail ($.92 \leq X \leq .97$) in the experiments. As will be discussed next, these differences in body geometry result in both a larger extent and magnitude of viscous-inviscid interaction for afterbody 5 than afterbody 1.

The calculations were performed for afterbody 1 for a body-length Reynolds number $Rn = 6.6 \times 10^6$ which corresponds to the experimental condition. The large- and small-domain grids used in the calculations are shown in figure 22 and 23 respectively. Referring to figures 22 and 1 for notation: the number of axial grid points is 60; the number of transverse grid points is 19; the inlet boundary S_I is at $x_u = .5$; the exit boundary S_E is at $x_d = 16.25$; the outer boundary is at $y_o = .8137$; and the first grid point off the body surface was located in the range $100 \leq y^+ \leq 160$. Referring to figure 23 and 1 for notation; the number of axial grid points is 60; the number of transverse grid points is 11; the inlet and exit boundaries have the same values as the large-domain grid; the outer boundary is at $y_o = \delta$ where $\delta(x)$ is the boundary-layer thickness which was specified based on the experimental results; and the first grid point off the surface was located in the range $80 \leq y^+ \leq 130$. The y-direction grid expansion was specified such that the first two grid nodes are within the log-law region. Simple turbulent flat-plate profiles were used to specify the initial conditions in both the large and small domain solutions. All other boundary conditions are prescribed as discussed in Section IV.D.

Figure 24 shows the pressure distribution on the surface of the body and along the wake centerline. Results are shown from the present methods both for a large solution domain and a small solution domain, including viscous-in-

viscid interaction. Also shown for comparison are the experimental results and the inviscid-flow solution without interaction. It is seen that both of the present methods are in good agreement with the experimental results. Actually, the interaction solution appears to be slightly in better agreement. This is probably due to the influence of the initial conditions which, in the case of the interaction solution, include a more proper matching with the external flow. Also, the grid resolution within the boundary-layer region is better for the interaction solution. Note the large gradients in pressure exhibited in both solutions in the immediate vicinity of the trailing edge (X = 1). A part of this behavior is no doubt a result of the rapid change in curvature of the streamlines associated with the closing of the body and transition into the wake. However, it was also found that the solution in this vicinity is sensitive to the grid and detailed numerical treatments at the trailing edge. A comparison of the present results with the inviscid-flow solution without interaction provides one indication of the magnitude of the viscous-inviscid interaction (47% reduction in the maximum value of C_p at x = .975). This comparison is made somewhat difficult by the inaccuracy of the inviscid-flow solution very near the trailing edge. In the present inviscid-flow method, as is the case with most other singularity-distribution methods, the solutions are not accurate in regions where the angles between adjacent panels are small. This inaccuracy is well known and was not removed since the inviscid-flow solution without interaction is not used in the present viscous-inviscid interaction approach.

Figure 25 shows the wall-shear velocity U_τ and is of similar format as the previous one. The experimental values were obtained from Preston tube measurements. In this case, the comparison between the calculations and the

experimental values is not quite as good. For $.9 \lesssim X \lesssim 1.$ the calculations show larger values than the experiment. This discrepancy is attributed to the well known deficiencies of the k-ϵ turbulence model for thick-boundary-layer flow as will be discussed further subsequently. Also, the large-domain solution predicts slightly higher values for U_τ than the interaction solution for $X \lesssim .9$. This is no doubt due to the influence of the initial conditions.

Figure 26 shows the wake-centerline velocity U_{CL} and is of similar format as the previous ones. The agreement between both the calculation methods and the limited experimental data is again quite good; however, the calculations show a slower recovery than that indicated by the limited near-wake experimental data. The largest differences between the large domain and interaction solutions are in the intermediate-wake region $2. \lesssim X \lesssim 5.$ and are consistent with differences in pressure as shown in figure 24.

Figures 27 and 28 show the convergence history (pressure distribution on the surface of the body and along the wake centerline and the displacement thickness) for the large-domain and interaction solutions respectively. Values are shown for every five global iterations. The planar definition of displacement thickness has been used for the large-domain solution. The interaction calculations were started with free-stream edge conditions (U_e = 1., p_e = 0.). After twenty iterations, the edge conditions were updated using the latest value of displacement thickness. Subsequently, the edge conditions were updated every five global iterations until convergence was achieved. A comparison of figures 27 and 28 shows that the convergence characteristics of the two solutions are quite different. The large-domain solution converges monotonically in 50 iterations. The interaction solutions converge with oscillations in 40 iterations. Basically the interaction solution converges

in two stages. The first stage is with free-stream edge conditions and leads to an underprediction of both C_p and δ^*. The second stage is with the displacement-body edge conditions and the solution converges quite rapidly. Figure 29 shows the iteration history of the edge velocity. The small changes in the displacement-body shape after 20 global iterations lead to imperceptible changes in U_e. Figure 30 shows a comparison between the converged edge pressure obtained from the displacement body with that obtained from the actual body, and the actual body including the equivalent-source method to represent the displacement effect of the boundary layer. It is seen that the displacement-body edge-pressure maximum is shifted upstream as compared to the actual-body edge pressure which results in greater edge pressures for $X \lesssim .95$ and lower values for $X \gtrsim .95$. Note that the equivalent-source method edge pressure shows the correct tendency but with only a minimal modification to the actual-body result. This clearly demonstrates, as was discussed previously, that the equivalent-source method is inaccurate for bodies with noncusped trailing edges. Figure 31 shows a comparison of the experimental and interaction solution displacement thickness. The calculated values are slightly below the experimental values.

Lastly, for afterbody 1, figure 32 shows the solution profiles (U,V,p,k,ε) for a number of X-stations between the inlet and the outlet. Note that in these figures the radial coordinate has been defined as $Y = \frac{Y-R_o}{R_{max}}$ where $R_o(x)$ is the local body radius and R_{max} is the maximum body radius. Wherever possible, a comparison has been made with the experimental data. In general the agreement between the large-domain and interaction solutions is very good and consistent with the previous discussions. Also, both solutions show good agreement with the experimental data. However, note the fact that

while both solutions indicate similar transverse pressure gradients p_y there is a systematic difference in pressure magnitude. The large-domain solution predicts lower pressures than the interaction solution which in general shows better agreement with the experimental data. The reason for this difference is not known. It may be related to the outer boundary conditions in the large-domain solution since its characteristics are similar to a blockage effect. The principal differences between the calculations and the experiments is that the calculations tend to overpredict the velocity and turbulent kinetic-energy profiles. This result is due to deficiencies of the standard turbulence model which is known to overpredict the level of turbulence in thick boundary layers, presumably caused by the use of an isotropic eddy viscosity and the neglection of curvature effects. Another cause may be the use of wall functions. Note the significant variation in pressure across the boundary layer in the vicinity of the trailing edge $.95 \lesssim X \leq 1.05$ indicating the necessity of including such effects in modeling the present flow.

The calculations were performed for afterbody 5 for a body-length Reynolds number $Rn = 9.3 \times 10^6$, which corresponds to the experimental condition. The large- and small-domain grids used in the calculations are shown in figures 33 and 34 respectively. Referring to figures 33 and 1 for notation: the number of axial grid points is 60; the number of transverse grid points is 19; the inlet boundary S_I is at $x_u = .5$; the exit boundary S_E is at $x_d = 16.25$; the outer boundary is at $y_o = .8137$; and the first grid point off the body surface was located in the range $120 \leq y^+ \leq 200$. Referring to figures 34 and 1 for notation: the number of axial grid points is 60; the number of transverse grid points is 11; the inlet and exit boundaries have the same values as the large-domain grid; the outer boundary is at $y_o = \delta$ where $\delta(x)$ is the

boundary layer thickness which was specified based on the experimental results; and the first grid point off the body surface was located in the range $100 \leq y+ \leq 160$. The y-direction grid expansion was specified such that the first two grid points are within the log-law region. Simple turbulent flat-plate profiles were used again to specify the initial conditions in both the large- and small-domain solutions. All other boundary conditions are prescribed as discussed in Section IV. D. In the discussion to follow, all figures for afterbody 5 are of a similar format as that described earlier for afterbody 1.

Figure 35 shows the pressure distribution on the surface of the body and along the wake centerline. Comparing figures 35 and 24, it is seen that the pressure distribution in the tail region of afterbody 5 shows even more radical variations than on afterbody 1. This includes both a lower minimum pressure upstream of the trailing edge and a higher maximum pressure at the trailing edge. It is seen that both the large-domain and interaction solutions are in good agreement with each other and the experimental data. The level of agreement is about the same as that obtained for afterbody 1. The magnitude of the viscous-inviscid interaction is larger for afterbody 5 than for afterbody 1 (50% reduction in the maximum value of C_p at X = .975).

Figure 36 shows the wall shear velocity U_τ and figure 37 the wake centerline velocity U_{CL}. The level of agreement is not as good as that obtained for afterbody 1. Figure 38 shows the converged value of displacement thickness and figure 39 the resulting edge velocity. A comparison of figures 38 and 28 shows that the viscous-inviscid interaction is larger for afterbody 5 than afterbody 1, resulting in an increased displacement thickness for afterbody 5. The displacement thickness is also shown in figure 40 where it is compared

with the experimental data. The agreement is very good. Lastly, the detailed solution profiles at various X-stations are shown in figure 41. The results are similar and consistent with those described earlier and do not require further elaboration. However, note the increase in pressure variation across the boundary layer as compared to afterbody 1, again indicating the larger viscous-inviscid interaction and thick-boundary-layer effects for afterbody 5 than 1.

For both afterbodies 1 and 5, the large-domain solutions converged in 50 global iterations and the interaction solutions in 40. For afterbody 1, the relaxation factors were $(\alpha, \alpha_p, \alpha_p^\wedge)$ = (1., .2-.5, 1.) for the large-domain solution and $(\alpha, \alpha_p, \alpha_p^\wedge)$ = (.6, .2-.5, 1.) for the interaction solution. For afterbody 5, the relaxation factors were $(\alpha, \alpha_p, \alpha_p^\wedge)$ = (.6, .2-.5,1.) for the large-domain solution and $(\alpha, \alpha_p, \alpha_p^\wedge)$ = (.5, .2-.5, 1.) for the interaction solution. In all cases, in the wake α_p = .05 for IT < 10 and α_p = .1 - .2 for IT $\geq$ 10. Also, in all cases, the solutions required about 10 minutes of cpu on a Prime 9950 minicomputer.

VII. CONCLUDING REMARKS

It has been shown that trailing-edge flows with thick boundary layers can be modeled using viscous-inviscid interaction procedures if all the important aspects of the flow, namely the pressure variation across the boundary layer and the displacement effect of the viscous flow on the external inviscid flow, are taken into account. The validation of the present interaction procedures has been accomplished by comparing the results for two-dimensional and axisymmetric flows with large-domain solutions, in which the entire zone of viscous-inviscid interaction is captured, obtained using the same numerical proced-

ures. Also, a direct comparison has been made with other methods, including the finite-analytic method of Chen and Patel (1985), and with available experimental data.

In general, the comparison between the present interaction and large-domain solutions is very satisfactory for all the cases investigated. Some small differences are evident, as might be expected. The direct comparison between the present methods and other methods and also the experimental data shows excellent agreement. Of particular interest is the comparison with the method of Chen and Patel; since, their method and the present ones have certain features in common and are quite different in other respects. Specifically, the velocity-pressure coupling procedures as well as the turbulence model are identical; however, the coordinate systems used in solving the governing equations, the discretization procedures employed, as well as other numerical treatments are very different. Chen and Patel (1985) and Patel and Chen (1985) also present results for afterbodies 1 and 5, including a comparison with the same experimental data. The level of agreement is very similar to that shown with the present methods. Thus, it would seem that the most critical aspect of computational methods for thick-boundary-layer trailing-edge flows is the velocity-pressure coupling rather than the discretization procedure (finite analytic vs. finite difference) and other numerical procedures employed.

As to the relative advantages of the interaction vs. large-domain solutions, the latter does not require any approximations with regard to the viscous-inviscid interaction as does the former; however, the interaction solution was shown to be just as accurate as the large-domain solution, indicating that the present viscous-inviscid interaction procedures can capture

this important influence on the flow. With regard to computational efficiency, when the equivalent-source method is used the interaction solution is more efficient; however, when the displacement-body method is used, which is the case for bodies of interest, then the large-domain solution is more efficient. This is because of the additional computational effort in calculating the inviscid flow. The prescription of the inviscid flow at the boundary-layer edge does speed up the convergence rate of the viscous-flow solution but not enough to offset the increase pointed out above. Note that we have used a three-dimensional source-panel method for the inviscid-flow solution. For three-dimensional applications, it is expected that the interactive solution will be more attractive since the saving in computational effort in the viscous-flow solution will have a more substantial effect on the overall computational efficiency. Calculations for three-dimensional body geometries are now in progress and will be reported on in the future. Lastly, it should be mentioned that, besides the academic interest in the nature of an interaction solution, it also has a practical value. For example, the modification of the external inviscid-flow solution due to the thick boundary layer and wake is obtained as part of the solution, and for applications to ship boundary layers, it is readily extendable to nonzero-Froude-number calculations.

REFERENCES

Abdelmeguid, A.M. Markatos, N.C., Muraoka, K. and Spalding, D.B., (1979), "A Comparison Between the Parabolic and Partially-Parabolic Solution Procedures for Three-Dimensional Turbulent Flows Around Ship's Hulls", Appl. Math. Modelling, Vol. 3, p. 249.

Anderson, D.A., Tannehill, J.C., and Pletcher, R.H., (1984), "Computational Fluid Mechanics and Heat Transfer", Hemisphere Publishing Corporation, New York, N.Y.

Brune, G.W., Rubbert, P.E., and Forester, C.K., (1975), "The Analysis of Flow Fields with Separation by Numerical Matching", AGARD Sym. on Flow Separation, Gottingen.

Cebeci, T., Chang, K.C., and Kaups, K., (1978), "A General Method for Calculating Three-Dimensional Laminar and Turbulent Boundary Layers on Ship Hulls", Mcdonnel Douglas Corp. Report No. MDCJ7998.

Chen, H.C. and Patel, V.C., (1985), "Calculation of Trailing Edge, Stern and Wake Flows by a Time-Marching Solution of the Partially-Parabolic Equations", Iowa Institute of Hydraulic Research, University of Iowa, IIHR Report 285.

Chen, H.C. and Patel, V.C., (1986), "Laminar Flow at the Trailing Edge of a Flat Plate", submitted to AIAA Journal.

Dietz, M.S., (1980), "An Axisymmetric, Strong Interaction Procedure to Include Large, Normal Pressure Gradients", Applied Research Lab., Penn. State Univ., Tech. Memo. 80-160.

Hoekstra, M., and Raven, H.C., (1985), "Ship Boundary Layer and Wake Calculation with a Parabolised Navier-Stokes Solution System", 4th Int. Conf. on Num. Ship Hydrodynamics, Washington, D.C.

Huang, T.T., Santelli, W., and Belt, G., (1978), "Stern Boundary-Layer Flow on Axisymmetric Bodies", 12th Sym. on Naval Hydrodynamics, Washington, D.C.

Huang, T.T., Groves, N.C., and Belt, G., (1980), "Boundary-Layer Flow on an Axisymmetric Body with an Inflected Stern", DTNSRDC Rept. 80/064.

Huang, T.T., Groves, N.C., and Belt, G., (1983), "Stern Boundary-Layer Flow on Two Three-Dimensional Bodies Having Elliptical Transverse Cross-Sections", 2nd Sym. on Numerical and Physical Aspects of Aerodynamic Flows, Long Beach, CA.

Landweber, L., (1978), "On Irrotational Flows Equivalent to the Boundary Layer and Wake", David Taylor Naval Ship Research and Development Center Report No. DTNSRDC-78/111.

Landweber, L., (1986), private communication.

Lee, Y.T., (1978), "Thick Axisymmetric Turbulent Boundary Layer and Wake of a Low-Drag Body", Ph.D. Thesis, The University of Iowa.

Lighthill, M.J., (1958), "On Displacement Thickness", J. of Fluid Mechanics, Vol. 4, pp. 383-392.

Marlin, M.R., Rosten, H.I., Spalding, D.B., and Tatchell, D.G., (1985), "Application of PHOENICS to Flow Around Ship's Hulls", Proc. 2nd Int. Sym. Ship Visc. Resistance, SSPA, Goteburg, Sweden, paper 11.

Markatos, N.C., (1984), "The Computation of Thick Axisymmetric Boundary Layers and Wakes around Bodies of Revolution", Proc. Inst. Mech. Engrs., London, Vol. 198, pp. 51-62.

Markatos, N.C., Marlin, M.R. and Tatchell, D.G., (1980), "Computer Analysis of Three-Dimensional Turbulent Flows Around Ship's Hulls", Proc. Inst. Mech. Engrs., London, Vol. 194, pp. 239-248.

McDonald, H. and Briley, W.R., (1983), "A Survey of Recent Work on Interacted Boundary Layer Theory for Flow with Separation", Proc. 2nd Sym. Numerical & Physical Aspects of Aerodynamic Flows, Long Beach, CA.

Mehta, V., Chang, K.C., and Cebeci, T.C., (1985), "Relative Advantages of Thin-Layer Navier-Stokes and Interactive Boundary Layer Procedures", NASATM-86778.

Melnik, R.E. and Chow, R., (1975), "Asymtotic Theory of Two-Dimensional Trailing Edge Flows", Grumman Research Dept., Rept RE-510J.

Moore, F.K., (1953), "Displacement Effect of a Three-Dimensional Boundary Layer", NACA Rep. No. 1124.

Muraoka, K., (1982), "Calculation of Viscous Flow around Ships with Parabolic and Partially Parabolic Flow Solution Procedure", Trans. West Japan Soc. Naval Arch., Vol. 63, pp. 13-29.

Muraoka, K., (1980), "Calculation of Thick Boundary Layer and Wake of Ships by a Partially Parabolic Method", Proc. 13th ONR Sym. Naval Hydrodynamics, Tokyo, Shipbuilding Res. Assoc, Japan, pp. 601-616.

Nash, J.F., and Patel, V.C., (1972), "Three Dimensional Turbulent Boundary Layers", SBC Tech Books, Atlanta.

Patankar, S.V., (1980), "Numerical Heat Transfer and Fluid Flow", McGraw-Hill.

Patel, V.C., (1982), "Some Aspects of Thick Three-Dimensional Boundary Layers", Proc. 14th ONR Sym. Naval Hydrodynamics, Ann Arbor, MI, pp. 999-1040.

Patel, V.C., and Scheuerer, G., (1982), "Calculation of Two-Dimensional Near and Far Wakes", AIAA Journal, Vol. 20, pp. 900-907.

Patel, V.C., and Chen, H.C., (1985), "The Flow Over the Tail and in the Wake of Axisymmetric Bodies a Review of the State of the Art", Proc. Osaka Int. Colloq. on Ship Visc. Flow, pp. 468-495.

Patel, V.C., and Chen, H.C., (1986), "Turbulent Wake of a Flat Plate", Submitted to AIAA Journal.

Piquet, J., and Visonneau, M., (1985), "Study of 3-D Ship Boundary Layers by Means of an Inverse Method", 4th Int. Conf. on Num. Ship Hydrodynamics, Washington, D.C.

Pot, P.J., (1979), "Measurement in a 2D Wake Merging into a Boundary Layer", NLR, The Netherlands, Rept. TR 19063 U.

Richmond, M.C., Chen, H.C., and Patel, V.C., (1986), "Equations of Laminar and Turbulent Flows in General Curvilinear Coordinates", Iowa Institute of Hydraulic Research, University of Iowa, IIHR Report 300.

Rouse, H. et al., (1976), "Advanced Mechanics of Fluids", Robert E. Krieger Publishing Company, Huntington, New York.

Tzabiras, G.D., (1983), "On a Method for the Calculation of Turbulent Flow at the Stern of a Double Model", Proc. 12th SMSSH Seminar, Varna, Bulgaria, p. 39-41.

Tzabiras, G.D. and Loukakis, T.A., (1983), "A Method for Predicting the Flow Around the Stern of Double Ship Hulls", Nat. Tech. Uni., Athens, Unpublished Report.

Veldman, A.E.P., (1979), "A Numerical Method for the Calculation of Laminar, Incompressible Boundary Layers with Strong Viscous-Inviscid Interaction", NLR, The Netherlands, Rept. TR 79023 U.

von Kerczek, C.H., Stern, F., Scragg, C.A., and Sandberg, W., (1983), "The Use of Theoretical and Computational Methods for Evaluating the Resistance of Appended Destroyer Hull Forms", SNAME Chesapeake Section Paper.

Weatherburn, C.E., (1926), "On Triple Systems of Surfaces and Nonorthogonal Curvilinear Coordinates", Proc. Roy. Soc., Edinburgh, Vol. 46.

Zhou, L-D., (1982), "A Streamline-Iteration Method for Calculating Turbulent Flow Around the Stern of a Body of Revolution and its Wake", Proc. 14th ONR sym. Naval Hydrodynamics, Ann Arbor, MI, pp. 1041-1069.

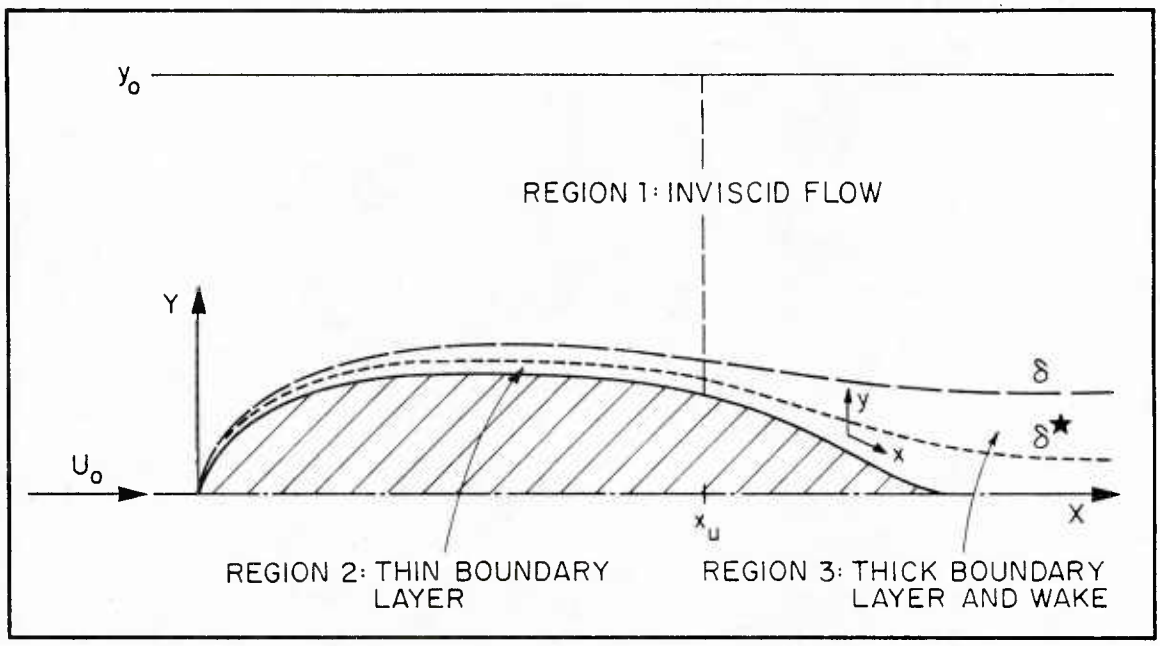

Fig. 1a (X,Y) Plane

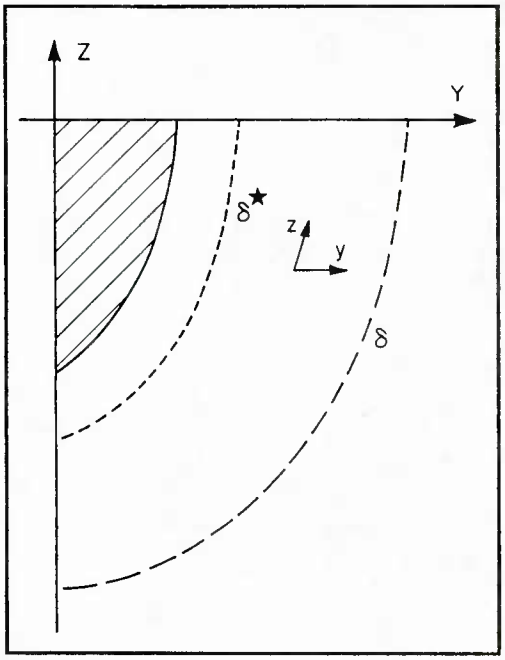

Fig. 1b (Y,Z) Plane

Figure 1. Definition Sketch of Flow-Field Regions

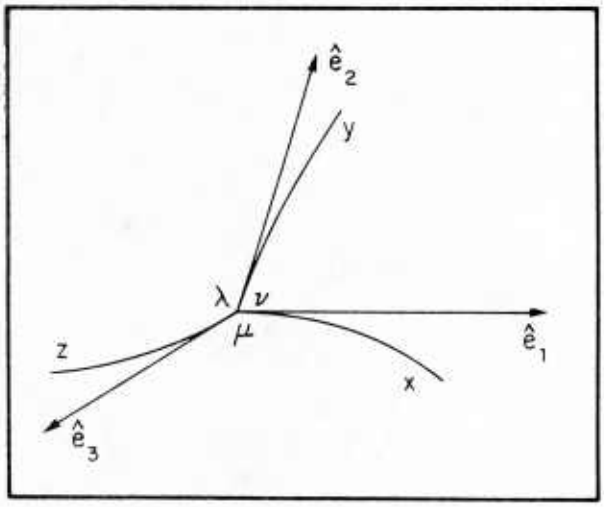

Figure 2. Nonorthogonal Curvilinear Coordinates

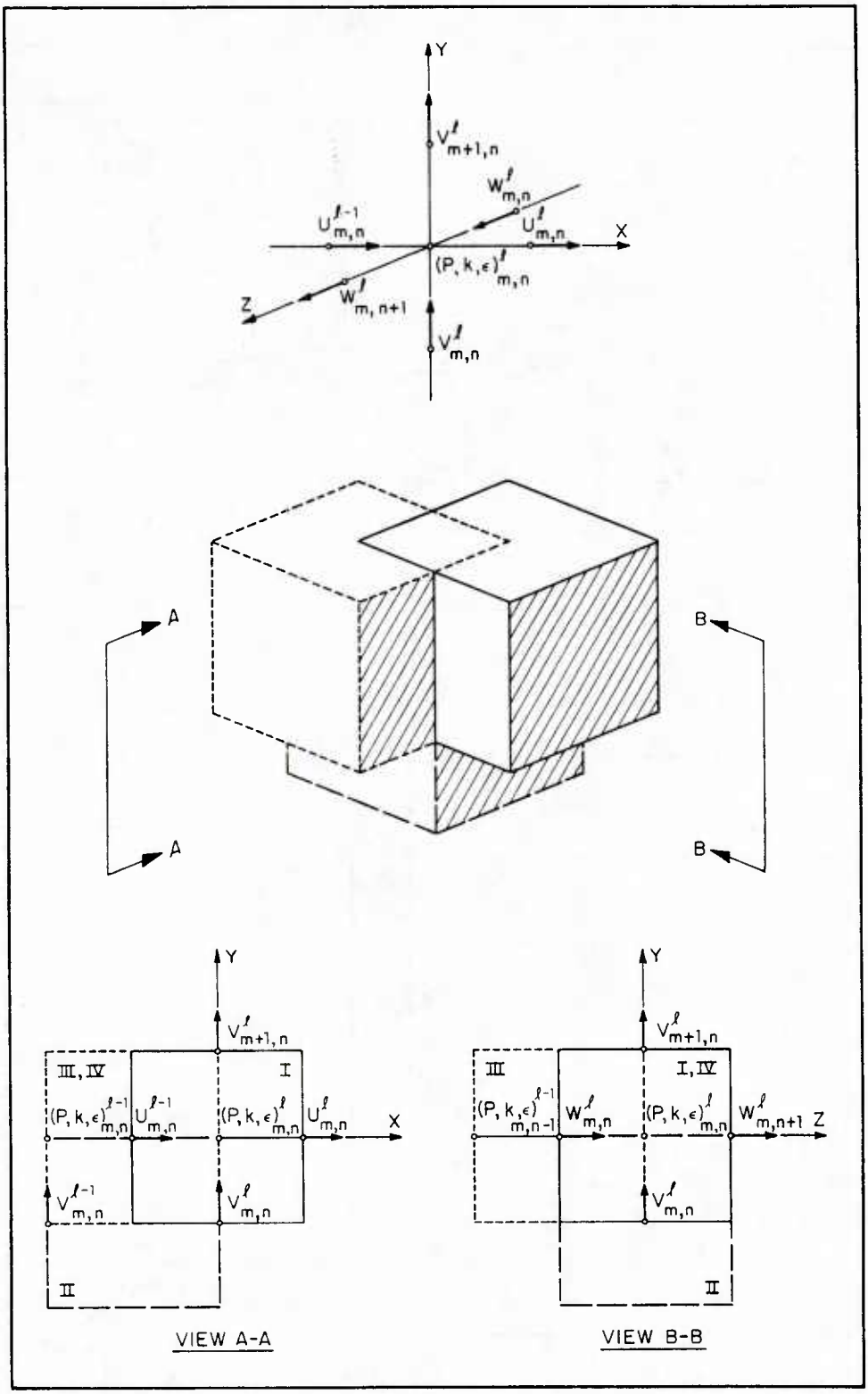

Figure 3. Finite-Difference Molecule

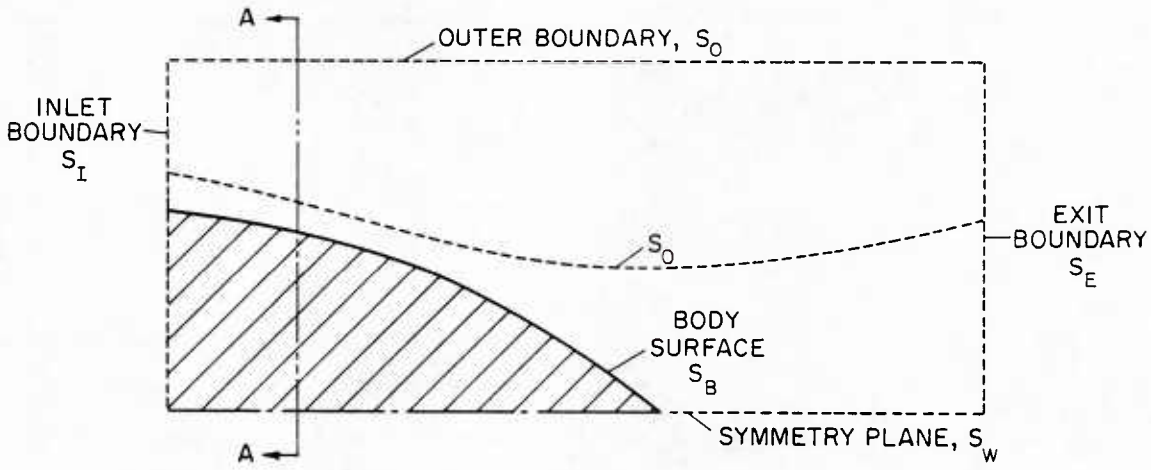

(a) DOMAIN BOUNDARIES IN THE (X,Y) PLANE

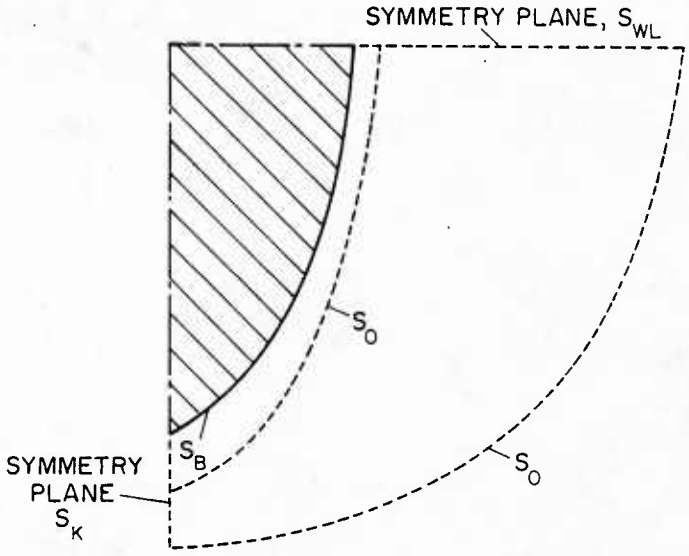

(b) DOMAIN BOUNDARIES IN THE (Y,Z) PLANE (VIEW A-A)

Figure 4. Definition Sketch of Boundary Surfaces

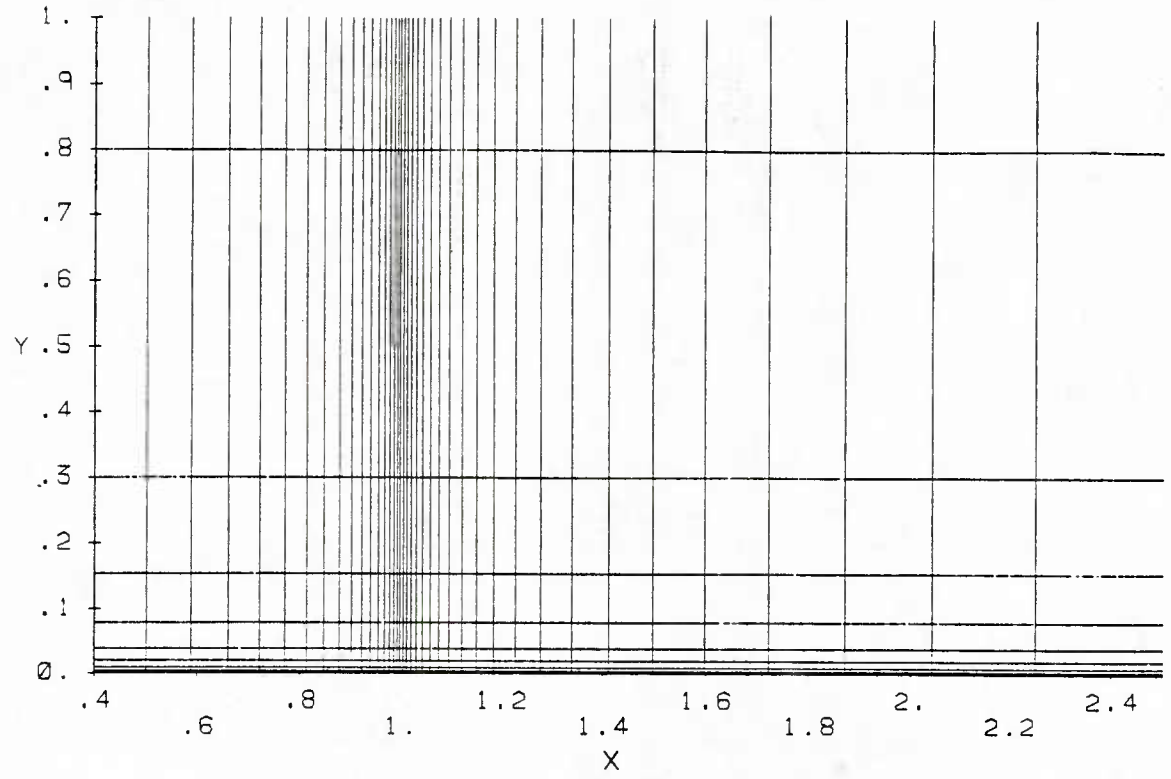

Figure 5. Large-Domain Grid for Flat-Plate Boundary Layer and Wake

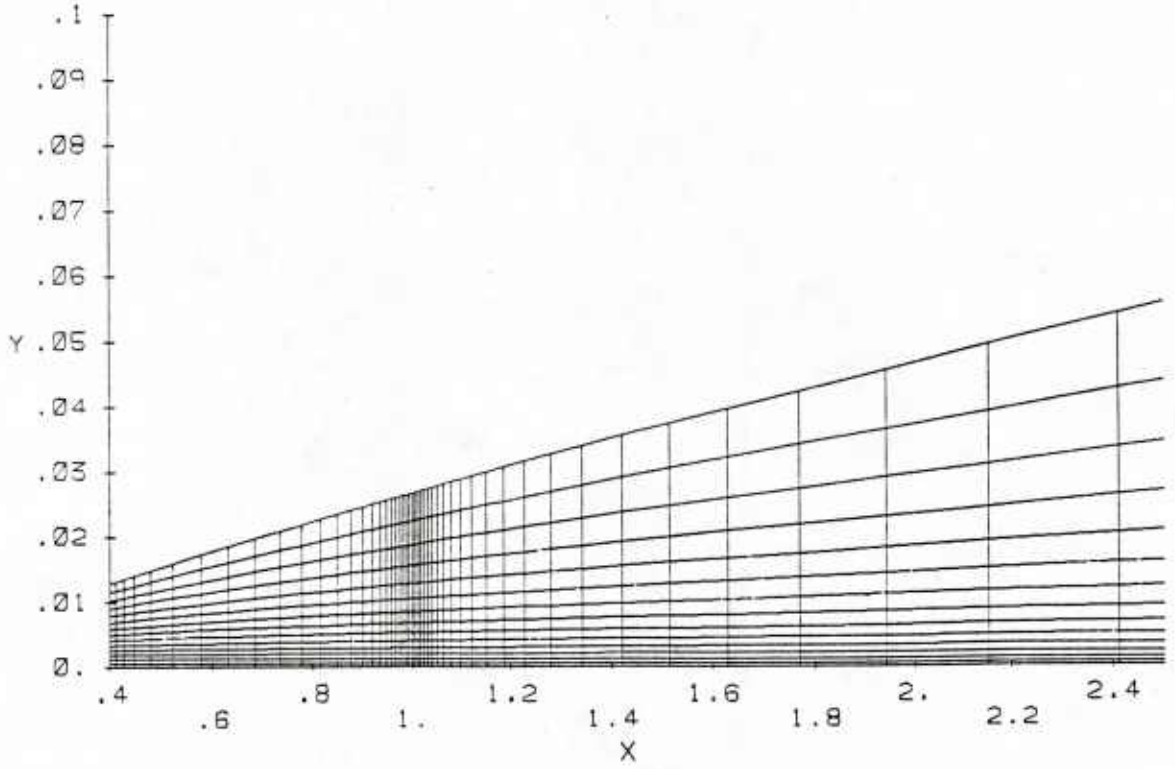

Figure 6. Small-Domain Grid for Flat-Plate Boundary Layer and Wake

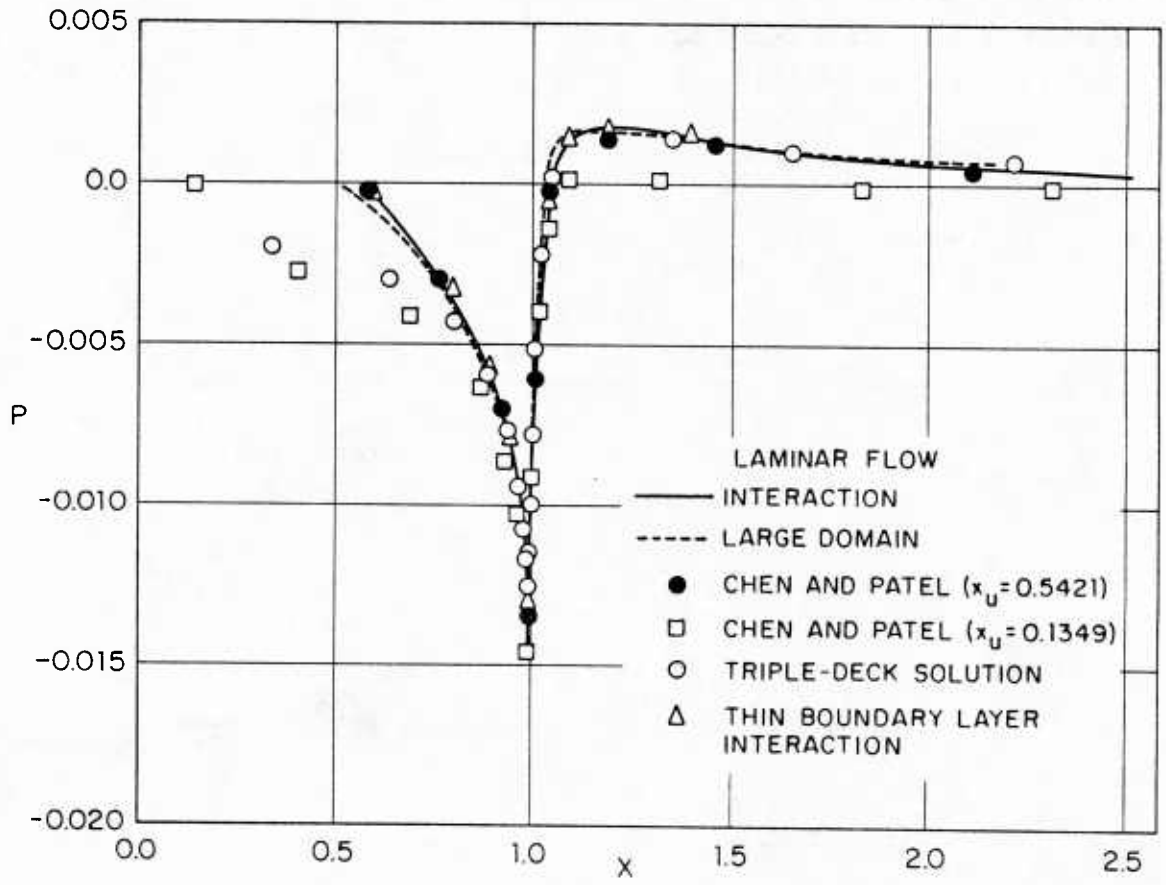

Figure 7. Pressure Distribution on the Surface of the Plate and along the Wake Centerline

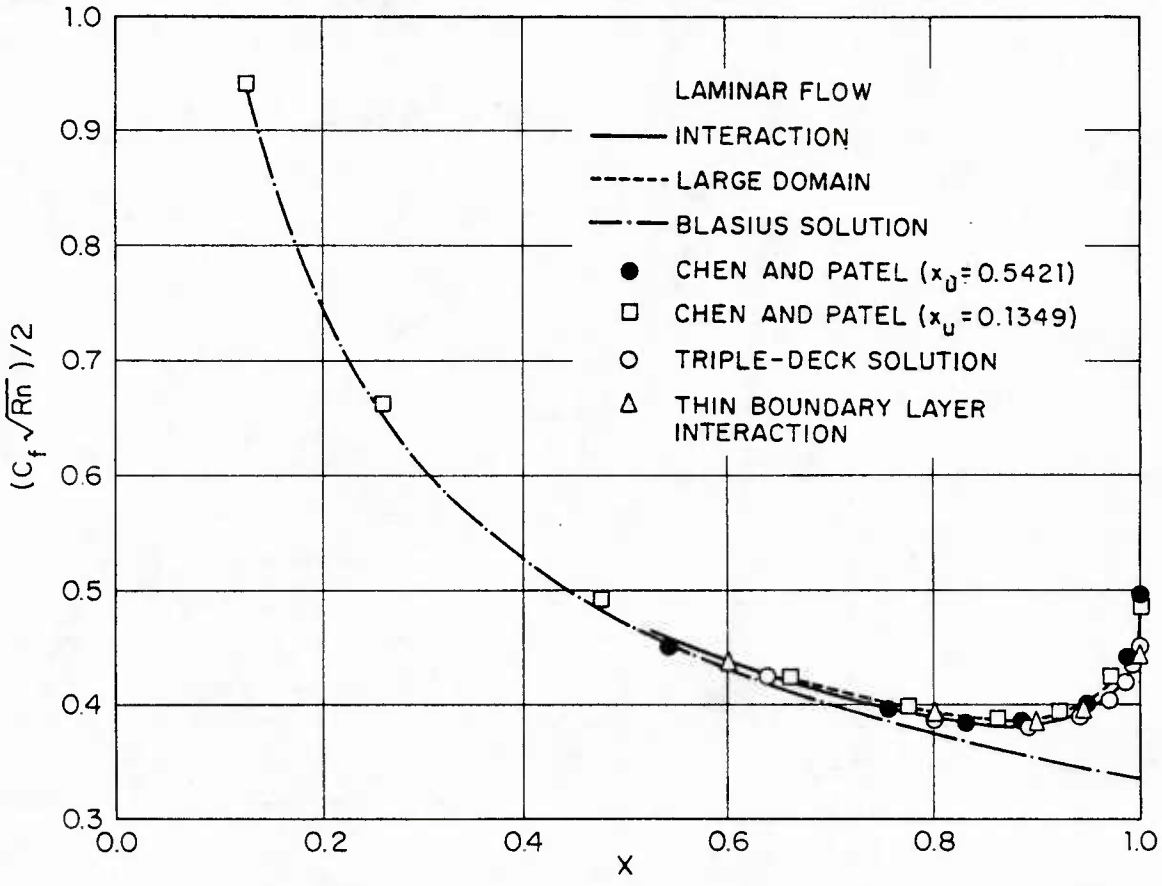

Figure 8. Skin-friction Coefficient

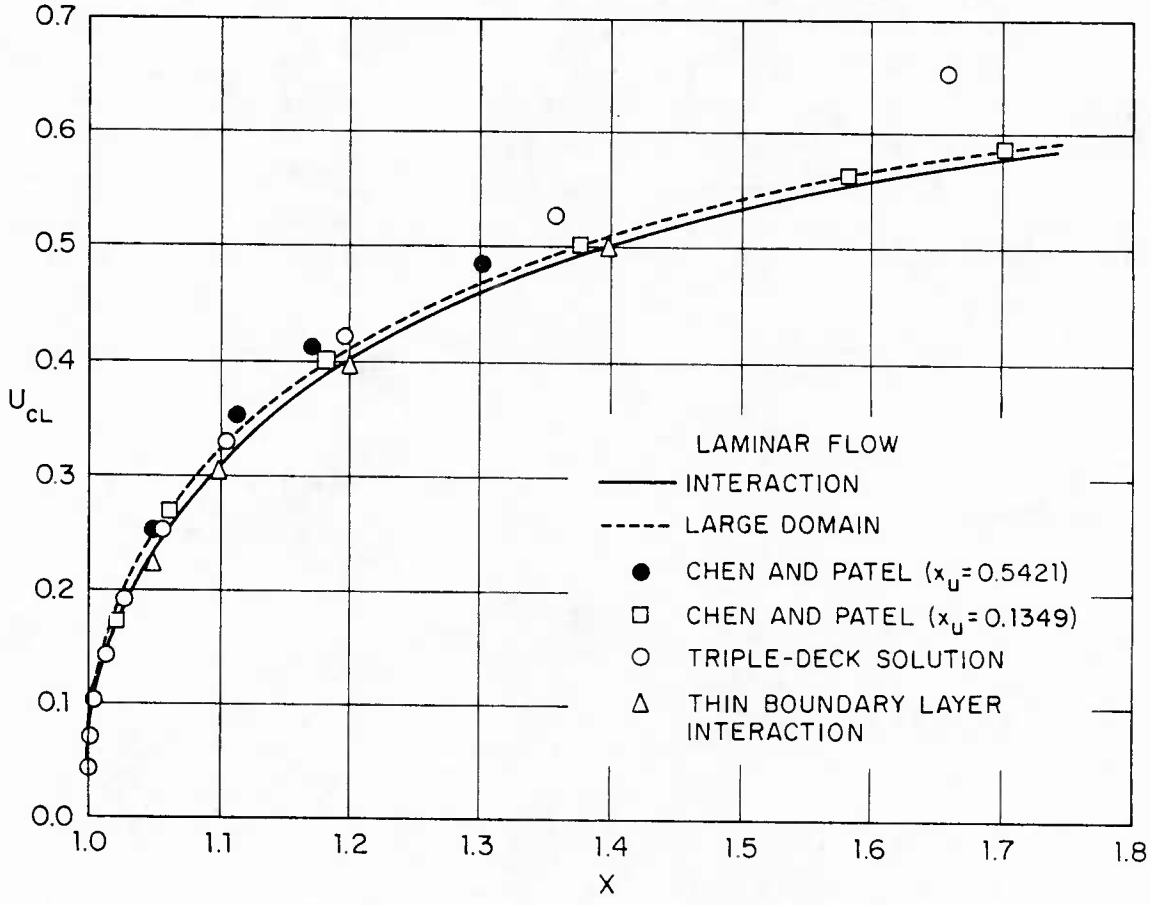

Figure 9. Wake-Centerline Velocity

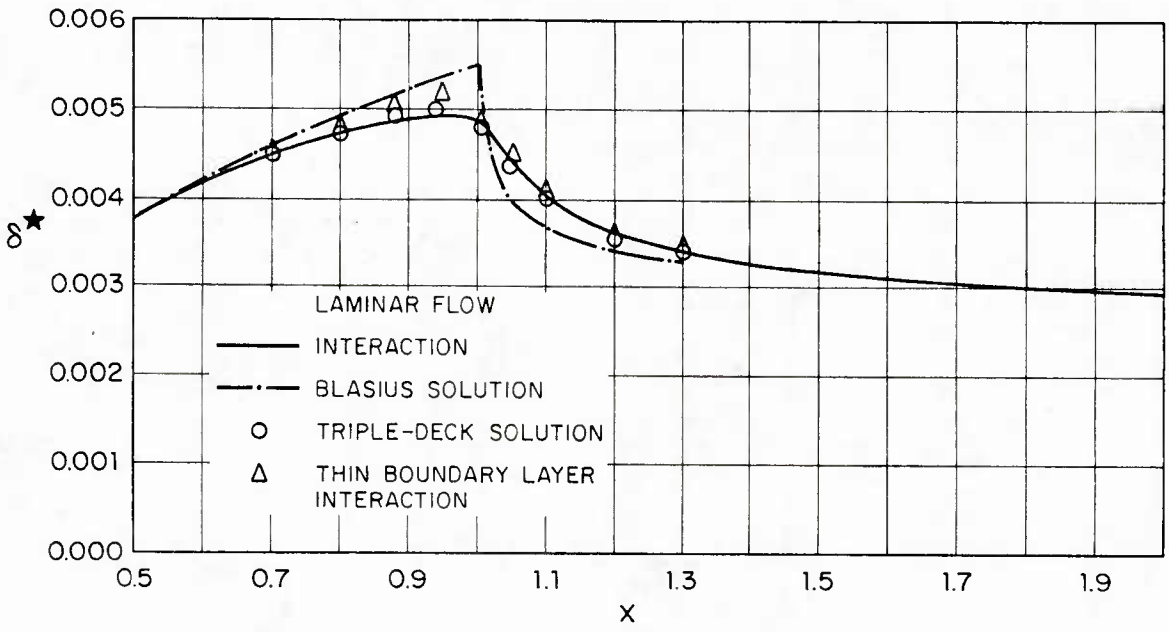

Figure 10. Displacement Thickness

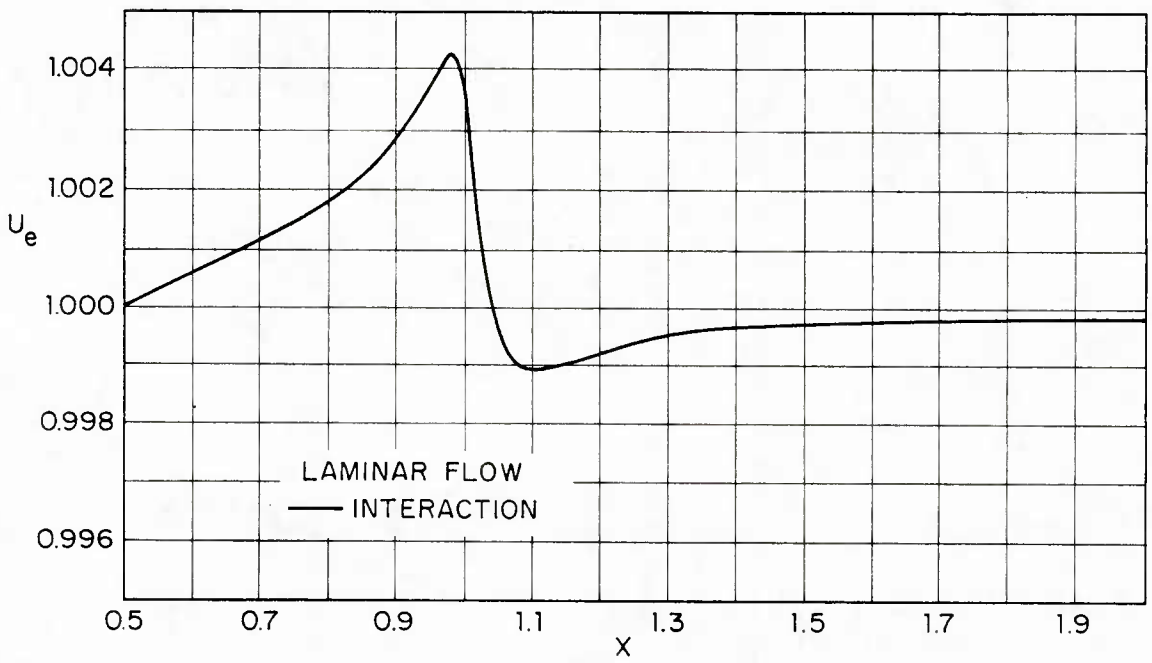

Figure 11. Edge Velocity

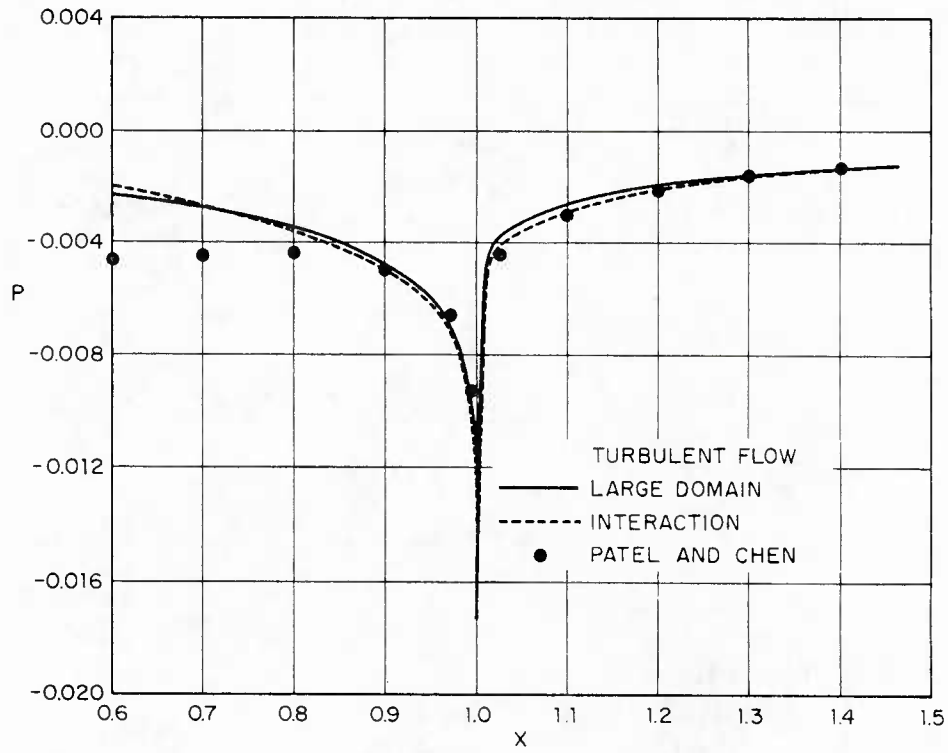

Figure 12. Pressure Distribution on the Surface of the Plate and Along the Wake Centerline

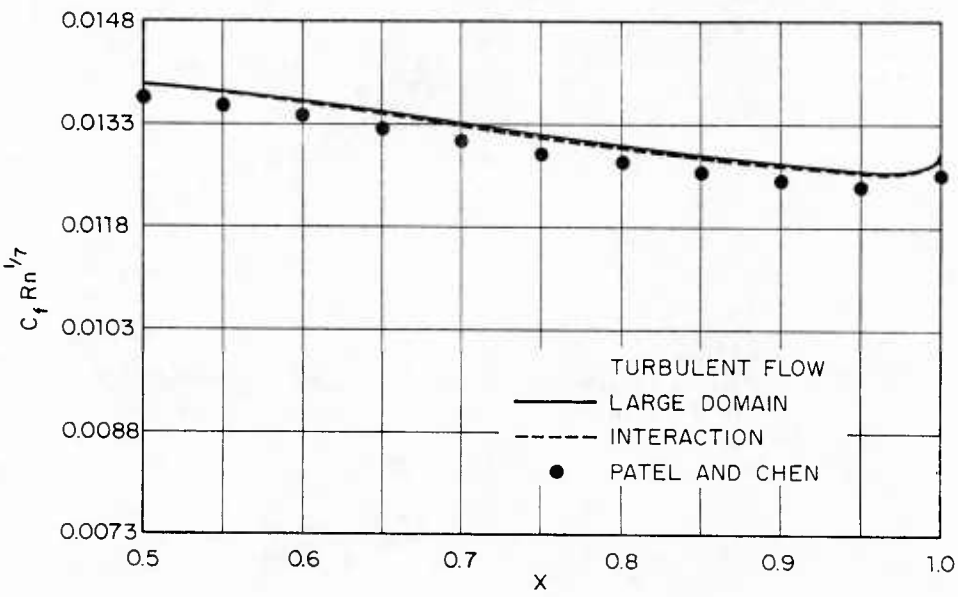

Figure 13. Skin-friction Coefficient

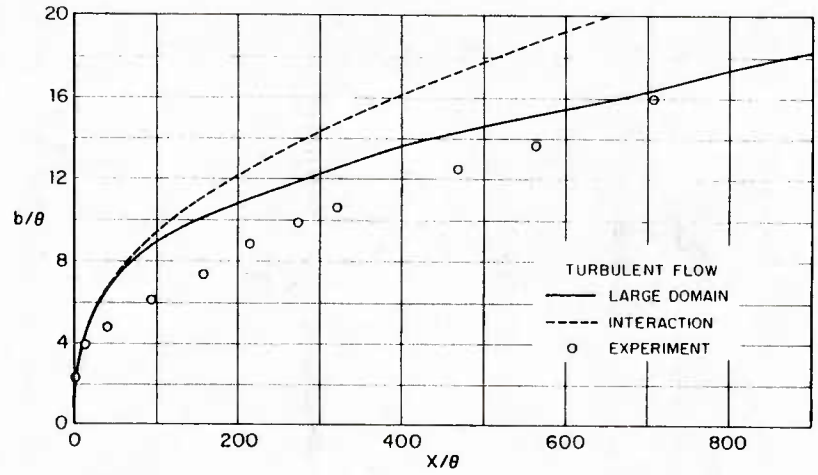

Half Width

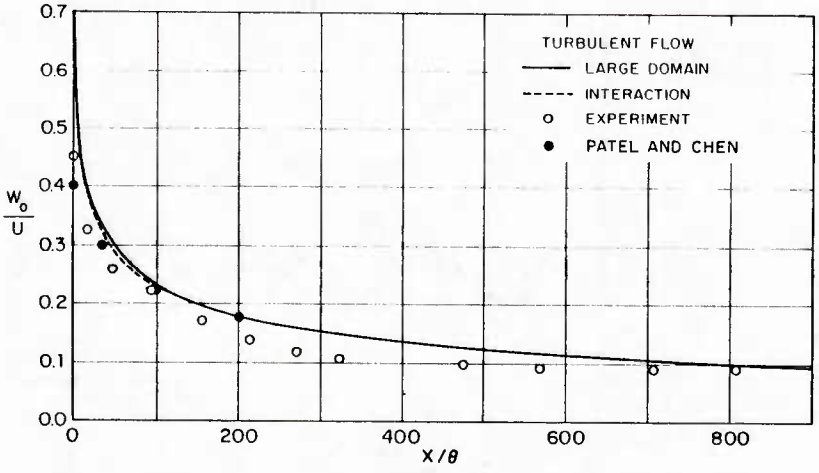

Maximum Velocity Defect

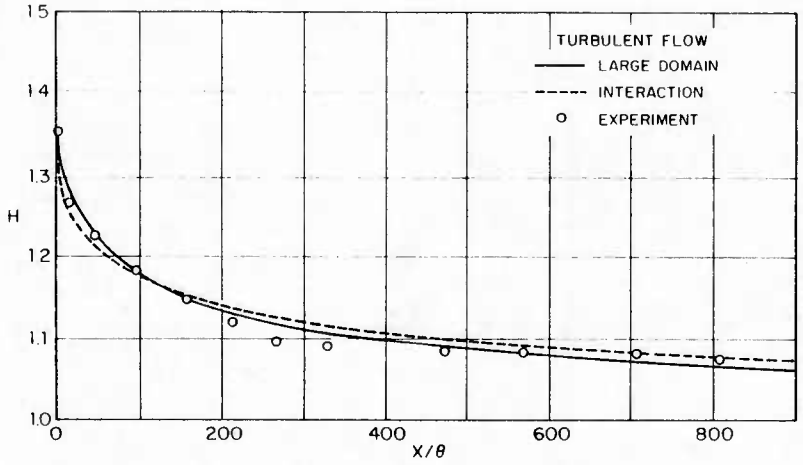

Shape Parameter

Figure 14. Near-Wake Parameters

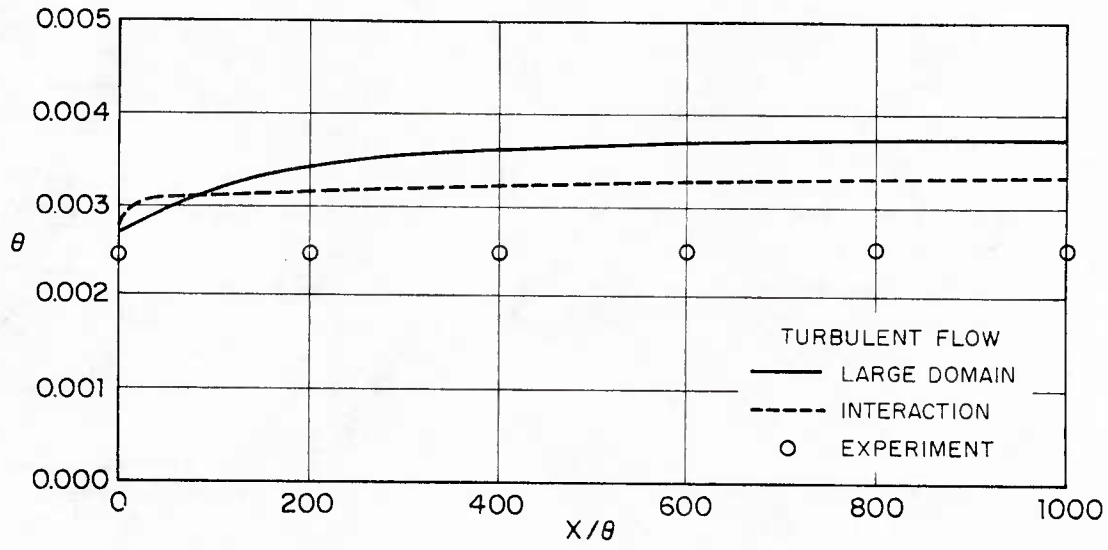

Figure 15. Wake Momentum Thickness

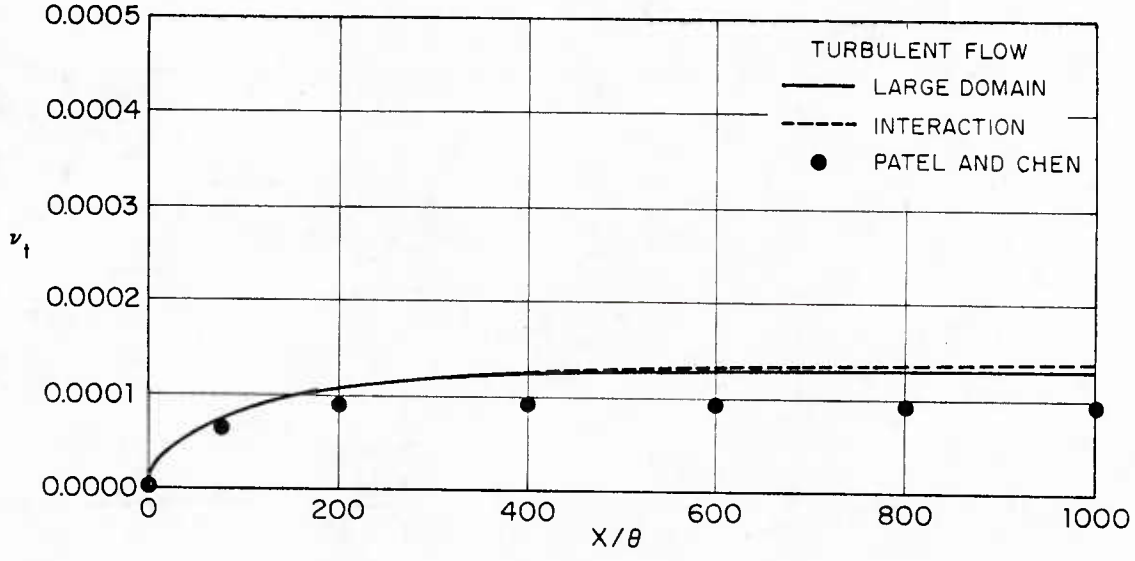

Figure 16. Wake-Centerline Eddy Viscosity

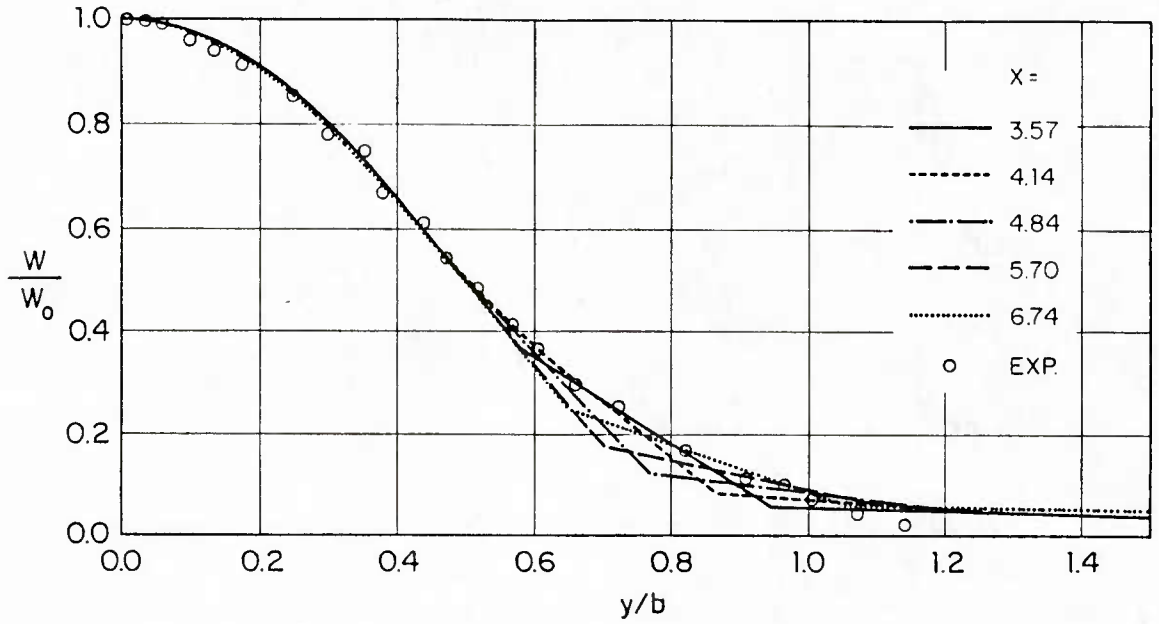

Asymptotic Velocity-Defect Profile

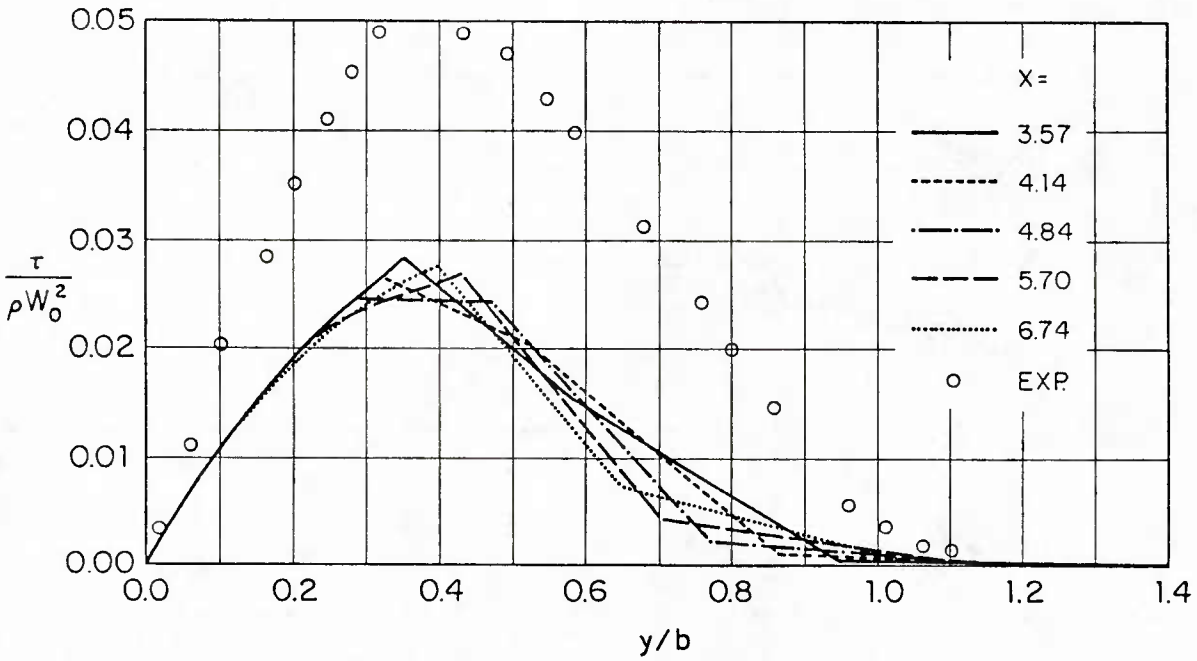

Asymptotic Stress Profile

Figure 17. Large-Domain Solution Asymptotic Profiles

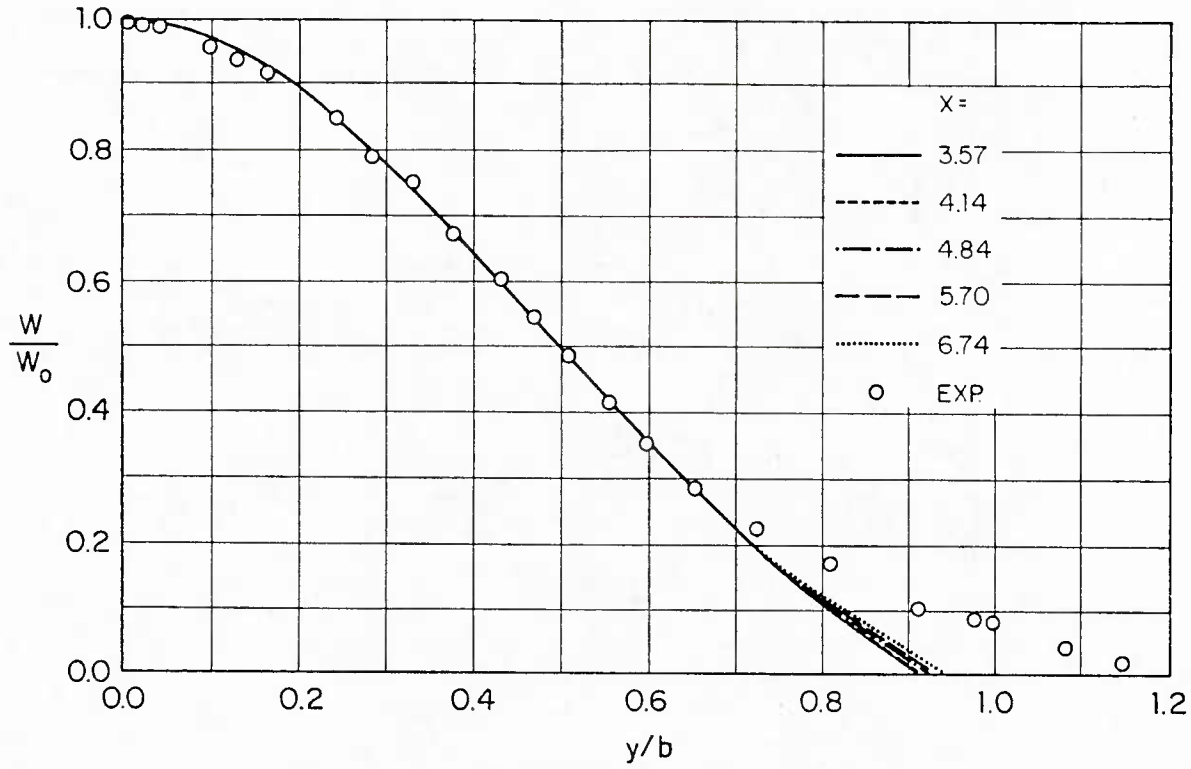

Asymptotic Velocity-Defect Profile

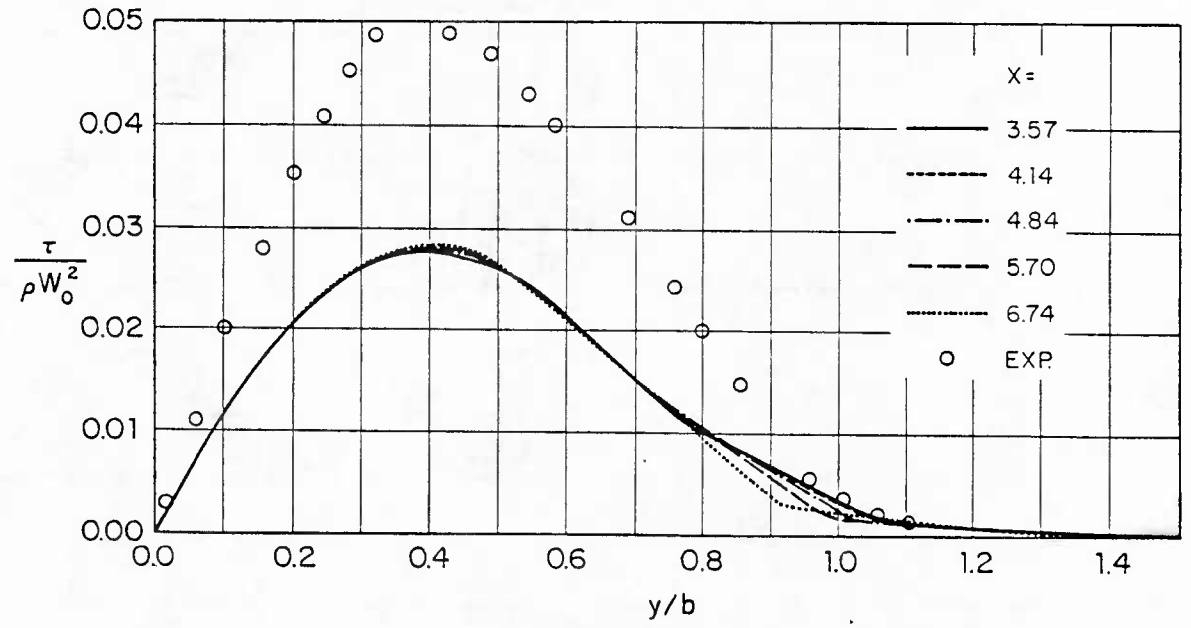

Asymptotic Stress Profile

Figure 18. Interaction Solution Asymptotic Profiles

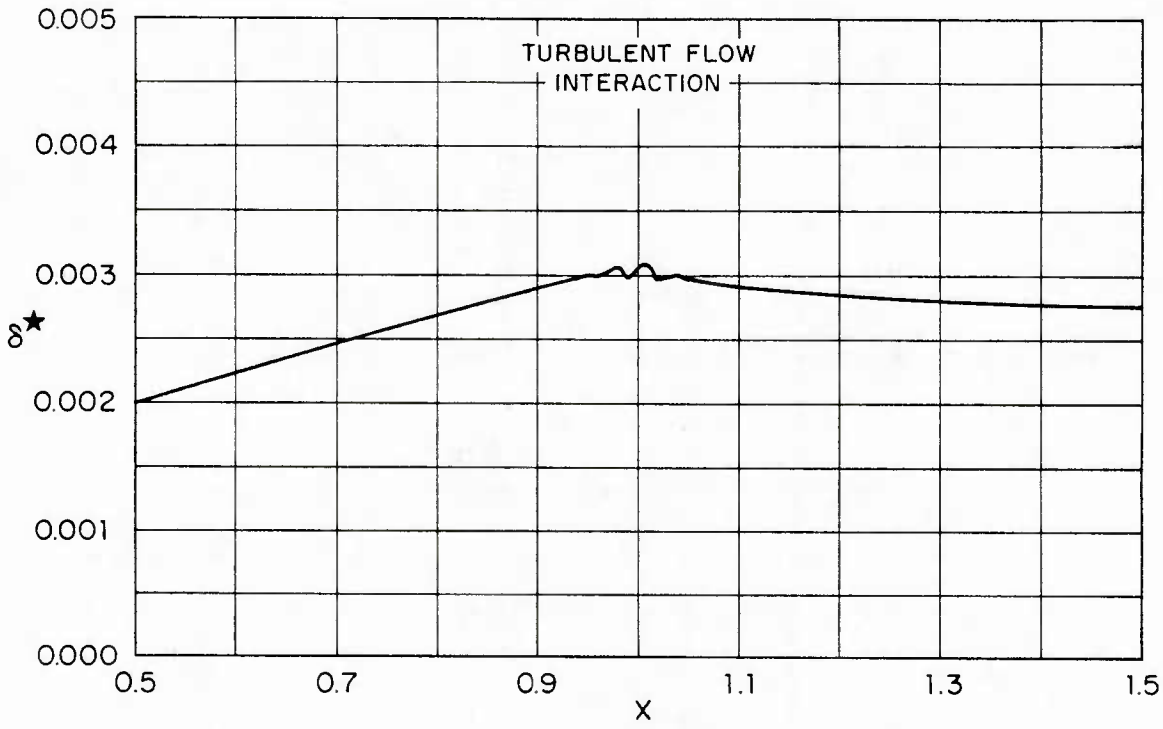

Figure 19. Displacement Thickness

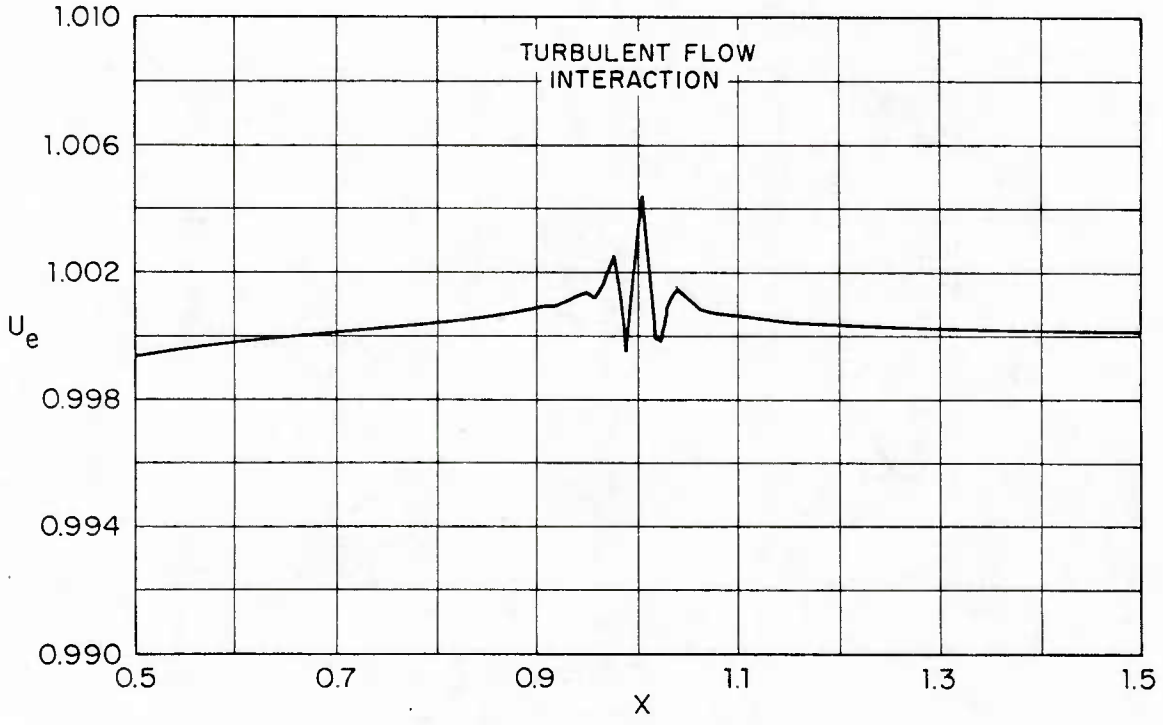

Figure 20. Edge Velocity

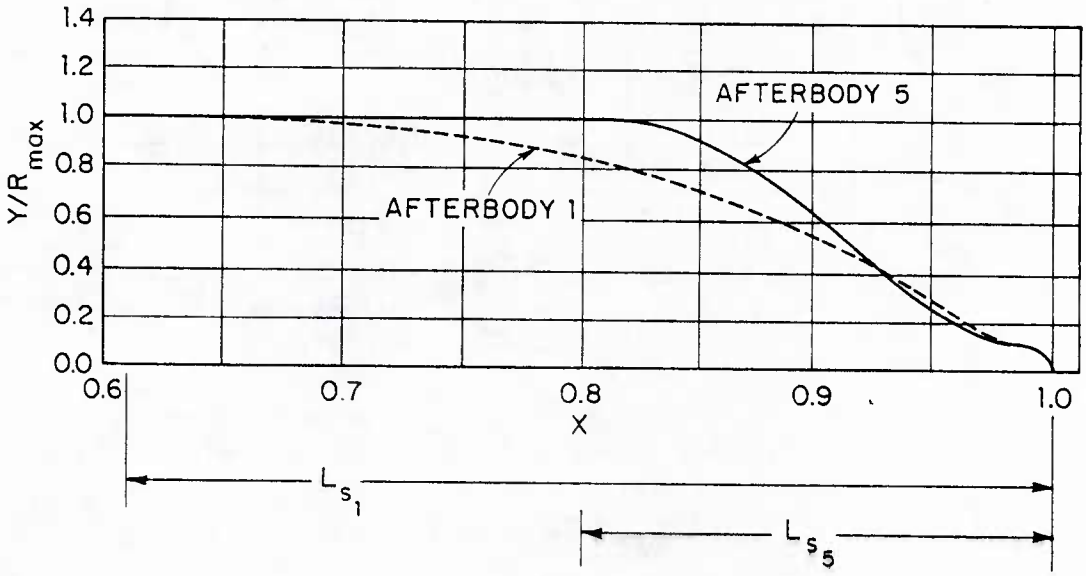

	AFTERBODY 1	AFTERBODY 5
L	3.066 m	2.91 m
D	0.2794 m	0.28 m
L_s/L	0.39	0.196
L_s/D	4.3	2.037
L/D	10.97	10.39

Figure 21. Geometric Data for DTNSRDC Afterbodies 1 and 5

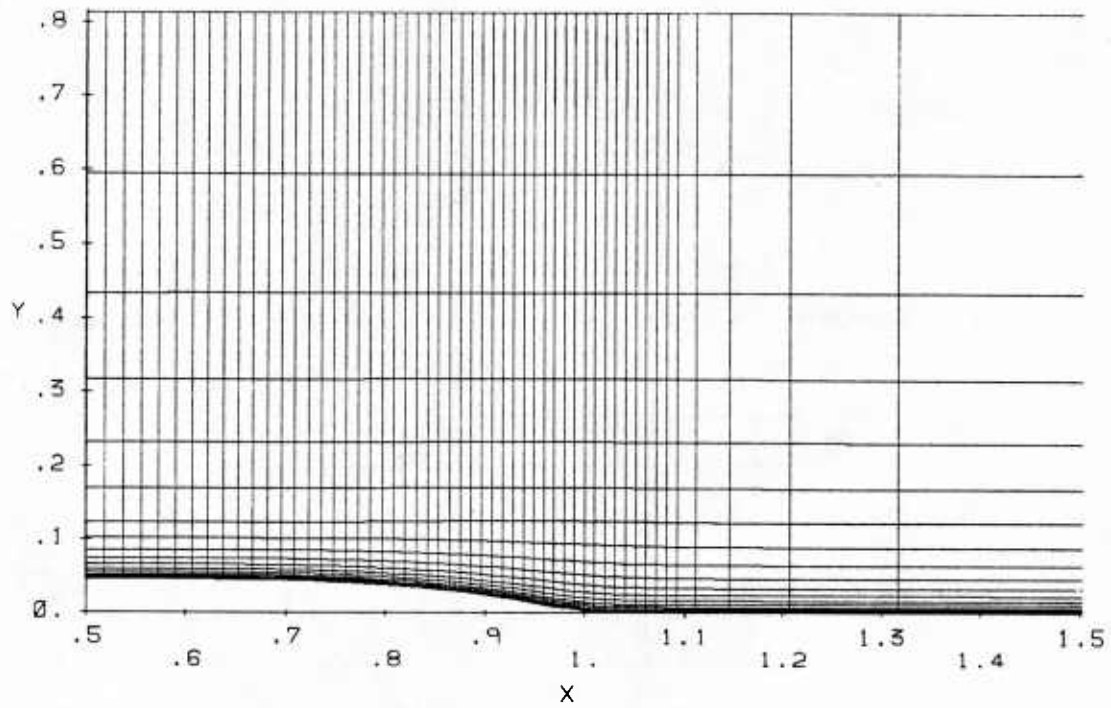

Figure 22. Large-Domain Grid for Afterbody 1

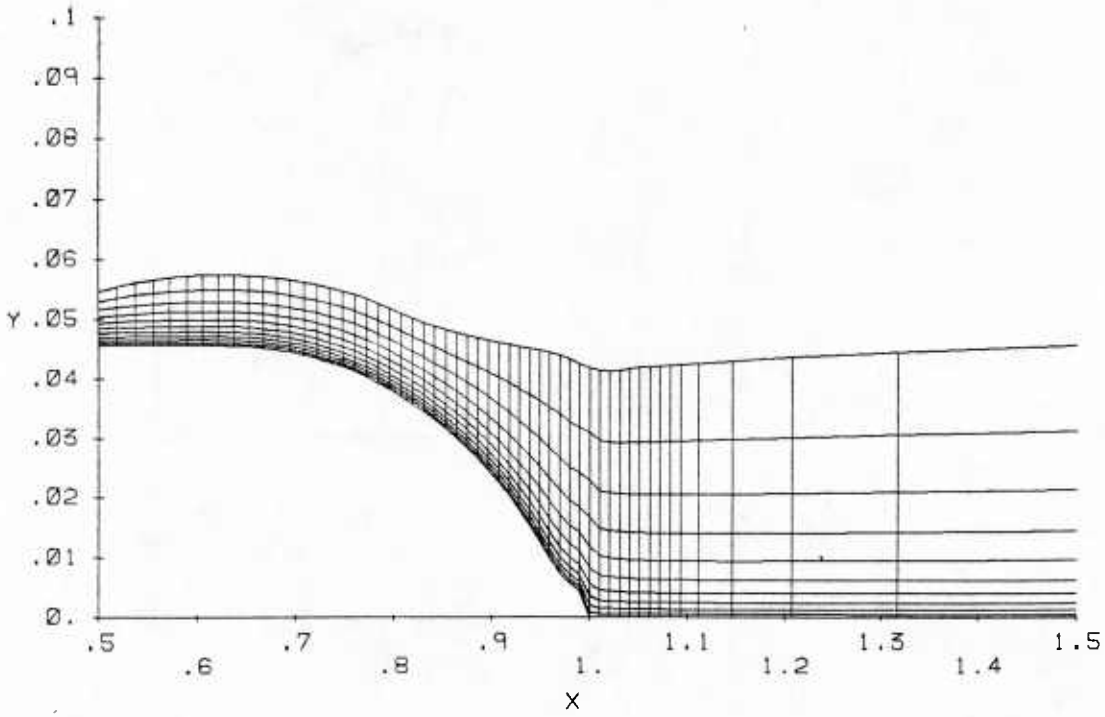

Figure 23. Small-Domain Grid for Afterbody 1

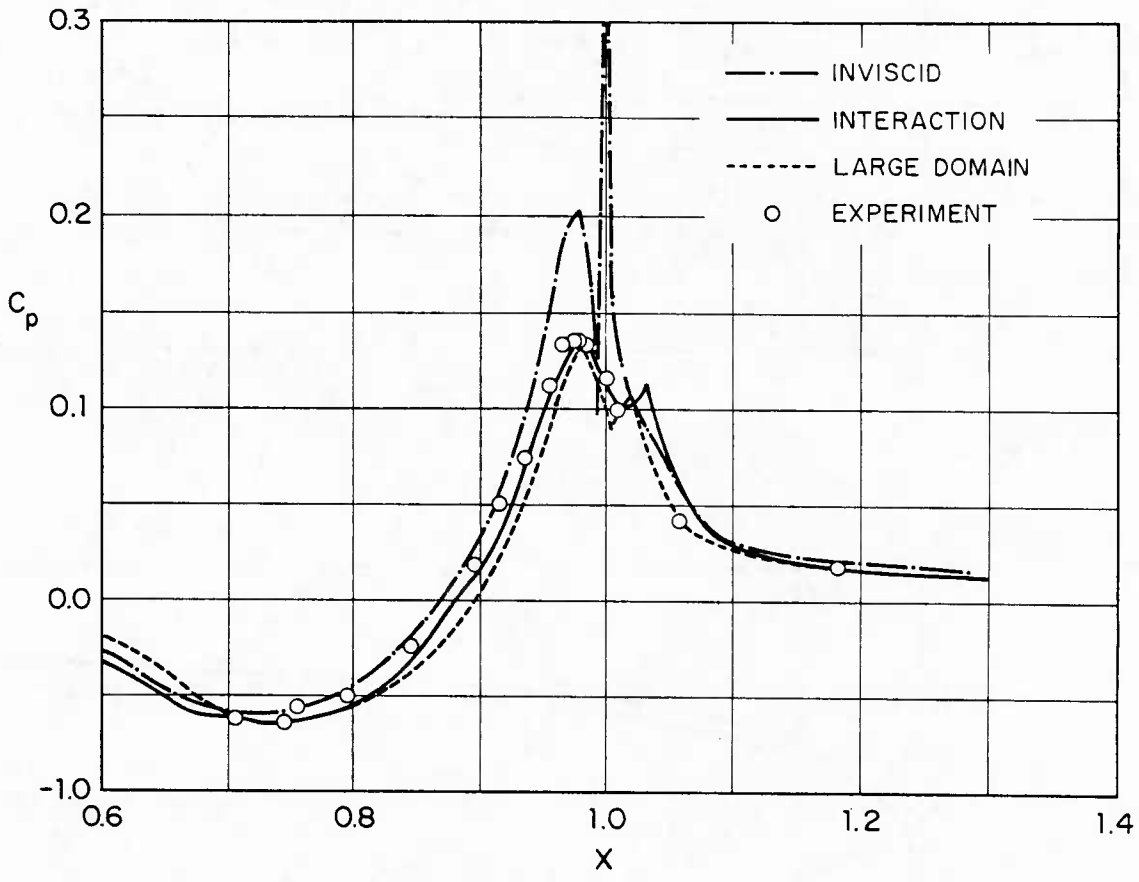

Figure 24. Pressure Distribution on the Surface of the Body and Along the Wake Centerline

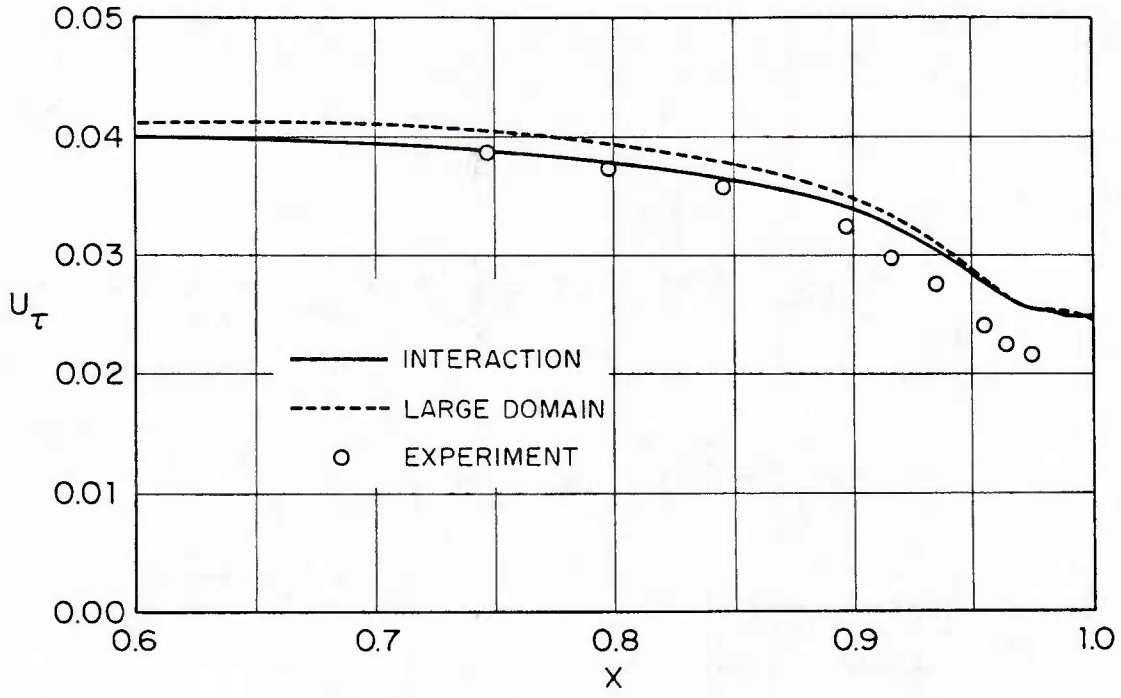

Figure 25. Wall-Shear Velocity

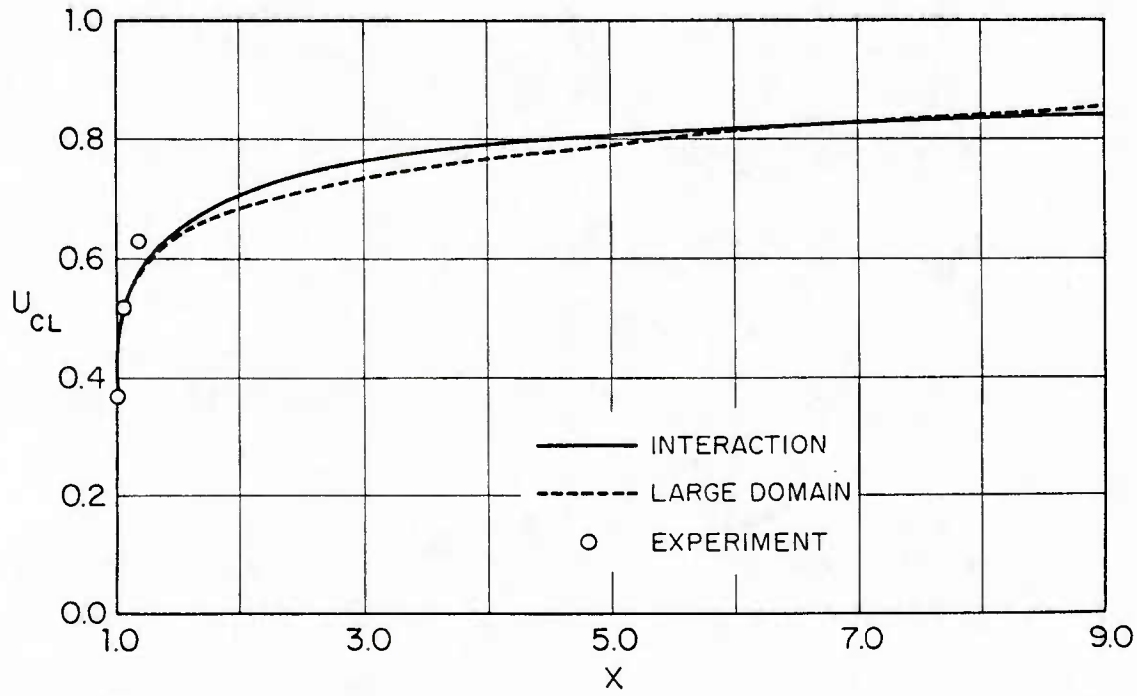

Figure 26. Wake-Centerline Velocity

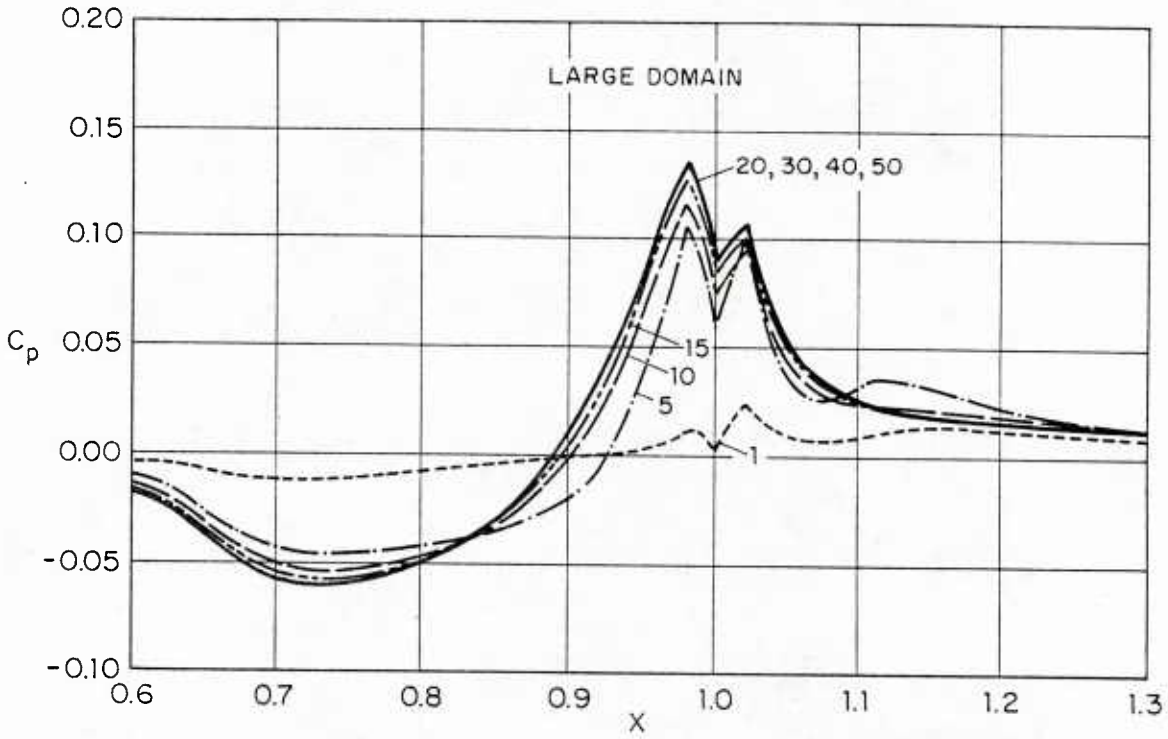

Pressure Distribution on the Surface of the Body and Along the Wake Centerline

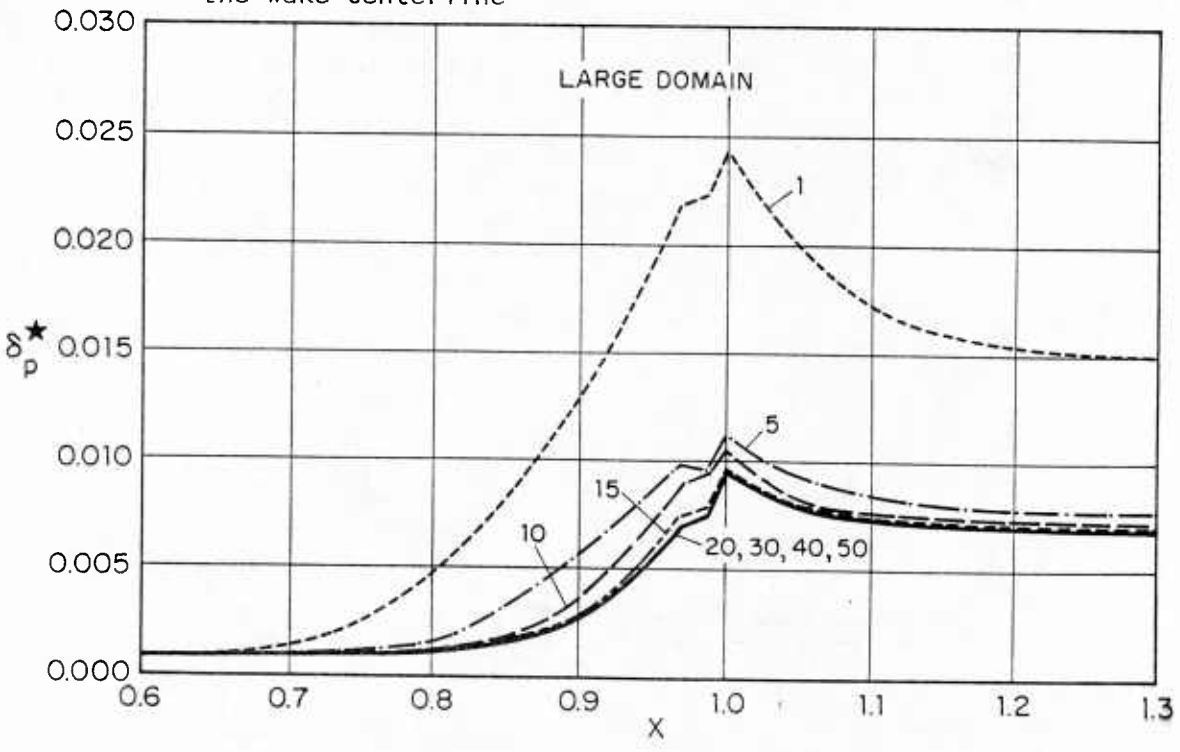

Displacement Thickness

Figure 27. Convergence History of Large-Domain Solution

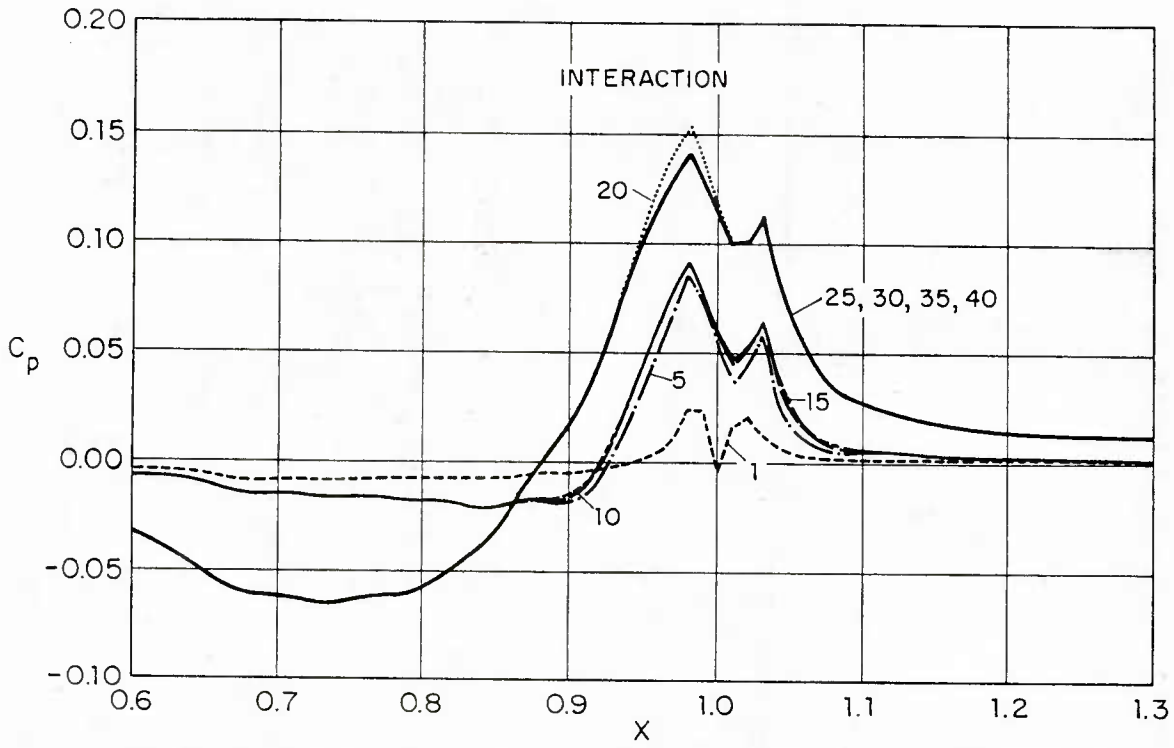

Pressure Distribution on the Surface of the Body and Along the Wake Centerline

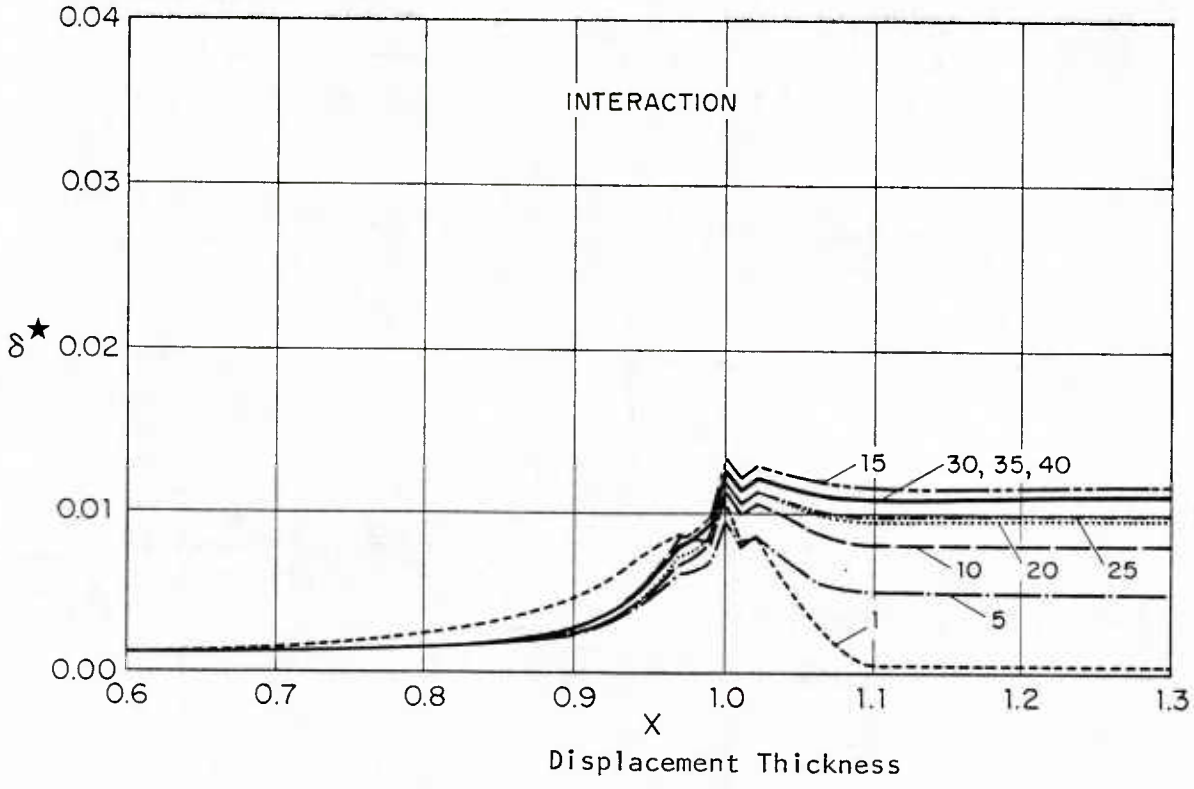

Displacement Thickness

Figure 28. Convergence History of Interaction Solution

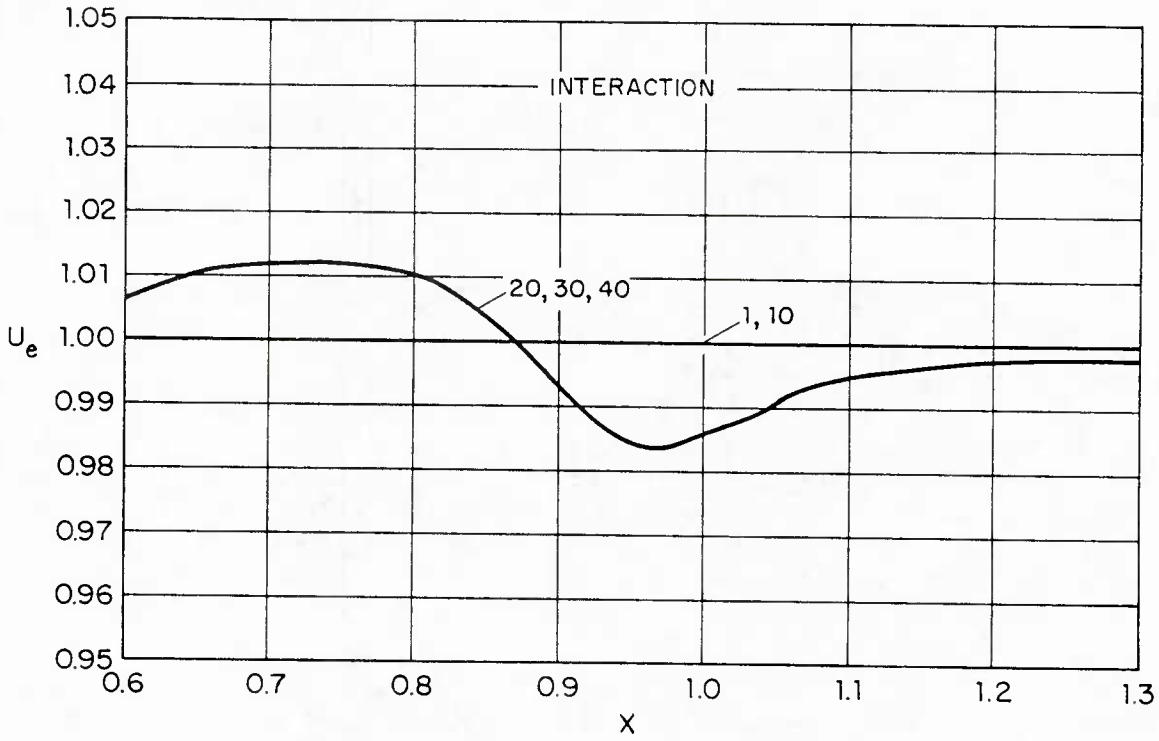

Figure 29. Edge Velocity

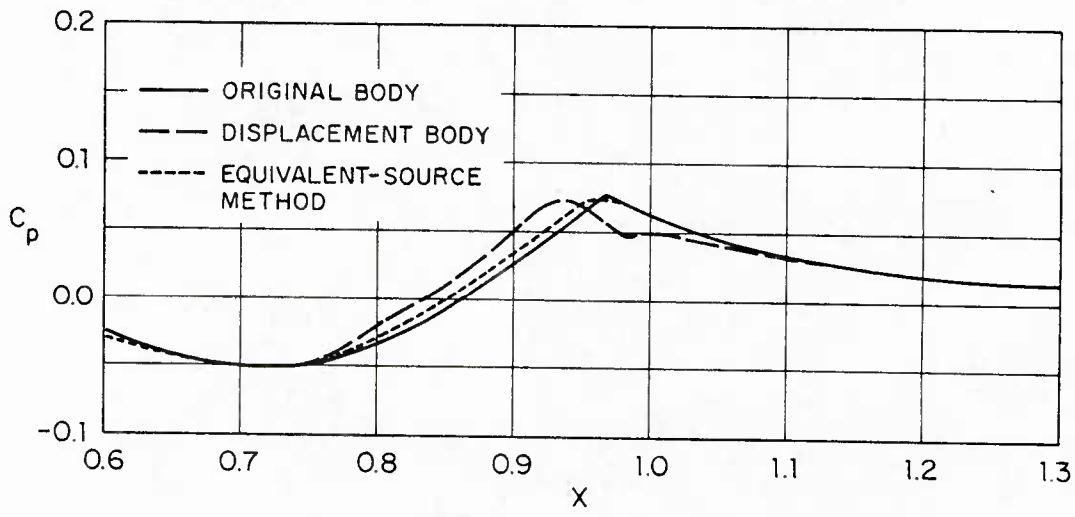

Figure 30. Edge Pressure

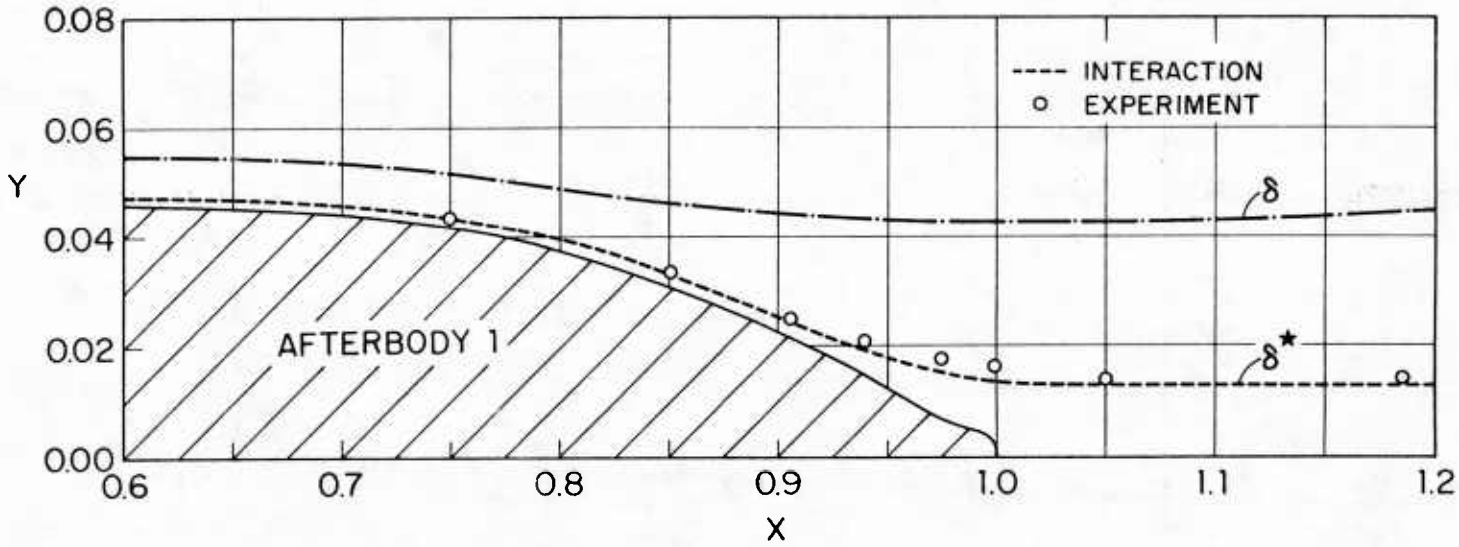

Figure 31. Boundary Layer and Displacement Thicknesses

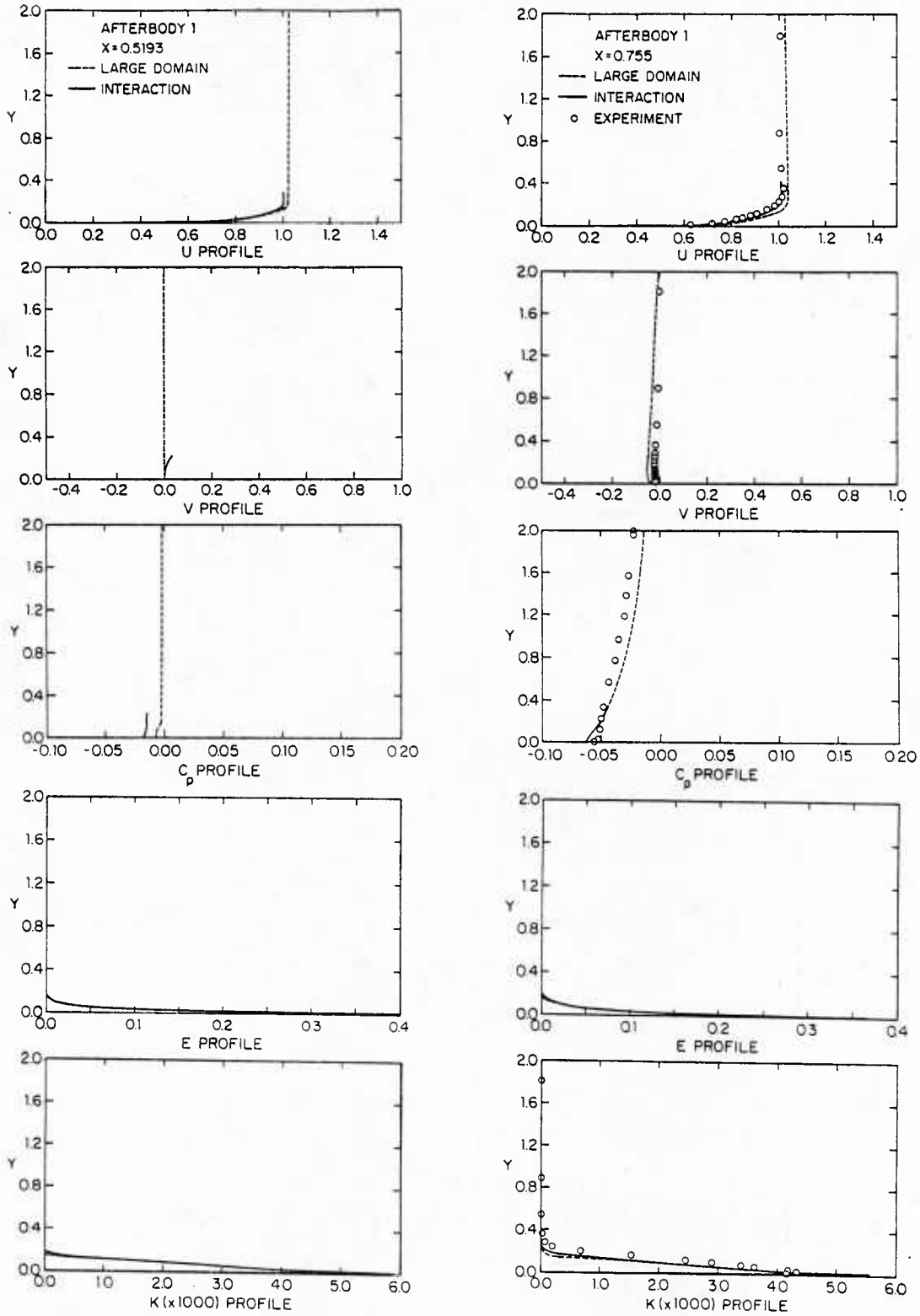

Figure 32. Solution Profiles

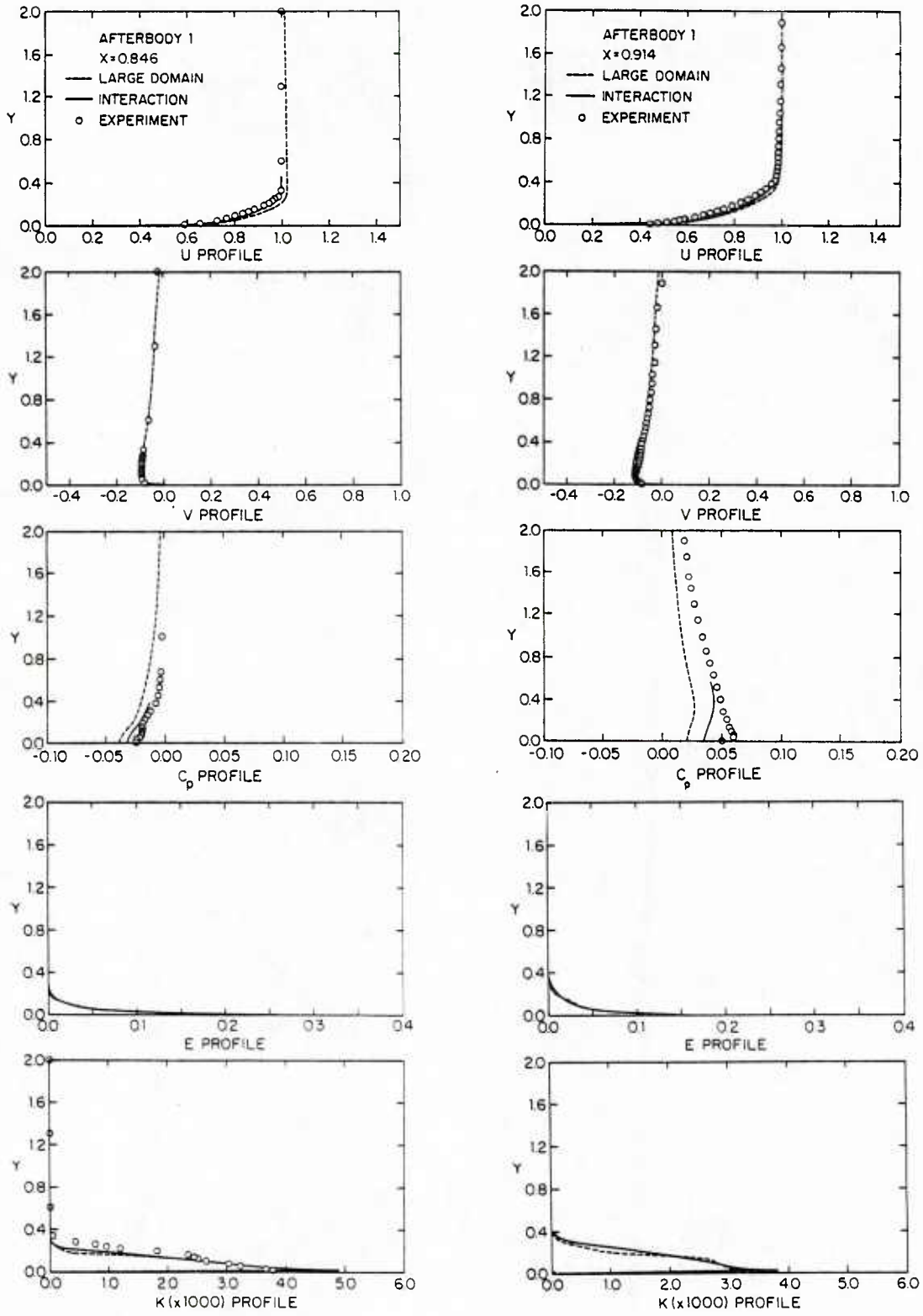

Figure 32. (Continued)

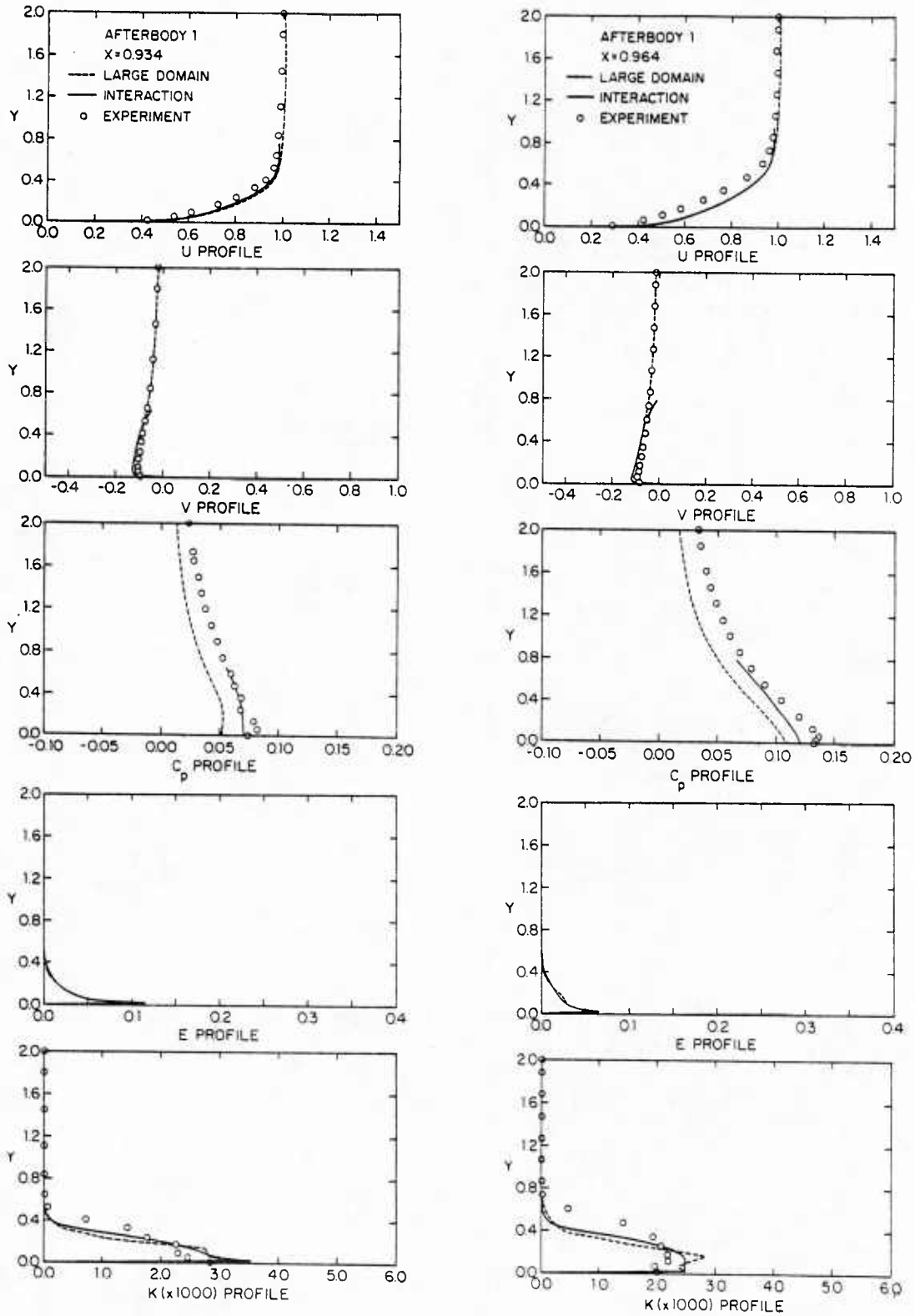

Figure 32. (Continued)

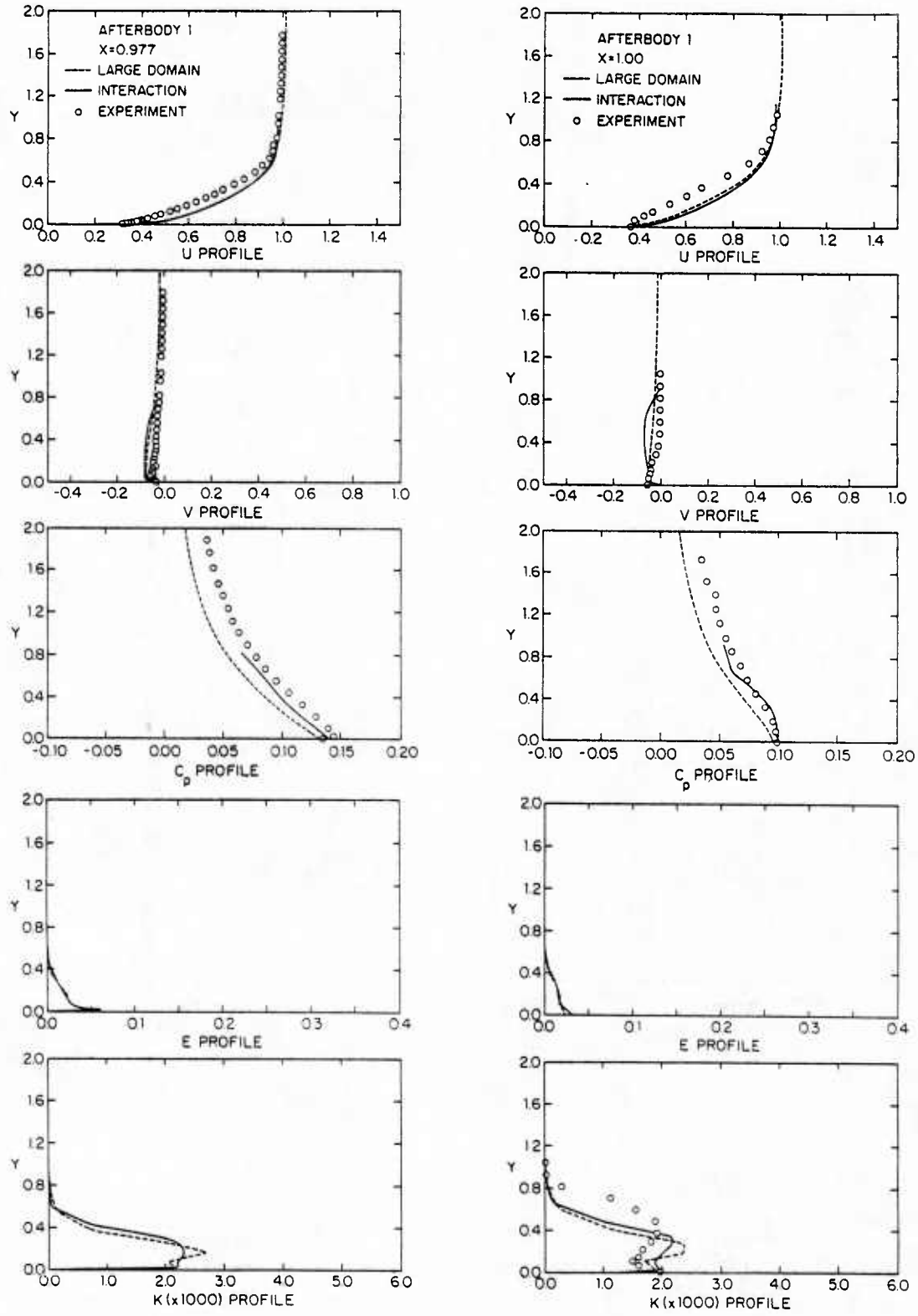

Figure 32. (Continued)

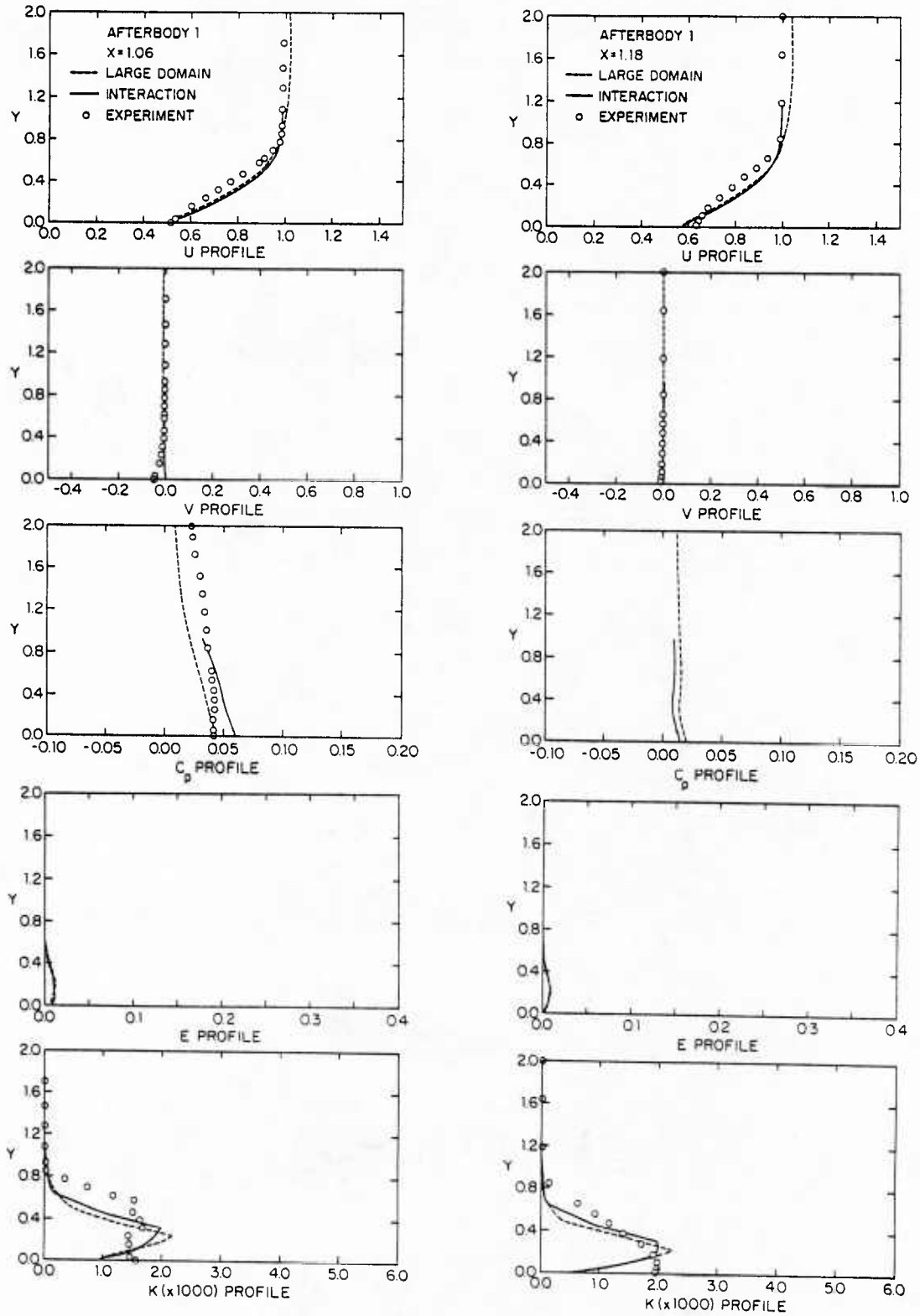

Figure 32. (Continued)

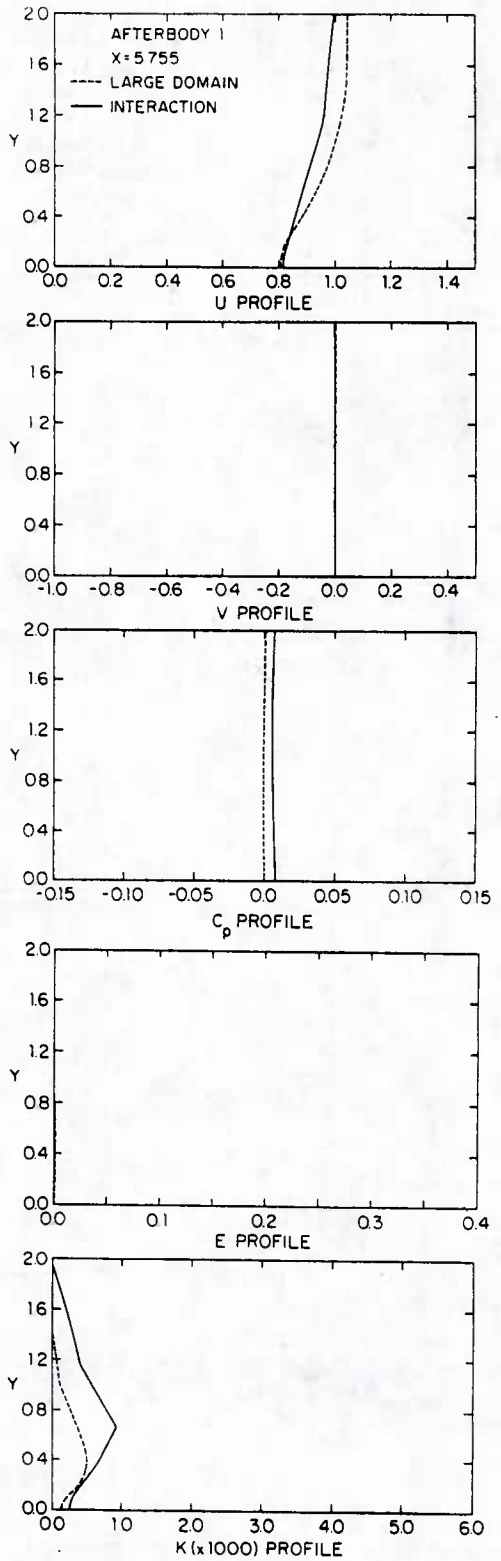

Figure 32. (Continued)

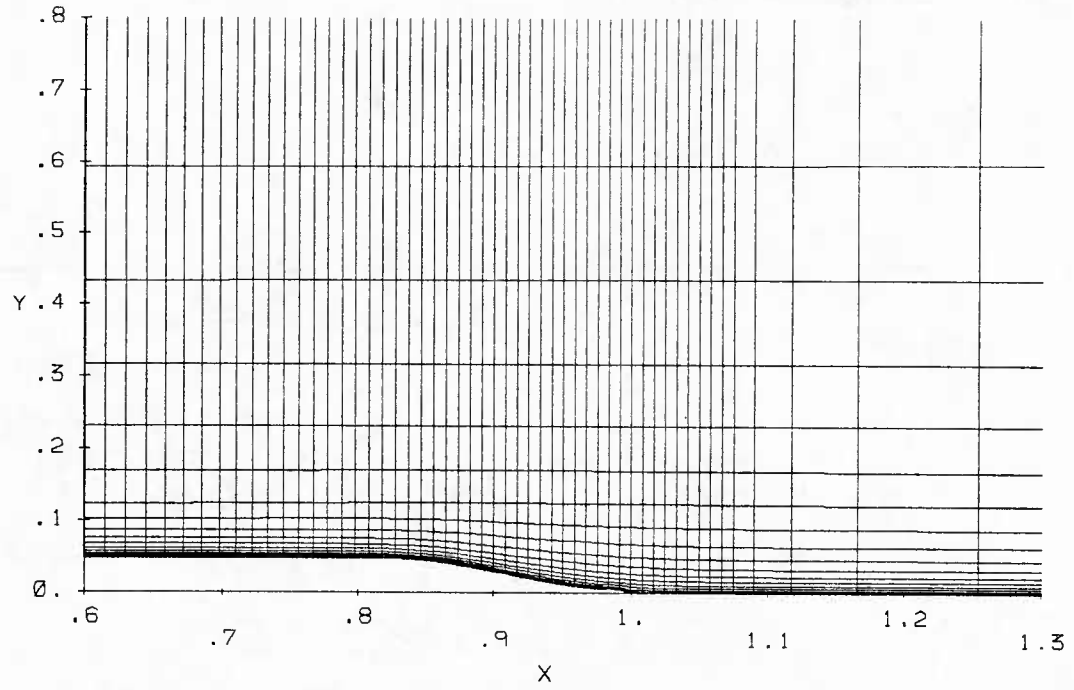

Figure 33. Large-Domain Grid for Afterbody 5

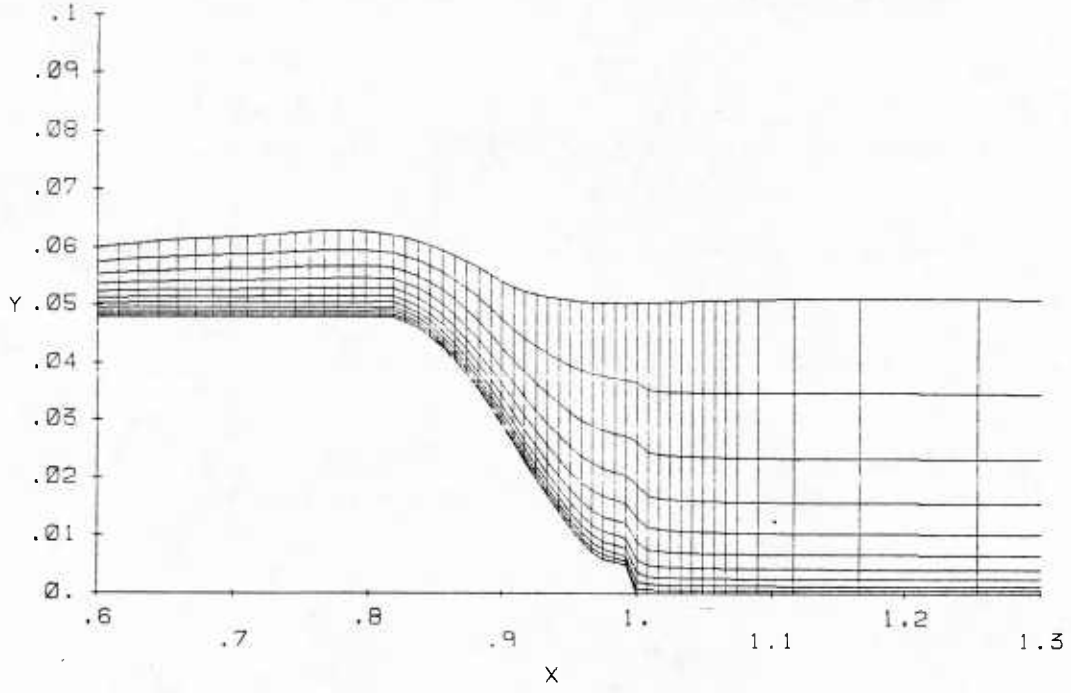

Figure 34. Small-Domain Grid for Afterbody 5

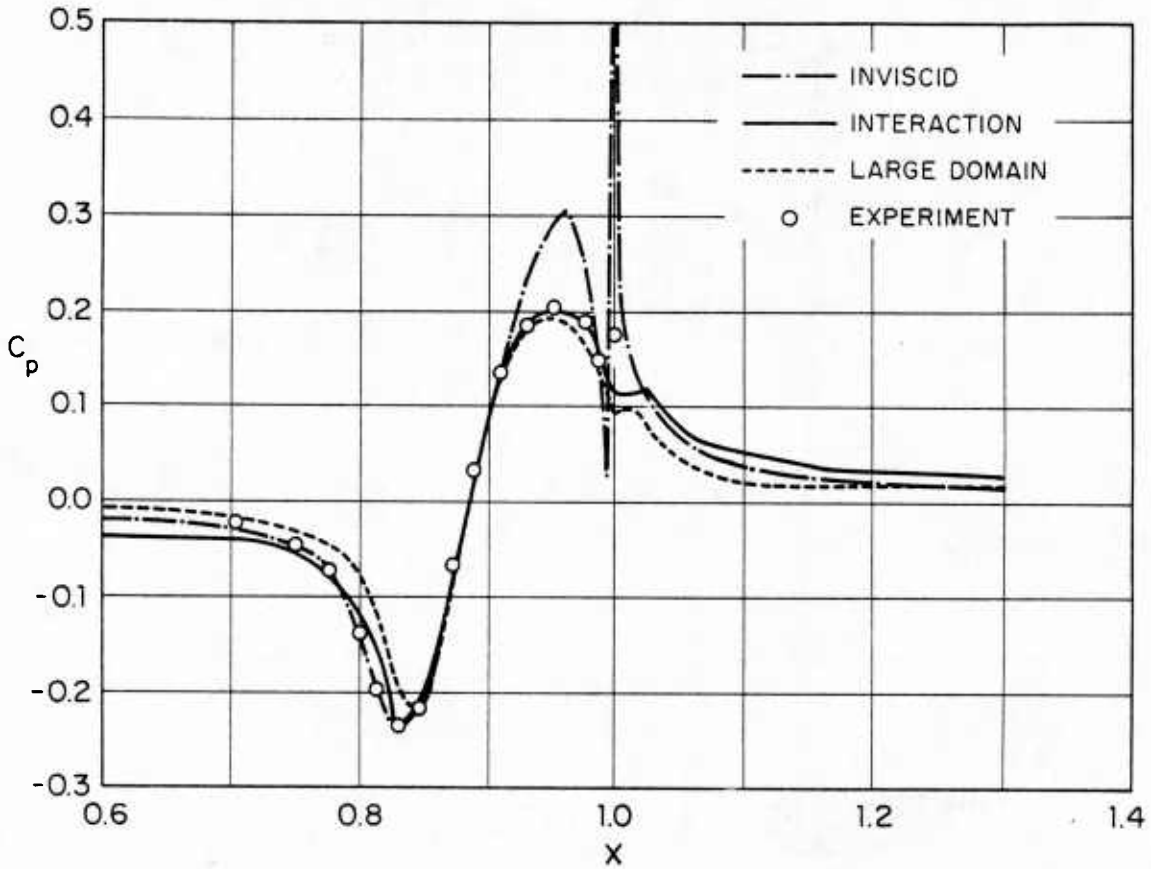

Figure 35. Pressure Distribution on the Surface of the Body and Along the Wake Centerline

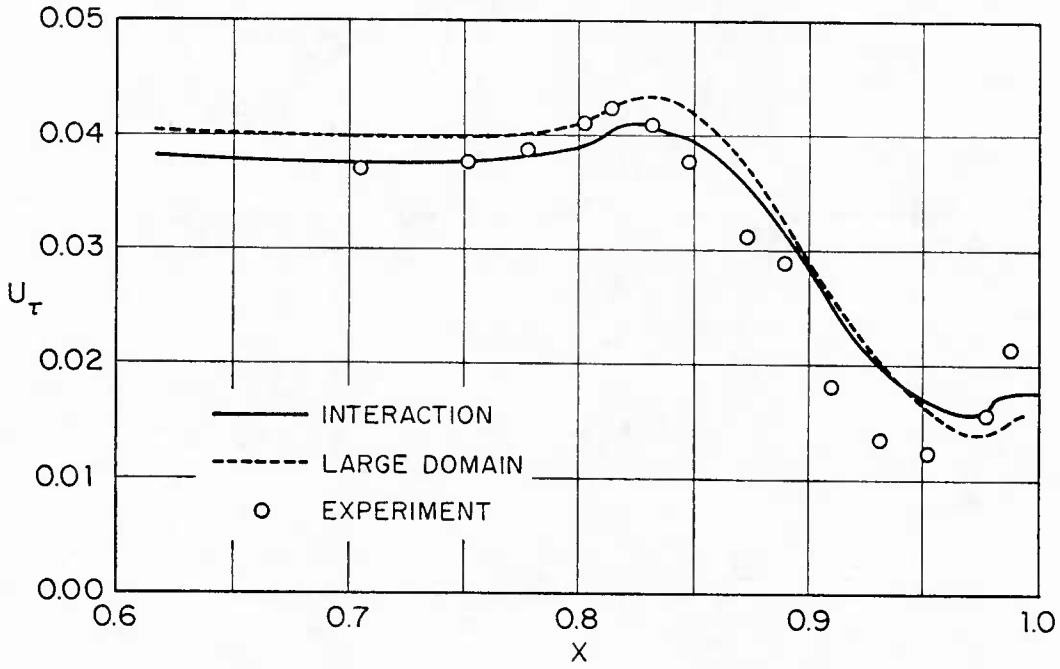

Figure 36. Wall-Shear Velocity

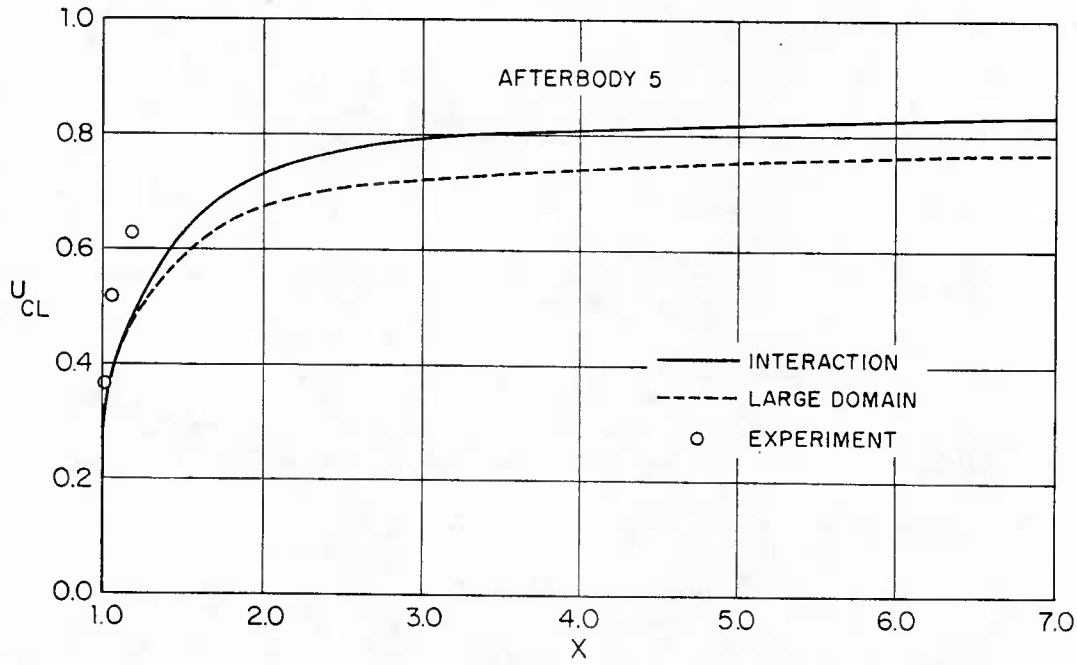

Figure 37. Wake-Centerline Velocity

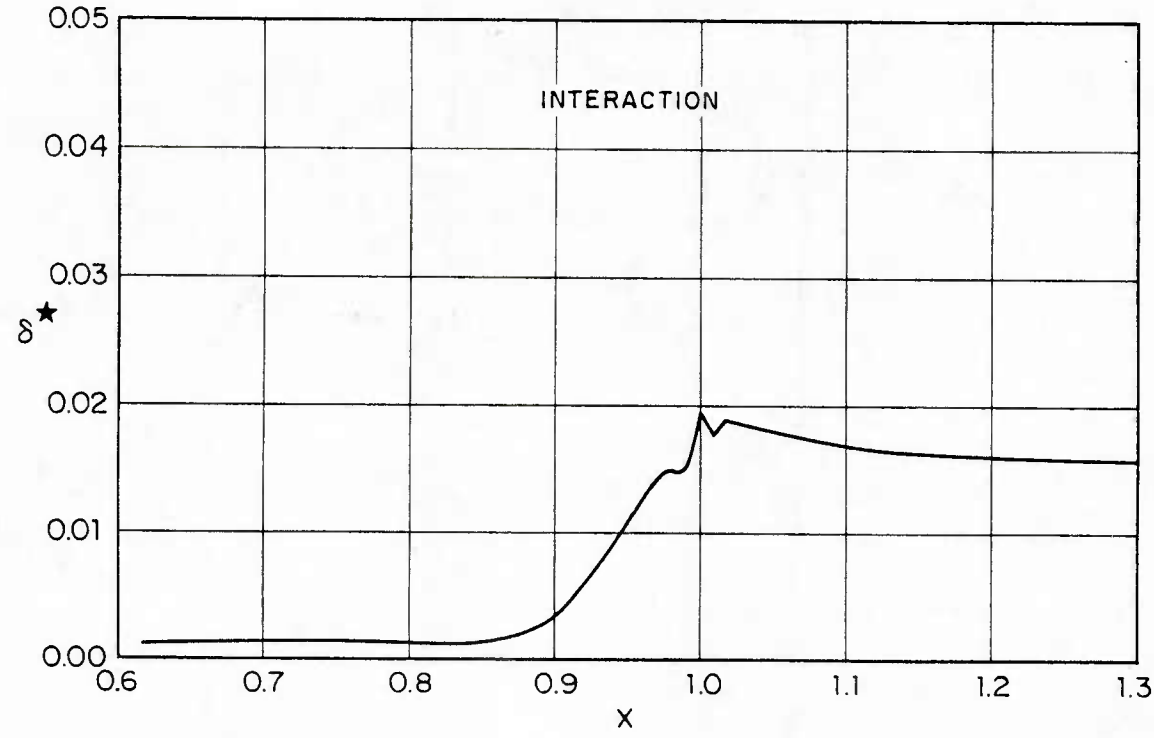

Figure 38. Displacement Thickness

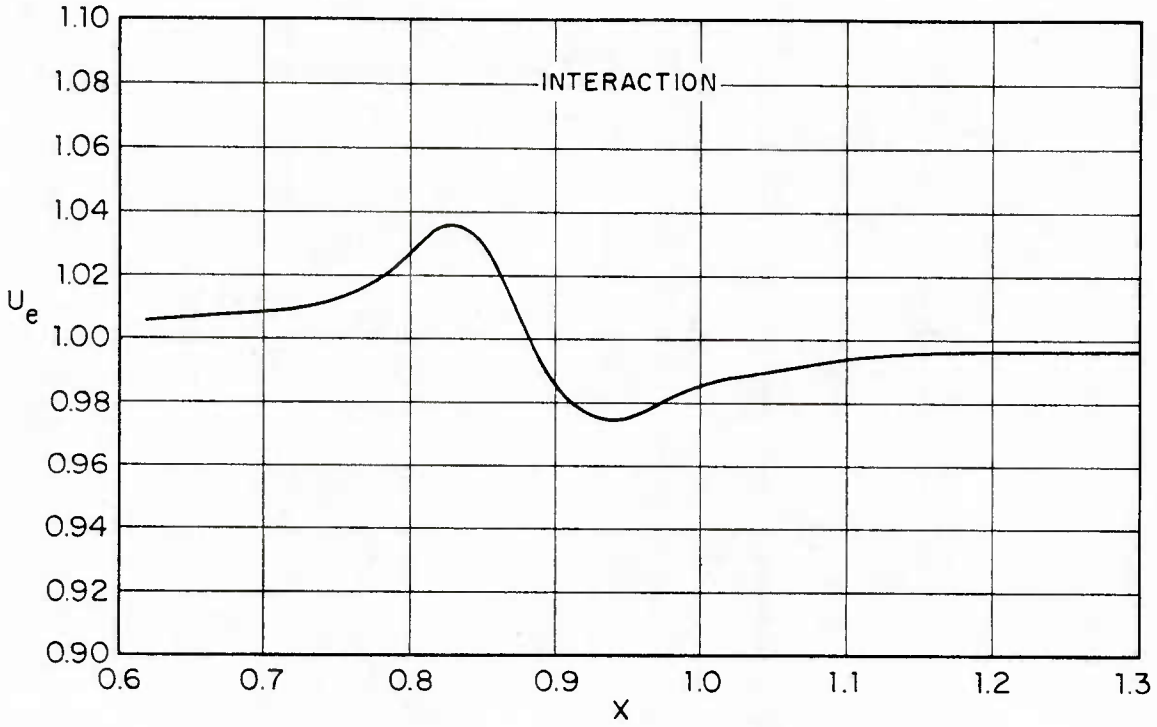

Figure 39. Edge Velocity

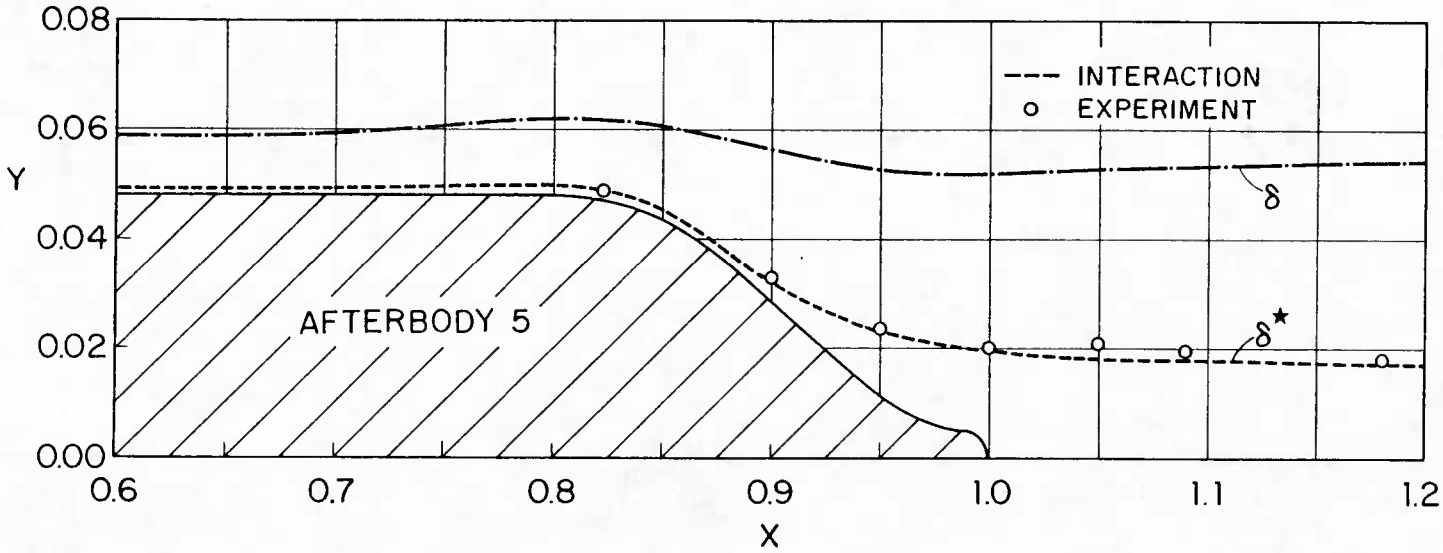

Figure 40. Boundary Layer and Displacement Thicknesses

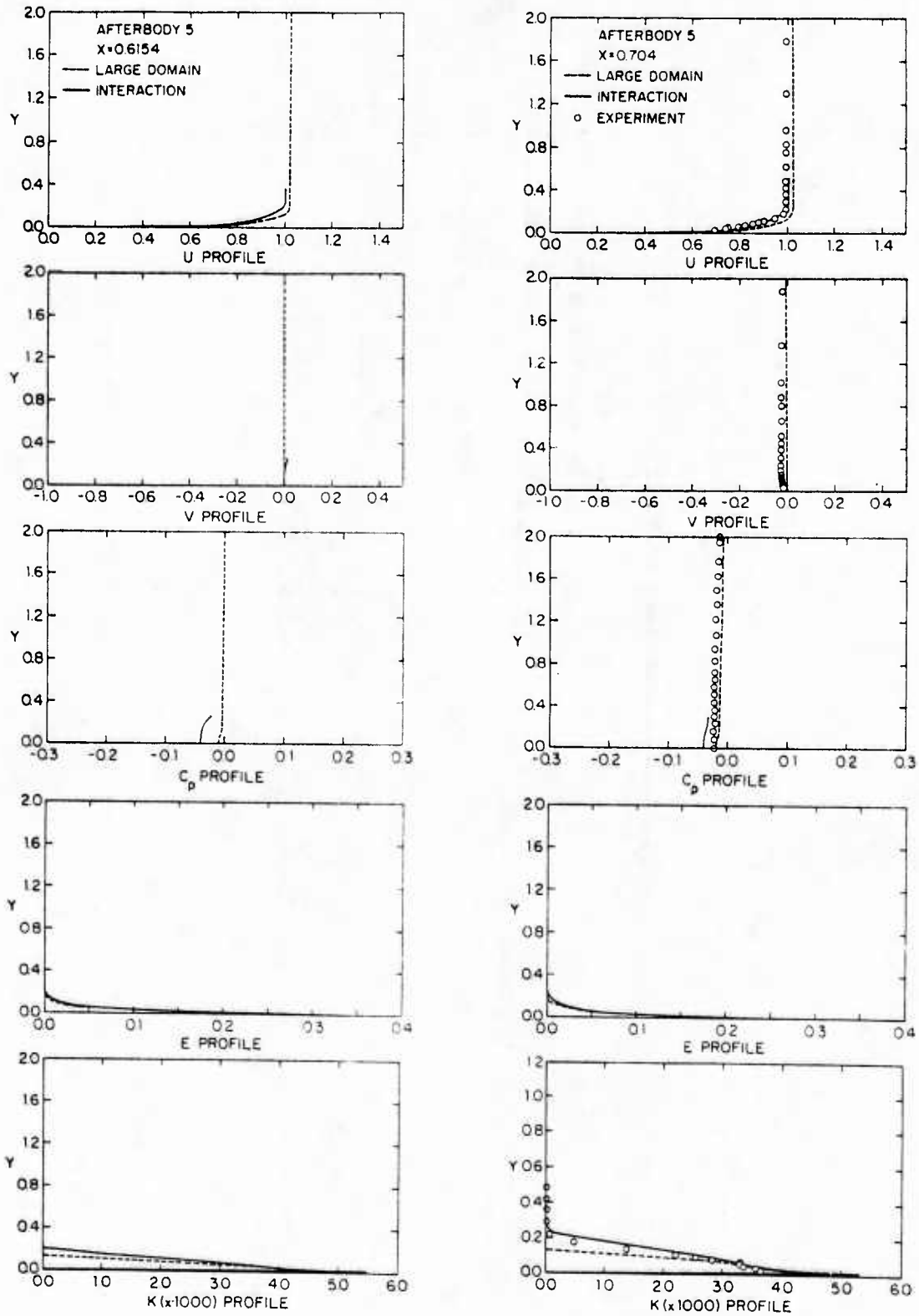

Figure 41. Solution Profiles

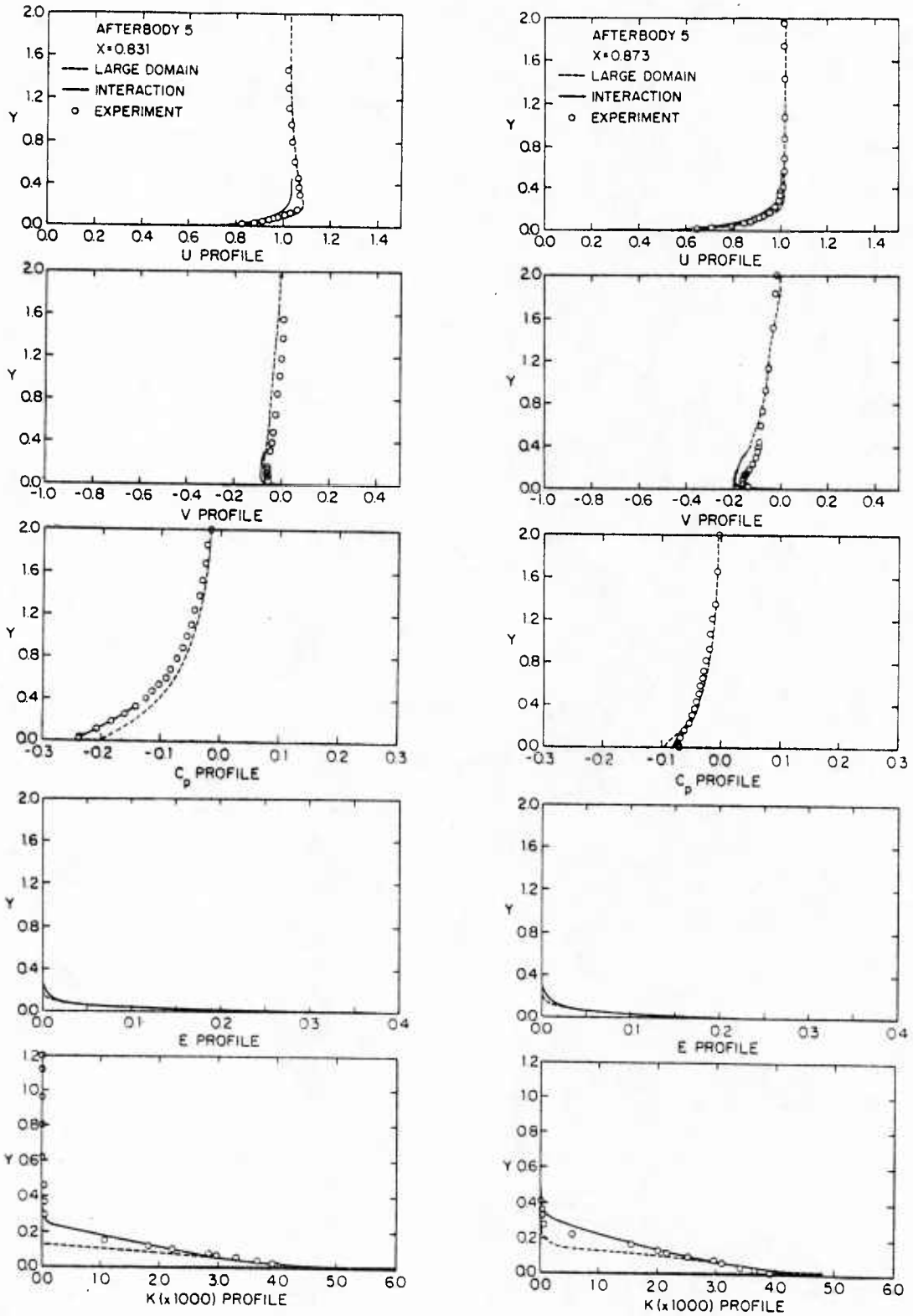

Figure 41. (Continued).

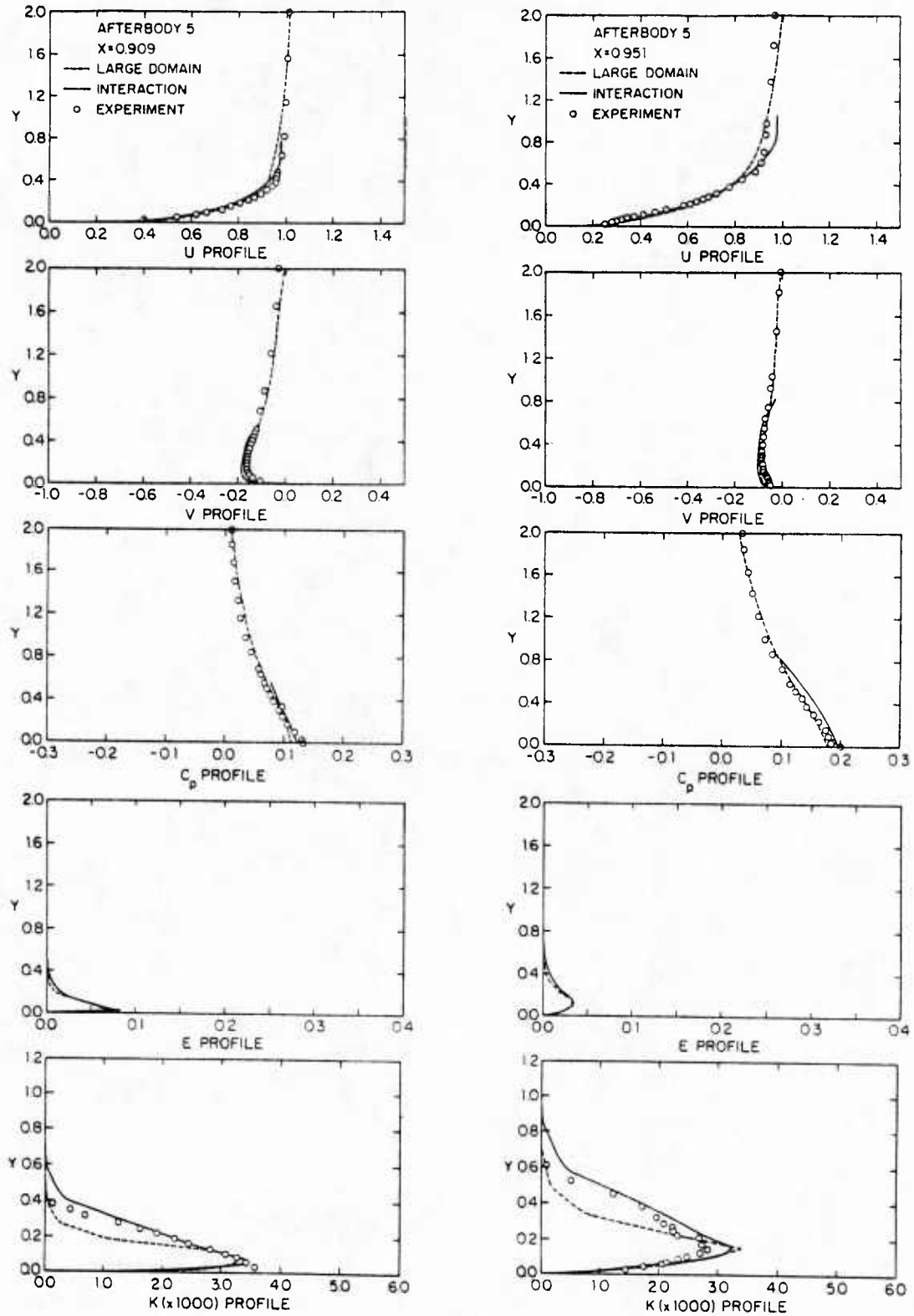

Figure 41. (Continued)

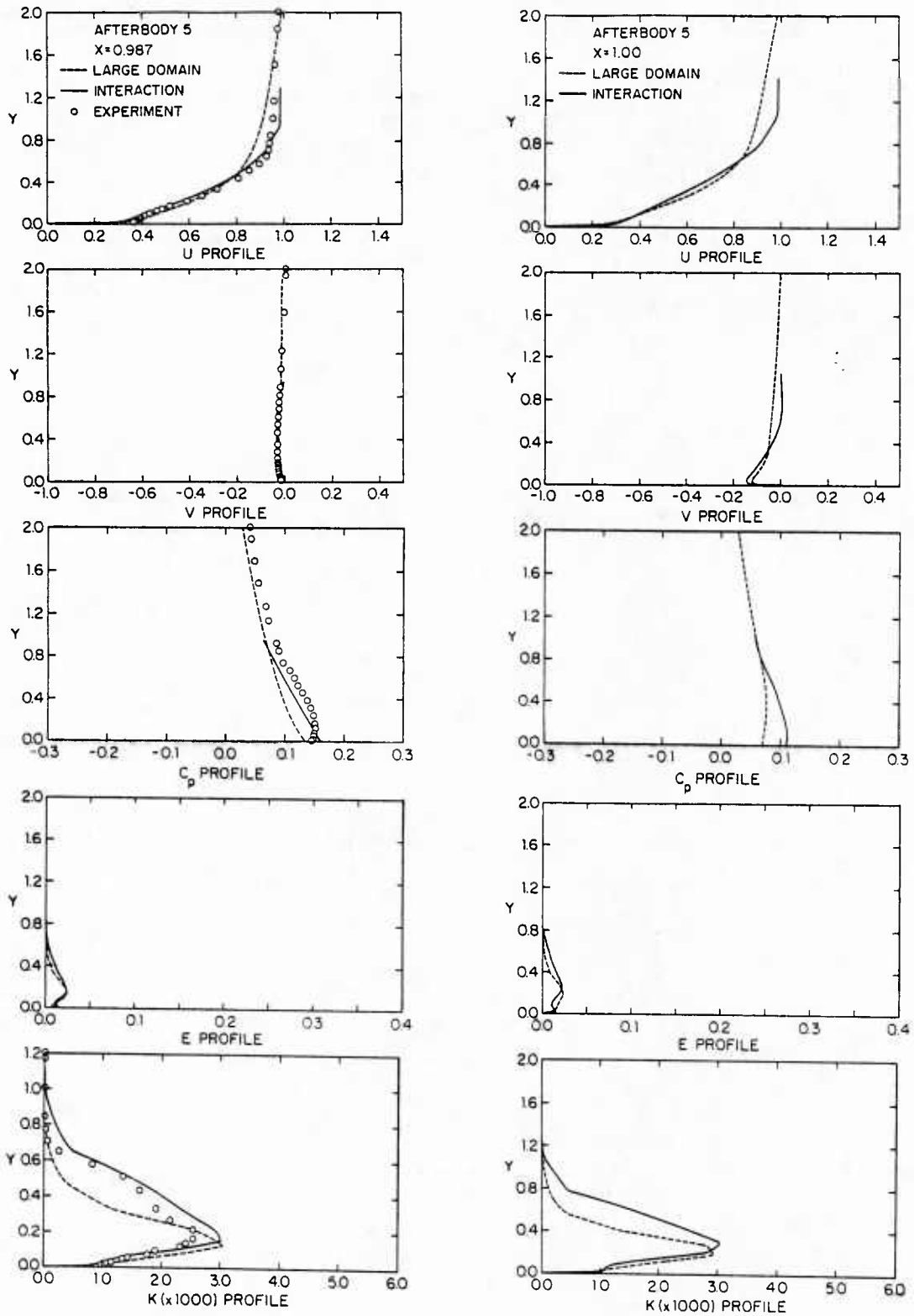

Figure 41. (Continued)

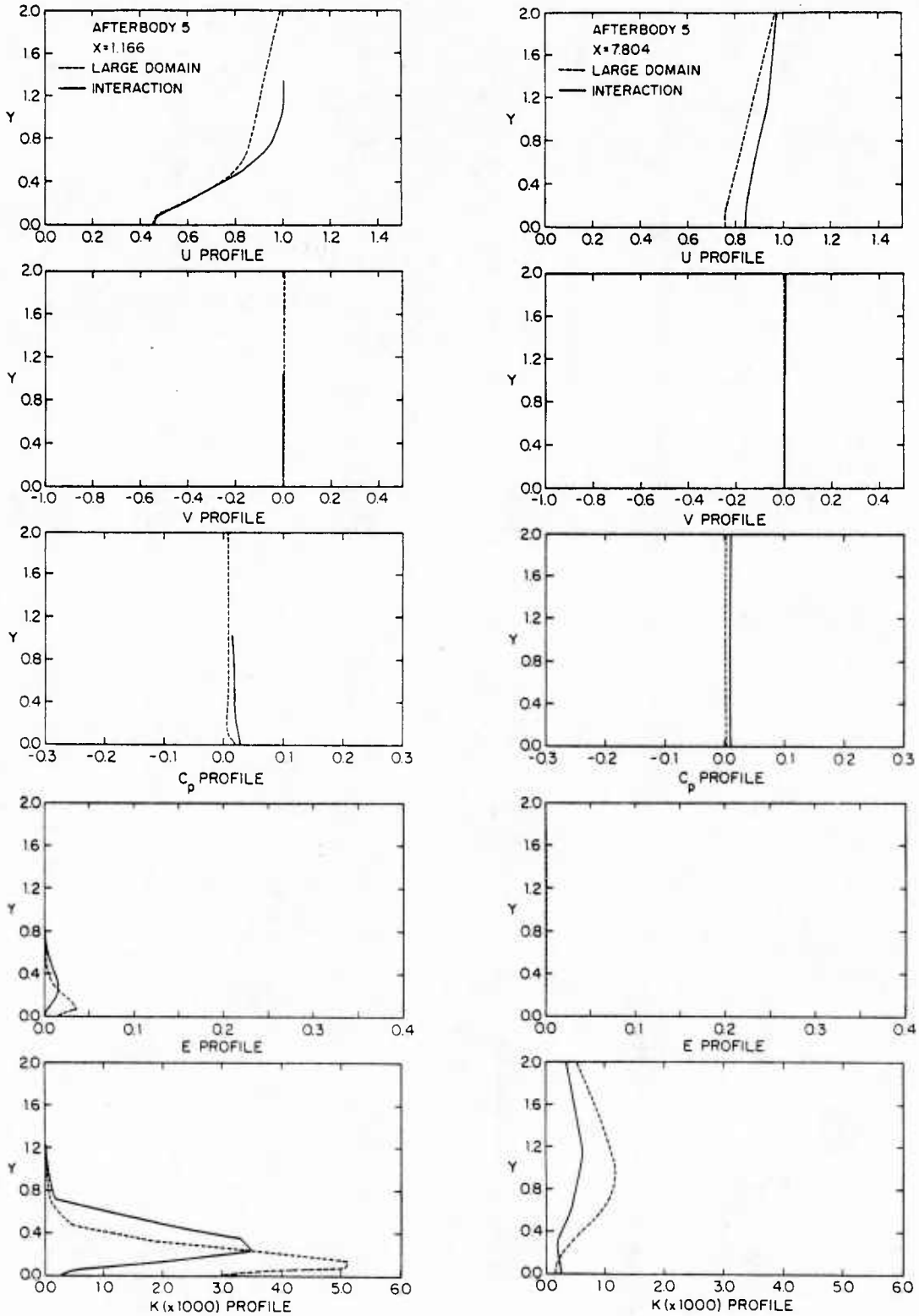

Figure 41. (Continued)

APPENDIX I: Equations in Nonorthogonal Curvilinear Coordinates

In Section IV.A the procedures for obtaining the governing equations in nonorthogonal curvilinear coordinates have been discussed. Since the resulting equations are quite lengthy they are provided in this Appendix. First, the continuity and momentum equations are presented. Subsequently, the equations of turbulent-kinetic-energy k and its dissipation-rate ε, which are used to model the Reynolds stresses in the momentum equations, are presented. The partially-parabolic forms of the Reynolds and turbulence-model equations are provided in Appendix II.

A. Continuity Equation

$$\frac{1}{h_1}\frac{\partial U}{\partial x} + \frac{1}{h_2}\frac{\partial V}{\partial y} + \frac{1}{h_3}\frac{\partial W}{\partial z} + Ua + Vb + Wc = 0 \qquad \text{(A-1)}$$

where

$$a = \frac{1}{h_1 h_2}\frac{\partial h_2}{\partial x} + \frac{1}{h_1 h_3}\frac{\partial h_3}{\partial x} + \frac{1}{h_1 S}\frac{\partial S}{\partial x}$$

$$b = \frac{1}{h_2 h_3}\frac{\partial h_3}{\partial y} + \frac{1}{h_1 h_2}\frac{\partial h_1}{\partial y} + \frac{1}{h_2 S}\frac{\partial S}{\partial y} \qquad \text{(A-2)}$$

$$c = \frac{1}{h_2 h_3}\frac{\partial h_2}{\partial z} + \frac{1}{h_1 h_3}\frac{\partial h_1}{\partial z} + \frac{1}{h_3 S}\frac{\partial S}{\partial z}$$

with

$$S = s/h_1 h_2 h_3 \qquad \text{(A-3)}$$

and s is the triple product defined by (IV-13).

B. Reynolds Equations

1. x-Momentum Equation

$$\frac{U}{h_1}\frac{\partial U}{\partial x} + \frac{V}{h_2}\frac{\partial U}{\partial y} + \frac{W}{h_3}\frac{\partial U}{\partial z} + \frac{1}{h_1}\frac{\partial \overline{u^2}}{\partial x} + \frac{1}{h_2}\frac{\partial \overline{uv}}{\partial y} + \frac{1}{h_3}\frac{\partial \overline{uw}}{\partial z} + R_1 UV + (R_1 + b)\,\overline{uv}$$

$$+ R_2(V^2 + \overline{v^2}) + R_3 (W^2 + \overline{w^2}) + R_4 U^2 + (R_4 + a)\overline{u^2} + R_5(VW + \overline{vw})$$

$$+ R_6 UW + (R_6 + c)\,\overline{uw} = -\frac{1}{\rho S^2}\left[\sin^2\lambda \frac{1}{h_1}\frac{\partial p}{\partial x} + \gamma \frac{1}{h_2}\frac{\partial p}{\partial y} + \beta \frac{1}{h_3}\frac{\partial p}{\partial z}\right]$$

$$+ \nu\left[\nabla^2 U + C_1 \frac{\partial U}{\partial x} + C_2 \frac{\partial U}{\partial y} + C_3 \frac{\partial U}{\partial z} + C_4 \frac{\partial V}{\partial x} + C_5 \frac{\partial V}{\partial y} + C_6 \frac{\partial V}{\partial z} + C_7 \frac{\partial W}{\partial x} + C_8 \frac{\partial W}{\partial y}\right.$$

$$\left. + C_9 \frac{\partial W}{\partial z} + C_{10} U + C_{11} V + C_{12} W\right] \qquad \text{(A-4)}$$

where (a,b,c) and S are given by (A-2) and (A-3), respectively, and

$$\alpha = \cos\nu \cos\mu - \cos\lambda$$

$$\beta = \cos\lambda \cos\nu - \cos\mu \qquad \text{(A-5)}$$

$$\gamma = \cos\mu \cos\lambda - \cos\nu$$

with (λ,μ,ν) defined by (IV-11). The Laplacian operator in nonorthogonal curvilinear coordinates is defined by (where Q is a scalar variable)

$$\nabla^2 Q = \frac{1}{s}\frac{\partial}{\partial x}\left[a_{11}\frac{\partial Q}{\partial x} + a_{12}\frac{\partial Q}{\partial y} + a_{13}\frac{\partial Q}{\partial z}\right] + \frac{1}{s}\frac{\partial}{\partial y}\left[a_{21}\frac{\partial Q}{\partial x} + a_{22}\frac{\partial Q}{\partial y} + a_{23}\frac{\partial Q}{\partial z}\right]$$

$$+ \frac{1}{s}\frac{\partial}{\partial z}\left[a_{31}\frac{\partial Q}{\partial x} + a_{32}\frac{\partial Q}{\partial y} + a_{33}\frac{\partial Q}{\partial z}\right] \qquad \text{(A-6)}$$

where

$$a_{11} = \frac{h_2^2 h_3^2 \sin^2\lambda}{s}, \qquad a_{12} = \frac{h_1 h_2 h_3^2 \gamma}{s}, \qquad a_{13} = \frac{h_1 h_2^2 h_3 \beta}{s}$$

$$a_{22} = \frac{h_1^2 h_3^2 \sin^2\mu}{s}, \qquad a_{23} = \frac{h_1^2 h_2 h_3 \alpha}{s}, \qquad a_{33} = \frac{h_1^2 h_2^2 \sin^2\nu}{s} \tag{A-7}$$

and $a_{ij} = a_{ji}$ for $i \neq j$. The R_i $(i = 1,6)$ and C_i $(i = 1, 12)$ coefficients are:

$$R_1 = \frac{\beta}{S^2}\left[\frac{1}{h_2 h_3}\frac{\partial}{\partial y}(h_3 \cos\mu) - \frac{1}{h_2 h_3}\frac{\partial}{\partial z}(h_2 \cos\nu) - \frac{\cos\nu}{h_1 h_3}\frac{\partial h_1}{\partial z} + \frac{1}{h_1 h_3}\frac{\partial}{\partial x}(h_3 \cos\lambda)\right]$$
$$+ \frac{(\gamma - \cos\nu \sin^2\lambda)}{h_1 h_2 S^2}\frac{\partial h_2}{\partial x} + \frac{(\sin^2\lambda - \gamma\cos\nu)}{h_1 h_2 S^2}\frac{\partial h_1}{\partial y} \tag{A-8}$$

$$R_2 = \frac{\beta}{h_2 h_3 S^2}\left[\frac{\partial(h_3 \cos\lambda)}{\partial y} - \frac{\partial h_2}{\partial z}\right] - \frac{\sin^2\lambda}{h_1 h_2 S^2}\left[\frac{\partial h_2}{\partial x} - \frac{\partial}{\partial y}(h_1 \cos\nu)\right] \tag{A-9}$$

$$R_3 = \frac{\sin^2\lambda}{h_1 h_3 S^2}\left[\frac{\partial}{\partial z}(h_1 \cos\mu) - \frac{\partial h_3}{\partial x}\right] - \frac{\gamma}{h_2 h_3 S^2}\left[\frac{\partial h_3}{\partial y} - \frac{\partial}{\partial z}(h_2 \cos\lambda)\right] \tag{A-10}$$

$$R_4 = \frac{\beta}{h_1 h_3 S^2}\left[\frac{\partial}{\partial x}(h_3 \cos\mu) - \frac{\partial h_1}{\partial z}\right] - \frac{\gamma}{h_1 h_2 S^2}\left[\frac{\partial h_1}{\partial y} - \frac{\partial}{\partial x}(h_2 \cos\nu)\right] \tag{A-11}$$

$$R_5 = \frac{\beta}{h_2 h_3 S^2}\left[\frac{\partial h_3}{\partial y} - \cos\lambda\frac{\partial h_2}{\partial z}\right] - \frac{\sin^2\lambda}{h_1 h_2 S^2}\left[\cos\lambda\frac{\partial h_2}{\partial x} - \frac{\partial}{\partial y}(h_1 \cos\mu)\right] + \frac{\sin^2\lambda}{h_1 h_3 S^2}$$
$$\left[\frac{\partial}{\partial z}(h_1 \cos\nu) - \frac{\partial}{\partial x}(h_3 \cos\lambda)\right] - \frac{\gamma}{h_2 h_3 S^2}\left[\cos\lambda\frac{\partial h_3}{\partial y} - \frac{\partial h_2}{\partial z}\right] \tag{A-12}$$

$$R_6 = \frac{\sin^2\lambda}{h_1 h_3 S^2}\left[\frac{\partial h_1}{\partial z} - \cos\mu\frac{\partial h_3}{\partial x}\right] - \frac{\beta}{h_1 h_3 S^2}\left[\cos\mu\frac{\partial h_1}{\partial z} - \frac{\partial h_3}{\partial x}\right] - \frac{\gamma}{h_2 h_3 S^2}\left[\cos\mu\frac{\partial h_3}{\partial y}\right.$$
$$\left. - \frac{\partial}{\partial z}(h_2 \cos\nu)\right] + \frac{\gamma}{h_1 h_2 S^2}\left[\frac{\partial}{\partial x}(h_2 \cos\lambda) - \frac{\partial}{\partial y}(h_1 \cos\mu)\right] \tag{A-13}$$

$$C_1 = -\frac{1}{s h_1}\left[\frac{\partial}{\partial x}\left(\frac{h_1 h_2^2 h_3^2 \sin^2\lambda}{s}\right) + \frac{\partial}{\partial y}\left(\frac{h_1^2 h_2 h_3^2 \gamma}{s}\right) + \frac{\partial}{\partial z}\left(\frac{h_1^2 h_2^2 h_3 \beta}{s}\right)\right]$$
$$+ \frac{h_1 h_2^2 h_3^2 \sin^2\lambda}{s^3}\frac{\partial}{\partial x}\left(\frac{s}{h_1}\right) + \frac{h_1 h_2 h_3 \cos\nu}{s^2}\left[\frac{\partial}{\partial z}(h_2 \cos\lambda) - \frac{\partial h_3}{\partial y}\right]$$

$$+\frac{h_1h_2h_3\cos\mu}{s^2}\left[\frac{\partial}{\partial y}(h_3\cos\lambda)-\frac{\partial h_2}{\partial z}\right]+\frac{h_1h_3}{s}\left[\cos\lambda\frac{\partial}{\partial y}\left(\frac{h_2h_3\cos\mu}{s}\right)\right.$$

$$\left.-\frac{\partial}{\partial y}\left(\frac{h_2h_3\cos\nu}{s}\right)\right]+\frac{h_1h_2}{s}\left[\cos\lambda\frac{\partial}{\partial z}\left(\frac{h_2h_3\cos\nu}{s}\right)-\frac{\partial}{\partial z}\left(\frac{h_2h_3\cos\mu}{s}\right)\right] \tag{A-14}$$

$$C_2=\frac{2h_1^2h_3\cos\mu}{s^2}\left[\frac{\partial}{\partial z}(h_2\cos\nu)-\frac{\partial}{\partial y}(h_3\cos\mu)\right]+\frac{h_1h_2h_3\cos\lambda}{s^2}$$

$$\left[\frac{\partial}{\partial x}(h_3\cos\mu)-\frac{\partial h_1}{\partial z}\right]+\frac{h_1h_3}{s^2}\left[\frac{\partial}{\partial z}(h_1h_2\cos\lambda)-\cos\mu\frac{\partial}{\partial z}(h_1h_2\cos\nu)\right]$$

$$-\frac{h_1h_3}{s^2}\left[h_3\frac{\partial}{\partial x}(h_2\cos\nu)+h_1\frac{\partial}{\partial z}(h_2\cos\lambda)\right]+\frac{h_1h_3\cos\mu}{s^2}\frac{\partial}{\partial y}(h_1h_3\cos\mu)$$

$$+\frac{h_1^2h_2h_3^2\gamma}{s^3}\frac{\partial}{\partial x}\left(\frac{s}{h_1}\right)-\frac{1}{s}\frac{\partial}{\partial x}\left(\frac{h_1h_2h_3^2\gamma}{s}\right) \tag{A-15}$$

$$C_3=\frac{h_1^2h_2^2h_3\beta}{s^3}\frac{\partial}{\partial x}\left(\frac{s}{h_1}\right)+\frac{h_1h_2}{s^2}\left[\frac{\partial}{\partial y}(h_1h_3\cos\lambda)-\cos\nu\frac{\partial}{\partial y}(h_1h_3\cos\mu)\right]$$

$$+\frac{h_1^2h_2}{s^2}\left[\cos\nu\frac{\partial}{\partial y}(h_3\cos\mu)-\frac{\partial}{\partial y}(h_3\cos\lambda)\right]+\frac{h_1^2h_2\cos\nu}{s^2}\left[\frac{\partial}{\partial y}(h_3\cos\mu)\right.$$

$$\left.-\frac{\partial}{\partial z}(h_2\cos\nu)\right]+\frac{h_1h_2^2}{s^2}\left[\cos^2\nu\frac{\partial h_1}{\partial z}-\frac{\partial}{\partial x}(h_3\cos\mu)\right]-\frac{1}{s}\frac{\partial}{\partial x}\left(\frac{h_1h_2^2h_3\beta}{s}\right)$$

$$+\frac{h_1h_2h_3\cos\lambda}{s^2}\left[\frac{\partial}{\partial x}(h_2\cos\nu)-\frac{\partial h_1}{\partial y}\right] \tag{A-16}$$

$$C_4=\frac{h_1h_2^2h_3^2\sin^2\lambda}{s^3}\frac{\partial}{\partial y}\left(\frac{s}{h_2}\right)+\frac{h_1h_3}{s}\left[\cos\lambda\frac{\partial}{\partial y}\left(\frac{h_2h_3\cos\lambda}{s}\right)-\frac{\partial}{\partial y}\left(\frac{h_2h_3}{s}\right)\right]$$

$$+\frac{h_1h_2}{s}\left[\cos\lambda\frac{\partial}{\partial z}\left(\frac{h_2h_3}{s}\right)-\frac{\partial}{\partial z}\left(\frac{h_2h_3\cos\lambda}{s}\right)\right]+\frac{h_1h_2h_3\cos\lambda}{s^2}\left[\frac{\partial}{\partial y}(h_3\cos\lambda)\right.$$

$$\left.-\frac{\partial h_2}{\partial z}\right]+\frac{h_1h_2h_3}{s^2}\left[\frac{\partial}{\partial z}(h_2\cos\lambda)-\frac{\partial h_3}{\partial y}\right] \tag{A-17}$$

$$C_5 = -\frac{h_1 h_3^2 \sin^2\lambda}{s^2}\frac{\partial h_2}{\partial x} + \frac{h_1^2 h_2 h_3^2 \gamma}{s^2}\left[\frac{1}{s}\frac{\partial}{\partial y}\left(\frac{s}{h_2}\right) - \frac{1}{h_2^2}\frac{\partial h_2}{\partial y}\right] - \frac{h_1^2 h_3 \beta}{s^2}\frac{\partial h_2}{\partial z}$$

$$- \frac{h_1 h_3 \cos\mu}{s}\left[\frac{h_1}{s}\frac{\partial}{\partial y}(h_3\cos\lambda) + \frac{\partial}{\partial y}\left(\frac{h_1 h_3 \cos\lambda}{s}\right) - \frac{h_1}{s}\frac{\partial h_2}{\partial z}\right] - \frac{h_1 h_3 \cos\lambda}{s}$$

$$\left[\frac{h_2}{s}\frac{\partial}{\partial y}(h_1\cos\nu) - \frac{h_2}{s}\frac{\partial}{\partial x}(h_3\cos\lambda)\right] - \frac{h_1 h_3}{s}\left[\frac{h_3}{s}\frac{\partial h_2}{\partial x} - \frac{h_3}{s}\frac{\partial}{\partial y}(h_1\cos\nu)\right.$$

$$\left. - \frac{\partial}{\partial y}\left(\frac{h_1 h_3 \cos\nu}{s}\right)\right] + \frac{h_1^2 h_3}{s^2}\left[\cos\nu\frac{\partial h_3}{\partial y} - \cos\lambda\frac{\partial}{\partial y}(h_3\cos\mu)\right]$$

$$+ \frac{h_1 h_2}{s}\left[\cos\nu\frac{\partial}{\partial z}\left(\frac{h_1 h_3 \cos\lambda}{s}\right) - \cos\lambda\frac{\partial}{\partial z}\left(\frac{h_1 h_3 \cos\nu}{s}\right)\right]$$

$$+ \frac{h_1^2 h_3}{s^2}\left[\cos\lambda\frac{\partial}{\partial z}(h_2\cos\nu) - \cos\nu\frac{\partial}{\partial z}(h_2\cos\lambda)\right] \qquad \text{(A-18)}$$

$$C_6 = \frac{h_1^2 h_2^2 h_3 \beta}{s^3}\frac{\partial}{\partial y}\left(\frac{s}{h_2}\right) + \frac{h_1 h_3}{s}\left[\cos\mu\frac{\partial}{\partial y}\left(\frac{h_1 h_2}{s}\right) - \cos\lambda\frac{\partial}{\partial y}\left(\frac{h_1 h_2 \cos\nu}{s}\right)\right]$$

$$+ \frac{h_1^2 h_2}{s^2}\left[\frac{\partial}{\partial y}(h_3\cos\mu) - \frac{\partial}{\partial z}(h_2\cos\nu)\right] + \frac{h_1^2 h_2 \cos\nu}{s^2}\left[\frac{\partial h_2}{\partial z} - \frac{\partial}{\partial y}(h_3\cos\lambda)\right]$$

$$+ \frac{h_1 h_2 \cos\nu}{s}\left[\frac{h_1}{s}\frac{\partial}{\partial y}(h_3\cos\lambda) - \frac{h_1}{s}\frac{\partial h_2}{\partial z} - \frac{\partial}{\partial z}\left(\frac{h_1 h_2}{s}\right)\right] + \frac{h_1 h_2}{s}\left[\frac{h_2}{s}\frac{\partial}{\partial z}(h_1\cos\nu)\right.$$

$$\left. + \frac{\partial}{\partial z}\left(\frac{h_1 h_2 \cos\nu}{s}\right) - \frac{h_2}{s}\frac{\partial}{\partial x}(h_3\cos\lambda)\right] + \frac{h_1 h_2 h_3 \cos\lambda}{s^2}\left[\frac{\partial h_2}{\partial x} - \frac{\partial}{\partial y}(h_1\cos\nu)\right]$$

(A-19)

$$C_7 = \frac{h_1 h_2}{s}\left[\cos\lambda\frac{\partial}{\partial z}\left(\frac{h_2 h_3 \cos\lambda}{s}\right) - \frac{\partial}{\partial z}\left(\frac{h_2 h_3}{s}\right)\right] + \frac{h_1 h_2^2 h_3^2 \sin^2\lambda}{s^3}\frac{\partial}{\partial z}\left(\frac{s}{h_3}\right)$$

$$+ \frac{h_1 h_2 h_3}{s^2}\left[\cos\lambda\frac{\partial}{\partial z}(h_2\cos\lambda) - \frac{\partial h_2}{\partial z}\right] \qquad \text{(A-20)}$$

$$C_8 = \frac{h_1^2 h_2 h_3^2 \gamma}{s^3}\frac{\partial}{\partial z}\left(\frac{s}{h_3}\right) - \frac{h_1 h_2 h_3 \cos\lambda}{s^2}\left[\frac{\partial}{\partial z}(h_1\cos\mu) - \frac{\partial h_3}{\partial x}\right] - \frac{h_1 h_3^2}{s^2}$$

$$[\frac{\partial}{\partial x}(h_2\cos\lambda) - \frac{\partial}{\partial y}(h_1\cos\mu)] + \frac{h_1h_2}{s}[\cos\nu\,\frac{\partial}{\partial z}(\frac{h_1h_3}{s}) - \cos\lambda\,\frac{\partial}{\partial z}$$

$$(\frac{h_1h_3\cos\mu}{s})] + \frac{h_1^2h_3}{s^2}[\frac{\partial}{\partial z}(h_2\cos\nu) - \cos\mu\,\frac{\partial h_3}{\partial y}] \qquad \text{(A-21)}$$

$$C_9 = -\frac{h_1h_2}{s^2}[h_2\sin^2\lambda\,\frac{\partial h_3}{\partial x} + h_1\gamma\,\frac{\partial h_3}{\partial y} + \frac{h_1h_2\beta}{h_3}\,\frac{\partial h_3}{\partial z}] + \frac{h_1^2h_2h_3\beta}{s^3}\,\frac{\partial}{\partial z}(\frac{s}{h_3})$$

$$+ \frac{h_1h_3}{s}[\cos\mu\,\frac{\partial}{\partial y}(\frac{h_1h_2\cos\lambda}{s}) - \cos\lambda\,\frac{\partial}{\partial y}(\frac{h_1h_2\cos\mu}{s})] + \frac{h_1^2h_2\cos\nu}{s^2}[\frac{\partial h_3}{\partial y}$$

$$- \frac{\partial}{\partial z}(h_2\cos\lambda)] + \frac{h_1^2h_2}{s^2}[\cos\lambda\,\frac{\partial}{\partial y}(h_3\cos\mu) - \cos\mu\,\frac{\partial}{\partial y}(h_3\cos\lambda)$$

$$- \cos\lambda\,\frac{\partial}{\partial z}(h_2\cos\nu) + \cos\mu\,\frac{\partial h_2}{\partial z}] + \frac{h_1h_2^2}{s^2}[\frac{\partial}{\partial z}(h_1\cos\mu) - \frac{\partial h_3}{\partial x}]$$

$$+ \frac{h_1h_2}{s}[\frac{\partial}{\partial z}(\frac{h_1h_2\cos\mu}{s}) - \cos\nu\,\frac{\partial}{\partial z}(\frac{h_1h_2\cos\lambda}{s})]$$

$$+ \frac{h_1h_2h_3\cos\lambda}{s^2}[\frac{\partial}{\partial x}(h_2\cos\lambda) - \frac{\partial}{\partial y}(h_1\cos\mu)] \qquad \text{(A-22)}$$

$$C_{10} = \frac{h_1h_2h_3}{s^2}[h_2h_3\sin^2\lambda\,\frac{\partial}{\partial x}\{\frac{1}{s}\frac{\partial}{\partial x}(\frac{s}{h_1})\} + h_2h_3\gamma\,\frac{\partial}{\partial y}\{\frac{1}{s}\frac{\partial}{\partial x}(\frac{s}{h_1})\} + h_1h_2\beta\,\frac{\partial}{\partial z}$$

$$\{\frac{1}{s}\frac{\partial}{\partial x}(\frac{s}{h_1})\}] + \frac{h_1}{s}[\frac{\partial}{\partial y}\{\frac{h_1h_3\cos\mu}{s}(\frac{\partial}{\partial z}(h_2\cos\nu) - \frac{\partial}{\partial y}(h_3\cos\mu))\}$$

$$+ \frac{\partial}{\partial y}\{\frac{h_2h_3\cos\lambda}{s}(\frac{\partial}{\partial x}(h_3\cos\mu) - \frac{\partial h_1}{\partial z})\} + \frac{\partial}{\partial y}\{\frac{h_3^2}{s}(\frac{\partial h_1}{\partial y} - \frac{\partial}{\partial x}(h_2\cos\nu))\} +$$

$$+ \frac{\partial}{\partial z}\{\frac{h_1h_2\cos\nu}{s}(\frac{\partial}{\partial y}(h_3\cos\mu) - \frac{\partial}{\partial z}(h_2\cos\nu))\} + \frac{\partial}{\partial z}\{\frac{h_2^2}{s}(\frac{\partial h_1}{\partial z}$$

$$- \frac{\partial}{\partial x}(h_3\cos\mu))\} + \frac{\partial}{\partial z}\{\frac{h_2h_3\cos\lambda}{s}(\frac{\partial}{\partial x}(h_2\cos\nu) - \frac{\partial h_1}{\partial y})\}] \qquad \text{(A-23)}$$

$$C_{11} = \frac{h_1 h_2 h_3}{s^2} [h_2 h_3 \sin^2\lambda \frac{\partial}{\partial x} \{\frac{1}{s} \frac{\partial}{\partial y} (\frac{s}{h_2})\} + h_1 h_3 \gamma \frac{\partial}{\partial y} \{\frac{1}{s} \frac{\partial}{\partial y} (\frac{s}{h_2})\} +$$

$$+ h_1 h_2 \beta \frac{\partial}{\partial z} \{\frac{1}{s} \frac{\partial}{\partial y} (\frac{s}{h_2})\}] + \frac{h_1}{s} [\frac{\partial}{\partial y} \{\frac{h_1 h_3 \cos\mu}{s} (\frac{\partial h_2}{\partial z} - \frac{\partial}{\partial y} (h_3 \cos\lambda))\}$$

$$+ \frac{\partial}{\partial y} \{\frac{h_2 h_3 \cos\lambda}{s} (\frac{\partial}{\partial x} (h_3 \cos\lambda) - \frac{\partial}{\partial z} (h_1 \cos\nu))\} + \frac{\partial}{\partial y} \{\frac{h_3^2}{s} (\frac{\partial}{\partial y} (h_1 \cos\nu) - \frac{\partial h_2}{\partial x})\}$$

$$+ \frac{\partial}{\partial z} \{\frac{h_1 h_2 \cos\nu}{s} (\frac{\partial}{\partial y} (h_3 \cos\lambda) - \frac{\partial h_2}{\partial z})\} + \frac{\partial}{\partial z} \{\frac{h_2^2}{s} (\frac{\partial}{\partial z} (h_1 \cos\nu)$$

$$- \frac{\partial}{\partial x} (h_3 \cos\lambda))\} + \frac{\partial}{\partial z} \{\frac{h_2 h_3 \cos\lambda}{s} (\frac{\partial h_2}{\partial x} - \frac{\partial}{\partial y} (h_1 \cos\nu))\}] \qquad \text{(A-24)}$$

$$C_{12} = \frac{h_1 h_2 h_3}{s^2} [h_2 h_3 \sin^2\lambda \frac{\partial}{\partial x} \{\frac{1}{s} \frac{\partial}{\partial z} (\frac{s}{h_3})\} + h_1 h_3 \gamma \frac{\partial}{\partial y} \{\frac{1}{s} \frac{\partial}{\partial z} (\frac{s}{h_3})\}$$

$$+ h_1 h_2 \beta \frac{\partial}{\partial z} \{\frac{1}{s} \frac{\partial}{\partial z} (\frac{s}{h_3})\}] + \frac{h_1}{s} [\frac{\partial}{\partial y} \{\frac{h_1 h_3 \cos\mu}{s} (\frac{\partial}{\partial z} (h_2 \cos\lambda) - \frac{\partial h_3}{\partial y})\}$$

$$+ \frac{\partial}{\partial y} \{\frac{h_2 h_3 \cos\lambda}{s} (\frac{\partial h_3}{\partial x} - \frac{\partial}{\partial z} (h_1 \cos\mu))\} + \frac{\partial}{\partial y} \{\frac{h_3^2}{s} (\frac{\partial}{\partial y} (h_1 \cos\mu) \frac{\partial}{\partial x} (h_2 \cos\lambda))\}$$

$$+ \frac{\partial}{\partial z} \{\frac{h_1 h_2 \cos\nu}{s} (\frac{\partial h_3}{\partial y} - \frac{\partial}{\partial z} (h_2 \cos\lambda))\} + \frac{\partial}{\partial z} \{\frac{h_2^2}{s} (\frac{\partial}{\partial z} (h_1 \cos\mu) - \frac{\partial h_3}{\partial x})\}$$

$$+ \frac{\partial}{\partial z} \{\frac{h_2 h_3 \cos\lambda}{s} (\frac{\partial}{\partial x} (h_2 \cos\lambda) - \frac{\partial}{\partial y} (h_1 \cos\mu))\}] \qquad \text{(A-25)}$$

2. y-Momentum Equation

$$\frac{U}{h_1}\frac{\partial V}{\partial x} + \frac{V}{h_2}\frac{\partial V}{\partial y} + \frac{W}{h_3}\frac{\partial V}{\partial z} + \frac{1}{h_1}\frac{\partial \overline{uv}}{\partial x} + \frac{1}{h_2}\frac{\partial \overline{v^2}}{\partial y} + \frac{1}{h_3}\frac{\partial \overline{vw}}{\partial z} + S_1 VW + (S_1+c)\,\overline{vw}$$

$$+ S_2(W^2 + \overline{w^2}) + S_3(U^2 + \overline{u^2}) + S_4 V^2 + (S_4+b)\,\overline{v^2} + S_5(UW + \overline{uw}) + S_6 UV$$

$$+ (S_6+a)\,\overline{uv} = -\frac{1}{\rho S^2}\left[\sin^2\mu\,\frac{1}{h_2}\frac{\partial p}{\partial y} + \alpha\,\frac{1}{h_3}\frac{\partial p}{\partial z} + \gamma\,\frac{1}{h_1}\frac{\partial p}{\partial x}\right] + \nu\left[\nabla^2 V + D_1\frac{\partial V}{\partial y}\right.$$

$$+ D_2\frac{\partial V}{\partial z} + D_3\frac{\partial V}{\partial x} + D_4\frac{\partial W}{\partial y} + D_5\frac{\partial W}{\partial z} + D_6\frac{\partial W}{\partial x} + D_7\frac{\partial U}{\partial y} + D_8\frac{\partial U}{\partial z} + D_9\frac{\partial U}{\partial x}$$

$$\left. + D_{10}V + D_{11}W + D_{12}U\right] \qquad \text{(A-26)}$$

where (a,b,c), S, (α,β,γ), and $\nabla^2 V$ are given by (A-2), (A-3), (A-5) and (A-6) respectively. The S_i (i = 1, 6) and the D_i (i = 1,12) coefficients are given by

$$S_1 = \frac{\gamma}{S^2}\left[\frac{1}{h_1 h_3}\frac{\partial}{\partial z}(h_1\cos\nu) - \frac{1}{h_1 h_3}\frac{\partial}{\partial x}(h_3\cos\lambda) - \frac{\cos\lambda}{h_1 h_2}\frac{\partial h_2}{\partial x} + \frac{1}{h_1 h_2}\frac{\partial}{\partial y}(h_1\cos\mu)\right]$$

$$+ \frac{(\alpha - \cos\lambda\sin^2\mu)}{h_2 h_3 S^2}\frac{\partial h_3}{\partial y} + \frac{(\sin^2\mu - \alpha\cos\lambda)}{h_2 h_3 S^2}\frac{\partial h_2}{\partial z} \qquad \text{(A-27)}$$

$$S_2 = \frac{\gamma}{h_1 h_3 S^2}\left[\frac{\partial}{\partial z}(h_1\cos\mu) - \frac{\partial h_3}{\partial x}\right] - \frac{\sin^2\mu}{h_2 h_3 S^2}\left[\frac{\partial h_3}{\partial y} - \frac{\partial}{\partial z}(h_2\cos\lambda)\right] \qquad \text{(A-28)}$$

$$S_3 = \frac{\sin^2\mu}{h_2 h_1 S^2}\left[\frac{\partial}{\partial x}(h_2\cos\nu) - \frac{\partial h_1}{\partial y}\right] - \frac{\alpha}{h_3 h_1 S^2}\left[\frac{\partial h_1}{\partial z} - \frac{\partial}{\partial x}(h_3\cos\mu)\right] \qquad \text{(A-29)}$$

$$S_4 = \frac{\gamma}{h_1 h_2 S^2}\left[\frac{\partial}{\partial y}(h_1\cos\nu) - \frac{\partial h_2}{\partial x}\right] - \frac{\alpha}{h_2 h_3 S^2}\left[\frac{\partial h_2}{\partial z} - \frac{\partial}{\partial y}(h_3\cos\lambda)\right] \qquad \text{(A-30)}$$

$$S_5 = \frac{\gamma}{h_3 h_1 S^2}\left[\frac{\partial h_1}{\partial z} - \cos\mu\,\frac{\partial h_3}{\partial x}\right] - \frac{\sin^2\mu}{h_2 h_3 S^2}\left[\cos\mu\,\frac{\partial h_3}{\partial y} - \frac{\partial}{\partial z}(h_2\cos\nu)\right]$$

$$+ \frac{\sin^2\mu}{h_2 h_1 S^2}\left[\frac{\partial}{\partial x}(h_2\cos\lambda) - \frac{\partial}{\partial y}(h_1\cos\mu)\right] - \frac{\alpha}{h_1 h_3 S^2}\left[\cos\mu\,\frac{\partial h_1}{\partial z} - \frac{\partial h_3}{\partial x}\right] \qquad \text{(A-31)}$$

$$S_6 = \frac{\sin^2\mu}{h_2 h_1 S^2}\left[\frac{\partial h_2}{\partial x} - \cos\nu\,\frac{\partial h_1}{\partial y}\right] - \frac{\gamma}{h_1 h_2 S^2}\left[\cos\nu\,\frac{\partial h_2}{\partial x} - \frac{\partial h_1}{\partial y}\right] - \frac{\alpha}{h_3 h_1 S^2}$$

$$\left[\cos\nu\,\frac{\partial h_1}{\partial z} - \frac{\partial}{\partial x}(h_3\cos\lambda)\right] + \frac{\alpha}{h_2 h_3 S^2}\left[\frac{\partial}{\partial y}(h_3\cos\mu) - \frac{\partial}{\partial z}(h_2\cos\nu)\right] \qquad \text{(A-32)}$$

$$D_1 = -\frac{1}{s h_2}\left\{\frac{\partial}{\partial y}\left(\frac{h_2 h_3^2 h_1^2 \sin^2\mu}{s}\right) + \frac{\partial}{\partial z}\left(\frac{h_2^2 h_3 h_1^2 \alpha}{s}\right) + \frac{\partial}{\partial x}\left(\frac{h_2^2 h_3^2 h_1 \gamma}{s}\right)\right\} + \frac{h_2 h_3^2 h_1^2 \sin^2\mu}{s^3}\,\frac{\partial}{\partial y}$$

$$\left(\frac{s}{h_2}\right) + \frac{h_1 h_2 h_3 \cos\lambda}{s^2}\left[\frac{\partial}{\partial x}(h_3\cos\mu) - \frac{\partial h_1}{\partial z}\right] + \frac{h_1 h_2 h_3 \cos\nu}{s^2}\left[\frac{\partial}{\partial z}(h_1\cos\mu)\right.$$

$$\left. - \frac{\partial h_3}{\partial x}\right] + \frac{h_1 h_2}{s}\left[\cos\mu\,\frac{\partial}{\partial z}\left(\frac{h_1 h_3 \cos\nu}{s}\right) - \frac{\partial}{\partial z}\left(\frac{h_1 h_3 \cos\lambda}{s}\right)\right]$$

$$+ \frac{h_2 h_3}{s}\left[\cos\mu\,\frac{\partial}{\partial x}\left(\frac{h_1 h_3 \cos\lambda}{s}\right) - \frac{\partial}{\partial x}\left(\frac{h_1 h_3 \cos\nu}{s}\right)\right] \qquad \text{(A-33)}$$

$$D_2 = \frac{2 h_2^2 h_1 \cos\nu}{s^2}\left[\frac{\partial}{\partial x}(h_3\cos\lambda) - \frac{\partial}{\partial z}(h_1\cos\nu)\right] + \frac{h_1 h_2 h_3 \cos\mu}{s^2}\left[\frac{\partial}{\partial y}(h_1\cos\nu) - \frac{\partial h_2}{\partial x}\right]$$

$$+ \frac{h_1 h_2}{s^2}\left[\frac{\partial}{\partial x}(h_2 h_3\cos\mu) - \cos\nu\,\frac{\partial}{\partial x}(h_2 h_3\cos\lambda)\right] - \frac{h_1 h_2}{s^2}\left[h_1\,\frac{\partial}{\partial y}(h_3\cos\lambda) +\right.$$

$$\left. + h_2\,\frac{\partial}{\partial x}(h_3\cos\mu)\right] + \frac{h_1 h_2 \cos\nu}{s^2}\,\frac{\partial}{\partial z}(h_1 h_2\cos\nu) + \frac{h_2^2 h_3 h_1^2 \alpha}{s^3}\,\frac{\partial}{\partial y}\left(\frac{s}{h_2}\right)$$

$$- \frac{1}{s}\,\frac{\partial}{\partial y}\left(\frac{h_2 h_3 h_1^2 \alpha}{s}\right) \qquad \text{(A-34)}$$

$$D_3 = \frac{h_2^2 h_3^2 h_1 \gamma}{s^3}\,\frac{\partial}{\partial y}\left(\frac{s}{h_2}\right) + \frac{h_2 h_3}{s^2}\left[\frac{\partial}{\partial z}(h_1 h_2\cos\mu) - \cos\lambda\,\frac{\partial}{\partial z}(h_1 h_2\cos\nu)\right]$$

$$+ \frac{h_2^2 h_3 \cos\lambda}{s^2}\left[\frac{\partial}{\partial z}(h_1\cos\nu) - \frac{\partial}{\partial x}(h_3\cos\lambda)\right] + \frac{h_2 h_3^2}{s^2}\left[\cos^2\lambda\,\frac{\partial h_2}{\partial x} - \frac{\partial}{\partial y}(h_1\cos\nu)\right]$$

$$- \frac{1}{s}\frac{\partial}{\partial y}\left(\frac{h_2 h_3^2 h_1 \gamma}{s}\right) + \frac{h_1 h_2 h_3 \cos\mu}{s^2}\left[\frac{\partial}{\partial y}(h_3 \cos\lambda) - \frac{\partial h_2}{\partial z}\right] \tag{A-35}$$

$$D_4 = \frac{h_2 h_3^2 h_1^2 \sin^2\mu}{s^3}\frac{\partial}{\partial z}\left(\frac{s}{h_3}\right) + \frac{h_1 h_2}{s}\left[\cos\mu\,\frac{\partial}{\partial z}\left(\frac{h_1 h_3 \cos\mu}{s}\right) - \frac{\partial}{\partial z}\left(\frac{h_1 h_3}{s}\right)\right]$$

$$+ \frac{h_1 h_2 h_3}{s^2}\left[\frac{\partial}{\partial x}(h_3 \cos\mu) - \frac{\partial h_1}{\partial z}\right] + \frac{h_2 h_3}{s}\left[\cos\mu\,\frac{\partial}{\partial x}\left(\frac{h_3 h_1}{s}\right)\right.$$

$$\left. - \frac{\partial}{\partial x}\left(\frac{h_3 h_1 \cos\mu}{s}\right)\right] + \frac{h_2 h_3 h_1 \cos\mu}{s^2}\left[\frac{\partial}{\partial z}(h_1 \cos\mu) - \frac{\partial h_3}{\partial x}\right] \tag{A-36}$$

$$D_5 = -\frac{h_2 h_1^2 \sin^2\mu}{s^2}\frac{\partial h_3}{\partial y} + \frac{h_2^2 h_3 h_1^2 \alpha}{s^2}\left[\frac{1}{s}\frac{\partial}{\partial z}\left(\frac{s}{h_3}\right) - \frac{1}{h_3^2}\frac{\partial h_3}{\partial z}\right] - \frac{h_2^2 h_1 \gamma}{s^2}\frac{\partial h_3}{\partial x}$$

$$- \frac{h_2 h_3 \cos\nu}{s}\left[\frac{h_2}{s}\frac{\partial}{\partial z}(h_1 \cos\mu) + \frac{\partial}{\partial z}\left(\frac{h_1 h_2 \cos\mu}{s}\right) - \frac{h_2}{s}\frac{\partial h_3}{\partial x}\right]$$

$$- \frac{h_3 h_2 h_1 \cos\mu}{s^2}\left[\frac{\partial}{\partial z}(h_2 \cos\lambda) - \frac{\partial}{\partial y}(h_1 \cos\mu)\right] - \frac{h_2 h_1}{s}\left[\frac{h_1}{s}\frac{\partial h_3}{\partial y} - \frac{h_1}{s}\frac{\partial}{\partial z}(h_2 \cos\lambda)\right.$$

$$\left. - \frac{\partial}{\partial z}\left(\frac{h_1 h_2 \cos\lambda}{s}\right)\right] + \frac{h_2^2 h_1}{s^2}\left[\cos\lambda\,\frac{\partial h_1}{\partial z} - \cos\mu\,\frac{\partial}{\partial z}(h_1 \cos\nu)\right] + \frac{h_2 h_3}{s}\left[\cos\lambda\,\frac{\partial}{\partial x}\right.$$

$$\left.\left(\frac{h_2 h_1 \cos\mu}{s}\right) - \cos\mu\,\frac{\partial}{\partial x}\left(\frac{h_2 h_1 \cos\lambda}{s}\right)\right] + \frac{h_2^2 h_1}{s^2}\left[\cos\mu\,\frac{\partial}{\partial x}(h_3 \cos\lambda)\right.$$

$$\left. - \cos\lambda\,\frac{\partial}{\partial x}(h_3 \cos\mu)\right] \tag{A-37}$$

$$D_6 = \frac{h_2^2 h_3^2 h_1 \gamma}{s^3}\frac{\partial}{\partial z}\left(\frac{s}{h_3}\right) + \frac{h_2 h_1}{s}\left[\cos\nu\,\frac{\partial}{\partial z}\left(\frac{h_2 h_3}{s}\right) - \cos\mu\,\frac{\partial}{\partial z}\left(\frac{h_2 h_3}{s}\cos\lambda\right)\right]$$

$$+ \frac{h_2^2 h_3}{s^2}\left[\frac{\partial}{\partial z}(h_1 \cos\nu) - \frac{\partial}{\partial x}(h_3 \cos\lambda)\right] + \frac{h_2^2 h_3 \cos\lambda}{s^2}\left[\frac{\partial h_3}{\partial x} - \frac{\partial}{\partial z}(h_1 \cos\mu)\right]$$

$$+ \frac{h_2 h_3 \cos\lambda}{s}\left[\frac{h_2}{s}\frac{\partial}{\partial z}(h_1 \cos\mu) - \frac{h_2}{s}\frac{\partial h_3}{\partial x} - \frac{\partial}{\partial x}\left(\frac{h_2 h_3}{s}\right)\right] + \frac{h_1 h_2 h_3 \cos\mu}{s^2}\left[\frac{\partial h_3}{\partial y}\right.$$

$$- \frac{\partial}{\partial z}(h_2 \cos\lambda)] + \frac{h_2 h_3}{s}\left[\frac{h_3}{s}\frac{\partial}{\partial x}(h_2\cos\lambda) + \frac{\partial}{\partial x}\left(\frac{h_2 h_3 \cos\lambda}{s}\right) - \frac{h_3}{s}\frac{\partial}{\partial y}(h_1\cos\mu)\right] \tag{A-38}$$

$$D_7 = \frac{h_2 h_3}{s}\left[\cos\mu\,\frac{\partial}{\partial x}\left(\frac{h_1 h_3}{s}\cos\mu\right) - \frac{\partial}{\partial x}\left(\frac{h_1 h_3}{s}\right)\right] + \frac{h_2 h_3^2 h_1^2 \sin^2\mu}{s^3}\frac{\partial}{\partial x}\left(\frac{s}{h_1}\right)$$

$$+ \frac{h_1 h_2 h_3}{s^2}\left[\cos\mu\,\frac{\partial}{\partial x}(h_3\cos\mu) - \frac{\partial h_3}{\partial x}\right] \tag{A-39}$$

$$D_8 = \frac{h_2^2 h_3 h_1^2 \alpha}{s^3}\frac{\partial}{\partial x}\left(\frac{s}{h_1}\right) - \frac{h_1 h_2 h_3 \cos\mu}{s^2}\left[\frac{\partial}{\partial x}(h_2\cos\nu) - \frac{\partial h_1}{\partial y}\right] - \frac{h_2 h_1^2}{s^2}\left[\frac{\partial}{\partial y}(h_3\cos\mu)\right.$$

$$\left. - \frac{\partial}{\partial z}(h_2\cos\nu)\right] + \frac{h_2 h_3}{s}\left[\cos\lambda\,\frac{\partial}{\partial x}\left(\frac{h_1 h_2}{s}\right) - \cos\mu\,\frac{\partial}{\partial x}\left(\frac{h_2 h_1 \cos\nu}{s}\right)\right]$$

$$+ \frac{h_2^2 h_1}{s^2}\left[\frac{\partial}{\partial x}(h_3\cos\lambda) - \cos\nu\,\frac{\partial h_1}{\partial z}\right] \tag{A-40}$$

$$D_9 = -\frac{h_2 h_3}{s^2}\left[h_3 \sin^2\mu\,\frac{\partial h_1}{\partial y} + h_2\alpha\,\frac{\partial h_1}{\partial z} + \frac{h_2 h_3 \gamma}{h_1}\frac{\partial h_1}{\partial x}\right] + \frac{h_2^2 h_3 h_1 \gamma}{s^3}\frac{\partial}{\partial x}\left(\frac{s}{h_1}\right)$$

$$+ \frac{h_2^2 h_3 \cos\lambda}{s}\left[\frac{\partial h_1}{\partial z} - \frac{\partial}{\partial x}(h_3\cos\mu)\right] + \frac{h_1 h_2}{s}\left[\cos\nu\,\frac{\partial}{\partial z}\left(\frac{h_2 h_3 \cos\mu}{s}\right)\right.$$

$$\left. - \cos\mu\,\frac{\partial}{\partial z}\left(\frac{h_2 h_3 \cos\nu}{s}\right)\right] + \frac{h_2 h_3^2}{s^2}\left[\frac{\partial}{\partial x}(h_2\cos\nu) - \frac{\partial h_1}{\partial y}\right]$$

$$+ \frac{h_2^2 h_3}{s^2}\left[\cos\mu\,\frac{\partial}{\partial z}(h_1\cos\nu) - \cos\nu\,\frac{\partial}{\partial z}(h_1\cos\mu) - \cos\mu\,\frac{\partial}{\partial x}(h_3\cos\lambda)\right.$$

$$\left. + \cos\nu\,\frac{\partial h_3}{\partial x}\right] + \frac{h_2 h_3}{s}\left[\frac{\partial}{\partial x}\left(\frac{h_2 h_3 \cos\nu}{s}\right) - \cos\lambda\,\frac{\partial}{\partial x}\left(\frac{h_2 h_3 \cos\mu}{s}\right)\right]$$

$$+ \frac{h_1 h_2 h_3 \cos\mu}{s^2}\left[\frac{\partial}{\partial y}(h_3\cos\mu) - \frac{\partial}{\partial z}(h_2\cos\nu)\right] \tag{A-41}$$

$$D_{10} = \frac{h_1 h_2 h_3}{s^2}\left[h_3 h_1 \sin^2\mu\,\frac{\partial}{\partial y}\left\{\frac{1}{s}\frac{\partial}{\partial y}\left(\frac{s}{h_2}\right)\right\} + h_3 h_1 \alpha\,\frac{\partial}{\partial z}\left\{\frac{1}{s}\frac{\partial}{\partial y}\left(\frac{s}{h_2}\right)\right\}\right.$$

$$\left. + h_2 h_3 \gamma\,\frac{\partial}{\partial x}\left\{\frac{1}{s}\frac{\partial}{\partial y}\left(\frac{s}{h_2}\right)\right\}\right] + \frac{h_2}{s}\left[\frac{\partial}{\partial z}\left\{\frac{h_2 h_1 \cos\nu}{s}\left(\frac{\partial}{\partial x}(h_3\cos\lambda) - \frac{\partial}{\partial z}(h_1\cos\nu)\right)\right\}\right.$$

$$+\frac{\partial}{\partial z}\{\frac{h_3h_1\cos\mu}{s}(\frac{\partial}{\partial y}(h_1\cos\nu)-\frac{\partial h_2}{\partial x})\}+\frac{\partial}{\partial z}\{\frac{h_1^2}{s}(\frac{\partial h_2}{\partial z}-\frac{\partial}{\partial y}(h_3\cos\lambda))\}+\frac{\partial}{\partial x}$$

$$\{\frac{h_2h_3\cos\lambda}{s}(\frac{\partial}{\partial z}(h_1\cos\nu)-\frac{\partial}{\partial x}(h_3\cos\lambda))\}+\frac{\partial}{\partial x}\{\frac{h_3^2}{s}(\frac{\partial h_2}{\partial x}-\frac{\partial}{\partial y}(h_1\cos\nu))\}$$

$$+\frac{\partial}{\partial x}\{\frac{h_1h_3\cos\mu}{s}(\frac{\partial}{\partial y}(h_3\cos\lambda)-\frac{\partial h_2}{\partial z})\}] \qquad \text{(A-42)}$$

$$D_{11}=\frac{h_1h_2h_3}{s^2}[h_3h_1\sin^2\mu\frac{\partial}{\partial y}\{\frac{1}{s}\frac{\partial}{\partial z}(\frac{s}{h_3})\}+h_2h_1\alpha\frac{\partial}{\partial z}\{\frac{1}{s}\frac{\partial}{\partial z}(\frac{s}{h_3})\}+$$

$$h_2h_3\gamma\frac{\partial}{\partial x}\{\frac{1}{s}\frac{\partial}{\partial z}(\frac{s}{h_3})\}]+\frac{h_2}{s}[\frac{\partial}{\partial z}\{\frac{h_2h_1\cos\nu}{s}(\frac{\partial h_3}{\partial x}-\frac{\partial}{\partial z}(h_1\cos\mu))\}+\frac{\partial}{\partial z}$$

$$\{\frac{h_3h_1\cos\mu}{s}(\frac{\partial}{\partial y}(h_1\cos\mu)-\frac{\partial}{\partial x}(h_2\cos\lambda))\}+\frac{\partial}{\partial z}\{\frac{h_1^2}{s}(\frac{\partial}{\partial z}(h_2\cos\lambda)-\frac{\partial h_3}{\partial y})\}$$

$$+\frac{\partial}{\partial x}\{\frac{h_2h_3\cos\lambda}{s}(\frac{\partial}{\partial z}(h_1\cos\mu)-\frac{\partial h_3}{\partial x})\}+\frac{\partial}{\partial x}\{\frac{h_3^2}{s}(\frac{\partial}{\partial x}(h_2\cos\lambda)$$

$$-\frac{\partial}{\partial y}(h_1\cos\mu))\}+\frac{\partial}{\partial x}\{\frac{h_3h_1\cos\mu}{s}(\frac{\partial h_3}{\partial y}-\frac{\partial}{\partial z}(h_2\cos\lambda))\}] \qquad \text{(A-43)}$$

$$D_{12}=\frac{h_1h_2h_3}{s^2}[h_3h_1\sin^2\mu\frac{\partial}{\partial y}\{\frac{1}{s}\frac{\partial}{\partial x}(\frac{s}{h_1})\}+h_2h_1\alpha\frac{\partial}{\partial z}\{\frac{1}{s}\frac{\partial}{\partial x}(\frac{s}{h_1})\}$$

$$+h_2h_3\gamma\frac{\partial}{\partial x}\{\frac{1}{s}\frac{\partial}{\partial x}(\frac{s}{h_1})\}]+\frac{h_2}{s}[\frac{\partial}{\partial z}\{\frac{h_2h_1\cos\nu}{s}(\frac{\partial}{\partial x}(h_3\cos\mu)-\frac{\partial h_1}{\partial z})\}$$

$$+\frac{\partial}{\partial z}\{\frac{h_3h_1\cos\mu}{s}(\frac{\partial h_1}{\partial y}-\frac{\partial}{\partial x}(h_2\cos\nu))\}+\frac{\partial}{\partial z}\{\frac{h_1^2}{s}(\frac{\partial}{\partial z}(h_2\cos\nu)-\frac{\partial}{\partial y}(h_3\cos\mu))\}$$

$$+\frac{\partial}{\partial x}\{\frac{h_2h_3\cos\lambda}{s}(\frac{\partial h_1}{\partial z}-\frac{\partial}{\partial x}(h_3\cos\mu))\}+\frac{\partial}{\partial x}\{\frac{h_3^2}{s}(\frac{\partial}{\partial x}(h_2\cos\nu)-\frac{\partial h_1}{\partial y})\}$$

$$+\frac{\partial}{\partial x}\{\frac{h_3h_1\cos\mu}{s}(\frac{\partial}{\partial y}(h_3\cos\mu)-\frac{\partial}{\partial z}(h_2\cos\nu))\}] \qquad \text{(A-44)}$$

3. z-Momentum Equation

$$\frac{U}{h_1}\frac{\partial W}{\partial x} + \frac{V}{h_2}\frac{\partial W}{\partial y} + \frac{W}{h_3}\frac{\partial W}{\partial z} + \frac{1}{h_1}\frac{\partial \overline{uw}}{\partial x} + \frac{1}{h_2}\frac{\partial \overline{vw}}{\partial y} + \frac{1}{h_3}\frac{\partial \overline{w^2}}{\partial z} + T_1 UW + T_2(U^2 + \overline{u^2})$$

$$+ (T_1 + a)\,\overline{uw} + T_3(V^2 + \overline{v^2}) + T_4 W^2 + (T_4 + c)\,\overline{w^2} + T_5(UV + \overline{uv}) + T_6 VW$$

$$+ (T_6 + b)\,\overline{vw} = -\frac{1}{\rho S^2}\left[\sin^2\nu\,\frac{1}{h_3}\frac{\partial p}{\partial z} + \beta\,\frac{1}{h_1}\frac{\partial p}{\partial x} + \alpha\,\frac{1}{h_2}\frac{\partial p}{\partial y}\right] + \nu\left[\nabla^2 W + E_1\frac{\partial W}{\partial z}\right.$$

$$+ E_2\frac{\partial W}{\partial x} + E_3\frac{\partial W}{\partial y} + E_4\frac{\partial U}{\partial z} + E_5\frac{\partial U}{\partial x} + E_6\frac{\partial U}{\partial y} + E_7\frac{\partial V}{\partial z} + E_8\frac{\partial V}{\partial x} + E_9\frac{\partial V}{\partial y} + E_{10}W$$

$$\left. + E_{11}U + E_{12}V\right] \qquad \text{(A-45)}$$

where (a,b,c), S, (α,β,γ), and $\nabla^2 W$ are given by (A-2), (A-3), (A-5) and (A-6) respectively. The T_i (i = 1, 6) and the E_i (i = 1,12) coefficients are given by

$$T_1 = \frac{\alpha}{S^2}\left[\frac{1}{h_2 h_1}\frac{\partial}{\partial x}(h_2\cos\lambda) - \frac{1}{h_2 h_1}\frac{\partial}{\partial y}(h_1\cos\mu) - \frac{\cos\mu}{h_2 h_3}\frac{\partial h_3}{\partial y} + \frac{1}{h_2 h_3}\frac{\partial}{\partial z}(h_2\cos\nu)\right]$$

$$+ \frac{(\beta - \cos\mu\,\sin^2\nu)}{h_3 h_1 S^2}\frac{\partial h_1}{\partial z} + \frac{(\sin^2\nu - \beta\,\cos\mu)}{h_3 h_1 S^2}\frac{\partial h_3}{\partial x} \qquad \text{(A-46)}$$

$$T_2 = \frac{\alpha}{h_2 h_1 S^2}\left[\frac{\partial}{\partial x}(h_2\cos\nu) - \frac{\partial h_1}{\partial y}\right] - \frac{\sin^2\nu}{h_3 h_1 S^2}\left[\frac{\partial h_1}{\partial z} - \frac{\partial}{\partial x}(h_3\cos\mu)\right] \qquad \text{(A-47)}$$

$$T_3 = \frac{\sin^2\nu}{h_3 h_2 S^2}\left[\frac{\partial}{\partial y}(h_3\cos\lambda) - \frac{\partial h_2}{\partial z}\right] - \frac{\beta}{h_1 h_2 S^2}\left[\frac{\partial h_2}{\partial x} - \frac{\partial}{\partial y}(h_1\cos\nu)\right] \qquad \text{(A-48)}$$

$$T_4 = \frac{\alpha}{h_2 h_3 S^2}\left[\frac{\partial}{\partial z}(h_2\cos\lambda) - \frac{\partial h_3}{\partial y}\right] - \frac{\beta}{h_3 h_1 S^2}\left[\frac{\partial h_3}{\partial x} - \frac{\partial}{\partial z}(h_1\cos\mu)\right] \qquad \text{(A-49)}$$

$$T_5 = \frac{\alpha}{h_1 h_2 S^2}\left[\frac{\partial h_2}{\partial x} - \cos\nu\,\frac{\partial h_1}{\partial y}\right] - \frac{\sin^2\nu}{h_3 h_1 S^2}\left[\cos\nu\,\frac{\partial h_1}{\partial z} - \frac{\partial}{\partial x}(h_3\cos\lambda)\right]$$

$$+ \frac{\sin^2\nu}{h_3 h_2 S^2}\left[\frac{\partial}{\partial y}(h_3\cos\mu) - \frac{\partial}{\partial z}(h_2\cos\nu)\right] - \frac{\beta}{h_2 h_1 S^2}\left[\cos\nu\,\frac{\partial h_2}{\partial x} - \frac{\partial h_1}{\partial y}\right] \qquad \text{(A-50)}$$

$$T_6 = \frac{\sin^2\nu}{h_3 h_2 S^2}\left[\frac{\partial h_3}{\partial y} - \cos\lambda\,\frac{\partial h_2}{\partial z}\right] - \frac{\alpha}{h_2 h_3 S^2}\left[\cos\lambda\,\frac{\partial h_3}{\partial y} - \frac{\partial h_2}{\partial z}\right] - \frac{\beta}{h_1 h_2 S^2}$$

$$\left[\cos\lambda\,\frac{\partial h_2}{\partial x} - \frac{\partial}{\partial y}(h_1\cos\mu)\right] + \frac{\beta}{h_3 h_1 S^2}\left[\frac{\partial}{\partial z}(h_1\cos\nu) - \frac{\partial}{\partial x}(h_3\cos\lambda)\right] \qquad \text{(A-51)}$$

$$E_1 = -\frac{1}{sh_3}\left\{\frac{\partial}{\partial z}\left(\frac{h_3 h_1^2 h_2^2}{s}\sin^2\nu\right) + \frac{\partial}{\partial x}\left(\frac{h_3^2 h_1 h_2^2 \beta}{s}\right) + \frac{\partial}{\partial y}\left(\frac{h_3^2 h_1^2 h_2 \alpha}{s}\right)\right\} + \frac{h_3 h_1^2 h_2^2 \sin^2\nu}{s^3}\frac{\partial}{\partial z}$$

$$\left(\frac{s}{h_3}\right) + \frac{h_1 h_2 h_3 \cos\mu}{s^2}\left[\frac{\partial}{\partial y}(h_1\cos\nu) - \frac{\partial h_2}{\partial x}\right] + \frac{h_1 h_2 h_3 \cos\lambda}{s^2}\left[\frac{\partial}{\partial x}(h_2\cos\nu) - \frac{\partial h_1}{\partial y}\right]$$

$$+ \frac{h_2 h_3}{s}\left[\cos\nu\,\frac{\partial}{\partial x}\left(\frac{h_2 h_1\cos\lambda}{s}\right) - \frac{\partial}{\partial x}\left(\frac{h_2 h_1\cos\mu}{s}\right) + \frac{h_3 h_1}{s}\left[\cos\nu\,\frac{\partial}{\partial y}\left(\frac{h_2 h_1\cos\mu}{s}\right)\right.\right.$$

$$\left.\left. - \frac{\partial}{\partial y}\left(\frac{h_2 h_1\cos\lambda}{s}\right)\right] \qquad \text{(A-52)}$$

$$E_2 = \frac{2h_3^2 h_2\cos\lambda}{s^2}\left[\frac{\partial}{\partial y}(h_1\cos\mu) - \frac{\partial}{\partial x}(h_2\cos\lambda)\right] + \frac{h_1 h_2 h_3\cos\nu}{s^2}\left[\frac{\partial}{\partial z}(h_2\cos\lambda) - \frac{\partial h_3}{\partial y}\right]$$

$$+ \frac{h_2 h_3}{s^2}\left[\frac{\partial}{\partial y}(h_3 h_1\cos\nu) - \cos\lambda\,\frac{\partial}{\partial y}(h_3 h_1\cos\mu)\right] - \frac{h_2 h_3}{s^2}\left[h_2\,\frac{\partial}{\partial z}(h_1\cos\mu)\right.$$

$$\left. + h_3\,\frac{\partial}{\partial y}(h_1\cos\nu)\right] + \frac{h_2 h_3\cos\lambda}{s^2}\,\frac{\partial}{\partial x}(h_2 h_3\cos\lambda) + \frac{h_3^2 h_1 h_2^2\beta}{s^3}\,\frac{\partial}{\partial z}\left(\frac{s}{h_3}\right)$$

$$- \frac{1}{s}\,\frac{\partial}{\partial z}\left(\frac{h_3 h_1 h_2^2\beta}{s}\right) \qquad \text{(A-53)}$$

$$E_3 = \frac{h_3^2 h_1^2 h_2\alpha}{s^3}\,\frac{\partial}{\partial z}\left(\frac{s}{h_3}\right) + \frac{h_3 h_1}{s^2}\left[\frac{\partial}{\partial x}(h_2 h_3\cos\nu) - \cos\mu\,\frac{\partial}{\partial x}(h_2 h_3\cos\lambda)\right]$$

$$+ \frac{h_3^2 h_1\cos\mu}{s^2}\left[\frac{\partial}{\partial x}(h_2\cos\lambda) - \frac{\partial}{\partial y}(h_1\cos\mu)\right] + \frac{h_3 h_1^2}{s^2}\left[\cos^2\mu\,\frac{\partial h_3}{\partial y} - \frac{\partial}{\partial z}(h_2\cos\lambda)\right]$$

$$- \frac{1}{s}\,\frac{\partial}{\partial z}\left(\frac{h_3 h_1^2 h_2\alpha}{s}\right) + \frac{h_1 h_2 h_3\cos\nu}{s^2}\left[\frac{\partial}{\partial z}(h_1\cos\mu) - \frac{\partial h_3}{\partial x}\right] \qquad \text{(A-54)}$$

$$E_4 = \frac{h_3 h_1^2 h_2^2 \sin^2\nu}{s^3} \frac{\partial}{\partial x}\left(\frac{s}{h_1}\right) + \frac{h_2 h_3}{s}\left[\cos\nu \frac{\partial}{\partial x}\left(\frac{h_2 h_1 \cos\nu}{s}\right) - \frac{\partial}{\partial x}\left(\frac{h_2 h_1}{s}\right)\right]$$

$$+ \frac{h_1 h_2 h_3}{s^2}\left[\frac{\partial}{\partial y}(h_1 \cos\nu) - \frac{\partial h_2}{\partial x}\right] + \frac{h_3 h_1}{s}\left[\cos\nu \frac{\partial}{\partial y}\left(\frac{h_1 h_2}{s}\right)\right.$$

$$\left. - \frac{\partial}{\partial y}\left(\frac{h_1 h_2 \cos\nu}{s}\right)\right] + \frac{h_3 h_1 h_2 \cos\nu}{s^2}\left[\frac{\partial}{\partial x}(h_2 \cos\nu) - \frac{\partial h_1}{\partial y}\right] \qquad \text{(A-55)}$$

$$E_5 = -\frac{h_3 h_2^2 \sin^2\nu}{s^2}\frac{\partial h_1}{\partial z} + \frac{h_3^2 h_1 h_2^2 \beta}{s^2}\left[\frac{1}{s}\frac{\partial}{\partial x}\left(\frac{s}{h_1}\right) - \frac{1}{h_1^2}\frac{\partial h_1}{\partial x}\right] - \frac{h_3^2 h_2 \alpha}{s^2}\frac{\partial h_1}{\partial y}$$

$$- \frac{h_3 h_1 \cos\lambda}{s}\left[\frac{h_3}{s}\frac{\partial}{\partial x}(h_2 \cos\nu) + \frac{\partial}{\partial z}\left(\frac{h_2 h_3 \cos\nu}{s}\right) - \frac{h_3}{s}\frac{\partial h_1}{\partial y}\right] - \frac{h_1 h_2 h_3 \cos\nu}{s^2}$$

$$\left[\frac{\partial}{\partial x}(h_3 \cos\mu) - \frac{\partial}{\partial z}(h_2 \cos\nu)\right] - \frac{h_3 h_2}{s}\left[\frac{h_2}{s}\frac{\partial h_1}{\partial z} - \frac{h_2}{s}\frac{\partial}{\partial x}(h_3 \cos\mu) - \frac{\partial}{\partial x}\right.$$

$$\left.\left(\frac{h_2 h_3 \cos\mu}{s}\right)\right] + \frac{h_3^2 h_2}{s^2}\left[\cos\mu \frac{\partial h_2}{\partial x} - \cos\nu \frac{\partial}{\partial x}(h_2 \cos\lambda)\right] + \frac{h_3 h_1}{s}\left[\cos\mu \frac{\partial}{\partial y}\right.$$

$$\left.\left(\frac{h_3 h_2 \cos\nu}{s}\right) - \cos\nu \frac{\partial}{\partial y}\left(\frac{h_3 h_2 \cos\mu}{s}\right)\right] + \frac{h_3^2 h_2}{s^2}\left[\cos\nu \frac{\partial}{\partial y}(h_1 \cos\mu) - \cos\mu \frac{\partial}{\partial y}\right.$$

$$\left.(h_1 \cos\nu)\right] \qquad \text{(A-56)}$$

$$E_6 = \frac{h_3^2 h_1^2 h_2 \alpha}{s^3}\frac{\partial}{\partial x}\left(\frac{s}{h_1}\right) + \frac{h_3 h_2}{s}\left[\cos\lambda \frac{\partial}{\partial x}\left(\frac{h_3 h_1}{s}\right) - \cos\nu \frac{\partial}{\partial x}\left(\frac{h_3 h_1 \cos\mu}{s}\right)\right]$$

$$+ \frac{h_3^2 h_1}{s^2}\left[\frac{\partial}{\partial x}(h_2 \cos\lambda) - \frac{\partial}{\partial y}(h_1 \cos\mu)\right] + \frac{h_3^2 h_1 \cos\mu}{s^2}\left[\frac{\partial h_1}{\partial y} - \frac{\partial}{\partial x}(h_2 \cos\nu)\right]$$

$$+ \frac{h_3 h_1 \cos\mu}{s}\left[\frac{h_3}{s}\frac{\partial}{\partial x}(h_2 \cos\nu) - \frac{h_3}{s}\frac{\partial h_1}{\partial y} - \frac{\partial}{\partial y}\left(\frac{h_3 h_1}{s}\right)\right] + \frac{h_1 h_2 h_3 \cos\nu}{s^2}\left[\frac{\partial h_1}{\partial z}\right.$$

$$\left. - \frac{\partial}{\partial x}(h_3 \cos\mu)\right] + \frac{h_3 h_1}{s}\left[\frac{h_1}{s}\frac{\partial}{\partial y}(h_3 \cos\mu) + \frac{\partial}{\partial y}\left(\frac{h_3 h_1 \cos\mu}{s}\right) - \frac{h_1}{s}\frac{\partial}{\partial z}(h_2 \cos\nu)\right]$$

$$\text{(A-57)}$$

$$E_7 = \frac{h_3 h_1}{s}\left[\cos\nu\,\frac{\partial}{\partial y}\left(\frac{h_2 h_1 \cos\nu}{s}\right) - \frac{\partial}{\partial y}\left(\frac{h_2 h_1}{s}\right)\right] + \frac{h_3 h_1^2 h_2^2 \sin^2\nu}{s^3}\,\frac{\partial}{\partial y}\left(\frac{s}{h_2}\right)$$

$$+ \frac{h_1 h_2 h_3}{s^2}\left[\cos\nu\,\frac{\partial}{\partial y}\left(h_1\cos\nu\right) - \frac{\partial h_1}{\partial y}\right] \qquad \text{(A-58)}$$

$$E_8 = \frac{h_3^2 h_1 h_2^2 \beta}{s^3}\,\frac{\partial}{\partial y}\left(\frac{s}{h_2}\right) - \frac{h_1 h_2 h_3 \cos\nu}{s^2}\left[\frac{\partial}{\partial y}\left(h_3\cos\lambda\right) - \frac{\partial h_2}{\partial z}\right] - \frac{h_3 h_2^2}{s^2}\left[\frac{\partial}{\partial z}\left(h_1\cos\nu\right)\right.$$

$$\left. - \frac{\partial}{\partial x}\left(h_3\cos\lambda\right)\right] + \frac{h_3 h_1}{s}\left[\cos\mu\,\frac{\partial}{\partial y}\left(\frac{h_2 h_3}{s}\right) - \cos\nu\,\frac{\partial}{\partial y}\left(\frac{h_3 h_2 \cos\lambda}{s}\right)\right] + \frac{h_3^2 h_2}{s^2}$$

$$\left[\frac{\partial}{\partial y}\left(h_1\cos\mu\right) - \cos\lambda\,\frac{\partial h_2}{\partial x}\right] \qquad \text{(A-59)}$$

$$E_9 = -\frac{h_3 h_1}{s^2}\left[h_1\sin^2\nu\,\frac{\partial h_2}{\partial z} + h_3\beta\,\frac{\partial h_2}{\partial x} + \frac{h_3 h_1 \alpha}{h_2}\,\frac{\partial h_2}{\partial y}\right] + \frac{h_3^2 h_1 h_2 \alpha}{s^3}\,\frac{\partial}{\partial y}\left(\frac{s}{h_2}\right) + \frac{h_3^2 h_1 \cos\mu}{s}$$

$$\left[\frac{\partial h_2}{\partial x} - \frac{\partial}{\partial y}\left(h_1\cos\nu\right)\right] + \frac{h_2 h_3}{s}\left[\cos\lambda\,\frac{\partial}{\partial x}\left(\frac{h_3 h_1 \cos\nu}{s}\right) - \cos\nu\,\frac{\partial}{\partial x}\left(\frac{h_3 h_1 \cos\lambda}{s}\right)\right]$$

$$+ \frac{h_3 h_1^2}{s^2}\left[\frac{\partial}{\partial y}\left(h_3\cos\lambda\right) - \frac{\partial h_2}{\partial z}\right] + \frac{h_3^2 h_1}{s^2}\left[\cos\nu\,\frac{\partial}{\partial x}\left(h_2\cos\lambda\right) - \cos\lambda\,\frac{\partial}{\partial x}\left(h_2\cos\nu\right)\right.$$

$$\left. - \cos\nu\,\frac{\partial}{\partial y}\left(h_1\cos\mu\right) + \cos\lambda\,\frac{\partial h_1}{\partial y}\right] + \frac{h_3 h_1}{s}\left[\frac{\partial}{\partial x}\left(\frac{h_3 h_1 \cos\lambda}{s}\right)\right.$$

$$\left. - \cos\mu\,\frac{\partial}{\partial y}\left(\frac{h_3 h_1 \cos\nu}{s}\right)\right] + \frac{h_1 h_2 h_3 \cos\nu}{s^2}\left[\frac{\partial}{\partial z}\left(h_1\cos\nu\right) - \frac{\partial}{\partial x}\left(h_3\cos\lambda\right)\right]$$

$$\qquad \text{(A-60)}$$

$$E_{10} = \frac{h_1 h_2 h_3}{s^2}\left[h_1 h_2 \sin^2\nu\,\frac{\partial}{\partial z}\left\{\frac{1}{s}\,\frac{\partial}{\partial z}\left(\frac{s}{h_3}\right)\right\} + h_1 h_2 \beta\,\frac{\partial}{\partial x}\left\{\frac{1}{s}\,\frac{\partial}{\partial z}\left(\frac{s}{h_3}\right)\right\} + h_3 h_1 \alpha\,\frac{\partial}{\partial y}\left\{\frac{1}{s}\,\frac{\partial}{\partial z}\right.\right.$$

$$\left.\left.\left(\frac{s}{h_3}\right)\right\}\right] + \frac{h_3}{s}\left[\frac{\partial}{\partial x}\left\{\frac{h_3 h_2 \cos\lambda}{s}\left(\frac{\partial}{\partial y}\left(h_1\cos\mu\right) - \frac{\partial}{\partial x}\left(h_2\cos\lambda\right)\right)\right\} + \frac{\partial}{\partial x}\left\{\frac{h_1 h_2 \cos\nu}{s}\left(\frac{\partial}{\partial z}\right.\right.\right.$$

$$\left.\left.\left.\left(h_2\cos\lambda\right) - \frac{\partial h_3}{\partial y}\right)\right\} + \frac{\partial}{\partial x}\left\{\frac{h_2^2}{s}\left(\frac{\partial h_3}{\partial x} - \frac{\partial}{\partial z}\left(h_1\cos\mu\right)\right)\right\} + \frac{\partial}{\partial y}\left\{\frac{h_3 h_1 \cos\mu}{s}\left(\frac{\partial}{\partial x}\left(h_2\cos\lambda\right)\right.\right.\right.$$

$$- \frac{\partial}{\partial y} (h_1 \cos \mu))\} + \frac{\partial}{\partial y} \{\frac{h_1^2}{s} (\frac{\partial h_3}{\partial y} - \frac{\partial}{\partial z} (h_2 \cos \lambda))\} + \frac{\partial}{\partial y} \{\frac{h_2 h_1 \cos \lambda}{s} (\frac{\partial}{\partial z} (h_1 \cos \mu)$$

$$- \frac{\partial h_3}{\partial x})\}] \qquad \text{(A-61)}$$

$$E_{11} = \frac{h_1 h_2 h_3}{s^2} [h_1 h_2 \sin^2 \nu \frac{\partial}{\partial z} \{\frac{1}{s} \frac{\partial}{\partial x} (\frac{s}{h_1})\} + h_3 h_2 \beta \frac{\partial}{\partial x} \{\frac{1}{s} \frac{\partial}{\partial x} (\frac{s}{h_2})\} + h_3 h_1 \alpha \frac{\partial}{\partial y} \{\frac{1}{s} \frac{\partial}{\partial x}$$

$$(\frac{s}{h_1})\}] + \frac{h_3}{s} [\frac{\partial}{\partial x} \{\frac{h_3 h_2 \cos \lambda}{s} (\frac{\partial h_1}{\partial y} - \frac{\partial}{\partial x} (h_2 \cos \nu))\} + \frac{\partial}{\partial x} \{\frac{h_1 h_2 \cos \nu}{s} (\frac{\partial}{\partial z} (h_2 \cos \nu)$$

$$- \frac{\partial}{\partial y} (h_3 \cos \mu))\} + \frac{\partial}{\partial x} \{\frac{h^2}{s} (\frac{\partial}{\partial x} (h_3 \cos \mu) - \frac{\partial h_1}{\partial z})\} + \frac{\partial}{\partial y} \{\frac{h_3 h_1 \cos \mu}{s} (\frac{\partial}{\partial x} (h_2 \cos \nu)$$

$$- \frac{\partial h_1}{\partial y})\} + \frac{\partial}{\partial y} \{\frac{h_1^2}{s} (\frac{\partial}{\partial y} (h_3 \cos \mu) - \frac{\partial}{\partial z} (h_2 \cos \nu))\} + \frac{\partial}{\partial y} \{\frac{h_1 h_2 \cos \nu}{s} (\frac{\partial h_1}{\partial z}$$

$$- \frac{\partial}{\partial x} (h_3 \cos \mu))\}] \qquad \text{(A-62)}$$

$$E_{12} = \frac{h_1 h_2 h_3}{s^2} [h_1 h_2 \sin^2 \nu \frac{\partial}{\partial z} \{\frac{1}{s} \frac{\partial}{\partial y} (\frac{s}{h_2})\} + h_3 h_2 \beta \frac{\partial}{\partial x} \{\frac{1}{s} \frac{\partial}{\partial y} (\frac{s}{h_2})\} + h_3 h_1 \alpha \frac{\partial}{\partial y}$$

$$\{\frac{1}{s} \frac{\partial}{\partial y} (\frac{s}{h_2})\}] + \frac{h_3}{s} [\frac{\partial}{\partial x} \{\frac{h_3 h_2 \cos \lambda}{s} (\frac{\partial}{\partial y} (h_1 \cos \nu) - \frac{\partial h_2}{\partial x})\} + \frac{\partial}{\partial x} \{\frac{h_1 h_2 \cos \nu}{s} (\frac{\partial h_2}{\partial z}$$

$$- \frac{\partial}{\partial y} (h_3 \cos \lambda))\} + \frac{\partial}{\partial x} \{\frac{h_2^2}{s} (\frac{\partial}{\partial x} (h_3 \cos \lambda) - \frac{\partial}{\partial z} (h_1 \cos \nu))\} + \frac{\partial}{\partial y} \{\frac{h_3 h_1 \cos \mu}{s} (\frac{\partial h_2}{\partial x}$$

$$- \frac{\partial}{\partial y} (h_1 \cos \nu))\} + \frac{\partial}{\partial y} \{\frac{h_1^2}{s} (\frac{\partial}{\partial y} (h_3 \cos \lambda) - \frac{\partial h_2}{\partial z}\} + \frac{\partial}{\partial y} \{\frac{h_1 h_2 \cos \nu}{s} (\frac{\partial}{\partial z} (h_1 \cos \nu)$$

$$- \frac{\partial}{\partial x} (h_3 \cos \lambda))\}] \qquad \text{(A-63)}$$

C. Turbulence Equations.

$$\frac{U}{h_1}\frac{\partial k}{\partial x} + \frac{V}{h_2}\frac{\partial k}{\partial y} + \frac{W}{h_3}\frac{\partial k}{\partial z} = \frac{1}{s}\left[\frac{\partial}{\partial x}\left\{\frac{\nu_t}{\sigma_k s}\left(A\frac{\partial k}{\partial x} + H\frac{\partial k}{\partial y} + G\frac{\partial k}{\partial z}\right)\right\} + \frac{\partial}{\partial y}\left\{\frac{\nu_t}{\sigma_k s}\right.\right.$$

$$\left.\left.\left(H\frac{\partial k}{\partial x} + B\frac{\partial k}{\partial y} + F\frac{\partial k}{\partial z}\right)\right\} + \frac{\partial}{\partial z}\left\{\frac{\nu_t}{\sigma_k s}\left(G\frac{\partial k}{\partial x} + F\frac{\partial k}{\partial y} + C\frac{\partial k}{\partial z}\right)\right\}\right] + \tilde{G} - \varepsilon \qquad \text{(A-64)}$$

$$\frac{U}{h_1}\frac{\partial \varepsilon}{\partial x} + \frac{V}{h_2}\frac{\partial \varepsilon}{\partial y} + \frac{W}{h_3}\frac{\partial \varepsilon}{\partial z} = \frac{1}{s}\left[\frac{\partial}{\partial x}\left\{\frac{\nu_t}{\sigma_\varepsilon s}\left(A\frac{\partial \varepsilon}{\partial x} + H\frac{\partial \varepsilon}{\partial y} + G\frac{\partial \varepsilon}{\partial z}\right)\right\} + \frac{\partial}{\partial y}\left\{\frac{\nu_t}{\sigma_\varepsilon s}\left(H\frac{\partial \varepsilon}{\partial x}\right.\right.\right.$$

$$\left.\left.\left. + B\frac{\partial \varepsilon}{\partial y} + F\frac{\partial \varepsilon}{\partial z}\right)\right\} + \frac{\partial}{\partial z}\left\{\frac{\nu_t}{\sigma_\varepsilon s}\left(G\frac{\partial \varepsilon}{\partial x} + F\frac{\partial \varepsilon}{\partial y} + C\frac{\partial \varepsilon}{\partial z}\right)\right\}\right] + C_{\varepsilon 1}\frac{\varepsilon}{k}\tilde{G} - C_{\varepsilon 2}\frac{\varepsilon^2}{k}$$

(A-65)

where s and the coefficients (A,B,C,F,G,H) are given by (IV-13) and (IV-14) respectively. The turbulence generation term is defined by

$$\tilde{G} = \nu_t\left[2(\varepsilon_{11}^2 + \varepsilon_{22}^2 + \varepsilon_{33}^2) + 4(\varepsilon_{12}^2 + \varepsilon_{23}^2 + \varepsilon_{31}^2)\right] \qquad \text{(A-66)}$$

where ε_{ij} is the rate-of-strain tensor

$$\varepsilon_{ij} = \frac{1}{2}\left[\nabla\underline{V} + \nabla\underline{V}^T\right] \qquad \text{(A-67)}$$

In (A-67) $\nabla\underline{V}$ is the deformation-rate tensor e_{ij} and $\nabla\underline{V}^T$ its transpose, i.e., $\nabla\underline{V}^T = e_{ji}$. The components of ε_{ij} are defined by:

$$\varepsilon_{11} = e_{11}$$
$$= \frac{1}{s^2}\left(h_1 AA_{11} + h_1 HA_{21} + h_1 GA_{31}\right) \qquad \text{(A-68)}$$

$$\varepsilon_{12} = \frac{1}{2}\left(e_{12} + e_{21}\right) = \varepsilon_{21}$$
$$= \frac{1}{2}\left[\frac{h_1}{s^2}\left(AA_{12} + HA_{22} + GA_{32}\right) + \frac{h_2}{s^2}\left(HA_{11} + BA_{21} + FA_{31}\right)\right] \qquad \text{(A-69)}$$

$$\varepsilon_{13} = \frac{1}{2}(e_{13} + e_{31}) = \varepsilon_{31}$$
$$= \frac{1}{2}\left[\frac{h_1}{s^2}(AA_{13} + HA_{23} + GA_{33}) + \frac{h_3}{s^2}(GA_{11} + FA_{21} + CA_{31})\right] \quad \text{(A-70)}$$

$$\varepsilon_{22} = \frac{h_2}{s^2}(HA_{12} + BA_{22} + FA_{32}) \quad \text{(A-71)}$$

$$\varepsilon_{23} = \frac{1}{2}(e_{23} + e_{32}) = \varepsilon_{32}$$
$$= \frac{1}{2}\left[\frac{h_2}{s^2}(HA_{13} + BA_{23} + FA_{33}) + \frac{h_3}{s^2}(GA_{12} + FA_{22} + CA_{32})\right] \quad \text{(A-72)}$$

$$\varepsilon_{33} = e_{33}$$
$$= \frac{h_3}{s^2}(GA_{13} + FA_{23} + CA_{33}) \quad \text{(A-73)}$$

where

$$\begin{aligned}
A_{11} &= U_1 + Ua_{11} + Va_{21} + Wa_{31} \\
A_{12} &= Ub_{11} + V_1 + Vb_{21} + Wb_{31} \\
A_{13} &= Uc_{11} + Vc_{21} + W_1 + Wc_{31} \\
A_{21} &= U_2 + Ua_{12} + Va_{22} + Wa_{32} \\
A_{22} &= Ub_{12} + V_2 + Vb_{22} + Wb_{32} \\
A_{23} &= Uc_{12} + Vc_{22} + W_2 + Wc_{32} \\
A_{31} &= U_3 + Ua_{13} + Va_{23} + Wa_{33} \\
A_{32} &= Ub_{13} + V_3 + Vb_{23} + Wb_{33} \\
A_{33} &= Uc_{13} + Vc_{23} + W_3 + Wc_{33}
\end{aligned} \quad \text{(A-74)}$$

and the notation

$$(U_i, V_i, W_i) = \left(\frac{\partial V}{\partial x_i}, \frac{\partial V}{\partial x_i}, \frac{\partial W}{\partial x_i}\right)$$

has been used. The coefficients (a_{ij}, b_{ij}, c_{ij}) in (A-74) are the components of the vectors representing the derivatives of the unit vectors $\hat{e}_i$ in the (x,y,z) coordinate directions, i.e.

$$\hat{e}_{i,j} = \frac{\partial}{\partial x_j}(\hat{e}_i) = a_{ij}\hat{e}_i + b_{ij}\hat{e}_2 + c_{ij}\hat{e}_3 \qquad \text{(A-75)}$$

where

$$\begin{aligned}
a_{11} &= (a'_{11} - h_{1,1})/h_1 & b_{11} &= b'_{11}/h_1 & c_{11} &= c'_{11}/h_1 \\
a_{12} &= (a'_{12} - h_{1,2})/h_1 & b_{12} &= b'_{12}/h_1 & c_{12} &= c'_{12}/h_1 \\
a_{13} &= (a'_{13} - h_{1,3})/h_1 & b_{13} &= b'_{13}/h_1 & c_{13} &= c'_{13}/h_1 \\
a_{21} &= a'_{21}/h_2 & b_{21} &= (b'_{21} - h_{2,1})/h_2 & c_{21} &= c'_{21}/h_2 \\
a_{22} &= a'_{22}/h_2 & b_{22} &= (b'_{22} - h_{2,2})/h_2 & c_{22} &= c'_{22}/h_2 \\
a_{23} &= a'_{23}/h_2 & b_{23} &= (b'_{23} - h_{2,3})/h_2 & c_{23} &= c'_{23}/h_2 \\
a_{31} &= a'_{31}/h_3 & b_{31} &= b'_{31}/h_3 & c_{31} &= (c'_{31} - h_{3,1})/h_3 \\
a_{32} &= a'_{32}/h_3 & b_{32} &= b'_{32}/h_3 & c_{32} &= (c'_{32} - h_{3,2})/h_3 \\
a_{33} &= a'_{33}/h_3 & b_{33} &= b'_{33}/h_3 & c_{33} &= (c'_{33} - h_{3,3})/h_3
\end{aligned} \qquad \text{(A-76)}$$

and the notation

$$\frac{\partial}{\partial x_j}(h_i) = h_{i,j}$$

has been used with

$$(a'_{11},\ b'_{11},\ c'_{11}) = D^{-1}\begin{Bmatrix} h_1 h_{1,1} \\ \nu'_{,1} - h_1 h_{1,2} \\ \mu'_{,1} - h_1 h_{1,3} \end{Bmatrix} \qquad \text{(A-77)}$$

$$(a'_{22},\ b'_{22},\ c'_{22}) = D^{-1}\begin{Bmatrix} h_2 h_{2,2} \\ \lambda'_{,2} - h_2 h_{2,3} \\ \nu'_{,2} - h_2 h_{2,1} \end{Bmatrix} \qquad \text{(A-78)}$$

$$(a'_{33},\ b'_{33},\ c'_{33}) = D^{-1}\begin{Bmatrix} h_3 h_{3,3} \\ \mu'_{,3} - h_3 h_{3,1} \\ \lambda'_{,3} - h_3 h_{3,2} \end{Bmatrix} \qquad \text{(A-79)}$$

$$(a'_{12},\ b'_{12},\ c'_{12}) = D^{-1}\begin{Bmatrix} h_1h_{1,2} \\ h_2h_{2,1} \\ \frac{1}{2}(\mu'_{,2} - \nu'_{,3} + \lambda'_{,1}) \end{Bmatrix} \tag{A-80}$$

$$(a'_{13},\ b'_{13},\ c'_{13}) = D^{-1}\begin{Bmatrix} h_1h_{1,3} \\ \frac{1}{2}(\lambda'_{,1} - \mu'_{,2} + \nu'_{,3}) \\ h_3h_{3,1} \end{Bmatrix} \tag{A-81}$$

$$(a'_{23},\ b'_{23},\ c'_{23}) = D^{-1}\begin{Bmatrix} \frac{1}{2}(\nu'_{,3} - \lambda'_{,1} + \mu'_{,2}) \\ h_2h_{2,3} \\ h_3h_{3,2} \end{Bmatrix} \tag{A-82}$$

and

$$D^{-1} = \frac{1}{h_1h_2h_3S^2}\begin{vmatrix} h_2h_3\sin^2\lambda & h_1h_3\gamma & h_1h_2\beta \\ h_2h_3\gamma & h_1h_3\sin^2\mu & h_1h_2\alpha \\ h_2h_3\beta & h_1h_3\alpha & h_1h_2\sin^2\nu \end{vmatrix} \tag{A-83}$$

$$\begin{aligned} \lambda' &= h_2h_3\cos\lambda \\ \mu' &= h_1h_3\cos\mu \\ \nu' &= h_1h_2\cos\nu \end{aligned} \tag{A-84}$$

Note that the coefficients $(a'_{ij},\ b'_{ij},\ c'_{ij})$ are symmetric, i.e., $(a'_{ij},\ b'_{ij},\ c'_{ij}) = (a'_{ji},\ b'_{ji},\ c'_{ji})$ for $i \neq j$.

APPENDIX II: Partially-Parabolic Equations

In Section IV-A the procedures for obtaining the partially-parabolic form of the governing equations have been discussed. The resulting equations are provided in this Appendix. The definitions of the various coefficients appearing in the equations are given in Appendix I.

x-Momentum Equation

$$\frac{U}{h_1}\frac{\partial U}{\partial x} + \frac{V}{h_2}\frac{\partial U}{\partial y} + \frac{W}{h_3}\frac{\partial U}{\partial z} + R_4^2 U^2 + \frac{1}{h_2}\frac{\partial \overline{uv}}{\partial y} + \frac{1}{h_3}\frac{\partial \overline{uw}}{\partial z} = -\frac{1}{\rho S^2}\left[\sin^2\lambda \frac{1}{h_1}\frac{\partial p}{\partial x} + \gamma \frac{1}{h_2}\frac{\partial p}{\partial y}\right.$$

$$\left. + \beta \frac{1}{h_3}\frac{\partial p}{\partial z}\right] + \frac{\nu}{s}\left[\frac{\partial}{\partial y}\left(a_{22}\frac{\partial U}{\partial y}\right) + \frac{\partial}{\partial y}\left(a_{23}\frac{\partial U}{\partial z}\right) + \frac{\partial}{\partial z}\left(a_{32}\frac{\partial U}{\partial y}\right) + \frac{\partial}{\partial z}\left(a_{33}\frac{\partial U}{\partial z}\right)\right] \qquad \text{(B-1)}$$

y-Momentum Equation

$$\frac{U}{h_1}\frac{\partial V}{\partial x} + \frac{V}{h_2}\frac{\partial V}{\partial y} + \frac{W}{h_3}\frac{\partial V}{\partial z} + \frac{1}{h_2}\frac{\partial \overline{v^2}}{\partial y} + \frac{1}{h_3}\frac{\partial \overline{vw}}{\partial z} - \nu D_7 \frac{\partial U}{\partial y} - \nu D_8 \frac{\partial U}{\partial z} + (S_1+c)\,\overline{vw}$$

$$+ S_2\overline{w^2} + S_3\left(U^2 + \overline{u^2}\right) + (S_4 + b)\,\overline{v^2} + S_5\left(UW + \overline{uw}\right) + S_6 UV + (S_6+a)\,\overline{uv}$$

$$= -\frac{1}{\rho S^2}\left[\sin^2\mu \frac{1}{h_2}\frac{\partial p}{\partial y} + \alpha \frac{1}{h_3}\frac{\partial p}{\partial z} + \gamma \frac{1}{h_1}\frac{\partial p}{\partial x}\right] + \frac{\nu}{s}\left[\frac{\partial}{\partial y}\left(a_{22}\frac{\partial V}{\partial y}\right) + \frac{\partial}{\partial y}\left(a_{23}\frac{\partial V}{\partial z}\right) +\right.$$

$$\left.\frac{\partial}{\partial z}\left(a_{32}\frac{\partial V}{\partial y}\right) + \frac{\partial}{\partial z}\left(a_{33}\frac{\partial V}{\partial z}\right)\right] \qquad \text{(B-2)}$$

z-Momentum Equation

$$\frac{U}{h_1}\frac{\partial W}{\partial x} + \frac{V}{h_2}\frac{\partial W}{\partial y} + \frac{W}{h_3}\frac{\partial W}{\partial z} + \frac{1}{h_3}\frac{\partial \overline{w^2}}{\partial z} + \frac{1}{h_2}\frac{\partial \overline{vw}}{\partial y} - \nu E_6 \frac{\partial U}{\partial y} - \nu E_4 \frac{\partial U}{\partial z} + T_1 UW$$

$$+ T_2 (U^2 + \overline{u^2}) + (T_1 + a)\,\overline{uw} + T_3\overline{v^2} + (T_4 + c)\,\overline{w^2} + T_5(UV + \overline{uv})$$

$$+ (T_6 + b)\,\overline{vw} = -\frac{1}{\rho S^2}\left[\sin^2\nu\,\frac{1}{h_3}\frac{\partial p}{\partial z} + \beta\,\frac{1}{h_1}\frac{\partial p}{\partial x} + \alpha\,\frac{1}{h_2}\frac{\partial p}{\partial y}\right] + \frac{\nu}{s}\left[\frac{\partial}{\partial y}\left(a_{22}\frac{\partial W}{\partial y}\right)\right.$$

$$\left. + \frac{\partial}{\partial y}\left(a_{23}\frac{\partial W}{\partial z}\right) + \frac{\partial}{\partial z}\left(a_{32}\frac{\partial W}{\partial y}\right) + \frac{\partial}{\partial z}\left(a_{33}\frac{\partial W}{\partial z}\right)\right] \qquad \text{(B-3)}$$

k-Equation

$$\frac{U}{h_1}\frac{\partial k}{\partial x} + \frac{V}{h_2}\frac{\partial k}{\partial y} + \frac{W}{h_3}\frac{\partial k}{\partial z} = \frac{1}{s}\left[\frac{\partial}{\partial y}\left(\frac{\nu_t^B}{\sigma_k s}\frac{\partial k}{\partial y} + \frac{\nu_t^F}{\sigma_k s}\frac{\partial k}{\partial z}\right) + \frac{\partial}{\partial z}\left(\frac{\nu_t^F}{\sigma_k s}\frac{\partial k}{\partial y} + \frac{\nu_t^C}{\sigma_k s}\frac{\partial k}{\partial z}\right)\right]$$

$$+ \tilde{G} - \varepsilon \qquad \text{(B-4)}$$

ε - Equation

$$\frac{U}{h_1}\frac{\partial \varepsilon}{\partial x} + \frac{V}{h_2}\frac{\partial \varepsilon}{\partial y} + \frac{W}{h_3}\frac{\partial \varepsilon}{\partial z} = \frac{1}{s}\left[\frac{\partial}{\partial y}\left(\frac{\nu_t^B}{\sigma_\varepsilon s}\frac{\partial \varepsilon}{\partial y} + \frac{\nu_t^F}{\sigma_\varepsilon s}\frac{\partial \varepsilon}{\partial z}\right) + \frac{\partial}{\partial z}\left(\frac{\nu_t^F}{\sigma_\varepsilon s}\frac{\partial \varepsilon}{\partial y} + \frac{\nu_t^C}{\sigma_\varepsilon s}\frac{\partial \varepsilon}{\partial z}\right)\right]$$

$$+ C_{\varepsilon 1}\frac{\varepsilon}{k}\tilde{G} - C_{\varepsilon 2}\frac{\varepsilon^2}{k} \qquad \text{(B-5)}$$

The Reynolds stress terms required in equations (B-1) - (B-3) are related to k-ε through the isotropic eddy viscosity concept:

$$\overline{v_i v_j} = -2\nu_t \varepsilon_{ij} + \frac{2}{3}k\,(h_i h_j g_{ij}) \qquad \text{(B-6)}$$

where $\nu_t = C_\mu k^2/\varepsilon$ is the eddy viscosity, ε_{ij} is the rate-of-strain tensor (A-68)-(A-73), h_i are the metric coefficients (IV-10), and g_{ij} is the inverse metric tensor (IV-14.1). Note that equations (B-1)-(B-3) were derived under the assump-

tion that $\overline{v_i v_j} \sim O(\varepsilon)$. Thus, the order-of-magnitude of $\nu_t \varepsilon_{ij} \sim O(\varepsilon)$; however, the order-of-magnitude of ν_t is difficult to assign and should be $O(\varepsilon) \leq \nu_t \leq O(\varepsilon^2)$. For this reason terms of $O(\varepsilon^{-1})$ and $O(1)$ have been retained in the partially-parabolic form of ε_{ij}. Note that ε_{ij} is also required for the evaluation of the turblence generation term $\tilde{G}$ (A-66). The terms (A-74) simplify to

$$
\begin{aligned}
A_{11} &= U_1 + Ua_{11} \\
A_{12} &= Ub_{11} \\
A_{13} &= Uc_{11} \\
A_{21} &= U_2 + Ua_{12} \\
A_{22} &= Ub_{12} + V_2 \\
A_{23} &= Uc_{12} + W_2 \\
A_{31} &= U_3 + Ua_{13} \\
A_{32} &= Ub_{13} + V_3 \\
A_{33} &= Uc_{13} + W_3
\end{aligned}
\qquad \text{(B-7)}
$$

and the components of ε_{ij} (A-68) - (A-78) become

$$\varepsilon_{11} = \frac{h_1}{s^2}\{A(U_1 + Ua_{11}) + H(U_2 + Ua_{12}) + G(U_3 + Ua_{13})\} \qquad \text{(B-8)}$$

$$\varepsilon_{12} = \frac{1}{2}\left[\frac{h_1}{s^2}\{AUb_{11} + H(Ub_{12} + V_2) + G(Ub_{13} + V_3)\} + \right.$$

$$\left. + \frac{h_2}{s^2}\{H(U_1 + Ua_{11}) + B(U_2 + Ua_{12}) + F(U_3 + Ua_{13})\}\right] \qquad \text{(B-9)}$$

$$\varepsilon_{13} = \frac{1}{2}\left[\frac{h_1}{s^2}\{AUc_{11} + H(Uc_{12} + W_2) + G(Uc_{13} + W_3)\right.$$

$$\left. + \frac{h_3}{s^2}\{G(U_1 + Ua_{11}) + F(U_2 + Ua_{12}) + C(U_3 + Ua_{13})\}\right] \qquad \text{(B-10)}$$

$$\varepsilon_{22} = \frac{h_2}{s^2}\{HUb_{11} + B(Ub_{12} + V_2) + F(Ub_{13} + V_3)\} \tag{B-11}$$

$$\varepsilon_{23} = \frac{1}{2}\left[\frac{h_2}{s^2}\{HUc_{11} + B(Uc_{12} + W_2) + F(Uc_{13} + W_3) + \frac{h_3}{s^2}\{GUb_{11} + F(Ub_{12} + V_2) + C(Ub_{13} + V_3)\}\right] \tag{B-12}$$

$$\varepsilon_{33} = \frac{h_3}{s^2}\{GUc_{11} + F(Uc_{12} + W_2) + C(Uc_{13} + W_3)\} \tag{B-13}$$

APPENDIX III: Equations in Discretized Form

This appendix provides the details of the finite-difference procedures used to put the partially-parabolic Reynolds and Turbulence equations, as well as the pressure-correction and pressure equations, into discretized form. A written description has already been provided in Section IV.B and IV.C. and will not be repeated here. As shown below, various terms in the equations have been grouped for convenience. All differences are labeled as to forward (FD), backward (BD), or central (CD). Lastly, the terms are collected and the coefficients in equations (IV-18) - (IV-22) and (IV-29) - (IV-30) are defined. The following definitions are used for the distances between nodes (see figure 3):

$$(\Delta x_+)^{\ell}_{m,n} = [(X^{\ell+1}_{m,n} - X^{\ell}_{m,n})^2 + (Y^{\ell+1}_{m,n} - Y^{\ell}_{m,n})^2 + (Z^{\ell+1}_{m,n} - Z^{\ell}_{m,n})^2]^{1/2}$$

$$(\Delta x_-)^{\ell}_{m,n} = [(X^{\ell}_{m,n} - X^{\ell-1}_{m,n})^2 + (Y^{\ell}_{m,n} - Y^{\ell-1}_{m,n})^2 + Z^{\ell}_{m,n} - Z^{\ell-1}_{m,n})^2]^{1/2}$$

$$(\Delta y_+)^{\ell}_{m,n} = [(Y^{\ell}_{m+1,n} - Y^{\ell}_{m,n})^2 + (Z^{\ell}_{m+1,n} - Z^{\ell}_{m,n})^2]^{1/2}$$

$$(\Delta y_-)^{\ell}_{m,n} = [(Y^{\ell}_{m,n} - Y^{\ell}_{m-1,n})^2 + (Z^{\ell}_{m,n} - Z^{\ell}_{m-1,n})^2]^{1/2}$$

$$(\Delta z_+)^{\ell}_{m,n} = [(Y^{\ell}_{m,n+1} - Y^{\ell}_{m,n})^2 + (Z^{\ell}_{m,n+1} - Z^{\ell}_{m,n})^2]^{1/2}$$

$$(\Delta z_-)^{\ell}_{m,n} = [(Y^{\ell}_{m,n} - Y^{\ell}_{m,n-1})^2 + (Z^{\ell}_{m,n} - Z^{\ell}_{m,n-1})^2]^{1/2}$$

$$(\Delta y_{--})^{\ell}_{m,n} = (\Delta y_-)^{\ell-1}_{m,n}$$

$$(\Delta z_{--})^{\ell}_{m,n} = (\Delta z_-)^{\ell-1}_{m,n}$$

$$(\Delta y_{++})^{\ell}_{m,n} = (\Delta y_+)^{\ell+1}_{m,n}$$

$$(\Delta z_{++})^{\ell}_{m,n} = (\Delta z_{+})^{\ell+1}_{m,n}$$

where (ℓ,m,n) are the indices in the (x,y,z) coordinate directions and (X,Y,Z) are the Cartesian coordinates. Note that in the present staggered grid arrangement the streamwise velocity component U is located at the grid node (ℓ,m,n) whereas the transverse velocity component V is located at $(\ell-1/2,\ m-1/2,\ n)$, the girthwise velocity component W is located at $(\ell-1/2,\ m,\ n-1/2)$, and the remaining variables $(p,\hat{p},k,\varepsilon)$ are located at $(\ell-1/2,\ m,\ n)$. All the required geometrical quantities are first evaluated at the grid nodes (ℓ,m,n) using a backward difference for x-derivatives and central differences for y- and z-derivatives. Subsequently, when the discretized equations are formed, all geometric quantities are evaluated at the location of the variable under consideration by taking the appropriate average of the neighboring values which is the reason that the notation $\ell \pm 1/2$, $m \pm 1/2$, $n \pm 1/2$ has been introduced below.

A. Reynolds Equations

1. x-Momentum Equation

a)

$$\frac{U}{h_1}\frac{\partial U}{\partial x} = \frac{U^{\ell}_{m,n}}{(\Delta x_{-})^{\ell}_{m,n}}\left(U^{\ell}_{m,n} - U^{\ell-1}_{m,n}\right) = xa_1\left(U^{\ell}_{m,n} - U^{\ell-1}_{m,n}\right) \quad (BD) \qquad (C\text{-}1)$$

b)

$$\frac{V\partial U}{h_2\partial y} = \frac{V^*}{\Delta y_v}\left\{(\Phi_y+1)\,U^{\ell}_{m+1,n} - 2\Phi_y U^{\ell}_{m,n} + (\Phi_y-1)\,U^{\ell}_{m-1,n}\right\} = xb_1 U^{\ell}_{m+1,n} - xb_2 U^{\ell}_{m,n} + xb_3 U^{\ell}_{m-1,n} \qquad (C\text{-}2)$$

where

$$V^* = \frac{1}{4}\left(V^{\ell}_{m,n} + V^{\ell+1}_{m,n} + V^{\ell}_{m+1,n} + V^{\ell+1}_{m+1,n}\right)$$

$$Re_c = R_e\, V^*(\Delta y_{+} + \Delta y_{-})^{\ell}_{m,n}/2$$

$$R_e = 1/(\nu_t + 1/R_n),$$

$$\Phi_y = -1 \text{ and } \Delta y_v = 2(\Delta y_-)^{\ell}_{m,n} \text{ if } Re_c > 2 \text{ (BD)}$$

$$\phi_y = 0 \text{ and } \Delta y_v = (\Delta y_+ + \Delta y_-)^{\ell}_{m,n} \text{ if } |Re_c| < 2 \text{ (CD)}$$

$$\phi_y = 1 \text{ and } \Delta y_v = 2(\Delta y_+)^{\ell}_{m,n} \text{ if } Re_c < -2 \text{ (FD)}$$

c)

$$\frac{W\partial U}{h_3 \partial z} = \frac{W^*}{\Delta z_w}\{(\Phi_z + 1)\, U^{\ell}_{m,n+1} - 2\Phi_z U^{\ell}_{m,n} + (\Phi_z - 1)\, U^{\ell}_{m,n-1}\} = xc_1 \qquad \text{(C-3)}$$

where

$$W^* = (W^{\ell}_{m,n} + W^{\ell}_{m,n+1} + W^{\ell+1}_{m,n} + W^{\ell+1}_{m,n+1})4$$

$$Re_c = W^* Re\, (\Delta z_+ + \Delta z_-)^{\ell}_{m,n}/2$$

$$\Phi_z = -1 \text{ and } \Delta z_w = 2(\Delta z_-)^{\ell}_{m,n} \text{ if } Re_c > 2 \text{ (BD)}$$

$$\phi_z = 0 \text{ and } \Delta z_w = (\Delta z_+ + \Delta z_-)^{\ell}_{m,n} \text{ if } |Re_c| < 2 \text{ (CD)}$$

$$\phi_z = 1 \text{ and } \Delta z_w = 2(\Delta z_+)^{\ell}_{m,n} \text{ if } Re_c < -2 \text{ (FD)}$$

d)

$$R_4 U^2 + 2\frac{\partial}{h_2 \partial y}(\nu_t \varepsilon_{12} - \frac{1}{3}\bar{k}_{12}) + 2\frac{\partial}{h_3 \partial z}(\nu_t \varepsilon_{13} - \frac{1}{3}\bar{k}_{13}) = R_4 U^2 + 2\{\frac{\partial}{h_2 \partial y}(\nu_t \bar{\varepsilon}_{12} -$$

$$\frac{1}{3}\bar{k}_{12}) + \frac{\partial}{h_3 \partial z}(\nu_t \varepsilon_{13} - \frac{1}{3}\bar{k}_{13}) - \frac{\partial}{h_2 \partial y}(\nu_t \frac{\partial U}{h_2 \partial y})\}$$

$$R_4 U^2 + 2\{\frac{\partial}{h_2 \partial y}(\nu_t \overline{\varepsilon_{12}} - \frac{1}{3}\bar{k}_{12}) + \frac{\partial}{h_3 \partial z}(\nu_t \varepsilon_{13} - \frac{1}{3}\bar{k}_{13})$$

$$= (R_4 U^2)^{\ell}_{m,n} + 2\,[\frac{1}{\Delta y_\varepsilon}\{(\nu_t \overline{\varepsilon_{12}} - \frac{1}{3}\bar{k}_{12})^{\ell}_{m+1,n}$$

$$- (\nu_t \overline{\varepsilon_{12}} - \frac{1}{3}\bar{k}_{12})^{\ell}_{m-1,n}\} + \frac{1}{\Delta z_\varepsilon}\{(\nu_t \varepsilon_{13} - \frac{1}{3}\bar{k}_{13})^{\ell}_{m,n+1} - (\nu_t \varepsilon_{13} - \frac{1}{3}\bar{k}_{13})^{\ell}_{m,n-1}\}]$$

$$= xd_1 \text{ (CD)} \qquad \text{(C-4)}$$

$$- \frac{\partial}{h_2 \partial y} \left(\nu_t \frac{\partial U}{h_2 \partial y}\right) = - \frac{2}{(\Delta y_+ + \Delta y_-)^{\ell}_{m,n}} \left\{ \frac{(\nu_t)^{\ell}_{m+1/2,n}}{(\Delta y_+)^{\ell}_{m,n}} (U^{\ell}_{m+1,n} - U^{\ell}_{m,n}) \right.$$

$$\left. - \frac{(\nu_t)^{\ell}_{m-1/2,n}}{(\Delta y_-)^{\ell}_{m,n}} (U^{\ell}_{m,n} - U^{\ell}_{m-1,n}) \right\} = - xd_2 \, U^{\ell}_{m+1,n} + xd_3 \, U^{\ell}_{m,n} - xd_4 \, U^{\ell}_{m-1,n} \quad \text{(CD)} \tag{C-5}$$

where

$$\overline{\varepsilon_{12}} = \varepsilon_{12} - \frac{\partial U}{2h_2 \partial y}$$

$$\overline{k}_{ij} = k h_i h_j g_{ij}$$

$$\Delta y_{\varepsilon} = (\Delta y_+ + \Delta y_-)^{\ell - 1/2}_{m,n}$$

$$\Delta z_{\varepsilon} = (\Delta z_+ + \Delta z_-)^{\ell - 1/2}_{m,n}$$

e)

$$- \frac{1}{\rho} \left(\frac{\sin^2 \lambda}{S^2} \frac{\partial p}{h_1 \partial x} + \frac{\gamma}{S^2} \frac{\partial p}{h_2 \partial y} + \frac{\beta}{S^2} \frac{\partial p}{h_3 \partial z}\right) = - \frac{1}{\rho} \left\{ \left(\frac{\sin^2 \lambda}{S^2}\right)^{\ell}_{m,n} \frac{p^{\ell+1}_{m,n} - p^{\ell}_{m,n}}{\Delta x_x} + \left(\frac{\gamma}{S^2}\right)^{\ell}_{m,n} \right.$$

$$\frac{1}{\Delta y_x} \left(p^{\ell+1}_{m+1,n} + p^{\ell}_{m+1,n} - p^{\ell+1}_{m-1,n} - p^{\ell}_{m-1,n}\right) + \left(\frac{\beta}{S^2}\right)^{\ell}_{m,n} \frac{1}{\Delta z_x} \left(p^{\ell+1}_{m,n+1} + p^{\ell}_{m,n+1} \right.$$

$$\left. \left. - p^{\ell+1}_{m,n-1} - p^{\ell}_{m,n-1}\right) \right\} = - xe_1 \text{ (FD), (CD), (CD)} \tag{C-6}$$

where

$$\Delta x_x = \left\{ (\Delta x_+)^{\ell}_{m,n} + (\Delta x_-)^{\ell}_{m,n} \right\} / 2$$

$$\Delta y_x = (\Delta y_+ + \Delta y_-)^{\ell}_{m,n}$$

$$\Delta z_x = (\Delta z_+ + \Delta z_-)^{\ell}_{m,n}$$

f)

$$\frac{\nu}{s}\{\frac{\partial}{\partial y}(a_{22}\frac{\partial U}{\partial y}) + \frac{\partial}{\partial y}(a_{23}\frac{\partial U}{\partial z}) + \frac{\partial}{\partial z}(a_{32}\frac{\partial U}{\partial y}) + \frac{\partial}{\partial z}(a_{33}\frac{\partial U}{\partial z})\}$$

$$= (I) + (II) + (III) + (IV)$$

$$(I) = \frac{\nu}{s}\frac{\partial}{\partial y}(a_{22}\frac{\partial U}{\partial y}) = \frac{\nu}{(h_1h_3S)^{\ell}_{m,n}}\{\frac{(h_2a_{22})^{\ell}_{m+1/2,n}}{(\Delta y_+)^{\ell}_{m,n}}(U^{\ell}_{m+1,n} - U^{\ell}_{m,n}) - \frac{(h_2a_{22})^{\ell}_{m-1/2,n}}{(\Delta y_-)^{\ell}_{m,n}}$$

$$(U^{\ell}_{m,n} - U^{\ell}_{m-1,n})\}\frac{2}{(\Delta y_- + \Delta y_+)^{\ell}_{m,n}} = xf_1\,U^{\ell}_{m+1,n} - xf_2\,U^{\ell}_{m,n} + xf_3u^{\ell}_{m-1,n}\ (CD) \qquad (C\text{-}7)$$

$$(II) = \frac{\nu}{s}\frac{\partial}{\partial y}(a_{23}\frac{\partial U}{\partial z}) = \{\frac{\nu}{h_1h_3S(\Delta y_- + \Delta y_+)}\}^{\ell}_{m,n}\{(\frac{h_3a_{23}}{\Delta z^+ + \Delta z^-})^{\ell}_{m+1,n}(U^{\ell}_{m+1,n+1} - U^{\ell}_{m+1,n-1})$$

$$-(\frac{h_3\,a_{23}}{\Delta z_+ + \Delta z_-})^{\ell}_{m-1,n}(U^{\ell}_{m-1,n+1} - U^{\ell}_{m-1,n-1})\} = xf_4\ (CD),\ (CD) \qquad (C\text{-}8)$$

$$(III) = \frac{\nu}{s}\frac{\partial}{\partial z}(a_{32}\frac{\partial U}{\partial y}) = \{\frac{\nu}{h_1h_2s(\Delta z_+ + \Delta z_-)}\}^{\ell}_{m,n}\{(\frac{h_2a_{32}}{\Delta y_- + \Delta y_+})^{\ell}_{m,n+1}(U^{\ell}_{m+1,n+1} - U^{\ell}_{m-1,n+1})$$

$$-(\frac{h_2\,a_{32}}{\Delta y_- + \Delta y})^{\ell}_{+m,n-1}(U^{\ell}_{m+1,n-1} - U^{\ell}_{m-1,n-1})\} = xf_5\ (CD),\ (CD) \qquad (C\text{-}9)$$

$$(IV) = \frac{\nu}{s}\frac{\partial}{\partial z}(a_{33}\frac{\partial U}{\partial z}) = \{\frac{2\nu}{h_1h_2S\,(\Delta z_- + \Delta z_+)}\}^{\ell}_{m,n}\{\frac{(h_3\,a_{33})^{\ell}_{m,n+1/2}}{(\Delta z_+)^{\ell}_{m,n}}(U^{\ell}_{m,n+1} - U^{\ell}_{m,n})$$

$$-\frac{(h_3a_{33})^{\ell}_{m,n-1/2}}{(\Delta z_-)^{\ell}_{m,n}}(U^{\ell}_{m,n} - U^{\ell}_{m,n-1})\} = xf_6\ (CD),\ (CD) \qquad (C\text{-}10)$$

Collecting all terms (C-1) - (C-10):

$$xa_1U^{\ell}_{m,n} - xa_1U^{\ell-1}_{m,n} + xb_1U^{\ell}_{m+1,n} - xb_2U^{\ell}_{m,n} + xb_3U^{\ell}_{m-1,n} + xc_1 + xd_1$$

$$- xd_2\,U^{\ell}_{m+1,n} + xd_3U^{\ell}_{m,n} - xd_4U^{\ell}_{m-1,n} + xe_1 - xf_1U^{\ell}_{m+1,n} + xf_2U^{\ell}_{m,n} - xf_3U^{\ell}_{m-1,n}$$

$$- xf_4 - xf_5 - xf_6 = 0$$

or

$$(xb_3 - xd_4 - xf_3)\, U^{\ell}_{m-1,n} + (xa_1 - xb_2 + xd_3 + xf_2)\, U^{\ell}_{m,n} + (xb_1 - xd_2 - xf_1)$$

$$U^{\ell}_{m+1,n} = xa_1 U^{\ell-1}_{m,n} - xc_1 - xd_1 + xf_4 + xf_5 + xf_6 - xe_1$$

Finally, the coefficients in equation (IV-18) are:

$$a_1 = xb_3 - xd_4 - xf_3$$

$$a_2 = xa_1 - xb_2 + xd_3 + xf_2 \qquad \text{(C-11)}$$

$$a_3 = xb_1 - xd_2 - xf_1$$

$$Su = xa_1 U^{\ell-1}_{m,n} - xc_1 - xd_1 + xf_4 + xf_5 + xf_6$$

$$Pu = - xe_1$$

2. y-Momentum Equation

a)

$$\frac{U \partial V}{h_1 \partial x} = \frac{U^*}{(\Delta x_-)^{\ell-1/2}_{m-1/2,n}} (V^{\ell}_{m,\bar{n}} V^{\ell-1}_{m,n}) = ya_1 (V^{\ell}_{m,n} - V^{\ell-1}_{m,n}) \text{ (BD)} \qquad \text{(C-12)}$$

where

$$U^* = (U^{\ell}_{m,n} + U^{\ell-1}_{m,n} + U^{\ell}_{m-1,n} + U^{\ell-1}_{m-1,n})/4.$$

b)

$$\frac{V\partial V}{h_2\partial y} = \frac{V^{\ell}_{m,n}}{\Delta y_V}\{(\Phi_y+1)\ V^{\ell}_{m+1,n} - 2\Phi_y V^{\ell}_{m,n} + (\Phi_y-1)V^{\ell}_{m-1,n}\} = yb_1\ V^{\ell}_{m+1,n} - yb_2 V^{\ell}_{m,n} + yb_3 V^{\ell}_{m-1,n} \tag{C-13}$$

where

$$\Phi_y = -1 \text{ and } \Delta y_V = 2(\Delta y)^{\ell-1/2}_{m-1/2,n} \text{ if } Re_c > 2 \text{ (BD)}$$

$$\Phi_y = 0 \text{ and } \Delta y_V = (\Delta y_+ + \Delta y_-)^{\ell-1/2}_{m-1/2,n} \text{ if } |Re_c| \leq 2 \text{ (CD)}$$

$$\Phi_y = 1 \text{ and } \Delta y_V = 2(\Delta y_+)^{\ell-1/2}_{m-1/2,n} \text{ if } Re_c < -2 \text{ (FD)}$$

$$Re_c = Re\ V^{\ell}_{m,n}(\Delta y_- + \Delta y_+)^{\ell-1/2}_{m-1/2,n}/2.$$

c)

$$\frac{W\partial V}{h_3\partial z} = \frac{W^*}{\Delta z_w}\{(\phi_z+1)V^{\ell}_{m,n+1} - 2\phi_z V^{\ell}_{m,n} + (\phi_z-1)\ V^{\ell}_{m,n-1}\} = yc_1 \tag{C-14}$$

where

$$\Phi_z = -1 \text{ and } \Delta z_w = 2(\Delta z_-)^{\ell-1/2}_{m-1/2,n-1/2} \text{ if } Re_c > 2 \text{ (BD)}$$

$$\phi_z = 0 \text{ and } \Delta z_w = (\Delta z_+ + \Delta z_-)^{\ell-1/2}_{m-1/2,n-1/2} \text{ if } |Re_c| < 2 \text{ (CD)}$$

$$\phi_z = 1 \text{ and } \Delta z_w = 2(\Delta z_+)^{\ell-1/2}_{m-1/2,n-1/2} \text{ if } Re_c < -2 \text{ (FD)}$$

$$W^* = (W^{\ell}_{m,n} + W^{\ell}_{m,n+1} + W^{\ell}_{m-1,n} + W^{\ell}_{m-1,n-1})/4.$$

$$Re_c = ReW^*\ (\Delta z_+ + \Delta z_-)^{\ell-\frac{1}{2}}_{m-\frac{1}{2},n}/2.$$

d)

$$2\{\frac{\partial}{h_2\partial y}(\nu_t\varepsilon_{22}) + \frac{\partial}{h_3\partial z}(\nu_t\varepsilon_{23} - \frac{1}{3}\overline{k}_{23})\} - \frac{2}{3}\frac{\partial k_{22}}{h_2\partial y} = 2\{-\frac{\partial}{h_2\partial y}(\nu_t\frac{\partial V}{2h_2\partial y}) + \frac{\partial(\nu_t\overline{\varepsilon}_{22})}{h_2\partial y}$$

$$+ \frac{\partial}{h_3\partial z}(\nu_t\varepsilon_{23} - \frac{1}{3}\overline{k}_{23})\} - \frac{2}{3}\frac{\partial\overline{k}_{22}}{h_2\partial y}$$

$$\frac{2\partial(\nu_t\varepsilon_{23}-\frac{1}{3}\bar{k}_{23})}{h_3\partial z} - \frac{2}{3}\frac{\partial\bar{k}_{22}}{h_2\partial y} + \frac{2\partial(\nu_t\overline{\varepsilon_{22}})}{h_2\partial y} = \frac{1}{\Delta z_\varepsilon}\{(\nu_t\varepsilon_{23}\frac{1}{3}\bar{k}_{23})^{\ell}_{m,n+1} + (\nu_t\varepsilon_{23}-$$

$$\frac{1}{3}\bar{k}_{23})^{\ell-1}_{m,n+1} - (\nu_t\varepsilon_{23}-\frac{1}{3}\bar{k}_{23})^{\ell}_{m,n-1} - (\nu_t\varepsilon_{23}-\frac{1}{3}\bar{k}_{23})^{\ell-1}_{m,n-1}\} - \frac{2}{3}\frac{(\bar{k}^{\ell}_{22m,n} - \bar{k}^{\ell}_{22m-1,n})}{\Delta y_\varepsilon} +$$

$$\frac{1}{\Delta y_\varepsilon}\{(\nu_t\overline{\varepsilon_{22}})^{\ell}_{m,n} + (\nu_t\overline{\varepsilon_{22}})^{\ell-1}_{m,n} - (\nu_t\overline{\varepsilon_{22}})^{\ell}_{m-1,n} - (\nu_t\overline{\varepsilon_{22}})^{\ell-1}_{m-1,n}\} = yd_1(CD), (BD), (BD) \quad (C\text{-}15)$$

$$-\frac{\partial}{h_2\partial y}(\nu_t\frac{\partial V}{h_2\partial y}) = -\frac{2}{(\Delta y_+ + \Delta y_-)^{\ell-1/2}_{m-1/2,n}}\{\frac{(\nu_t)^{\ell-1/2}_{m,n}}{(\Delta y_+)^{\ell-1/2}_{m-1/2,n}}(V^{\ell}_{m+1,n} - V^{\ell}_{m,n})$$

$$-\frac{(\nu_t)^{\ell-1/2}_{m-1,n}}{(\Delta y_-)^{\ell-1/2}_{m-1/2,n}}(V^{\ell}_{m,n} - V^{\ell}_{m-1,n})\} = -yd_2V^{\ell}_{m+1,n} + yd_3V^{\ell}_{m,n} - yd_4V^{\ell}_{m-1,n}(CD) \quad (C\text{-}16)$$

where

$$\Delta z_\varepsilon = (\Delta z_+ + \Delta z_-)^{\ell-1/2}_{m,n}$$

$$\Delta y_\varepsilon = (\Delta y_-)^{\ell-1/2}_{m,n}$$

$$\bar{\varepsilon}_{22} = \varepsilon_{22} - \frac{1}{2h_2}\frac{\partial v}{\partial y}$$

e)

$$-\frac{1}{\rho}(\frac{\gamma}{S^2h_1}\frac{\partial p}{\partial x} + \frac{\sin^2\mu}{S^2h_2}\frac{\partial p}{\partial y} + \frac{\alpha}{S^2h_3}\frac{\partial p}{\partial z}) = -\frac{1}{\rho}\{(\frac{\gamma}{S^2})^{\ell-1/2}_{m-1/2,n}\frac{1}{\Delta x_y}(p^{\ell+1}_{m,n} + p^{\ell+1}_{m-1,n} - p^{\ell-1}_{m,n}$$

$$- p^{\ell-1}_{m-1,n}) + (\frac{\sin^2\mu}{S^2})^{\ell-1/2}_{m-1/2,n}\frac{1}{\Delta y_y}(p^{\ell}_{m,n} - p^{\ell}_{m-1,n}) + (\frac{\alpha}{S^2})^{\ell-1/2}_{m-1/2,n}\frac{1}{\Delta z_y}(p^{\ell}_{m,n+1} + p^{\ell}_{m-1,n+}$$

$$- p^{\ell}_{m,n-1} - p^{\ell}_{m-1,n-1})\} = -ye_1(CD), (BD), (CD) \quad (C\text{-}17)$$

where

$$\Delta x_y = \{\Delta x_+ + (\Delta x_- + \Delta x_{++})/2\}^{\ell}_{m,n}$$

$$\Delta y_y = (\Delta y_-)^{\ell-1/2}_{m,n}$$

$$\Delta z_y = (\Delta z_+ + \Delta z_-)^{\ell-1/2}_{m-1/2,n}$$

f)

$$\frac{\nu}{s}\left\{\frac{\partial}{\partial y}\left(a_{22}\frac{\partial V}{\partial y}\right) + \frac{\partial}{\partial y}\left(a_{23}\frac{\partial V}{\partial z}\right) + \frac{\partial}{\partial z}\left(a_{32}\frac{\partial V}{\partial y}\right) + \frac{\partial}{\partial z}\left(a_{33}\frac{\partial V}{\partial z}\right)\right\} = (I)$$

$$+ (II) + (III) + (IV)$$

$$(I) = \frac{\nu}{s}\frac{\partial}{\partial y}\left(a_{22}\frac{\partial V}{\partial y}\right) = \frac{2\nu}{\{h_1 h_3 S(\Delta y_- + \Delta y_+)\}^{\ell-1/2}_{m-1/2,n}}\left\{\frac{(h_2 a_{22})^{\ell-1/2}_{m,n}}{(\Delta y_+)^{\ell-1/2}_{m-1/2,n}}(V^{\ell}_{m+1,n} - V^{\ell}_{m,n})\right.$$

$$\left. - \frac{(h_2 a_{22})^{\ell-1/2}_{m-1,n}}{(\Delta y_-)^{\ell-1/2}_{m-1/2,n}}(V^{\ell}_{m,n} - V^{\ell}_{m-1,n})\right\} = yf_1\, V^{\ell}_{m+1,n} - yf_2\, V^{\ell}_{m,n} + yf_3\, V^{\ell}_{m-1,n}\,(CD) \qquad (C\text{-}18)$$

$$(II) = \frac{\nu}{s}\frac{\partial}{\partial y}\left(a_{23}\frac{\partial V}{\partial z}\right) = \frac{\nu}{(h_1 h_3 S)^{\ell-1/2}_{m-1/2,n}}\frac{1}{\Delta y_a}\left\{\frac{(h_3 a_{23})^{\ell-1/2}_{m,n}}{(\Delta z_+ + \Delta z_-)^{\ell-1/2}_{m+1/2,n}}(V^{\ell}_{m+1,n+1} - V^{\ell}_{m+1,n-1})\right.$$

$$\left. - \frac{(h_3 a_{23})^{\ell-1/2}_{m-1,n}}{(\Delta z_+ + \Delta z_-)^{\ell-1/2}_{m-1/2,n}}(V^{\ell}_{m-1,n+1} - V^{\ell}_{m-1,n-1})\right\} = yf_4\,(CD),\,(CD) \qquad (C\text{-}19)$$

where

$$\Delta y_a = \{\Delta y_- + \frac{1}{2}(\Delta y_+ + \Delta y_{--})\}^{\ell-1/2}_{m,n}$$

$$(III) = \frac{\nu}{s}\frac{\partial}{\partial z}\left(a_{32}\frac{\partial V}{\partial y}\right) = \frac{\nu}{\{h_1 h_2 S(\Delta z_- + \Delta z_-)\}^{\ell-1/2}_{m-1/2,n}}\left\{\frac{(h_2\, a_{32})^{\ell-1/2}_{m-1/2,n+1}}{\Delta y_b}(V^{\ell}_{m+1,n+1}\right.$$

$$- V^{\ell}_{m-1,n+1}) - \frac{(h_2\, a_{32})^{\ell-1/2}_{m-1/2,n-1}}{\Delta y_c}\,(V^{\ell}_{m+1,n+1} - V^{\ell}_{m-1,n-1})\} = yf_5(CD),\ (CD) \tag{C-20}$$

where

$$\Delta y_b = \{\Delta y_- + \frac{1}{2}\,(\Delta y_+ + \Delta y_-)\}^{\ell-1/2}_{m,n+1}$$

$$\Delta y_c = \{\Delta y_- + \frac{1}{2}\,(\Delta y_+ + \Delta y_-)\}^{\ell-1/2}_{m,n-1}$$

$$(IV) = \frac{\nu}{s}\frac{\partial}{\partial z}\left(a_{33}\frac{\partial V}{\partial z}\right) = \frac{2\nu}{(h_1 h_2 S)^{\ell-1/2}_{m-1/2,n}}\,\frac{1}{(\Delta z_- + \Delta z_+)^{\ell-1/2}_{m-1/2,n}}\,\{\frac{(h_3 a_{33})^{\ell-1/2}_{m-1/2,n+1/2}}{(\Delta z_+)^{\ell-1/2}_{m-1/2,n}}$$

$$(V^{\ell}_{m,n+1} - V^{\ell}_{m,n}) - \frac{(h_3 a_{33})^{\ell-1/2}_{m-1/2,n-1/2}}{(\Delta z_-)^{\ell-1/2}_{m-1/2,n}}\,(V^{\ell}_{m,n} - V^{\ell}_{m,n-1})\} = yf_6\ (CD),\ (CD) \tag{C-21}$$

g)

$$\{(S_1+c)(-2\nu_t\varepsilon_{23} + \frac{2}{3}\,\bar{k}_{23}) + S_2(\frac{2}{3}\,k_{33} - 2\nu_t\varepsilon_{33}) + S_3(U^2 - 2\nu_t\varepsilon_{11} + \frac{2}{3}\,\bar{k}_{11})$$

$$+ (S_4+b)\,(\frac{2}{3}\,\bar{k}_{22} - 2\nu_t\varepsilon_{22}) + S_5(UW - 2\nu_t\varepsilon_{13} + \frac{2}{3}\,\bar{k}_{13}) + S_6 UV - 2(S_6+a)(\nu_t\varepsilon_{12} -$$

$$- \frac{1}{3}\,\bar{k}_{12})\}^{\ell-1/2}_{m-1/2,n} = yg_1 \tag{C-22}$$

h)

$$\nu D_7\frac{\partial U}{\partial y} + \nu D_8\frac{\partial U}{\partial z} = \nu D_{7\,m-1/2,n}^{\ell-1/2}\,(U^{\ell}_{m,n} - U^{\ell}_{m-1,n} + U^{\ell-1}_{m,n} - U^{\ell-1}_{m-1,n})/2$$

$$+ \nu D_{8\,m-1/2,n}^{\ell-1/2}\,(U^{\ell}_{m,n+1} + U^{\ell-1}_{m,n+1} + U^{\ell}_{m-1,n+1} + U^{\ell-1}_{m-1,n+1}$$

$$- U^{\ell}_{m,n-1} - U^{\ell-1}_{m,n-1} - U^{\ell}_{m-1,n-1} - U^{\ell-1}_{m-1,n-1})/8 = yh_1 \text{ (BD), (CD)} \qquad \text{(C-23)}$$

Collecting all terms (C-12) - (C-23):

$$ya_1(V^{\ell}_{m,n} - V^{\ell-1}_{m,n}) + yb_1 V^{\ell}_{m+1,n} - yb_2 V^{\ell}_{m,n} + yb_3 V^{\ell}_{m-1,n} + yc_1 + yd_1$$

$$- yd_2 V^{\ell}_{m+1,n} + yd_3 V^{\ell}_{m,n} - yd_4 V^{\ell}_{m-1,n} + ye_1 - yf_1 V^{\ell}_{m+1,n} + yf_2 V^{\ell}_{m,n}$$

$$- yf_3 V^{\ell}_{m-1,n} - yf_4 - yf_5 - yf_6 + yg_1 - yh_1 = 0$$

or

$$(yb_3 - yd_4 - yf_3) V^{\ell}_{m-1,n} + (ya_1 - yb_2 + yd_3 + yf_2) V^{\ell}_{m,n}$$

$$+ (yb_1 - yd_2 - yf_1) V^{\ell}_{m+1,n} = ya_1 V^{\ell-1}_{m,n} - yc_1 - yd_1 + yf_4 + yf_5 + yf_6 - yg_1 - ye_1 + yh_1$$

Finally, the coefficients in equation (IV-19) are:

$$b_1 = yb_3 - yd_4 - yf_3$$

$$b_2 = ya_1 - yb_2 + yd_3 + yf_2 \qquad \text{(C-24)}$$

$$b_3 = yb_1 - yd_2 - yf_1$$

$$Sv = ya_1 V^{\ell-1}_{m,n} - yc_1 - yd_1 + yf_4 + yf_5 + yf_6 - yg_1 + yh_1$$

$$Pv = - ye_1$$

3. z-Momentum Equation

a)

$$\frac{U\partial W}{h_1\partial x} = \frac{U^*}{(\Delta x_-)^{\ell-1/2}_{m,n-1/2}} (W^{\ell}_{m,n} - W^{\ell-1}_{m,n}) = za_1 (W^{\ell}_{m,n} - W^{\ell-1}_{m,n}) \quad (BD) \qquad (C\text{-}25)$$

where

$$U^* = (U^{\ell}_{m,n} + U^{\ell-1}_{m,n} + U^{\ell-1}_{m,n} + U^{\ell}_{m,n-1})/4.$$

b)

$$\frac{V\partial W}{h_2\partial y} = \frac{V^*}{\Delta y_V} \{(\phi_y+1)\, W^{\ell}_{m+1,n} - 2\phi_y W^{\ell}_{m,n} + (\phi_y-1)\, W^{\ell}_{m-1,n}\} \equiv zb_1 \qquad (C\text{-}26)$$

where

$$\phi_y = -1 \text{ and } \Delta y_V = 2(\Delta y_-)^{\ell-1/2}_{m,n-1/2} \text{ if } Re_c > 2 \text{ (BD)}$$

$$\phi_y = 0 \text{ and } \Delta y_V = (\Delta y_+ + \Delta y_-)^{\ell-1/2}_{m,n-1/2} \text{ if } |Re_c| \leq 2 \text{ (CD)}$$

$$\phi_y = 1 \text{ and } \Delta y_V = 2(\Delta y_+)^{\ell-1/2}_{m,n-1/2} \text{ if } Re_c < -2 \text{ (FD)}$$

$$Re_c = Re\, V^{\ell}_{m,n} (\Delta y_- + \Delta y_+)^{\ell-1/2}_{m,n-1/2}/2.$$

$$V^* = (V^{\ell}_{m,n} + V^{\ell}_{m+1,n} + V^{\ell}_{m,n+1} + V^{\ell}_{m+1,n+1})/4.$$

c)

$$\frac{W\partial W}{h_3\partial z} = \frac{W^{\ell}_{m,n}}{\Delta z_w} \{(\phi_z+1)\, W^{\ell}_{m,n+1} - 2\phi_z W^{\ell}_{m,n} + (\phi_z-1)\, W^{\ell}_{m,n-1}\}$$

$$= zc_1 W^{\ell}_{m,n+1} - zc_2 W^{\ell}_{m,n} + zc_3 W^{\ell}_{m,n-1} \qquad (C\text{-}27)$$

where

$$\phi_z = -1 \text{ and } \Delta z_w = 2(\Delta z_-)^{\ell-1/2}_{m,n-1/2} \text{ if } Re_c > 2 \text{ (BD)}$$

$$\phi_z = 0 \text{ and } \Delta z_w = (\Delta z_+ + \Delta z_-)^{\ell-1/2}_{m,n-1/2} \text{ if } |Re_c| \leq 2 \text{ (CD)}$$

$$\phi_z = 1 \text{ and } \Delta z_w = 2(\Delta z_+)^{\ell-1/2}_{m,n-1/2} \text{ if } Re_c < -2 \text{ (FD)}$$

$$Re_c = Re\ W^{\ell}_{m,n}(\Delta z_- + \Delta z_+)^{\ell-1/2}_{m,n-1/2}$$

d)

$$2\frac{\partial}{h_2\partial y}(\nu_t\varepsilon_{23} - \frac{1}{3}\bar{k}_{23}) + \frac{2}{h_3}\frac{\partial}{\partial z}(\nu_t\varepsilon_{33}) - \frac{2}{3}\frac{\partial \bar{k}_{33}}{h_3\partial z} = 2\frac{\partial}{h_2\partial y}(\nu_t\varepsilon_{23} - \frac{1}{3}\bar{k}_{23}) +$$

$$2\frac{\partial}{h_3\partial z}(\nu_t\overline{\varepsilon_{33}}) - \frac{\partial}{h_3\partial z}(\nu_t\frac{\partial W}{h_3\partial z}) - \frac{2}{3}\frac{\partial \bar{k}_{33}}{h_3\partial z}$$

$$2\{\frac{\partial}{h_2\partial y}(\nu_t\varepsilon_{23} - \frac{1}{3}\bar{k}_{23}) + \frac{\partial}{h_3\partial z}(\nu_t\varepsilon_{33})\} - \frac{2\partial \bar{k}_{33}}{3h_3\partial z} = \frac{1}{\Delta y_e}\{(\nu_t\varepsilon_{23} - \frac{1}{3}\bar{k}_{23})^{\ell}_{m+1,n}$$

$$+ (\nu_t\varepsilon_{23} - \frac{1}{3}\bar{k}_{23})^{\ell-1}_{m+1,n} - (\nu_t\varepsilon_{23} - \frac{1}{3}\bar{k}_{23})^{\ell}_{m-1,n} - (\nu_t\varepsilon_{23} - \frac{1}{3}\bar{k}_{23})^{\ell-1}_{m-1,n}\} - \frac{2}{3}$$

$$\frac{(\bar{k}_{33}{}^{\ell}_{m,n} - \bar{k}_{33}{}^{\ell}_{m,n-1})}{(\Delta z_-)^{\ell-1}_{m,n}} + \frac{1}{\Delta z_e}\{\nu_t\overline{\varepsilon_{33}})^{\ell}_{m,n} + (\nu_t\overline{\varepsilon_{33}})^{\ell-1}_{m,n} - (\nu_t\overline{\varepsilon_{33}})^{\ell}_{m,n-1} - (\nu_t\overline{\varepsilon_{33}})^{\ell-1}_{m,n-1}\}$$

$$= zd_1 \text{ (CD), (BD), (BD)} \qquad \text{(C-28)}$$

where

$$\Delta y_e = (\Delta y_- + \Delta y_+)^{\ell-1/2}_{m,n}$$

$$\Delta z_e = (\Delta z_- + \Delta z_+)^{\ell-1/2}_{m,n} \ /2$$

$$\bar{\varepsilon}_{33} = \varepsilon_{33} - \frac{1}{2h_3}\frac{\partial W}{\partial z}$$

$$-\frac{\partial}{h_3\partial z}(\nu_t\frac{\partial W}{h_3\partial z}) = -\frac{2}{\{\Delta z_+ + \Delta z_-\}^{\ell-1/2}_{m,n-1/2}}\{\frac{(\nu_t)^{\ell-1/2}_{m,n}}{(\Delta z_+)^{\ell-1/2}_{m,n-1/2}}(W^{\ell}_{m,n+1} - W^{\ell}_{m,n})$$

$$- \frac{(\nu_t)^{\ell-1/2}_{m,n-1}}{(\Delta z_-)^{\ell-1/2}_{m,n-1/2}} (W^{\ell}_{m,n} - W^{\ell}_{m,n-1})\} = - zd_2 W^{\ell}_{m,n+1} + zd_3 W^{\ell}_{m,n} - zd_4 W^{\ell}_{m,n-1} \quad (CD) \qquad (C\text{-}29)$$

e)

$$- \frac{1}{\rho} \left(\frac{\beta}{S^2 h_1} \frac{\partial p}{\partial x} + \frac{\alpha \partial p}{S^2 h_2 \partial y} + \frac{\sin^2 \nu \, \partial p}{S^2 h_3 \partial z}\right) = - \frac{1}{\rho} \{ \left(\frac{\beta}{S^2}\right)^{\ell-1/2}_{m,n-1/2} \frac{1}{\Delta x_z} (p^{\ell+1}_{m,n} + p^{\ell+1}_{m,n-1} - p^{\ell-1}_{m,n}$$

$$- p^{\ell-1}_{m,n-1}) + \left(\frac{\alpha}{S^2}\right)^{\ell-1/2}_{m,n-1/2} \frac{1}{\Delta y_z} (p^{\ell}_{m+1,n} + p^{\ell}_{m+1,n-1} - p^{\ell}_{m-1,n} - p^{\ell}_{m-1,n-1})$$

$$+ \left(\frac{\sin^2 \nu}{S^2}\right)^{\ell-1/2}_{m,n-1/2} \frac{1}{\Delta z_z} (p^{\ell}_{m,n} - p^{\ell}_{m,n-1})\} = ze_1 \quad (CD), \quad (CD), \quad (BD) \qquad (C\text{-}30)$$

where

$$\Delta x_z = \frac{1}{2} \{\Delta x_- + \frac{1}{2} (\Delta x_+ + \Delta x_-)\}^{\ell}_{m,n}$$

$$\Delta y_z = (\Delta y_+ + \Delta y_-)^{\ell-1/2}_{m,n-1/2}$$

$$\Delta z_z = (\Delta z)^{\ell-1/2}_{m,n}$$

f)

$$\frac{\nu}{s} \{\frac{\partial}{\partial y} (a_{22} \frac{\partial W}{\partial y}) + \frac{\partial}{\partial y} (a_{23} \frac{\partial W}{\partial z}) + \frac{\partial}{\partial z} (a_{32} \frac{\partial W}{\partial y}) + \frac{\partial}{\partial z} (a_{33} \frac{\partial W}{\partial z})\}$$

$$= (I) + (II) + (III) + (IV)$$

$$(I) = \frac{\nu}{s} \frac{\partial}{\partial y} (a_{22} \frac{\partial W}{\partial y}) = \frac{2}{\{h_1 h_3 S(\Delta y_+ + \Delta y_-)\}^{\ell-1/2}_{m,n-1/2}} \{\frac{(h_2 a_{22})^{\ell-1/2}_{m+1/2,n-1/2}}{(\Delta y_+)^{\ell-1/2}_{m,n-1/2}} (W^{\ell}_{m+1,\bar{n}} W^{\ell}_{m,n})$$

$$- \frac{(h_2 \, a_{22})^{\ell-1/2}_{m-1/2,n-1/2}}{(\Delta y_-)^{\ell-1/2}_{m,n-1/2}} (W^{\ell}_{m,n} - W^{\ell}_{m-1,n})\} = zf_1 (CD) \qquad (C\text{-}31)$$

$$(II) = \frac{\nu}{s} \frac{\partial}{\partial y} (a_{23} \frac{\partial W}{\partial z}) = \frac{1}{\{h_1 h_3 S \, (\Delta y_- + \Delta y_+)\}^{\ell-1/2}_{m,n-1/2}} \{\frac{(h_3 a_{23})^{\ell-1/2}_{m+1,n-1/2}}{\Delta z_a} (W^{\ell}_{m+1,n+1}$$

$$- W^{\ell}_{m+1,n-1}) - \frac{(h_3 a_{33})^{\ell-1/2}_{m-1,n-1/2}}{\Delta z_b} (W^{\ell}_{m-1,n+1} - W^{\ell}_{m-1,n-1})\} = zf_2(CD), \quad (CD) \tag{C-32}$$

where

$$\Delta z_a = \{\Delta z_- + \frac{1}{2} (\Delta z_+ + \Delta z_{--})\}^{\ell-1/2}_{m+1,n}$$

$$\Delta z_b = \{\Delta z_- + \frac{1}{2} (\Delta z_+ + \Delta z_{--})\}^{\ell-1/2}_{m-1,n}$$

$$(III) = \frac{\nu}{s} \frac{\partial}{\partial z} (a_{32} \frac{\partial W}{\partial y}) = \frac{1}{(h_1 h_2 S \Delta z_c)^{\ell-1/2}_{m,n}} \{\frac{(h_2 a_{22})^{\ell-1/2}_{m,n+1/2}}{(\Delta y_- + \Delta y_+)^{\ell-1/2}_{m,n+1}} (W^{\ell}_{m+1,n+1} - W^{\ell}_{m-1,n+1})$$

$$- \frac{(h_2 a_{32})^{\ell-1/2}_{m,n-1/2}}{(\Delta y_- + \Delta y_+)^{\ell-1/2}_{m-1,n-1/2}} (W^{\ell}_{m+1,n-1} - W^{\ell}_{m-1,n-1})\} = zf_3 (CD), \quad (CD) \tag{C-33}$$

where

$$\Delta z_c = \{\Delta z_- + \frac{1}{2} (\Delta z_+ + \Delta z_{--})\}^{\ell-1/2}_{m,n}$$

$$(IV) = \frac{\partial}{\partial z} (a_{33} \frac{\partial W}{\partial z}) = \frac{2}{(h_1 h_2 S \Delta z_a)^{\ell-1/2}_{m,n-1/2}} \{\frac{(h_3 a_{33})^{\ell-1/2}_{m,n}}{(\Delta z_+)^{\ell-1/2}_{m,n-1/2}} (W^{\ell}_{m,n+1} - W^{\ell}_{m,n})$$

$$- \frac{(h_3 a_{33})^{\ell-1/2}_{m,n-1}}{(\Delta z_-)^{\ell-1/2}_{m,n-1/2}} (W^{\ell}_{m,n} - W^{\ell}_{m,n-1})\} = zf_4 W^{\ell}_{m,n+1} - zf_5 W^{\ell}_{m,n} + zf_6 W^{\ell}_{m,n-1} \quad (CD) \tag{C-34}$$

where

$$\Delta z_a = \frac{1}{2} (\Delta z_+ + \Delta z_-)^{\ell-1/2}_{m,n-1/2}$$

g)

$$\{T_1 UW + T_2(U^2 + \frac{2}{3} \bar{k}_{11} - 2\nu_t \varepsilon_{11}) + (T_1 + a)(-2\nu_t \varepsilon_{13} + \frac{2}{3} \bar{k}_{13}) + T_3(\frac{2}{3} \bar{k}_{22} - 2\nu_t \varepsilon_{22})$$

$$+ (T_4 + c)(\frac{2}{3} \bar{k}_{33} - 2\nu_t \varepsilon_{33}) + T_5(UV - 2\nu_t \varepsilon_{12} + \frac{2}{3} \bar{k}_{12}) + (T_6 + b)$$

$$(- 2\nu_t \varepsilon_{23} + \frac{2}{3} \bar{k}_{23})\}^{\ell-1/2}_{m,n-1/2} = zg_1 \tag{C-35}$$

h)

$$\nu E_6 \frac{\partial U}{\partial y} + \nu E_4 \frac{\partial U}{\partial z} = \nu E^{\ell-1/2}_{6m,n-1/2} \left(U^{\ell}_{m+1,n} + U^{\ell-1}_{m+1,n} + U^{\ell}_{m+1,n-1}\right.$$

$$\left. + U^{\ell-1}_{m+1,n-1} - U^{\ell}_{m-1,n} - U^{\ell-1}_{m-1,n} - U^{\ell}_{m-1,n-1} - U^{\ell-1}_{m-1,n-1}\right)/8$$

$$+ \nu E^{\ell-1/2}_{4m,n-1/2} \left(U^{\ell}_{m,n} + U^{\ell-1}_{m,n} - U^{\ell}_{m,n-1} - U^{\ell-1}_{m,n-1}\right)/2 = zh_1 \text{ (CD), (BD)} \qquad \text{(C-36)}$$

Collecting all the terms (C-25) - (C-36):

$$za_1(W^{\ell}_{m,n} - W^{\ell-1}_{m,n}) + zb_1 + zc_1 W^{\ell}_{m,n+1} - zc_2 W^{\ell}_{m,n} + zc_3 W^{\ell}_{m,n-1}$$

$$+ zd_1 - zd_2 W^{\ell}_{m,n+1} + zd_3 W^{\ell}_{m,n} - zd_4 W^{\ell}_{m,n-1} + ze_1 - zf_1 - zf_2 - zf_3$$

$$- zf_4 W^{\ell}_{m,n+1} + zf_5 W^{\ell}_{m,n} - zf_6 W^{\ell}_{m,n-1} + zg_1 - zh_1 = 0$$

or

$$(zc_3 - zd_4 - zf_6) W^{\ell}_{m,n-1} + (za_1 - zc_2 + zd_3 + zf_5) W^{\ell}_{m,n}$$

$$+ (zc_1 - zd_2 - zf_4) W^{\ell}_{m,n+1} = za_1 W^{\ell-1}_{m,n} - zb_1 - zd_1 + zf_1 + zf_2 + zf_3$$

$$- zg_1 - ze_1 - zh_1$$

Finally, the coefficients in equation (IV-20) are:

$$c_1 = zc_3 - zd_4 - zf_6$$

$$c_2 = za_1 - zc_2 + zd_3 + zf_5$$

$$c_3 = zc_1 - zd_2 - zf_4 \qquad \text{(C-37)}$$

$$Pw = - ze_1$$

$$Sw = za_1 W^{\ell-1}_{m,n} - zb_1 - zd_1 + zf_1 + zf_2 + zf_3 - zg_1 + zh_1$$

B. Turbulence-Model Equations

F stands for k or ε

a)

$$\frac{U\partial F}{h_1 \partial x} = \frac{U^*}{\Delta x}\left(F^{\ell}_{m,n} - F^{\ell-1}_{m,n}\right) = Fa_1\left(F^{\ell}_{m,n} - F^{\ell-1}_{m,n}\right) \text{ (BD)} \qquad \text{(C-38)}$$

where

$$U^* = \left(U^{\ell}_{m,n} + U^{\ell-1}_{m,n}\right)/\Delta x$$

$$\Delta x = \frac{1}{2}\left\{\Delta x_{-} + \Delta x_{--}\right\}^{\ell}_{m,n}$$

b)

$$V\frac{\partial F}{h_2 \partial y} = \frac{V^{\ell}_{m,n}}{\Delta y}\left(F^{\ell}_{m+1,n} - F^{\ell}_{m-1,n}\right) = Fb_1\left(F^{\ell}_{m+1,n} - F^{\ell}_{m-1,n}\right) \text{ (CD)} \qquad \text{(C-39)}$$

where

$$\Delta y = \left(\Delta y_{+} + \Delta y_{-}\right)^{\ell-1/2}_{m,n}$$

c)

$$W\frac{\partial F}{\partial z} = \frac{W^*}{\Delta z_w}\left\{\left(\phi_z + 1\right)F^{\ell}_{m,n+1} - 2\phi_z F^{\ell}_{m,n} + \left(\phi_z - 1\right)F^{\ell}_{m,n-1}\right\} = Fc_1 \qquad \text{(C-40)}$$

where

$$\phi_z = -1 \text{ and } \Delta z_w = 2\left(\Delta z_{-}\right)^{\ell-1/2}_{m,n} \text{ if } Re_c > 2 \text{ (BD)}$$

$$\phi_z = 0 \text{ and } \Delta z_w = \left(\Delta z_{+} + \Delta z_{-}\right)^{\ell-1/2}_{m,n} \text{ if } \left|Re_c\right| < 2 \text{ (CD)}$$

$$\phi_z = 1 \text{ and } \Delta z_w = 2(\Delta z_+)^{\ell-1/2}_{m,n} \text{ if } Re_c < -2 \text{ (FD)}$$

$$Re_c = Re \Delta z W^*$$

$$W^* = (W^{\ell}_{m,n} + W^{\ell}_{m,n+1})/2$$

$$\Delta z = (\Delta z_+ + \Delta z_-)^{\ell-1/2}_{m,n}$$

d)

$$\frac{1}{s}\{\frac{\partial}{\partial y}(C_\nu\, a_{22}\frac{\partial F}{\partial y}) + \frac{\partial}{\partial y}(C_\nu\, a_{23}\frac{\partial F}{\partial z}) + \frac{\partial}{\partial z}(C_\nu a_{32}\frac{\partial F}{\partial y}) + \frac{\partial}{\partial z}(C_\nu a_{33}\frac{\partial F}{\partial z})\}$$

$$= (I) + (II) + (III) + (IV)$$

$$C_\nu = \nu_t/\sigma_k \text{ for } k$$

$$C_\nu = \nu_t/\sigma_\varepsilon \text{ for } \varepsilon$$

$$(I) = \frac{1}{s}\frac{\partial}{\partial y}(C_\nu\, a_{22}\frac{\partial F}{\partial y}) = \frac{1}{\{h_1 h_3 S\}^{\ell-1/2}_{m,n}} \frac{2}{(\Delta y_+ + \Delta y_-)^{\ell-1/2}_{m,n}} \{\frac{(h_2 C_\nu a_{22})^{\ell-1/2}_{m+1/2,n}}{(\Delta y_+)^{\ell-1/2}_{m,n}}$$

$$(F^{\ell}_{m+1,n} - F^{\ell}_{m,n}) - \frac{(h_2 C_\nu a_{22})^{\ell-1/2}_{m-1/2,n}}{(\Delta y_-)^{\ell-1/2}_{m,n}}(F^{\ell}_{m,n} - F^{\ell}_{m-1,n})\} = Fd_1 F^{\ell}_{m+1,n} - Fd_2 F^{\ell}_{m,n}$$

$$+ Fd_3 F^{\ell}_{m-1,n} \text{ (CD)} \qquad \text{(C-41)}$$

$$(II) = \frac{1}{s}\frac{\partial}{\partial y}(C_\nu a_{23}\frac{\partial F}{\partial z}) = \frac{1}{\{h_1 h_3 S(\Delta y_- + \Delta y_+)\}^{\ell-1/2}_{m,n}} \{(\frac{h_3 a_{23} C_\nu}{\Delta z_- + \Delta z_+})^{\ell-1/2}_{m+1,n}(F^{\ell}_{m+1,n+1} - F^{\ell}_{m+1,n-1})$$

$$- (\frac{h_3 a_{23} C_\nu}{\Delta z_- + \Delta z_+})^{\ell-1/2}_{m-1,n}(F^{\ell}_{m-1,n+1} - F^{\ell}_{m-1,n-1})\} = Fd_4 \text{ (CD), (CD)} \qquad \text{(C-42)}$$

$$(III) = \frac{1}{s}\frac{\partial}{\partial z}(C_\nu a_{32}\frac{\partial F}{\partial y}) = \frac{1}{\{h_1 h_2 S(\Delta z_- + \Delta z_+)\}^{\ell-1/2}_{m,n}} \{(\frac{h_2 a_{32} C_\nu}{\Delta y_- + \Delta y_+})^{\ell-1/2}_{m,n+1}$$

$$(F^{\ell}_{m+1,n+1} - F^{\ell}_{m-1,n+1}) - \left(\frac{h_2 a_{32} C_\nu}{\Delta y_- + \Delta y_+}\right)^{\ell-1/2}_{m,n-1} (F^{\ell}_{m+1,n-1} - F^{\ell}_{m-1;n-1})\}$$
$$= Fd_5\ (CD),\ (CD) \qquad (C\text{-}43)$$

$$(IV) = \frac{1}{s}\frac{\partial}{\partial z}\left(C_\nu a_{33}\frac{\partial F}{\partial z}\right) = \frac{2}{\{h_1 h_2 S(\Delta z_- + \Delta z_+)\}^{\ell-1/2}_{m,n}}\left\{\left(\frac{h_3 a_{33} C_\nu}{\Delta z_+}\right)^{\ell-1/2}_{m,n+1/2}(F^{\ell}_{m,n+\bar{1}} F^{\ell}_{m,n})\right.$$
$$\left. - \left(\frac{h_3 a_{33} C_\nu}{\Delta z_-}\right)^{\ell-1/2}_{m,n-1/2}(F^{\ell}_{m,n} - F^{\ell}_{m,n-1})\right\} = Fd_6\ (CD) \qquad (C\text{-}44)$$

e)

$$\tilde{G} - \varepsilon = Sk$$

$$C_{1\varepsilon}\frac{\varepsilon}{k}\tilde{G} - C_{2\varepsilon}\frac{\varepsilon^2}{k} = S\varepsilon$$

i) For k, $\tilde{G} - \varepsilon = \tilde{G} - \frac{C_\mu}{\nu_t}k^2 = (\tilde{G})^{\ell}_{m,n} - \left(\frac{C_\mu k}{\nu_t}\right)^{\ell}_{m,n} k^{\ell}_{m,n} = Fe_1 - Fe_2 k^{\ell}_{m,n}$ (C-45)

ii) For ε, $C_{1\varepsilon}\frac{\varepsilon}{k}\tilde{G} - C_{2\varepsilon}\frac{\varepsilon^2}{k} = (C_{1\varepsilon}\frac{\varepsilon}{k}\tilde{G})^{\ell}_{m,n} - (C_{2\varepsilon}\frac{\varepsilon}{k})^{\ell}_{m,n}\varepsilon^{\ell}_{m,n} = Fe_1 - Fe_2\,\varepsilon^{\ell}_{m,n}$ (C-46)

Collecting all terms (C-38) - (C-46):

$$Fa_1(F^{\ell}_{m,n} - F^{\ell-1}_{m,n}) + Fb_1(F^{\ell}_{m+1,n} - F^{\ell}_{m-1,n}) + Fc_1 - Fd_1 F^{\ell}_{m+1,n}$$
$$+ Fd_2 F^{\ell}_{m,n} - Fd_3 F^{\ell}_{m-1,n} - Fd_4 - Fd_5 - Fd_6 - Fe_1 + Fe_2 F^{\ell}_{m,n} = 0$$

or

$$-(Fb_1 + Fd_3)\,F^{\ell}_{m-1,n} + (Fa_1 + Fd_2 + Fe_2)\,F^{\ell}_{m,n} + (Fb_1 - Fd_1)\,F^{\ell}_{m+1,n}$$
$$= -Fc_1 + Fd_4 + Fd_5 + Fd_6 + Fe_1$$

Finally, the coefficients in equations IV-21 and (IV-22) are:

$$(d,e)_1 = - Fb_1 - Fd_3$$

$$(d,e)_2 = Fa_1 + Fd_2 + Fe_2 \qquad \text{(C-47)}$$

$$(d,e)_3 = Fb_1 - Fd_1$$

$$SF = - Fc_1 + Fd_4 + Fd_5 + Fd_6 + Fe_1$$

C. Pressure-Correction and Pressure Equations The discretized form of the momentum equations (IV-18)-(IV-20) can be put in the form

$$U^{\ell}_{m,n} = \tilde{U}^{\ell}_{m,n} + \frac{1}{a_2} Pu^{\ell}_{m,n} \qquad \text{(C-48)}$$

$$V^{\ell}_{m,n} = \tilde{V}^{\ell}_{m,n} + \frac{1}{b_2} Pv^{\ell}_{m,n} \qquad \text{(C-49)}$$

$$W^{\ell}_{m,n} = \tilde{W}^{\ell}_{m,n} + \frac{1}{c_2} Pw^{\ell}_{m,n} \qquad \text{(C-50)}$$

where the pseudovelocities are defined as

$$\tilde{U}^{\ell}_{m,n} = - \frac{1}{a_2} (a_1 U^{\ell}_{m-1,n} + a_3 U^{\ell}_{m+1,n} - Su^{\ell}_{m,n}) \qquad \text{(C-51)}$$

$$\tilde{V}^{\ell}_{m,n} = - \frac{1}{b_2} (b_1 V^{\ell}_{m-1,n} + b_3 V^{\ell}_{m+1,n} - Sv^{\ell}_{m,n}) \qquad \text{(C-52)}$$

$$\tilde{W}^{\ell}_{m,n} = - \frac{1}{c_2} (c_1 W^{\ell}_{m,n-1} + c_3 W^{\ell}_{m,n+1} - Sw^{\ell}_{m,n}) \qquad \text{(C-53)}$$

and the pressure-gradient term can be expanded to yield

$$\frac{1}{a_2} Pu^{\ell}_{m,n} = a_7 (p^{\ell+1}_{m,n} - p^{\ell}_{m,n}) + a_8 (p^{\ell+1}_{m+1,n} + p^{\ell}_{m+1,n} - p^{\ell+1}_{m-1,n} - p^{\ell}_{m-1,n})$$

$$+ a_9 (p^{\ell+1}_{m,n+1} + p^{\ell}_{m,n+1} - p^{\ell+1}_{m,n-1} - p^{\ell}_{m,n-1}) \text{ (FD), (CD), (CD)} \qquad \text{(C-54)}$$

$$\frac{1}{b_2} Pv^{\ell}_{m,n} = b_7 (p^{\ell+1}_{m,n} + p^{\ell+1}_{m-1,n} - p^{\ell-1}_{m,n} - p^{\ell-1}_{m-1,n}) + b_8 (p^{\ell}_{m,n} - p^{\ell}_{m-1,n})$$

$$+ b_9 (p^{\ell}_{m,n+1} + p^{\ell}_{m-1,n+1} - p^{\ell}_{m,n-1} - p^{\ell}_{m-1,n-1}) \text{ (CD), (BD), (CD)} \qquad \text{(C-55)}$$

$$\frac{1}{c_2} Pw^{\ell}_{m,n} = c_7(p^{\ell+1}_{m,n} + p^{\ell+1}_{m,n-1} - p^{\ell-1}_{m,n} - p^{\ell-1}_{m,n-1}) + c_8 (p^{\ell}_{m+1,n} + p^{\ell}_{m+1,n-1}$$

$$- p^{\ell}_{m-1,n} - p^{\ell}_{m-1,n-1}) + c_9(p^{\ell}_{m,n} - p^{\ell}_{m,n-1}) \text{ (CD), (CD), (BD)} \qquad \text{(C-56)}$$

in which the $(a_i, b_i, c_i, i = 7,8,9)$ coefficients are defined by

$$\begin{matrix} a_7 & a_8 & a_9 \\ b_7 & b_8 & b_9 \\ c_7 & c_8 & c_9 \end{matrix} = \begin{matrix} \frac{\sin^2\lambda}{S^2\Delta x_x a_2}, & \frac{\gamma}{S^2\Delta y_x a_2}, & \frac{\beta}{S^2\Delta z_x a_2} \\ \frac{\gamma}{S^2\Delta x_y b_2}, & \frac{\sin^2\mu}{S^2\Delta y_y b_2}, & \frac{\alpha}{S^2\Delta z_y b_2} \\ \frac{\beta}{S^2\Delta x_z c_2}, & \frac{\alpha}{S^2\Delta y_z c_2}, & \frac{\sin^2\nu}{S^2\Delta z_z c_2} \end{matrix} \qquad \text{(C-57)}$$

and evaluated at the grid node (ℓ,m,n) .

Substituting (C-48)-(C-50) and (IV-27) into (IV-26) results in the desired equation for pressure:

$$\frac{1}{(\Delta x_-)^{\ell}_{m,n}} [(h_2h_3S)^{\ell}_{m,n}\{\tilde{U}^{\ell}_{m,n} - (a_7)^{\ell}_{m,n} (p^{\ell+1}_{m,n} - p^{\ell}_{m,n}) - (a_8)^{\ell}_{m,n}(p^{\ell+1}_{m+1,n} + p^{\ell}_{m+1,n}$$

$$- p^{\ell+1}_{m-1,n} - p^{\ell}_{m-1,n}) - (a_9)^{\ell}_{m,n} (p^{\ell+1}_{m,n+1} + p^{\ell}_{m,n+1} - p^{\ell+1}_{m,n-1} - p^{\ell}_{m,n-1})\}$$

$$- (h_2h_3S)^{\ell-1}_{m,n} \{\tilde{U}^{\ell-1}_{m,n} - (a_7)^{\ell-1}_{m,n} (p^{\ell}_{m,n} - p^{\ell-1}_{m,n}) - (a_8)^{\ell-1}_{m,n} (p^{\ell}_{m+1,n} + p^{\ell-1}_{m+1,n}$$

$$- p^{\ell}_{m-1,n} - p^{\ell-1}_{m-1,n}) - (a_9)^{\ell-1}_{m,n} (p^{\ell}_{m,n+1} + p^{\ell-1}_{m,n+1} - p^{\ell}_{m,n-1} - p^{\ell-1}_{m,n-1})\}]$$

$$+ \frac{1}{(\Delta y_-)^{\ell-1/2}_{m+1/2,n}} [(h_1h_3S)^{\ell}_{m+1/2,n}\{\tilde{V}^{\ell}_{m+1,n} - (b_8)^{\ell}_{m+1/2,n}(p^{\ell}_{m+1,n} - p^{\ell}_{m,n}) - (b_7)^{\ell}_{m+1/2,n}$$

$$(p^{\ell+1}_{m+1,n} + p^{\ell+1}_{m,n} - p^{\ell-1}_{m,n} - p^{\ell-1}_{m+1,n}) - (b_9)^{\ell}_{m+1/2,n}(p^{\ell}_{m,n+1} + p^{\ell}_{m+1,n+1} - p^{\ell}_{m,n-1} - p^{\ell}_{m+1,n-1})\}$$

$$- (h_1h_3S)^{\ell}_{m-1/2,n}\{\tilde{V}^{\ell}_{m,n} - (b_8)^{\ell}_{m-1/2,n}(p^{\ell}_{m,n} - p^{\ell}_{m-1,n}) - (b_7)^{\ell}_{m-1/2,n}$$

$$(p^{\ell+1}_{m,n} + p^{\ell+1}_{m-1,n} - p^{\ell-1}_{m,n} - p^{\ell-1}_{m-1,n}) - (b_9)^{\ell}_{m-1/2,n}(p^{\ell}_{m,n+1} + p^{\ell}_{m-1,n+1} - p^{\ell}_{m,n-1} - p^{\ell}_{m-1,n-1})\}]$$

$$+ \frac{1}{(\Delta z_-)^{\ell-1/2}_{m,n+1/2}} [(h_1h_2S)^{\ell}_{m,n+1}\{\tilde{W}^{\ell}_{m,n+1} - (c_9)^{\ell}_{m,n+1/2}(p^{\ell}_{m,n+1} - p^{\ell}_{m,n}) - (c_8)^{\ell}_{m,n+1/2}$$

$$(p^{\ell}_{m+1,n+1} + p^{\ell}_{m+1,n} - p^{\ell}_{m-1,n+1} - p^{\ell}_{m-1,n}) - (c_7)^{\ell}_{m,n+1/2}(p^{\ell+1}_{m,n} + p^{\ell+1}_{m,n+1} - p^{\ell-1}_{m,n} - p^{\ell-1}_{m,n+1})\}$$

$$- (h_1h_2S)^{\ell}_{m,n-1}\{\tilde{W}^{\ell}_{m,n} - (c_9)^{\ell}_{m,n-1/2}(p^{\ell}_{m,n} - p^{\ell}_{m,n-1}) - (c_8)^{\ell}_{m,n-1/2}(p^{\ell}_{m+1,n} + p^{\ell}_{m+1,n-1}$$

$$- p^{\ell}_{m-1,n} - p^{\ell}_{m-1,n-1}) - (c_7)^{\ell}_{m,n-1/2}(p^{\ell+1}_{m,n} + p^{\ell+1}_{m,n-1} - p^{\ell-1}_{m,n} - p^{\ell-1}_{m,n-1})\}\ ] = 0 \qquad (C\text{-}58)$$

Through the use of the following definitions

$$cx_1 = (h_2h_3S)^{\ell}_{m,n}/(\Delta x_-)^{\ell}_{m,n},\quad cx_2 = (h_2h_3S)^{\ell-1}_{m,n}/(\Delta x_-)^{\ell}_{m,n}$$

$$cy_1 = (h_1h_3S)^{\ell}_{m+1/2,n}/(\Delta y_-)^{\ell-1/2}_{m+1/2,n},\quad cy_2 = (h_1h_3S)^{\ell}_{m-1/2,n}/(\Delta y_-)^{\ell-1/2}_{m+1/2,n}$$

$$cz_1 = (h_1h_2S)^{\ell}_{m,n+1/2}/(\Delta z_-)^{\ell-1/2}_{m,n+1/2},\quad cz_2 = (h_1h_2S)^{\ell}_{m,n-1/2}/(\Delta z_-)^{\ell-1/2}_{m,n+1/2}$$

$$\dot{m} = cx_1\tilde{U}^{\ell}_{m,n} - cx_2\tilde{U}^{\ell-1}_{m,n} + cy_1\tilde{V}^{\ell}_{m+1,n} - cy_2\tilde{V}^{\ell}_{m,n} + cz_1\tilde{W}^{\ell}_{m,n+1} - cz_2\tilde{W}^{\ell}_{m,n}$$

$$a_{1x} = (a_7)^{\ell}_{m,n},\quad a_{1y} = (a_8)^{\ell}_{m,n},\quad a_{1z} = (a_9)^{\ell}_{m,n}$$

$$a_{2x} = (a_7)^{\ell-1}_{m,n},\quad a_{2y} = (a_8)^{\ell-1}_{m,n},\quad a_{2z} = (a_9)^{\ell-1}_{m,n}$$

$$a_{3x} = (b_7)^{\ell}_{m+1/2,n},\quad a_{3y} = (b_8)^{\ell}_{m+1/2,n},\quad a_{3z} = (b_9)^{\ell}_{m+1/2,n}$$

$$a_{4x} = (b_7)^{\ell}_{m-1/2,n},\quad a_{4y} = (b_8)^{\ell}_{m-1/2,n},\quad a_{4z} = (b_9)^{\ell}_{m-1/2,n}$$

$$a_{5x} = (c_7)^{\ell}_{m,n+1/2},\quad a_{5y} = (c_8)^{\ell}_{m,n+1/2},\quad a_{5z} = (c_9)^{\ell}_{m,n+1/2}$$

$$a_{6x} = (c_7)^{\ell}_{m,n-1/2},\quad a_{6y} = (c_8)^{\ell}_{m,n-1/2},\quad a_{6z} = (c_9)^{\ell}_{m,n-1/2}$$

the pressure equation can be put in the form

$$f_1p^{\ell+1}_{m,n} + f_2p^{\ell}_{m,n} + f_3p^{\ell-1}_{m,n} + f_4p^{\ell}_{m+1,n} + f_5p^{\ell}_{m-1,n} + f_6p^{\ell}_{m,n+1} + f_7p^{\ell}_{m,n-1} = Sp \qquad (C\text{-}59)$$

where

$$f_1 = - a_{1x}cx_1 - a_{3x}cy_1 + a_{4x}cy_2 + a_{6x}cz_2 - a_{5x}cz_1$$

$$f_2 = a_{1x}cx_1 + a_{2x}cx_2 + a_{3y}cy_1 + a_{4y}cy_2 + a_{5z}cz_1 + a_{6z}cz_2$$

$$f_3 = - a_{2x}cx_2 + a_{3x}cy_1 - a_{4x}cy_2 + a_{5x}cz_1 - a_{6x}cz_2 \qquad \text{(C-60)}$$

$$f_4 = - a_{1y}cx_1 + a_{2y}cx_2 - a_{3y}cy_1 - a_{5y}cz_1 + a_{6y}cz_2$$

$$f_5 = a_{1y}cx_1 - a_{2y}cx_2 - a_{4y}cy_2 + a_{5y}cz_1 - a_{6y}cz_2$$

$$f_6 = -a_{1z}cx_1 + a_{2z}cx_2 - a_{3z}cy_1 + a_{4z}cy_2 - a_{5z}cz_1$$

$$f_7 = a_{1z}cx_1 - a_{2z}cx_2 + a_{3z}cy_1 - a_{4z}cy_2 - a_{6z}cz_2$$

and

$$\begin{aligned} Sp = &- \dot{m} + (a_{1y}cx_1 + a_{3x}cy_1)\, p^{\ell+1}_{m+1,n} + (a_{1z}cx_1 + a_{5x}cz_1)\, p^{\ell+1}_{m,n+1} \\ &- (a_{1z}cx_1 + a_{6x}cz_2)\, p^{\ell+1}_{m,n-1} - (a_{1y}cx_1 + a_{4x}cy_2)\, p^{\ell+1}_{m-1,n} \\ &+ (a_{3z}cy_1 + a_{5y}cz_1)\, p^{\ell}_{m+1,n+1} - (a_{3z}cy_1 + a_{6y}cz_2)\, p^{\ell}_{m+1,n-1} \\ &- (a_{4z}cy_2 + a_{5y}cz_1)\, p^{\ell}_{m-1,n+1} + (a_{4z}cy_2 + a_{6y}cz_2)\, p^{\ell}_{m-1,n-1} \\ &- (a_{2y}cx_2 + a_{3x}cy_1)\, p^{\ell-1}_{m+1,n} - (a_{2z}cx_2 + a_{5x}cz_1)\, p^{\ell-1}_{m,n+1} \\ &+ (a_{2z}cx_2 + a_{6x}cz_2)\, p^{\ell-1}_{m,n-1} + (a_{2y}cx_2 + a_{4x}cy_2)\, p^{\ell-1}_{m-1,n} \end{aligned} \qquad \text{(C-61)}$$

U.S. DISTRIBUTION LIST

Commander
David W. Taylor Naval Ship
R & D Center (ATTN: Code 1505)
Bldg. 19, Room 129B
Bethesda, Maryland 20084

Commander
Naval Sea Systems Command
Washington, D.C. 20362
ATTN: 05R22

Commander
Naval Sea Systems Command
Washington, D.C. 20362
ATTN:55W (R. Keane, Jr.)

Commander
Naval Sea Systems Command
Washington, D.C. 20362
ATTN: 55W3 (W. Sandberg)

Commander
Naval Sea Systems Command
Washington, D.C. 20362
ATTN: 50151 (C. Kennell)

Commander
Naval Sea Systems Command
Washington, D.C. 20362
ATTN: 56X12 (C.R. Crockett)

Commander
Naval Sea Systems Command
Washington, D.C. 20362
ATTN: 63R31 (T. Pierce)

Commander
Naval Sea Systems Command
Washington, D.C. 20362
ATTN: 55X42 (A. Paladino)

Commander
Naval Sea Systems Command
Washington, D.C. 20362
ATTN: 99612 (Library)

Director
Defense Documentation Center
5010 Duke Street
Alexandria, VA 22314

Library of Congress
Science & Technology Division
Washington, D.C. 20540

Naval Underwater Weapons Research
& Engineering Station (Library)
Newport, RI 02840

Office of Naval Research
800 N. Quincy Street
Arlington, VA 22217
ATTN: Dr. C.M. Lee, Code 432

Commanding Officer (L31)
Naval Civil Engineering Laboratory
Port Hueneme, CA 93043

Commander
Naval Ocean Systems Center
San Diego, CA 92152
ATTN: Library

Library
Naval Underwater Systems Center
Newport, RI 02840

Charleston Naval Shipyard
Technical Library
Naval Base
Charleston, SC 29408

Norfolk Naval Shipyard
Technical Library
Portmoth, VA 23709

Puget Sound Naval Shipyard
Engineering Library
Bremerton, WA 98314

Long Beach Naval Shipyard
Technical Library (246L)
Long Beach, CA 90801

Mare Island Naval Shipyard
Shipyard Technical Library (202.3)
Vallejo, CA 94592

Assistant Chief Design Engineer
for Naval Architecture (Code 250)
Mare Island Naval Shipyard
Vallejo, CA 94592

U.S. Naval Academy
Annapolis, MD 21402
ATTN: Technical Library

Naval Postgraduate School
Monterey, CA 93940
ATTN: Library (2124)

Study Center
National Maritime Research Center
U.S. Merchant Marine Academy
Kings Point, LI, New York 11024

The Pennsylvania State University
Applied Research Laboratory (Library)
P.O. Box 30
State College, PA 16801

Dr. B. Parkin, Director
Garfield Thomas Water Tunnel
Applied Research Laboratory
P.O. Box 30
State College, PA 16801

Bolt, Beranek & Newman (Library)
50 Moulton Street
Cambridge, MA 02138

Cambridge Acoustical Associates, Inc.
54 Rindge Ave Extension
Cambridge, MA 02140

R & D Manager
Electric Boat Division
General Dynamics Corporation
Groton, Conn 06340

Gibbs & Cox, Inc. (Tech. Info. Control)
21 West Street
New York, NY 10006

Tracor Hydronautics, Inc. (Library)
Pindell School Rd.
Laurel, MD 20810

Newport New Shipbuilding and
Dry Dock Co. (Tech. Library)
4101 Washington Ave.
Newport News, VA 23607

Society of Naval Architects and
Marine Engineers (Tech. Library)
One World Trade Center, Suite 1369
New York, NY 10048

Sperry Systems Management Division
Sperry Rand Corporation (Library)
Great Neck, NY 10020

Stanford Research Institute
Menlo Park, CA 94025
ATTN: Library

Southwest Research Institute
P.O. Drawer 28510
San Antonio, TX 78284
ATTN: Dr. H. Abramson

Mr. Robert Taggart
9411 Lee Highway, Suite P
Fairfax, VA 22031

Ocean Engr. Department
Woods Hole Oceanographic Inc.
Woods Hole, Mass 02543

Worcester Polytechnic Inst.
Alden Research Lab (Tech Library)
Worcester, MA 01609

Applied Physics Laboratory
University of Washington (Tech. Library)
1013 N. E. 40th Street
Seattle, WA 98105

University of California
Naval Architecture Department
Berkeley, CA 94720
ATTN: Profs. Webster, Paulling,
Wehausen & Library

California Institute of Technology
Pasadena, CA 91109
ATTN: Library

Engineering Research Center
Reading Room
Colorado State University
Foothills Campus
Fort Collins, CO 80521

Florida Atlantic University
Ocean Engineering Department
Boca Raton, Florida 33432
ATTN: Technical Library

Gordon McKay Library
Harvard University
Pierce Hall
Cambridge, MA 02138

Department of Ocean Engineering
University of Hawaii (Library)
2565 The Mall
Honolulu, Hawaii 96822

Institute of Hydraulic Research
The University of Iowa
Iowa City, Iowa 52242
ATTN: Library, Landweber, Patel

Prof. O. Phillips
Mechanics Department
The John Hopkins University
Baltimore, MD 21218

Kansas State University
Engineering Experiment Station
Seaton Hall
Manhattan, Kansas 66502
ATTN: Prof. D. Nesmith

University of Kansas
Chm Civil Engr Department Library
Lawrence, Kansas 60644

Fritz Engr. Laboratory Library
Department of Civil Engr
Lehigh University
Bethelehem, Pa 18015

Department of Ocean Engineering
Massachusetts Institute of Technology
Cambridge, MA 02139
ATTN: Profs. Leehey & Kerwin

Engineering Technical Reports
Room 10-500
Massachusetts Institute of Technology
Cambridge, MA 02139

St. Anthony Falls Hydraulic Laboratory
University of Minnesota
Mississippi River at 3rd Av., SE
Minneapolis, MN 55414
ATTN: Dr. Arndt & Library

Department of Naval Architecture
and Marine Engineering-North Campus
University of Michigan
Ann Arbor, Michigan 48109
ATTN: Library

Davidson Laboratory
Stevens Institute of Technology
711 Hudson Street
Hoboken, NJ 07030
ATTN: Library

Applied Research Laboratory
University of Texas
P.O. Box 8029
Austin, TX 78712

Stanford University
Stanford, CA 94305
ATTN: Engineering Library, Dr. Street

Webb Institute of Naval Architecture
Crescent Beach Road
Glen Cove, LI, NY 11542
ATTN: Library

National Science Foundation
Engineering Divison Library
1800 G Street NW
Washington, DC 20550

Mr. John L. Hess
4338 Vista Street
Long Beach, CA 90803

Dr. Tuncer Cebeci
Mechanical Engineering Dept.
California State University
Long Beach, CA 90840

Science Applications, Inc.
134 Holiday Court, Suite 318
Annapolis, MD 21401